Quaternary Sedimentology East of Thunder Bay, Ontario; Implications for Five Paleoindian Sites

Christine Shultis

Geology Department

Lakehead University

Thunder Bay, Ontario

A thesis submitted to the Faculty of Graduate Studies in partial fulfillment of the requirements for the degree of Master of Science

PERMISSION TO USE

In presenting this thesis in partial fulfillment of the requirements for a Masters of Science degree in Geology from Lakehead University, I agree that copies of this thesis shall be deposited in the University Library and the Department of Geology to be freely available for public use. I further agree that permission for copying of this thesis in any manner, in whole or in part, for scholarly purposes may be granted by my supervisors Dr. Matthew Boyd and Dr. Philip Fralick, the graduate coordinator Dr. Andrew Conly, or in their absence, by the chair of the Department of Geology or the Dean of the Faculty of Science and Environmental Studies. It is understood that any copying or publication of this thesis, or parts thereof for financial gain shall not be allowed without my written permission. Also it is understood that due recognition will be given to me and Lakehead University in any scholarly use which may be made of any material in this thesis.

ABSTRACT

A geoarchaeological investigation was north of Highway 11/17, 34km east of Thunder Bay, Ontario. Five archaeological sites (Mackenzie 1, Mackenzie 2, RLF, Woodpecker 1, and Woodpecker 2) and seven additional sediment exposures were examined for stratigraphic analysis to accompany the archaeological excavations. River-mouth sediments at 268m asl and a series of deltas indicate that the study area was subaqueous while placement of the Superior lobe prevented drainage to the Superior basin. This elevation is consistent with Lake Beaver Bay, an ice-contact lake that received glacial meltwater from the north (the Hudson Bay lobe) as well as the south (the Superior lobe). This is demonstrated by southward and northward prograding deltaic sequences within the study area.

As the Superior lobe made its final retreat, Lake Beaver Bay dissipated into the Superior basin marking the beginning of the Minong phase, likely around 9,900 ^{14}C yrs BP. Additional sequences representing river-mouth, beach shoreface, and deltaic depositional environments indicate that a series of shorelines within the study area represent subsequent Minong lake levels. The highest, and likely oldest of these strandlines is an erosional feature at 256m asl, consistent with wave-cut terraces previously identified in the Thunder Bay region.

Relative lake level drops occurred, likely due to a combination of gradual erosion of the Nadoway Point sill and isostatic rebound of the recently deglaciated land. Beach and river-mouth sequences representing subsequent shorelines are located at 249m, 243m, and 240m asl. Artifacts on each of these beach terraces suggest they were occupied by Paleoindian groups.

The occupation layer(s) at the Mackenzie 1 site are strongly bioturbated, although the sediment matrix is consistent with underlying beach sediments in the north and river-mouth sequences in the south. The site is about 10,000 m^2, and 378 Paleoindian projectile points were recovered along with additional bifaces, other formal and expedient tools, as well as lithic debitage. The frequency of artifacts and site size likely indicate that Mackenzie 1 was successively occupied over an extended time period of time. However, absence

of an unconformity separating the visible stratigraphy from the massive occupation layer(s) may indicate that the site was inhabited soon after deposition ceased. This likely places site occupation within the Minong phase (dating to ~10,500 to 9,000 cal BP).

Artifacts recovered from the RLF archaeological site are also within a bioturbated sediment matrix consistent with underlying stratigraphy. Lithofacies indicate that soon after the beach shoreface sediments were deposited, the beach terrace was utilized by mobile Paleoindian groups.

A shoreline at 240m asl is evidenced by a wave-cut feature and beach sediments at the Woodpecker sites, river-mouth sequences at the Mackenzie 2 site, and beach shoreface deposits at a roadcut exposure. Presence of artifacts and charcoal within beach sediments at the Woodpecker 2 site provides evidence that occupation was contemporaneous with active beach formation. However, the majority of recovered artifacts at Woodpecker 1 and Woodpecker 2 are associated with bioturbated sediments consistent with underlying stratigraphy. Most likely, the Woodpecker sites were occupied along an active Lake Minong margin, and subsequently inhabited soon after the relative lake level dropped again. The artifact matrix at the Mackenzie 2 site similarly suggests that occupation occurred soon after deposition of the underlying river-mouth sequences

Two additional exposures revealing a deltaic sequence and beach sediments suggest that the relative lake level lowered to 233m, and subsequently to 224m asl. This lowest shoreline identified within the study area likely represents the beginning of the Post-Minong phase.

All five archaeological sites are strategically placed on beach terraces, which is consistent with most presently known Paleoindian habitations in Northwestern Ontario. As well, The Mackenzie and Woodpecker sites likely had access to a river, making them ideal for fishing as well as hunting at the river crossings. The study area provides additional evidence that lake margins and river-mouths were highly attractive campsites for mobile Paleoindian groups. In addition, artifacts recovered from within beach sediments at Woodpecker 2 suggest that the Thunder Bay region was first occupied soon after deglaciation.

The Mackenzie, RLF, and Woodpecker sites were likely inhabited between about 9,900 and 9,000 ^{14}C yrs BP.

ACKNOWLEDGEMENTS

I would like to thank the many people that were integral to this thesis project. My supervisors Dr. Matt Boyd (Anthropology Department, Lakehead University) and Dr. Phil Fralick (Geology Department, Lakehead University) both assisted and guided me through the process of data collection, interpretation, and writing. In addition, I want to thank the Lakehead University Geology Department, and Dr. Vance Holliday (Anthropology and Geosciences Department, University of Arizona) for the feedback and complements I was given throughout the review process.

There were many inquisitive people that caused me to think critically and helped me form interpretatios and conclusions. These include Dr. Scott Hamilton (Anthropology Department, Lakehead University), Dave Norris, Sam Markham, Gjende Bennett, Gary Wowchuck, Mark Paxton-MacRae, and Dale Langford. I want them to know that their discussions were invaluable.

While collecting data for this thesis, my colleagues helped considerably, and made the field work enjoyable. Thank you to all of the Western Heritage employees involved with this project, especialy to Sylvia Szymczak, Breana McCulloch, Sam Markham, and Gjende Bennett. Their assistance and optimism is greatly appreciated. In addition, it was an honour to work with Dr. Paul Adderley (University of Sterling) and Dr. Krista Gilliland (Western Heritage). Discussions with them were an invaluable part of this thesis.

A warm thank you also goes to Western Heritage, the company completing archaeological mitigation. I would not have had such an incredible project to complete my Masters had it not been for Jim Finnigan (President of Western Heritage) and Terry Gibson (Senior Manager and Founding Partner of Western Heritage).

To my fellow graduate students at Lakehead, specifically Vicki Stinson and Bre Beh, thank you for the motivation. Lastly, I would like to thank my friends, family, and Fort Frances family for their unconditional support.

TABLE OF CONTENTS

TABLE OF FIGURES

Table of Tables

1. INTRODUCTION

This thesis was undertaken as a geoarchaeological investigation of site stratigraphy at five archaeological sites discovered during archaeological assessment required as part of the highway improvements near Thunder Bay, Ontario. During stage two and stage three investigations, diagnostic artifacts were recovered indicating extensive Paleoindian occupations that would be impacted by the construction. As a result, ongoing mitigation of five archaeological sites was required (Fig. 1.1).

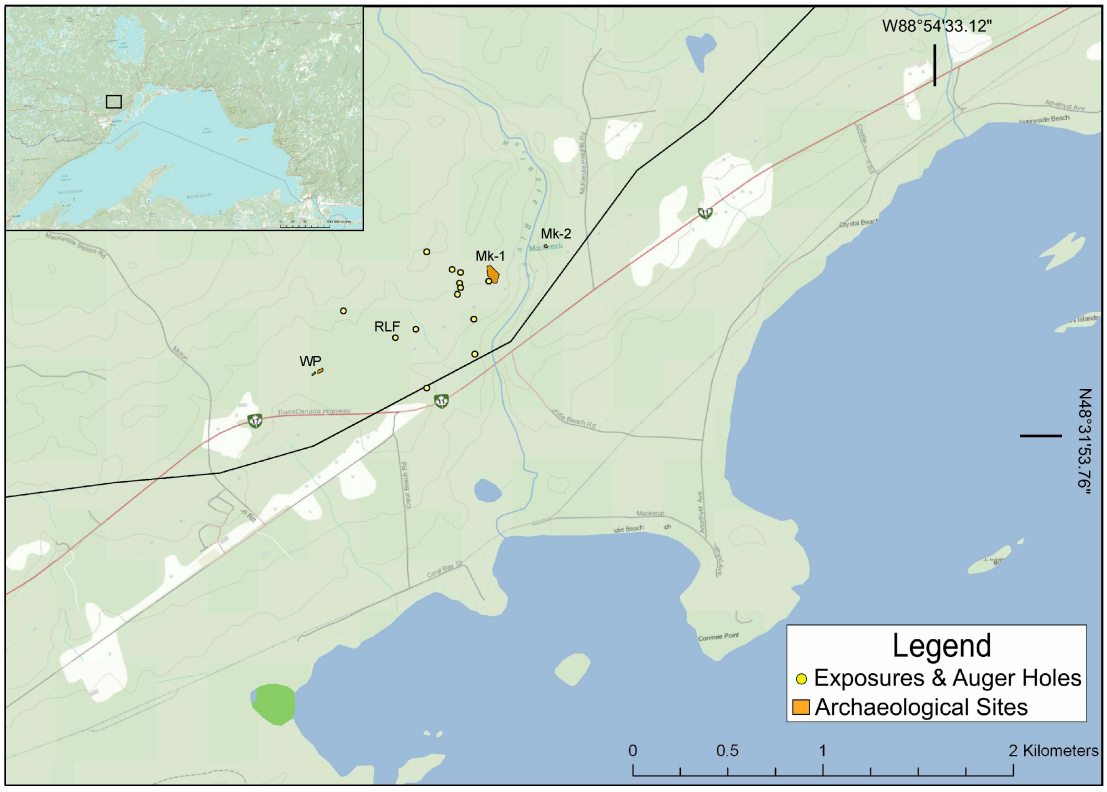

Figure 1.1. Location of study area. Sites shown are: Mk-1, Mackenzie 1; Mk-2, Mackenzie 2; RLF; WP, Woodpecker 1 and Woodpecker 2.

1.1 Background

The first human occupation of the Lake Superior basin was after the Pleistocene, when the deglaciated land became habitable. Although many Paleoindian sites have been identified along the Northwestern Lake Superior basin (e.g., Fox, 1976; Dawson, 1983; Julig, 1984), few have been excavated. This makes it difficult to interpret the nature and timing of initial occupation. As well, this initial occupation appears to be concentrated along relict beaches deposited during proglacial lake phases (e.g., Minong). The presence of water is commonly indicative of abundant food resources, making lake margins and river systems a focal area for human foraging and settlement. However, contemporaneity of site occupation and active beach formation has not been demonstrated at many of these Paleoindian sites due to a general lack of geoarchaeological research and absolute dating in the Thunder Bay region.

The modern landscape of Northwestern Ontario retains a visible imprint of geological processes that have occurred over the last 12,000 years. Successive glacial advances and retreats, the formation of proglacial lakes, and glacial meltwater outflow along with other events have produced a wide variety of sedimentary landforms visible today. Among these features are relict strandlines, which provide evidence of significant fluctuations in water-level due to meltwater influx, differential isostatic rebound, and other factors (Farrand & Drexler, 1985; Teller & Mahnic, 1988; Boyd et al., 2012). Between ~9,500 to 8,000 ^{14}C yrs BP (radiocarbon years before present) water levels remained high in the Superior basin at ~230m above sea level (asl), ~47m above the modern water plane, during the Minong phase due to a morainal sill crossing from Nadoway Point (Michigan) to Gross Cap (Ontario) (Farrand & Drexler, 1985; Yu et al., 2010).

The Minong phase in the Superior basin coincides with the Paleoindian tradition (13,400 to 8,300 cal BP), when small mobile hunting groups likely utilized the high and dry ridges of former water planes as transportation corridors (Deller, 1979; Peers, 1985). Archaeologists have long recognized northwestern Ontario as a location of Paleoindian settlement in Canada (e.g., Fox, 1976),

although few Paleoindian sites in the Thunder Bay region have been excavated making the nature and timing of this occupation unknown. Continued research can rectify this issue with the aid of geoarchaeological investigations, which connect the human occupation at an archaeological site to the stratigraphic record of noncultural depositional events. Examination of sediment stratigraphy at archaeological sites in the Superior basin located near known lake margins can indicate whether site occupation is contemporaneous with active beach formation. This relationship, established at additional archaeological sites, can be used to understand land use patterns.

1.2 Study Objectives

The central purpose of this thesis was to reconstruct the depositional environments prior to, during, and after occupation of five archaeological sites near Thunder Bay, Ontario (Fig. 1.1). Absolute ages determined by Western Heritage are assessed in combination with paleogeography to provide some additional insight into the deglaciation sequence in northwestern Ontario, and history of proglacial Lake Minong. In addition, the relationship between site setting and lake history will be inferred. This research will provide new insight into the timing and nature of Paleoindian settlement in the Upper Great Lakes.

1.3 Study Area and Access

The thesis study area spans from the east side of the Mackenzie River at the Mackenzie 2 site to ~1.5km southwest, where the Electric Woodpecker sites are located (Fig. 1.1). This region lies within the Canadian Shield, where Proterozoic sedimentary and intrusive rocks dominate the north shore of Lake Superior and in the Nipigon basin (Zoltai, 1965). Existing relief is the result of erosion and deposition by glacial ice (features include ablation till, high morainic ridges, and esker ridges), as well as outwash sand and glacial lake sediment infilling some depressions (Zoltai, 1965). North of the study area, a complex of glaciofluvial material including esker-like ridges and kames parallels the shore of

modern Lake Superior, occupying a belt ~1.6km wide (Zoltai, 1965). Associated with the archaeological sites within the study area are prominent relict beaches that provide margins for proglacial Lake Minong (Steinbring, 1976; Burwasser, 1977). Although eight separate Lake Minong levels have been acknowledged (Farrand & Drexler, 1985), and few of these have been identified in Northwestern Ontario, one Minong level strandline does parallel HWY 11/17 along the exposures and archaeological sites with the study area (Fig. 1.1).

2. DEGLACIATION AND LAKE HISTORY OF THE SUPERIOR BASIN

The Great Lakes watershed covers about 765,990km^2 (Fig. 2.1), encompassing lake basins originating from channeling of ice flow along major bedrock valley systems that existed prior to glaciation, as well as glacial scouring and erosion (Larson & Schaetzl, 2001). Deglaciation and lake evolution in the Great Lakes region is complex resulting in part from glacial readvances, outlet erosion, meltwater inflow, and differential isostatic rebound. As the Laurentide Ice Sheet (LIS) retreated, proglacial lakes formed temporarily in basins, as well as low-lying areas adjacent to ice boundaries (Larson & Schaetzl, 2001). Many archaeological sites have been discovered along margins of these large and interconnected proglacial lakes (discussed in Chapter 3), making it important to accurately reconstruct lake-level fluctuations. This chapter provides a summary of the history of deglaciation and associated proglacial lakes in the Great Lakes region, with a focus on the Minong phase of the Lake Superior basin.

Figure 2.1. The Great Lakes Watershed. After Larson and Schaetzl, 2001.

2.1 Cordilleran and Laurentide Ice Sheets

The Last Glacial Maximum occurred around 18,000 to 21,000 ^{14}C yrs BP when there was relative climate stability, and a period of low global sea level (Dyke et al., 2002). During this time there were two major ice sheets in Canada: the Cordilleran and Laurentide. At their maximum extent ~18,000 ^{14}C yrs BP, the Cordilleran and Laurentide ice sheets coalesced (Fig. 2.2) (Dyke, 2004). After the LIS had reached its maximum extent and oscillated near that position for several thousands of years, the southern margin began retreating northward into the Great Lakes watershed, interrupted by major readvances that culminated at about 15,500, 13,000, 11,800, and 10,000 ^{14}C yrs BP (Larson & Schaetzl, 2001).

Figure 2.2. Coalescence of Cordilleran and Laurentide ice sheets at their maximum extent ~18,000 ^{14}C yrs BP. After Dyke (2004).

2.1.1 Deglaciation of Northwestern Ontario (12,000 - 10,000 ^{14}C yr BP)

As the LIS retreated from northwestern Ontario, end moraines were created by till deposition, documenting ice position throughout the Early and

Middle Holocene (Fig. 2.3) (Lowell et al., 2009). These were initially mapped by Zoltai (1963, 1965), and have been used to determine a deglaciation chronology utilizing radiocarbon dates from basal organics preserved in depressions (Dyke, 2004), as well as in lake sediments (Bjorck, 1985; Teller et al., 2005; Loope, 2006; Lowell et al., 2009). In order to develop a better understanding of the deglaciation sequence of the Thunder Bay region, Lowell et al. (2009) incorporated 17 radiocarbon ages from previous work with their 26 dates on basal organics from lake sediments deposited in front of and behind moraines. This sequence begins with the LIS initially retreating to the Vermilion Moraine ~12,000 ^{14}C yr BP (south of area shown in Fig. 2.3), remaining at or near this position for nearly 2,500 yr (Lowell et al., 2009).

Figure 2.3. Moraines in Northwestern Ontario. After Zoltai (1965)

The Brule Creek Moraine marks the position of the Patrician ice mass as it retreated from the region (Burwasser, 1977), and may be a continuation of the Eagle-Finlayson Moraine (Zoltai, 1965). Although contemporaneity has not been confirmed for Brule Creek and Eagle-Finlayson, these and Steep Rock likely formed 10,200 ^{14}C yr BP, in a brief interval of time (Lowell et al., 2009). West of Thunder Bay, minimum dates indicates that the Patrician ice mass retreated to the Hartman Moraine between 11,000 and 10,100 ^{14}C yr BP (Lowell et al., 2009).

The Dog Lake lobe of the Hudson Bay glacier advanced from the northeast, halting at the Dog Lake moraine during or at the end of the Younger Dryas between 11,000 and 10,100 ^{14}C yr BP (Lowell et al., 2009). The Dog Lake lobe also formed the Lac Seul/Kaiashk Interlobate Moraine while the Patrician ice mass stagnant at the Hartmann Moraine (Burwasser, 1977) between 10,900 and 9,000 ^{14}C yr BP (Lowell et al., 2009).

The Superior lobe advanced in a western direction, halting at the Marks Moraine while also forming the Mackenzie Interlobate Moraine with the Dog Lake ice lobe ~10,000 ^{14}C yr BP (Burwasser, 1977; Clayton & Moran, 1982).

2.1.2 Marquette Readvance (~10,000 ^{14}C yr BP)

During the Marquette readvance, the LIS extended from about 1,000km east of Dululth, Minnesota across the northern and southern shores of Lake Superior (Lowell et al., 1999). This advance partially covered the Lake Gribben forest, while depositing the ice contact moraine Grand Marais I (Fig. 2.4; Lowell et al., 1999). Along with moraine sediments, the Gribben forest organics were buried completely by lacustrine and outwash deposits which preserved the organics. Dating of the Lake Gribben forest organics indicates that the Marquette readvance reached its greatest extent at ~10,000 ^{14}C yr BP (Lowell et al., 1999), coinciding with formation of the terminal Marks Moraine on the north shore of the Superior basin (Burwasser, 1977; Clayton & Moran, 1982).

Two terminal moraines north of Grand Marais I mark brief stagnant periods as the LIS made its final retreat from the Superior basin (Farrand & Drexler, 1985). These are Grand Marais II and Grand Marais III (Fig. 2.4).

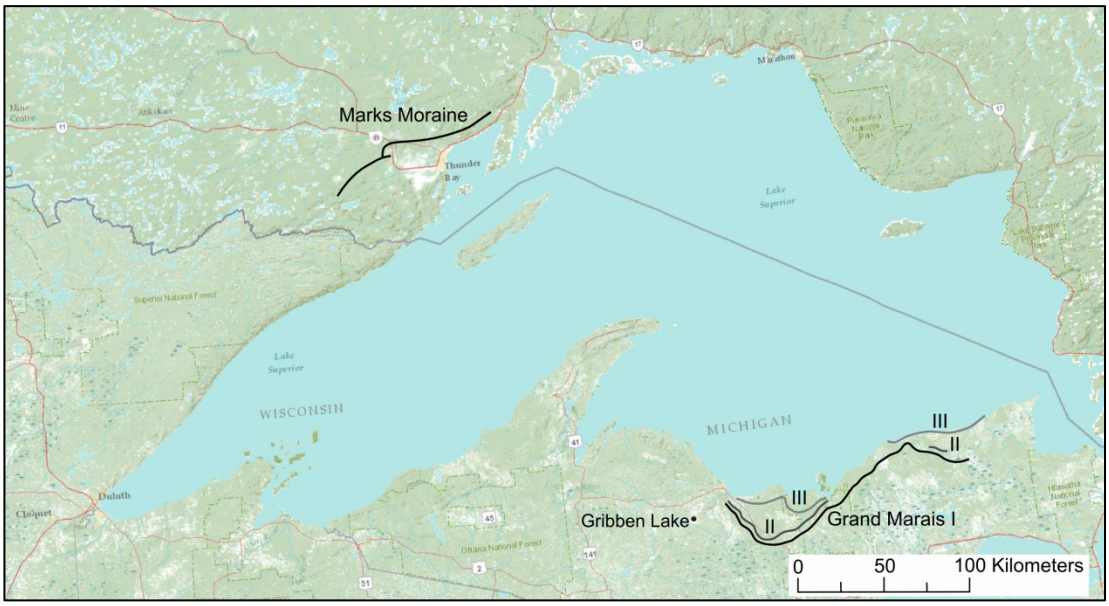

Figure 2.4. Terminal moraines deposited during the Marquette readvance, and subsequent retreat: Marks Moraine, Grand Marais I, Grand Marais II (II), and Grand Marais III (III). After Zoltai (1963) and Farrand & Drexler (1985).

A deltaic sequence has been identified at the KOA campground south of the Mackenzie Moraine indicating northward progradation (Patricia Craig, 1991). Glacial striae on the Sibley Peninsula and east of the KOA delta exposure (Zoltai, 1965) were utilized to conclude that there was a glacial ice margin to the north (at roughly the Mackenzie Moraine location) as well as to the south, which would have caused water to accumulate between the ice margins (Patricia Craig, 1991) (B or C of Fig. 2.5). However, the glacial striae could indicate the direction of glacial movement during the Marquette readvance. In this scenario, glacial meltwater would have pooled between the Superior lobe to the south and high topography to the north as the glacier made its final retreat from northwestern Ontario.

Similarly, Phillips and Fralick (1994b) identified three deltaic features on the flanks of Mount Baldy, Thunder Bay, Ontario with northward paleocurrent directions. The deltaic sequences are located at higher elevations than inferred

post-glacial lake-levels in the area, therefore they are interpreted to represent the previously unrecognized proglacial Lake Baldy (Figure 2.5; Phillips & Fralick, 1994b). Dropstone units are present within the deltaic sequences, indicating that icebergs were actively involved in deposition (Phillips & Fralick, 1994b). These deltaic sequences likely represent a proglacial lake that persisted for a short time between the Mackenzie moraine and the Superior lobe as depicted in Figure 2.5 (Phillips & Fralick, 1994b). This sequence likely occurred after the Marquette readvance, between about 9,900 and 9,500 ^{14}C yr BP (Phillips & Fralick, 1994b). As the LIS was retreating from the region, the Hudson Bay and Superior lobes separated allowing ice contact lakes to form between them (A of Fig. 2.5). The gradual retreat of the two lobes provided meltwater that flowed from the Hudson Bay lobe into Upper Lake Beaver Bay and Lake Baldy, as well as northward runoff from the Superior lobe (B and C of Fig. 2.5). This is also consistent with interpretations of the KOA delta (Patricia Craig, 1991), explaining how it is possible that water flowed north in this part of northwestern Ontario.

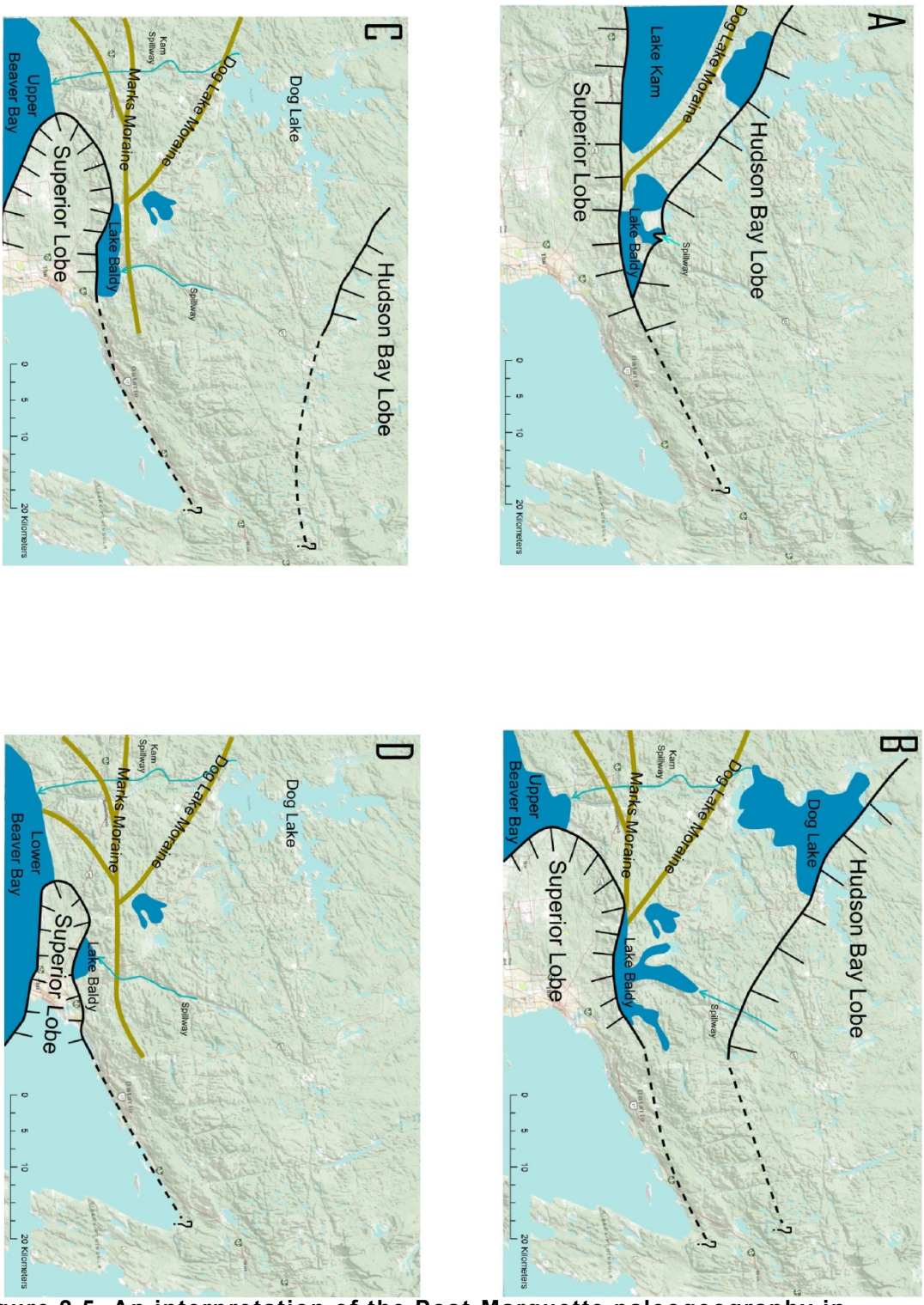

Figure 2.5. An interpretation of the Post-Marquette paleogeography in northwestern Ontario, about 9,900 to 9,500 ^{14}C yr BP. After Phillips and Fralick (1994b).

2.2 Development of the Great Lakes

As the southern margin of the Laurentide Ice Sheet receded, large proglacial lakes formed in the lake basins between high topography to the south and ice margins to the north (Larson & Schaetzl, 2001), and in the ice and meltwater-scoured valleys that had isostatically reversed gradients, sloping to the north as opposed to the south as they do today (Teller, 1995). However, few ice contact lakes formed until the Laurentide Ice Sheet had retreated into the Great Lakes basin since the regional slope of the North American continent was south, forcing most water to briefly drain into the Gulf of Mexico (Teller, 1995). As glacial ice retreated northward, with periodic surging southward, the routing of overflow from, as well as between, proglacial lakes changed frequently and abruptly along with the depth and areal extent of the lakes (Teller, 1995). The large glacial lakes in Canada and USA had very complex histories of changing water levels as outlets opened and closed in response to isostatic uplift and fluctuations in ice margin positions (Teller, 1995). Rates of isostatic rebound indicate that in the late Winsconsin, glacial ice was thickest over the Hudson Bay (Andrews, 1983), causing a relatively faster rate of isostatic rebound in this region following deglaciation.

The record of glacial and postglacial lakes in the Great Lakes watershed consists of lake floor sediments, bars, abandoned spillways and channels, wave-cut cliffs, beach ridges, and deltas providing evidence of former water levels (Larson & Schaetzl, 2001). Strandlines can also be investigated for an understanding of glacial retreat and isostatic uplift (Farrand & Drexler, 1985).

Proglacial lakes in the Great Lakes region first formed ~16,000 ^{14}C yrs BP. These include Lake Milwaukee which occupied the southern part of the Michigan basin (Schneider & Need, 1985), and glacial Lake Leverett which occupied the Erie basin (Barnett, 1992). A third unnamed lake likely existed in the southern part of the Huron basin and drained south into the Erie basin, although all of these basins were abandoned by the ice readvance ~15,500 ^{14}C yrs BP (Larson & Schaetzl, 2001). Subsequent ice retreat allowed for lake formation in the southernmost portions of the Michigan and Erie basins~14,000 ^{14}C yrs BP. In

the Superior basin, lake formation began ~11,000 ^{14}C yrs BP, however these drained through the Brule and Portage outlets allowing glacial Lake Algonquin to flood northward from the Huron basin (Farrand & Drexler, 1985). Lake Algonquin survived in the Superior basin until it was displaced by ice during the Marquette readvance (Farrand & Drexler, 1985). One of the most significant influences on lake development and history was glacial Lake Agassiz, which discharged both directly into the Great Lakes basin and indirectly through Lake Nipigon.

2.3 The Glacial Lake Agassiz – Superior Basin Connection

Glacial Lake Agassiz (Fig. 2.6) formed after the Last Glacial Maximum between ice and recently deglaciated land. Its level and extent were controlled by the elevation of spillways, the position of the Laurentide Ice Sheet (LIS), as well as terrain morphology, which was itself influenced by dynamic processes such as fluvial erosion and differential isostatic rebound (Teller, 1995; Leverington et al., 1999; Teller et al., 2005). Following deglaciation, continual differential isostatic rebound caused a relatively rapid rise in the northeastern part of the Agassiz basin, which resulted in southern transgressions (Leverington et al., 1999). Throughout the history of Lake Agassiz, major drops in water level occurred due to outlet erosion or the opening of lower outlets due to Laurentide Ice Sheet retreat; at other times, lake levels rose due to closing of outlets by glacial readvances or isostatic rebounding of outlets (Leverington et al., 1999). Five main drainage systems were utilized throughout Lake Agassiz's history (Fig. 2.6), and a sixth carried the final outburst either subglacially (LaJeunesse & St-Onge, 2008), or when ice in the Hudson Bay no longer provided a barrier (Teller et al., 2005). As the largest lake in North America during the last deglaciation, Lake Agassiz had considerable impacts on the dynamics of the rivers and lakes that received its overflow (Leverington et al., 1999). The Eastern drainage route, when occupied, routed glacial meltwater to the Superior basin either directly (E in Figure 2.6) or indirectly through the Nipigon basin (K in Figure 2.6), and strongly influenced lake levels prior to and throughout the Minong phase (Leverington & Teller, 2003; Teller et al., 2005).

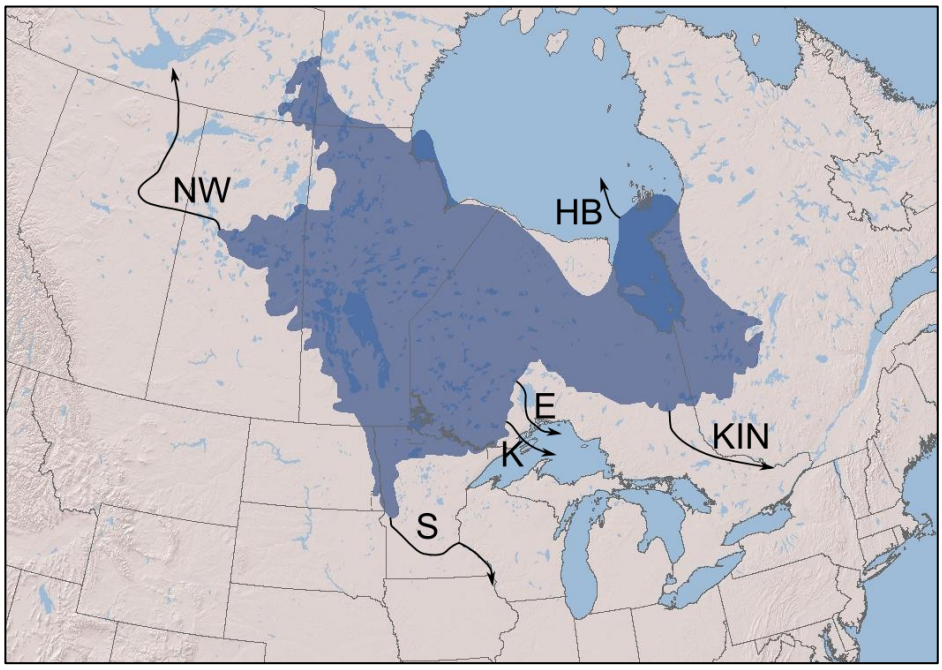

Figure 2.6. Total area covered by Glacial Lake Agassiz, main routes of overflow indicated by arrows and letters. NW: northwestern outlet, S: southern outlet, K: eastern outlets through the Thunder Bay area, E: eastern outlets through the Nipigon basin, KIN: Kinojevis outlet, HB: Hudson Bay route of final drainage. After Teller et al. (2005).

After ~11,800 ^{14}C yrs BP, the ice front began its northward retreat with glacial Lake Algonquin forming to the south (Farrand & Drexler, 1985). At this time, glacial Lake Agassiz experienced high water levels during the Lockhart phase, from its inception until 10,800 ^{14}C yr BP, when regression caused a lowstand that resulted in abandonment of the southern outlet during the Moorhead phase (Boyd, 2007b; Fisher et al., 2008). Eastward drainage during the Moorhead phase provided meltwater for the transgression of Lake Agassiz (Lewis & Anderson, 1989), although strandlines in the Superior basin representing this lake would have been destroyed by the Marquette readvance (Farrand & Drexler, 1985). In the western portion of the Superior basin, the earliest lakes recorded were narrow ice-marginal lakes that ponded between the ice front and the bedrock highlands from the Keweenaw Peninsula to Duluth, where meltwater was trapped in embayments (Farrand & Drexler, 1985). As the glacier retreated, overflow moved from east to west through bedrock channels,

through channels of which one wall was the ice front, or directly across the surface of the thin edge of the ice sheet (Farrand & Drexler, 1985).

After ~11,000 ^{14}C yrs BP, when Late Wisconsinan ice retreated from the Superior basin, Lake Agassiz initially drained south through the Minnesota and Mississippi River valleys to the Gulf of Mexico (Teller et al., 2005; Breckenridge, 2007. As deglaciation continued, a series of outlets along the eastern side of Lake Agassiz were successively occupied providing a connection with the Superior basin (Fig. 2.7).

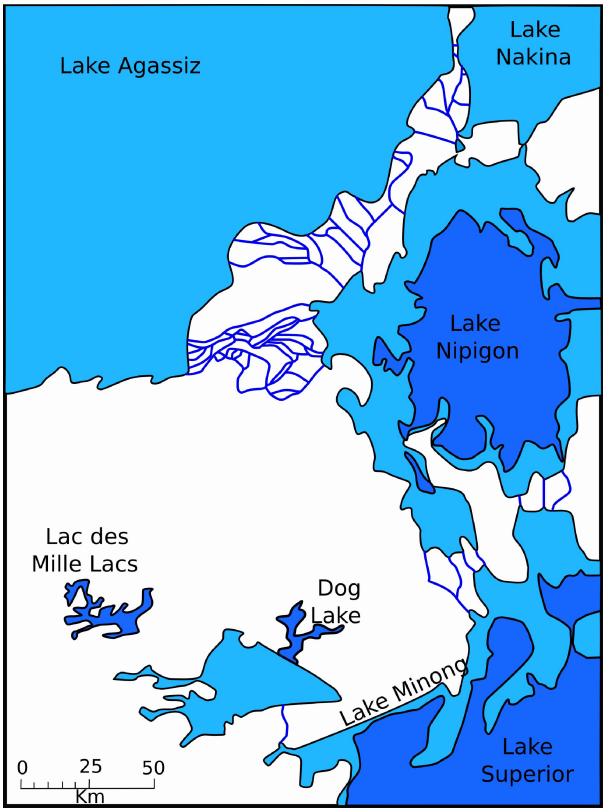

Figure 2.7. Outlets along the eastern side of Lake, draining through Lake Nipigon to the Superior basin. Modern lakes are dark blue. After Teller & Thorleifson (1983).

One on-going debate concerns the routing of glacial Lake Agassiz during the Younger Dryas (12,900~-10,000 cal [11,000 – 10,100 ^{14}C yr] BP), which coincides with a water level drop in the Agassiz basin of ~100m (Leverington et al., 2000; Fisher, 2003). It has been proposed that this meltwater outburst

temporarily interrupted thermohaline circulation in the North Atlantic Ocean causing the Younger Dryas cooling period (Broecker et al., 1989; Murton et al., 2010). Belief that the LIS blocked all northward drainage until about 10,000 ^{14}C yrs BP led to the conclusion that around 10,800 years ago, eastward outlets into the Superior basin opened, allowing the eastern outlets to be occupied as meltwater flowed throught the Great Lakes-St. Lawrence Valley to the North Atlantic Ocean (Breckenridge, 2007). However, due to the absence of catastrophic meltwater flood deposits in the Thunder Bay region and recent AMS dates (radiocarbon dates using accelerator mass spectrometry) (Teller et al., 2005; Lowell et al., 2009), it has more recently been proposed that Lake Agassiz discharge may have flowed northwest to the Arctic Ocean, possibly between 11,200 and 10,100 ^{14}C yrs BP (Murton et al., 2010). This direction of flow could have occurred if the LIS had not yet retreated from the Superior basin, blocking the eastern routes (Teller et al., 2005; Murton et al., 2010). Whether meltwater drained through the eastern route or the northwestern route, a significant drop in the lake level of Agassiz occurred, resulting in the Moorhead low stand (Leverington et al., 1999).

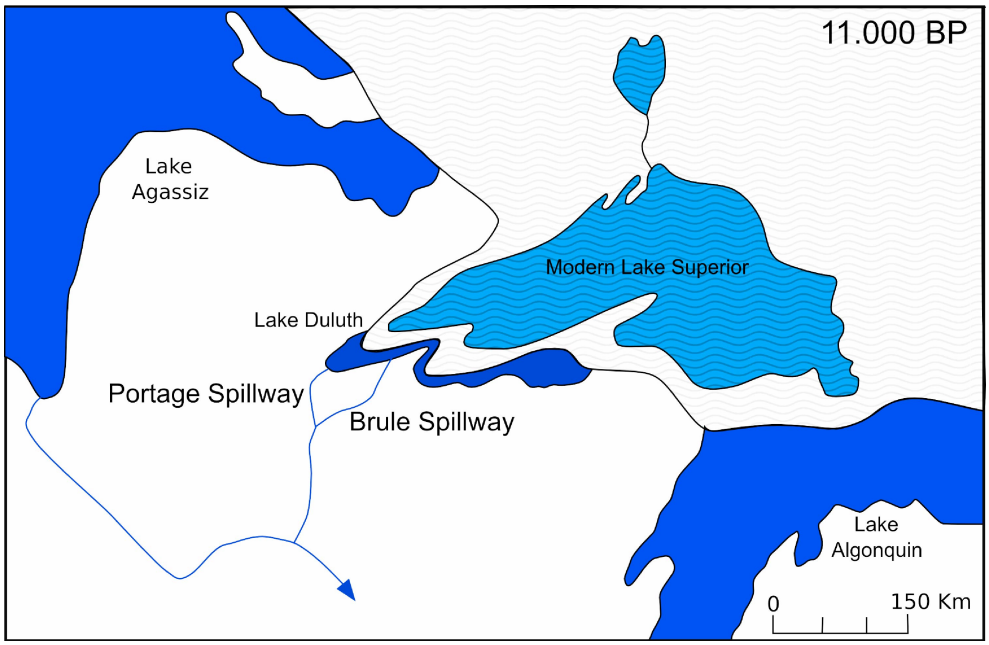

Figure 2.8. Brule and Portage outlet channels from the Superior basin. After Farrand & Drexler (1985).

As early as 11,000 ^{14}C yrs BP, there were two outlet channels from the southwestern corner of the Superior basin (Fig. 2.8) (Farrand & Drexler, 1985). The most prominent is the Brule outlet, which converges with the lake Agassiz southern drainage route at ~312m (1022ft) above sea level. The other is the Portage outlet, which is slightly higher than Brule at 320m. Originally, Lake Brule utilized the Brule outlet, while glacial lake Nemadji discharged through the Portage outlet. Later, Lakes Brule and Nemadji merged to form Lake Duluth (Farrand & Drexler, 1985). The two outlets likely functioned simultaneously when the lake stood at lake Duluth level, however the Portage outlet could have functioned alone when ice plugged the Brule outlet, and at lower lake levels solely the Brule outlet would have been used (Farrand & Drexler, 1985).

The ice front retreated more rapidly from the western basin than it did from the Marquette area, thus the water level remained at the Duluth levels until outlets lower than the Brule outlet were exposed (Farrand & Drexler, 1985). As outlets were opened or deepened by erosion, lake levels began to fall, marking the Post-Duluth phase. During the Marquette readvance (10,000 ^{14}C yrs BP), Lake Washburn (one of the Post-Duluth phase lakes) occupied the western portion of the Superior basin while Early Lake Minong occupied the eastern portion (Fig. 2.9) (Phillips & Fralick, 1994b; Booth et al., 2002). As the LIS retreated from its Marquette position Lake Washburn expanded (Fig. 2.9b) (Farrand & Drexler, 1985). Later, after the ice front retreated from Keweenaw Point (~9,500 ^{14}C yrs BP), Lakes Washburn and Minong coalesced into Lake Minong, which occupied the entire basin (Fig. 2.9c) (Farrand & Drexler, 1985; Booth et al., 2002).

Around 10,100 ^{14}C yrs BP water may have flowed northwest through the Clearwater and Athabasca River Valleys to the Mackenzie Valley and Arctic Ocean, or through the southern route mentioned previously (Teller et al., 2005). Another date of about 9,700 ^{14}C yrs BP, when Lake Agassiz merged with Lake Churchill in eastern Saskatchewan, has more recently been proposed as the opening of the southern outlet (Fisher et al., 2009). The Marquette re-advance blocked the Eastern outlets with glacial ice, isolating Lake Agassiz from the Great

lakes allowing it to attain its greatest extent and stability (Teller, 1995; Breckenridge, 2007). Leverington et al. (1999), argue that following the Marquette
readvance water flowed through the Northwestern route around 9,800 ^{14}C yrs BP then as more rapid rebound occurred, around 9,300 ^{14}C yrs BP, southern transgressions allowed the southernmost (Mississippi River Valley) route to be occupied. However, Fisher (2003) demonstrates that the southern outlet was occupied sometime between 9,900 and 9,400 ^{14}C yrs, although the duration and number of occupations are uncertain. This is supported by a study reporting evidence of freshwater discharge in the Gulf of Mexico at 9,900, 9,700, and 9,400 ^{14}C yrs BP (Aharon, 2003). It is likely that around 10,000 ^{14}C yrs BP, the lower northwestern outlet was temporarily closed due to the Marquette readvance which allowed water levels to rise to the Campbell level (Boyd, 2007b).

The end of the Moorhead phase (lowstand of Lake Agassiz) was thought to be ~10,000 ^{14}C yrs BP (e.g. Fisher, 2003; Boyd, 2007b), however there are conflicting arguments on this. It is also argued that the Emerson phase began about 10,000 ^{14}C yrs BP, culminating in the formation of the upper Campbell beach and the reopening of the southern outlet around 9,400 to 9,300 ^{14}C yrs BP (Teller et al., 2000; Fisher et al., 2008). The dates this argument rely upon are minimum ages from the southern outlet (Fisher et al., 2008), and based on radiocarbon dates that range from 10,040 to 9,300 ^{14}C yrs BP (Teller et al., 2000), therefore there are potential issues with these dates. Additional work is required for a more accurate chronology of the Emerson phase.

After the southern outlet was utilized by at least 9,400 ^{14}C yrs BP, discharge from glacial Lake Agassiz was again routed east, this time into the Nipigon basin before discharging through the Superior basin, and the Great Lakes-St. Lawrence Valley to the North Atlantic Ocean (Teller et al., 2005). The southeastern outlet was used 8,000 ^{14}C yrs BP allowing water to flow from amalgamated Lake Agassiz-Ojibway through the Ottawa River Valley to the St. Lawrence Valley and to the North Atlantic Ocean (Teller et al., 2005). Lastly,

from 7,700 ^{14}C yrs BP Lake Agassiz drained north into the Hudson Bay then east through Hudson Strait to the Labrador Sea-North Atlantic Ocean (Teller et al., 2005).

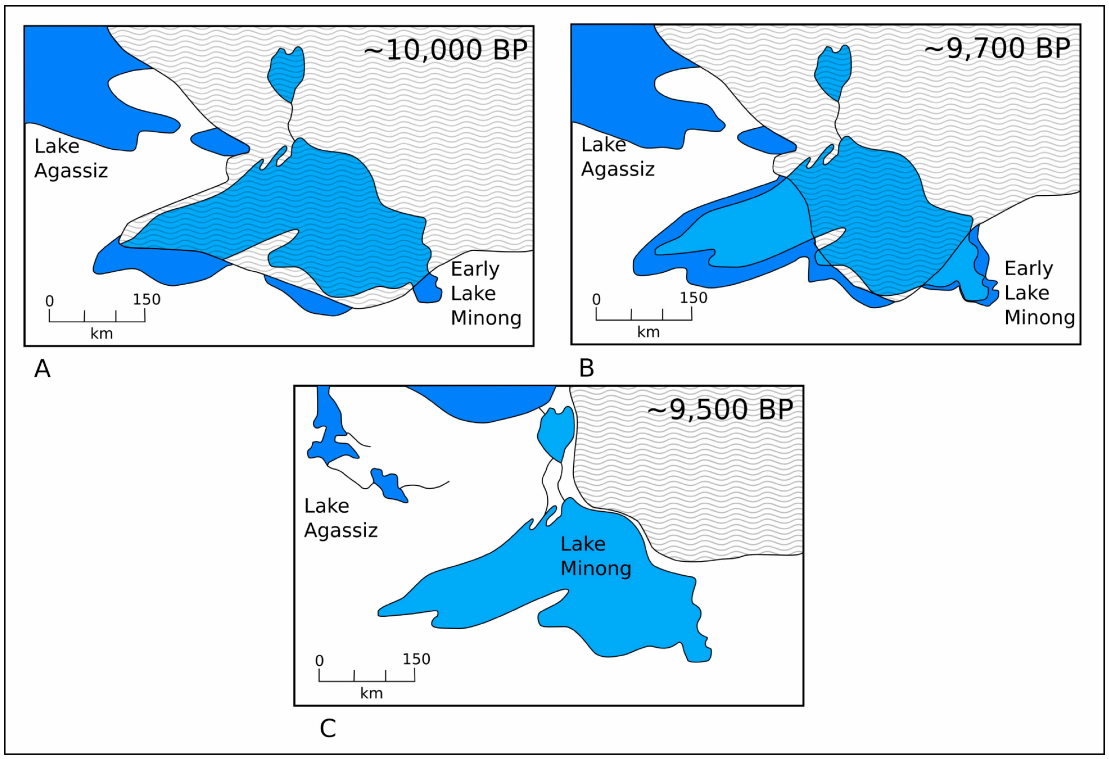

Figure 2.9. A) The LIS extent during the Marquette readvance (~10,000 ^{14}C yrs BP), with the appearance of Early Lake Minong shown with modern Lake Superior. B) Extent of the LIS ~9,700 ^{14}C yrs BP shown with Early Lake Minong and modern Lake Superior extents. C) Lakes Minong and Agassiz ~9,500 ^{14}C yrs BP, with simplified spillways. After Phillips and Fralick (1994a and 1994b).

2.4 The Lake Superior Basin (~9,000-~4,500 ^{14}C yrs BP)

Lake Minong's evolution is depicted in Figures 2.9a-c. The drainage route of Lake Agassiz 9,500 ^{14}C yrs BP is shown to be east, channeled downslope into major channels and flowing through Lake Nipigon, then through the Great Lakes (Leverington & Teller, 2003). Also by 9,500 ^{14}C yrs BP the Hudson Bay lobe had retreated from Dog Lake Moraine and the Superior lobe had retreated from Marks Moraine, both of which are situated just outside the city of Thunder Bay (Phillips & Fralick, 1994b).

From about 9,500 to 8,000 ^{14}C yrs BP, the existence of generally high but variable lake phases in the Upper Great Lakes is attributed to meltwater from glacial Lake Agassiz across the continental divide (Lewis & Anderson, 1989). Lake levels in the Superior basin would have been higher than 213m (Booth et al., 2002). During this time, overflow water was routed from Lake Agassiz through a complex system of eastern outlets decreasing elevation toward the north (Leverington & Teller, 2003). A rapid drop in the level of glacial Lake Agassiz and a corresponding catastrophic release of water may have accompanied the deglaciation and opening of each new outlet into the Nipigon basin (Leverington & Teller, 2003). As the southern margin of the Laurentide Ice Sheet retreated northward during the Nipigon phase, progressively lower outlets were opened to glacial Lake Nipigon, and correspondingly, the level of Lake Agassiz declined (Leverington & Teller, 2003). These drainage routes connecting Lake Agassiz and Lake Nipigon allowed water to flow in both directions, but since the Laurentide Ice Sheet retreated from the eastern Superior basin first, Superior levels dropped earlier allowing higher levels in the Agassiz basin to drain eastward (Farrand & Drexler, 1985).

Early in the Nipigon phase of Lake Agassiz, discharge would have entered the Minong level of Lake Superior, and likely eroded the Nadoway Point sill (Farrand & Drexler, 1985) approximately 9,300 ^{14}C yrs BP (Yu et al., 2010). The level of Lake Minong then lowered to the Houghton level, and was stabilized when the bedrock sill in the St. Marys River was reached (Farrand & Drexler, 1985). This dropped the lake level about 31m, resulting in a minimum and relative elevation around 182m (Saarnisto, ; Booth et al., 2002; Yu et al., 2010; Boyd et al., 2012). This also coincides with the routing of discharge from Lake Agassiz north of the Great Lakes, flowing instead into Lake Barlow-Ojibway. The Houghton low, attributed to erosion of the Nadoway Point sill, is contemporaneous with diversion of Agassiz meltwater away from the Superior basin into the Hudson Bay lowlands. Reduction of meltwater inflow coupled with a mid-Holocene dry period (8,000 - 5000 cal BP) may have caused water levels in Lake Michigan (Chippewa low phase) (Booth et al., 2002; Lewis et al., 2007),

and the Huron basin (Stanley low phase) to drop below the level of their outlets making them hydrologically closed (Booth et al., 2002; Lewis et al., 2007). A closed lake phase is also evident in the Superior basin between at least 9,100 and 8,900 cal BP (Boyd et al., 2012).

Rising water levels through the Nipissing phase produced the highest Holocene water levels of the Great Western Lakes by ~4,500 ^{14}C yrs BP (Booth et al., 2002). This high stand resulted from isostatic uplift raising the elevation of the North Bay outlet, backflooding upstream lake outlets bringing water levels of contiguous basins into confluence (Lewis & Anderson, 1989). By 7,700 ^{14}C yrs BP all the Upper Great Lakes except Superior had coalesced with waters of the Nipissing basin (Lewis & Anderson, 1989). In the Superior basin, the Nipissing transgression occurred in two phases (Booth et al., 2002): Nippising I occurred around 6,800 to 5,700 ^{14}C yrs BP, and has been explained by differential uplift between the outlet at North Bay and the Sault Sill which caused a water rise in the Superior basin, bringing Superior to the same level as the other Great Lakes, at an elevation about 195m (Booth et al., 2002; Lewis & Anderson, 1989); Nipissing II occurred between 4,600 and 4,400 ^{14}C yrs BP (Booth et al., 2002), when the Nipissing Great Lakes reached their maximum elevation and began to regress (Lewis & Anderson, 1989). At this time, differential uplift had completed the transfer of discharge from North Bay to southern outlets at Chicago and Port Huron, so the Great Lakes were fed solely by inflow from local precipitation and runoff (Lewis & Anderson, 1989).

2.5 Lake Minong Strandlines in the Thunder Bay Region

The elevations of all mapped Lake Minong shoreline features are drawn relative to isobases estimated by Lewis et al. (2005) using regional uplift rates (Fig. 2.10) (Breckenridge et al., 2010). Many strandlines have been inferred or correlated by extrapolating known isobases to other parts of the basin by Farrand & Drexler (1985). At least eight separate Lake Minong levels have been identified: Minong I-III, Post-Minong I-IV (Post-Minong IV also named Dorion), and Houghton (Fig. 2.10). All water planes with an outlet at Sault Ste. Marie are

drowned southwest of the Sault-Pigeon River isobase, causing the Houghton low shoreline to be submerged throughout the United States part of the Superior basin (Farrand & Drexler, 1985). Similarly, the Minong shoreline can be traced into Minnesota only to about as far as Grand Portage where it is intersected by the younger and stronger Nipissing shoreline, eventually dipping below the present water level (Fig. 2.10) (Farrand & Drexler, 1985).

Few dates constrain Minong and subsequent strandlines in the Thunder Bay region. Three dates have been presented from what is assumed to be Post-Minong I: 9,380 ± 150 ^{14}C yrs BP using wood from the base of the beach at Rosslyn (~230 m asl) (see Table 1 in Boyd et al., 2012); 9,260 ± 170 ^{14}C yrs BP from the base of Cummins Pond (Julig, 1988); and 9,345 ± 240 ^{14}C yrs BP from a beach at Grand Marais (Drexler et al., 1983).

The Nakina moraine contains ice-contact deltas contemporaneous with either Minong III or Post-Minong I. A tentative date of 9,000 ^{14}C yrs BP has been presented (Saarnisto, 1975), however a later date of 8,200 ^{14}C yrs BP was also proposed (Teller & Thorleifson, 1983; Teller et al., 1996).

The transition from Post-Minong III to Dorion (Fig. 2.10) is younger, and poorly constrained by three samples (9,240 ± 280, 8,310 ± 200, and 8,070 ± 180 ^{14}C yrs BP) (Bajc et al., 1997).

Another significant time period in this sequence of events is the lake level drop to the Houghton level in the Superior basin following erosion of the Nadoway point sill. It has been proposed that catastrophic discharge released from the Superior basin ~9,300 cal BP drained into the North Atlantic Ocean, triggering the cold event (Yu et al., 2010). While it does appear that substantial changes occurred in both deep and surface oceanic conditions at this time, to be caused by glacial meltwater from the Superior basin there must have been an extremely rapid lake level drop catastrophically discharging into the ocean. While Farrand and Drexler (1985) suggest that the outlet across the Nadoway dam was eroded progressively, Yu et al. (2010) suggested a rapid lake level drop of ~45m (from 226 to 181m asl relative to Saut Ste. Marie), which may have been capable of shutting down thermohaline circulation. This theory, however, is in

conflict with the known water planes in the Superior basin. A rapid lake level drop of ~45m implies that there may not have been sufficient time for a beach ridge to form. The transition from Post-Minong III to Dorion is roughly 9,200 cal BP (Bajc et al., 1997), providing evidence that the Dorion strandline formed while water in the Superior basin was regressing to the Houghton level. In fact, if the older date of >10,000 cal (9,240 ^{14}C yrs) (Bajc et al., 1997) is more accurate, the Post-Minong III strandline would have formed as lake levels were dropping as well. These strandlines need to be investigated further and require better constrained dates to substantiate the hypothesis proposed by Yu et al. (2010), although the radiocarbon chronology does support their scenario.

Minong-level strandlines have been identified between Kakabeka Falls and Nipigon, although a literature review has not revealed any additional dates or discussion of them. Extensive examination of the oldest and highest groups of strandlines across the Lake Agassiz basin has led to some new interpretations, which may prove useful when additional research on the Minong strandlines is conducted. McMillan and Teller (2012) propose that the majority of eight Herman level strandlines, eleven Norcross strandlines, and nine Tintah strandlines are storm beaches emplaced during a regressing shoreline. This conclusion is based on overall poor stratification and poorly-sorted sediments recovered by coring the strandlines, in addition to the small size, discontinuous nature, and multiplicity of beach ridges which formed over only a few centuries (McMillan & Teller, 2012). These conclusions may prove relevant for the Minong strandlines, which are similarly abundant, small, and discontinuous. They also would have formed under the same cold-climate conditions as the Agassiz strandlines. Under cold climate conditions, fair-weather waves occur during a limited portion of the year, and their cumulative energy is spread over a much longer period than the duration of one storm event (Taylor & McCann, 1983). Thus, cold-climate conditions are more likely to promote storm beaches.

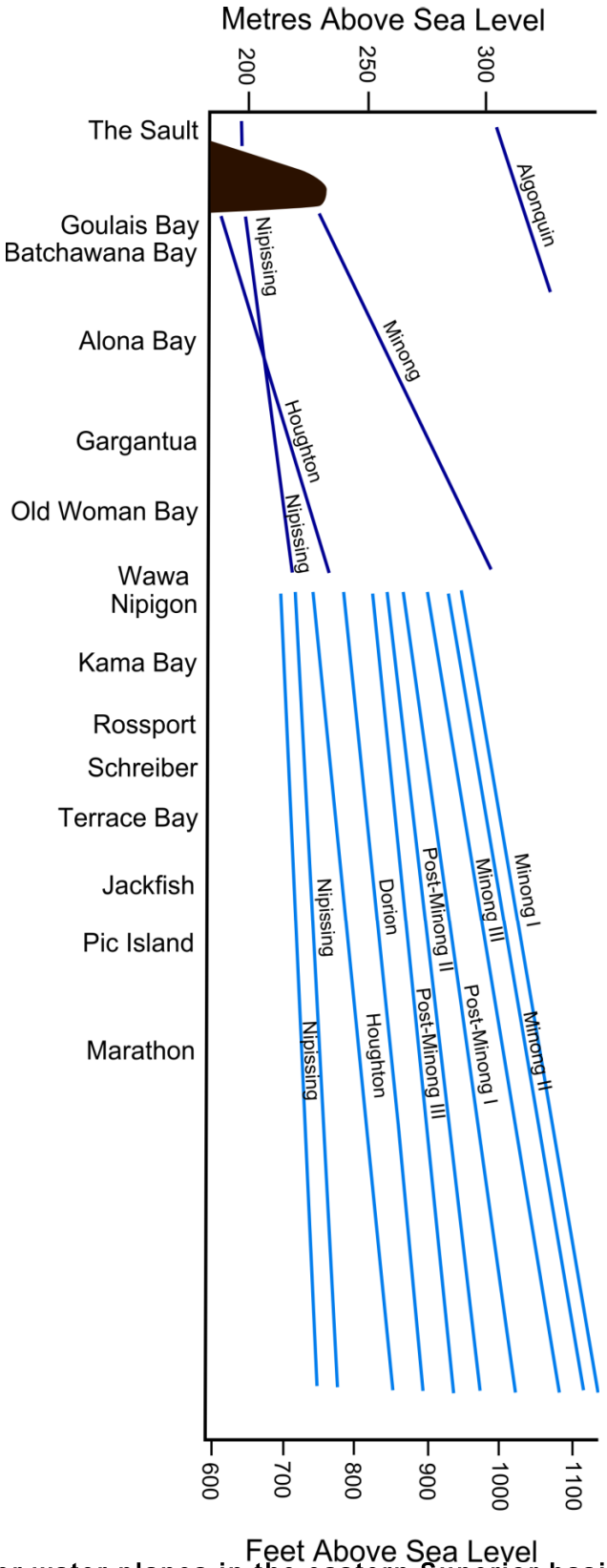

Figure 2.10. Former water planes in the eastern Superior basin (The Sault to Wawa), and in the western and northern Superior basin (Nipigon to Marathon). After Farrand & Drexler (1985) and Slattery et al. (2007)

2.6 Summary of Deglaciation and Lake History in the Superior basin

In northwestern Ontario, the history of deglaciation and lake levels was largely established by the work of Zoltai (1966), Burwasser (1977), and Farrand and Drexler (1985). As the LIS retreated from the Superior basin, a sequence of proglacial lakes formed in the southwest arm while a separate lake formed in the southeastern portion of the basin (Farrand & Drexler, 1985; Phillips & Fralick, 1994b). After the Marquette re-advance, which isolated glacial Lake Agassiz from the Superior basin, the two lakes merged to become proglacial Lake Minong. Dating from ~10,500 to 9,000 cal BP, the Minong phase coincides with episodic catastrophic discharge from glacial Lake Agassiz (Lewis & Anderson, 1989) that caused the numerous lake level fluctuations indicated by eight identified Minong strandlines (Slattery et al., 2007). This complex phase, when Lake Agassiz discharged through a system of eastern outlets and into the Great lakes (Leverington & Teller, 2003), is one of the highest levels recorded in the history of the Superior basin (Booth et al., 2002).

Strandlines indicate that the high lake levels in the Superior basin during the Minong phase experienced fluctuations as outlets from Lake Agassiz were opened to glacial Lake Nipigon (Leverington & Teller, 2003). However, determining an accurate chronology for the Minong phase in the Superior basin is complicated by differential isostatic rebound, the complexity of glacial Lake Agassiz, and a scarcity of organic material suitable for radiocarbon dating.

Following the Minong phase, there was a significant recession in the Superior basin to the Houghton level ~9,000 ^{14}C yrs BP when the morainal sill at Nadoway point was eroded (Booth et al., 2002). Subsequent transgressions occurred as northern outlets isostatically rebounded in the Superior basin causing the Nipissing transgression that culminated ~4,500 ^{14}C yrs BP, when the Great Lakes were in confluence, at their highest elevation of ~195m (Lewis & Anderson, 1989; Booth et al., 2002). Lake Superior separated from Lake Huron-Michigan ~2,000 ^{14}C yrs BP following isostatic rebound of the Sault Ste. Marie threshold (Farrand & Drexler, 1985).

3. CULTURE HISTORY OF NORTHWESTERN ONTARIO AND THE SURROUNDING AREAS

This chapter provides a review of the archaeological record in the Great Lakes region for the period between 10,500 and 10,000 cal BP, during the Plano complex. The earliest widely recognized theory of occupation of the Americas began ~11,500 cal BP with the Clovis culture during the early Paleoindian tradition (Waters and Stafford, 2007). Although subsequent early Paleoindian cultures occupied the southern Superior shore, deglaciation was later in northwestern Ontario than the rest of the Great Lakes region, and the first evidence of occupants reaching the northern Superior shore date to the late Paleoindian tradition (Phillips, 1993). The strong relationship between Plano groups and beach ridge occupation is explored for site bias and differential visibility.

3.1 Paleoindian Tradition

The Paleoindian tradition encompasses a variety of separate cultural complexes which are represented by sites throughout North America (Fig. 3.1 and Table 3.1). Early Paleoindian sites discovered in Alaska contain microlithics associated with the Paleoarctic tradition (Reanier, 1995; Dixon, 2001), while fluted points in South America are distinctively different from those in North America and not considered a culture of the Paleoindian tradition (having indented stems, flaring bases, and broad shoulders referred to as “fishtail”, proposed to have evolved from North American fluted points) (Morrow & Morrow, 1999).

Determining the chronological sequence of the Paleoindian tradition required considerable work and the involvement of geoscientists to provide archaeologists with basic stratigraphic principles used in dating. Until geoarchaeological work at the Clovis site on the southern High Plains identified intact stratigraphy proving that Folsom is younger than Clovis, the temporal

relationship of these and other cultures was poorly understood (Holliday, 2000). The advent of radiocarbon dating used in conjunction with stratigraphy further clarified the Paleoindian tradition: Early Paleoindian encompasses the fluted point tradition of Clovis and Folsom, and is succeeded by Late Paleoindian or Plano unfluted points (Holliday, 2000). Fluted points are lanceolate points with concave bases and a longitudinal groove or flute produced by the removal of one flake from the base (Mason, 1997). Clovis points are commonly fluted on only one face, and the scar rarely exceeds a third to half the length of the point while Folsom points typically have longer flutes on both faces (Mason, 1997). Although fluting was extremely common in the early Paleoindian time period, it likely did not improve the point and this final step in point production was eventually abandoned marking the beginning of the Plano period (Mason, 1997).

Figure 3.1. Selected sites representing the Paleoindian tradition. See Table 1 for references.

Table 3.1. Selected sites shown in Figure 3.2, and associated references.

Site Number	Site Name	Reference(s)
0	Horner	Frison & Todd, 1987; Jepson, 1953
1	Hanson	Frison & Bradley, 1980
2	Agate Basin (including Sheaman and Brewster)	Agogino, 1972; Agogino & Frankfortner, 1960; Frison & Stanford, 1982
3	Hell Gap	Irwin-Williams et al., 1973; Rapson & Niven, 2007
4	Scottsbluff	Barbour & Schultz, 1932; Schulz & Eiseley, 1935
5	Medicine Creek	Bamforth, 2002; Hudson, 2007
6	Lindenmeier	Haynes & Agogino, 1960; Wilmsen & Roberts, 1978
7	Olsen-Chubbock	Wheat, 1972
8	Sutter	Katz, 1971, 1973
9	Folsom	Cook, 1972, 1928; Figgins, 1927; Meltzer et al., 2002
10	Clovis	Haynes, 1975, 1995; Haynes & Agogino, 1966; Hester, 1972
11	Plainview	Holliday, 1997; Sellards et al., 1947
12	Lipscomb	Hofman, 1995; Schulz, 1943
13	Lubbock Lake	Green, 1962; Johnson, 1987; Sellards, 1952
14	Midland	Holliday & Meltzer, 1996; Wendorf & Krieger, 1959; Wendorf et al., 1955
15	Debert	MacDonald, 1966, 1968
16	Bull Brook	Byers, 1954, 1955, 1959
17	Crowfield	Deller, 1988; Deller & Ellis, 1984; Ellis, 1984
18	Parkhill	Deller, 1980; Ellis, 1979; Roosa, 1977; Roosa & Deller, 1982
19	Fisher	Storck, 1983
20	Hi-Lo	Fitting, 1963
21	Schaefer and Hebior	Hall, 1985
22	Holcombe	Fitting et al., 1966; DeVisscher et al., 1969
23	Hiscock	Laub, 1994; Laub et al., 1988
24	Paleo Crossing	Brose, 1994
25	Cummins	Dawson, 1983a; Julig, 1984, Julig et al., 1990
26	Mackenzie 1	Unpublished
27	Assiniboine Delta Sites	Boyd, 2007a
28	Flintstone Hill	Boyd, 2003
29	Sheguiandah	Julig, 2002
30	Spein Mountain	Ackerman, 1996a, 1996b
31	Mesa	Kunz & Reanier, 1996
32	Charlie Lake Cave	Driver, 1996
33	Vermilion Lakes	Driver, 1982; Fedje et al., 1995
34	Barton Gulch	Davis et al., 1988, 1989
35	Indian Creek	Davis & Greiser, 1992
36	Sibbald Creek	Gryba, 1983

3.2 The Clovis and Folsom Complexes (11,000 -10,500 cal BP)

Clovis and Folsom points occur primarily in the southwestern United States, on the Great Plains, in the Rocky Mountain foothills (Mason, 1981), and rarely in the Great Lakes region. A potential Clovis point is reported from Hurley in Northern Wisconsin (Mulholland et al., 1997), though other less controversial Clovis points have been recovered as lithic scatters in Wisconsin (Stoltman, 1998), and a broken point was discovered from a submerged area on Island Lake Reservoir north of Duluth, Minnesota (Mulholland et al., 1997). In addition, a modest Clovis assemblage was identified at the Anderson site in Illinois interpreted to be a hunting camp; however, the abstract indicates there is a possibility it is a Gainey site (Koldehoff et al., 1999). Folsom points have also been discovered in the Great Lakes region from Round Lake north of St. Cloud, Minnesota (Mulholland et al., 1997), from the Assiniboine Delta region (Boyd, 2007a) and at the Mile Long site in southern Wisconsin (Stoltman, 1998).

The early Paleoindian Anderson site is located in northeastern Illinois on the western edge of the Michigan basin (Koldehoff et al., 1999). While the site was occupied, the nearby floodplain supported a mixed growth of pine, fir, and tamarack while the uplands supported a more open, spruce-dominated parkland (Koldehoff et al., 1999). Inhabitants of the site would have been able to take advantage of both upland and riparian habitats, and since the site is located on a terrace, occupants could have easily monitored and intercepted game (Koldehoff et al., 1999).

Potts, another early Paleoindian site located in Oswego County, New York, was also strategically placed for overlooking the region and procuring game (Gramly & Lathrop, 1984). The encampment occupies a 150 metre-long section along the highest point of a drumlin (Gramly & Lathrop, 1984). Gramly and Lathrop (1984) interpret the landscape west of the inhabited drumlin as a plausible transportation corridor with a gully directly west of the Potts site and easily seen from it. It is possible that as game was migrating through the region, the gully would have acted as a natural barrier, slowing animals down enough for them to be easier prey for early Paleoindian hunters (Gramly & Lathrop, 1984).

In some areas of the Great Lakes region such as Michigan and southern Ontario, Clovis and Folsom complexes have not been recognized; instead Gainey points are generally accepted as the earliest evidence of occupation. Gainey points represent one of three early Paleoindian fluted complexes, which are likely different groups of closely related bands identified in southwestern Ontario. These are (oldest to youngest) Gainey, Parkhill, and Crowfield (Storck, 1984; Deller & Ellis, 1988). The Gainey phase is characterized by a number of technological attributes including the Gainey point (Jackson, 1996), which are partly fluted and occur in Michigan and probably Ontario (Roosa & Deller, 1982). They have a variant of Folsom type fluting (Roosa & Deller, 1982), and the Gainey phase is suspected of being immediately post-Clovis in age (roughly contemporaneous with Folsom) (Stoltman, 1998). The Parkhill complex has been defined based on material from the Barnes site in central Michigan, Parkhill in southwestern Ontario, the Leavitt site in southern Michigan, Fisher in the southern Georgian Bay region, and the Thedford II and McLeod sites in southwestern Ontario (Storck, 1984). Barnes points, with a strong resemblance to the Folsom complex of the West and the Bull Brook and Debert complexes of the northeastern United States and southeastern Canada, are characteristic of the Parkhill complex (Roosa & Deller, 1982). The Crowfield site in southwestern Ontario was used to establish the major characteristics of the Crowfield complex. Although additional Crowfield points have been discovered in southcentral Ontario as well (Storck, 1984), the complex is represented mainly by isolated finds and possibly three small sites (Deller & Ellis, 1988).

Some reported sites in southwestern Ontario are large (covering hectares and yielding hundreds of tools), and are interpreted as communal hunting sites (Deller & Ellis, 1988). Data from the study area and surrounding regions suggest that these larger sites are associated with the Gainey and Parkhill complexes, becoming more northerly distributed through time until the Crowfield complex which is relatively less well represented (Deller & Ellis, 1988).

In the northern regions of the Great Lakes, glaciation delayed occupation of Paleoindian populations. The pattern of fluted point recoveries suggests that

early Paleoindian peoples occupied the southern Superior shore, but the later Plano culture was the first to inhabit the northern shore (Phillips, 1993). It is possible that early Paleoindian populations reached the northern Superior shore before the Marquette Readvance (11,500 cal [10,000 ^{14}C yrs] BP), but either the subsequent glaciation destroyed evidence of occupation this early (Phillips, 1993), or existing early Paleoindian sites have not yet been discovered in northern Ontario.

3.3 Plano complex (10,500-10,000 cal BP)

The Late Paleoindian period, also known as the Plano complex, is defined by the disappearance of fluting on lanceolate points and the emergence of stemmed projectile points (Mason, 1997). Plano is thought to represent the expansion of Paleoindian occupation northward into recently deglaciated lands (Mason, 1997). Three unfluted leaf-shaped points, specific to the Great Lakes area, that likely show morphological and temporal continuity with early Paleoindian types are Holcombe, Plainview and Hi-Lo (Roosa & Deller, 1982; Deller & Ellis, 1988; Jackson, 2004). Based on morphological similarities, Holcombe may be the immediate successor of the Crowfield culture (Deller & Ellis, 1988; Jackson, 2004), and is likely followed by Plainview (Jackson, 2004). Hi-Lo points have three variants (Hi-Ho, stemmed, and side-notched), are broadly distributed, and more commonly found in southern Ontario than Holcombe (Ellis, 2004; Jackson, 2004). It is suggested that the Hi-Lo and "classic" Hi-Lo stemmed points are late Paleoindian, while the side-notched variant likely dates to the early Archaic (Ellis, 2004).

The Hell Gap site in eastern Wyoming has provided assemblages of eight Paleoindian groups (in chronological order), including Plainview, Agate Basin, Hell Gap, Alberta, Cody (Eden-Scottsbluff), and Frederick (Irwin and Wormington, 1970). All are well represented on the Plains, though recoveries from the Great Lakes region are predominantly Plainview, Agate Basin, Hell Gap, Madina, and Cody points (Steinbring, 1967; Jackson, 2004).

In summation, seven known types of Plano points have been identified in southern Ontario, including the "southern groups": Holcombe and Hi-Lo (~10,000-9,500 ^{14}C yrs BP); "northern groups" distributed in southwestern and south-central Ontario: Agate Basin (~10,300-10,000 ^{14}C yrs BP), Hell Gap (10,000-9,500 ^{14}C yrs BP), and Madina (10,200-9,800 ^{14}C yrs BP); as well as Cody (~9,500 ^{14}C yrs BP), which appears to be an eastern type centred on the St. Lawrence River (Jackson, 2004). The earliest inhabitants of the Thunder Bay region appear to be Agate Basin and Hell Gap cultures (McLeod, 2000), and are two cultures represented by the Lakehead Complex discussed below (Fox, 1967).

The end of the late Paleoindian period occurs with the invention and diffusion of side-notched points (associated with the Archaic Tradition), a time transgressive event that occurred later in northern Ontario. The date above indicates that the Paleoindian-Archaic transition occurred ~10,000 ^{14}C yrs BP which is true in the Great Plains. It has been proposed that appearance of Archaic cultural remains occurred closer to ~7,000 ^{14}C yrs BP in the Thunder Bay region (Dawson, 1983b), although there are very few dates in the area to confirm this theory. Some researchers prefer to use a date range of 10,000 to 7,000 ^{14}C yrs BP as the time of gradual change from late Paleoindian to Archaic culture (e.g. Julig, 1994). However, without more accurate dates and considering the absence of site survey in much of northwestern Ontario, there is very little evidence to support this transition period. It is just as likely that additional excavation work and more precise dates will provide an accurate transition date from Paleoindian to Archaic cultures closer 10,000 ^{14}C yrs BP, which is the transitional date in the northeast and Plains (see Figure 3.1 in Julig, 1994)

3.4 Lakehead Complex

Lake level fluctuations in the Great Lakes produced numerous strandlines representing former proglacial lakes that occupied their basins (Larson and Schaetzl, 2001). Although rugged terrain and thick vegetation impede site survey, biasing the archaeological record to accessible locations such as modern

waterways (Mulholland et al., 1997), Paleoindian sites are commonly associated with these paleoshorelines (e.g. Deller, 1979; Dawson, 1983a ; Buchner & Pettipas, 1990; Jackson et al., 2000; Boyd et al., 2003; Boyd, 2007a). This relationship between Plano sites and former water planes is likely because beach ridges were high and well-drained ridges utilized as transportation corridors by Paleoindian groups as well as the caribou they hunted (Deller, 1979; Peers, 1985). Furthermore, open ridges would have been more appealing than the poorly-drained and more forested areas further inland (Hinshelwood, 2004). Strandlines preserved above the present Lake Superior water levels in the northern part of the basin dip below the water plane in the southern part of the basin due to differential isostatic rebound (Slattery et al., 2007). This has provided the Thunder Bay region with a series of raised strandlines that represent former water-planes in the Superior basin (Teller & Mahnic, 1988). The proglacial Minong phase in the Superior basin near Thunder Bay, Ontario dates to ~10,500-9,000 cal (9,500-8,000 ^{14}C yrs) BP (Farrand & Drexler, 1985), at an elevation of ~230m asl (47 m above the modern water plane) (see Boyd et al., 2012).

Abandoned shorelines of post-glacial Lake Minong and outcrops of Gunflint Formation taconite (chert) are associated with the Lakehead complex, which was first defined by Fox (1976). A critical defining characteristic of this complex is association with the middle to late stages of Lake Minong (Fox, 1976) although at the time it was proposed, none of the Lakehead complex sites had been directly dated. Fox (1976) speculated that sites associated with the Minong beach ridge were contemporaneous with it, although Plano groups could have utilized the strandline after water levels receded. There is evidence of Archaic reoccupations at Paleoindian sites in northwestern Ontario, interpreted to represent occupation along well-drained shorelines that would have been convenient for travel and habitation (Hinshelwood, 2004).

In summary, the Lakehead Complex as originally defined (Fox, 1976) includes sites with Plano points. A heavy reliance on Gunflint Formation cherts, and an association with the middle to late stages of Lake Minong are also

characteristic. Ross (1995) more recently proposed " The Interlakes Composite", which encompasses the Lakehead Complex as well as the Lake of the Woods/Rainy River, Quetico/Superior, and Reservoir Lakes complexes identified from the eastern Manitoba border and around the southern shore of Lake Superior. These complexes all show a general association with either Lake Minong or Lake Agassiz (discussed below) (Hinshelwood, 2004).

Recoveries from Lakehead Complex sites include projectile points that have been tentatively identified as Agate Basin, Angostura, Scottsbluff variants and Minocqua (MacNeish, 1952; Fox, 1975; Julig, 1984; Ross, 1995), although Ross (1995) suggests that typological associations are uncertain and many points should probably remain unclassified. This diversity may reflect intermittent occupation by a range of non-resident groups (Jackson, 2004).

3.4.1 Paleoindian Site Distribution in Northwestern Ontario

Lakehead Complex sites range in elevation from ~225m to 240m asl (Dawson, 1983), and are strongly associated with streams and rivers as well as a prominent Minong strandline (Fig. 3.2). Although Paleoindian sites are not always associated with Holocene Shorelines (Hamilton, 1996), there is strong evidence of site occupation at both Brohm and Cummins while their associated beaches were active (discussed below). This relationship has yet to be demonstrated at the other Plano sites. Initial investigations at Lakehead Complex sites led to suggestions of occupation during active beach formation (e.g. Fox, 1975), although some Archaic sites are also associated with the Minong shoreline (see Fig. 3.2). Presence of later (Archaic) sites on these same landforms indicates that beaches were also occupied well after the proglacial lake phase of the Superior basin (Hinshelwood, 2004).

3.5 Geoarchaeology of Paleoindian Sites

Numerous Plano sites have been identified near Thunder Bay (Fig. 3.2). However, few have been extensively excavated making accurate interpretations regarding contemporaneity with beach formation, and therefore dating of the sites problematic. In addition, the acidic nature of soils in the boreal forest inhibits preservation of organic remains, and commonly the only artifacts that remain from Paleoindian sites are lithics (Hinshelwood and Webber, 1987), which makes dating difficult (MacDonald, 1971). Clear separation of archaeological components is complicated by seasonal frost action, disturbances due to vegetation (root action and tree-throws), and faunal burrows (Dawson, 1983a). For these reasons, it is common for hundreds of years of human activity to be compacted into a depth of only a few centimetres at archaeological sites in the boreal forest (Dawson, 1983b). This combination of factors coupled with a general lack of geoarchaeological work at most Plano sites, has resulted in a poor understanding of depositional context at most archaeological sites in the Thunder Bay region. Biloski and Simmonds are two such Plano sites with a representative sample of artifacts but very little context within which to place them. In addition, post-depositional processes were not examined at either site, making it extremely difficult to interpret artifact recoveries. I will introduce these sites, and discuss the geoarchaeology of the Brohm site. Lastly, I will review two more extensively studied sites (Cummins and Sheguiandah), to highlight the more thorough interpretations that can be made when geoarchaeological investigations are conducted.

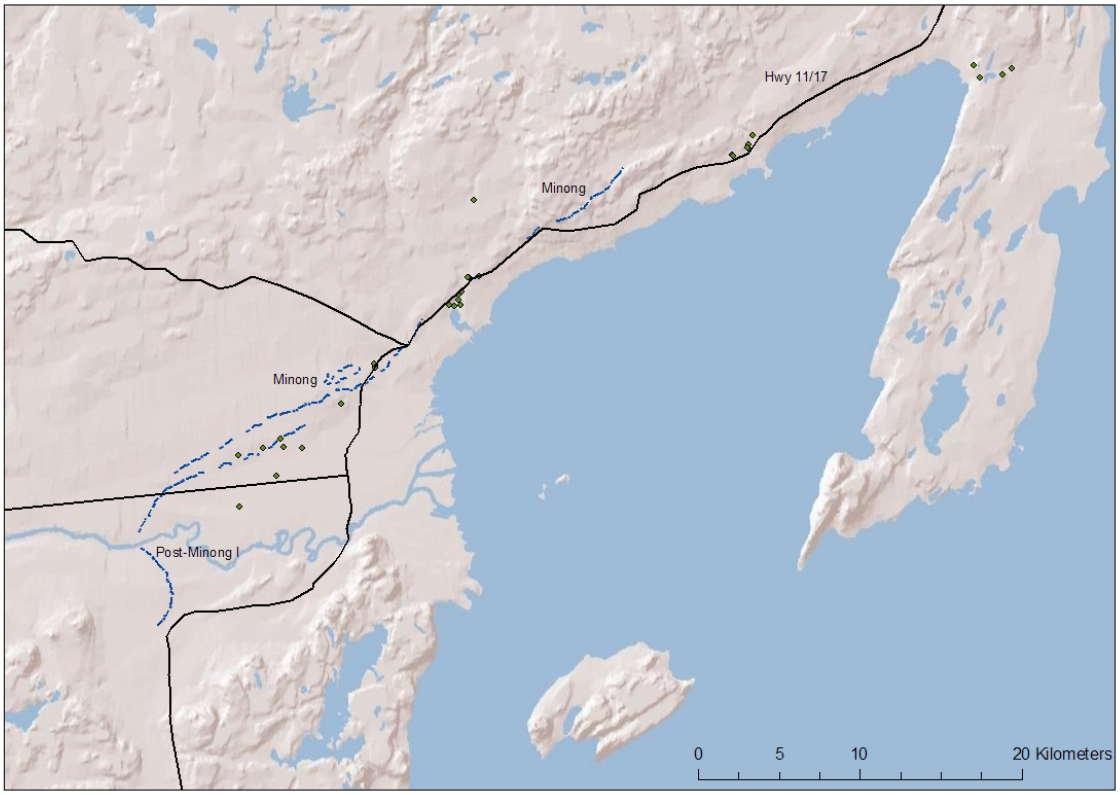

Figure 3.2. Distribution of Plano sites in the Thunder Bay region relative to the main Minong shoreline as well as the Post-Minong shoreline. After Burwasser (1977) and Steinbring (1976).

3.5.1 Biloski (DcJh-9)

Located on a sandy point along a Minong strandline, the Biloski site was bounded by water on three sides adjacent to a spruce-pine forest when it was occupied (Hinshelwood & Webber, 1987). Originally considered a small occupation with little interpretable data to contribute, recoveries during the 1895 and 1986 field seasons were fairly dense over much of the main beach terrace (Hinshelwood & Webber, 1987).

Hinshelwood and Webber (1987) suggest that a strong association between geomorphological features and the cultural components indicates that the Minong beach was inhabited while it was active (Hinshelwood & Webber, 1987). Biloski is one of the many sites considered to be contemporaneous with its associated strandline even though there is no evidence to support the claim. Without more accurate dates constraining the Paleoindian occupation of

northwestern Ontario, Paleoindian sites could have been utilized as recently as 7,000 ^{14}C yrs BP (e.g. Julig, 1994).

3.5.2 Simmonds (DeJh-4)

The Simmonds site is situated along the Current River within Thunder Bay, below a prominent bedrock bluff (Halverson, 1992). Geomorphic features associated with the site include a post-Minong series of bars through which a river truncated and downcut (Halverson, 1992). Examination of landscape features indicates that there was a river-mouth adjacent to Simmonds (Halverson, 1992), although no stratigraphic work has been done to infer whether site habitation coincides with an active river.

3.5.3 Brohm (DdJe-1)

Initially excavated in 1950 (MacNeish, 1952), Brohm is located west of Pass Lake near Thunder Bay, Ontario (Hinshelwood, 1990). Pass Lake is interpreted as a former embayment of Lake Minong, connected to it on the West side of Pass Lake by a channel. However, longshore drift caused deposition of a baymouth bar that eventually separated Pass Lake from Lake Minong. Brohm is adjacent to this bar, and artifacts were recovered within the upper 23 cm of beach gravel, providing evidence that the Brohm site was occupied during active beach formation (MacNeish, 1952). This provides evidence that Brohm was occupied during active beach formation.

3.5.4 Cummins (DcJi-1)

The Cummins site is probably the best-known Lakehead Complex sites because it was carefully excavated and subject to extensive analysis. Both a quarry and campsite are represented at this site, which is situated on a Lake Minong beach (Dawson, 1983; Julig, 1984). Much of the site is poorly drained due to bedrock near the surface, lacustrine clays in surface sediments, and generally low relief (Julig et al., 1990). Beach ridges adjacent to the Gunflint

Formation (taconite source) were well drained during occupation, providing a good campsite location among the generally poorly drained environment (Julig, 1984). A tributary of the Neebing River cuts through the beach ridges in the middle of the site, part of this drainage system is Cummins Pond, which formed in a depression of the bedrock (Julig, 1990). Cummins Pond was likely a lagoon or embayment of Lake Minong (Julig, 1990). Dune formation beginning ~8,000 ^{14}C yrs BP overlies some of the site and adjacent area, ranging in depth up to 2m (Julig, 1984; Julig et al., 1990).

Cultural features discovered during excavation include hearths, fire pit features, and a possible hearth pit for heating taconite prior to flaking (Dawson, 1983). Disturbed remnants of a cremation burial were recovered from Cummins, representing one of the earliest recorded burial in Ontario dating to 8,480 ± 390 ^{14}C yrs BP (Dawson, 1983). However, according to Wright (1963), the remains were recovered from the exposed face of a gravel pit, and appeared to be heavily disturbed (Julig, 1994). This date must therefore be utlilized with some caution.

Parts of the site are culturally stratified; an Archaic horizon is present below the humus layer, which is underlain by Plano artifacts (Julig et al., 1990). Below is a water-reworked geological lag gravel containing water-worn artifacts, indicating contemporaneity with an active post-Minong beach ~9,500 ^{14}C yrs BP or slightly earlier (Julig, 1984; Julig et al., 1990). Part of the site is on a lower Minong terrace, where there is no evidence of cultural stratigraphy and lithics are distributed throughout the upper 40 cm of homogenized fine sandy soil (Julig, 1994).

Areas of Cummins have been designated the dozer trench section (DT), west test trench section (WTT), and Lower Minong (LM) (Fig. 3.3) (Dawson, 1983). The DT section contains poorly-sorted beach sands, gravels, and lag deposits (Julig, 1994). The deep water-worn artifacts indicate a fairly high energy environment with subsequent Minong beach deposits overlying them (Julig, 1994). At the WTT section, dunes topographically enhance the existing beach ridge likely formed in the nearshore zone (Julig, 1994). Below is an abrupt contact with coarse cobble gravel containing occasional small boulders,

interpreted to possibly represent storm or flood gravel (Julig, 1994). Lower Minong is interpreted to be a beach bar that mimics the shape of the main Minong beach (Julig, 1994), thought to have formed offshore as water levels declined (Phillips, 1982, cited in Julig, 1994). However, this "bar" could be a beach deposit that formed as Lake Minong was transgressing, and was subsequently drowned without significant erosion (cf. Reading and Collinson, 1996).

After the site was occupied, Cummins was subjected to lacustrine processes, aeolian deposition and deflation, frost action, root growth and tree throws, and burrowing by small mammals (Julig et al., 1990). In addition, artifacts and other objects had been thrown into a bog at the site, likely affecting artifact and assemblage context (Julig et al., 1990). At two locations of the site, the original lower surface was completely reworked by wave action, though in other parts of the site the lower artifact assemblage was only partly modified wave action and artifacts ranged from essentially undamaged to battered (Julig et al., 1990). Wind action also affected part of the site, lightly polishing artifacts during brief surface exposure (Julig et al., 1990).

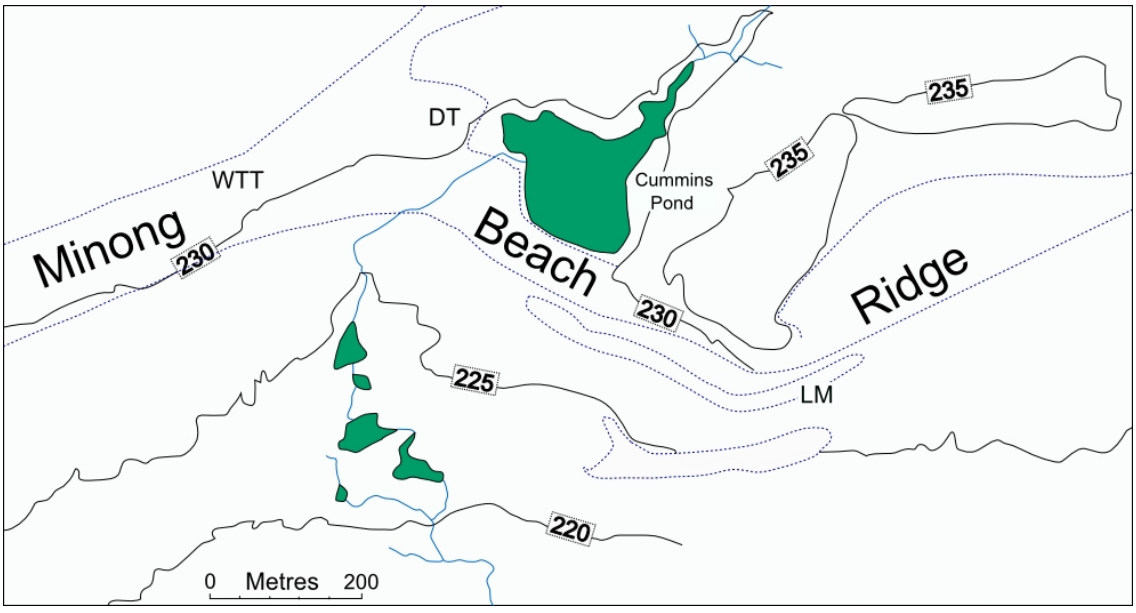

Figure 3.3. Cummins site map showing dozer trench section (DT), west test trench (WTT), and lower Minong (LM) in relation to the main Minong beach ridge and Cummins Pond. After Julig et al. (1990).

3.5.5 The Sheguiandah Site (BeHl-2)

Initial excavations of the Sheguiandah site located on Manitoulin Island, Ontario, began in the 1950s leading to claims that very early cultural material found at the base of the site was among “till-like” deposits indicating a pre-Clovis occupation, though work was never completed and the site remained enigmatic and controversial (Julig & Storck, 2002). More recent investigations were pursued to complete a re-analysis of selected artifacts and soil/sediment samples obtained during previous work, and to re-excavate and re-sample selected squares/trenches opened in the early 1950s (Julig & Storck, 2002).

Sheguiandhah is a rare stratified site (Julig & Storck, 2002). Long-term multiple occupations and archaeological deposits extend from the modern water level of Sheguiandah Bay (Lake Huron) to the tip of a hill; Middle Woodland artifacts were recovered at the Algoma water level, Archaic occupation was below the Nipissing beach level, and Paleoindian and later occupations are both stratified and mixed at the Korah level of Lake Agonquin (Julig & Storck, 2002).

Lee (1957) reported at least five occupation levels within the habitation area of the site: Level 1) Middle Woodland artifacts at or near the surface to ~10 cm; Level 2) extending to ~12 cm containing bifaces; Level 3) containing projectile points until ~17cm; Level 4) representing the upper half of the “till” unit containing small to a depth of ~60 cm, large thin bifaces were recovered; Level 5, the lower half of the “till” containing thicker bifaces; and deeper unnumbered levels below the “till” consisting of water-sorted sands and a lower-lying boulder pavement which contained scattered flakes and other “battered objects” (Lee, 1957). More recent excavations identified a somewhat different artifact distribution (Julig & Mahaney, 2002). Instead, artifacts were found to be concentrated in the upper 10 cm and above the “till”, with very little artifact recovery from Lee’s (1957) Levels 3 and 4 (Julig & Mahaney, 2002). Although a more extensive excavation is required to confirm Lee’s stratigraphic artifact distribution, it is likely that post-depositional disturbance and mixing has affected the lower levels of site stratigraphy (Julig & Mahaney, 2002). More specifically, the few recoveries from Lee’s (1957) “till” may have been mixed in after

deposition. Water level fluctuations possibly reworked artifacts from initial occupations, while frost heave and tree throws displaced artifacts from subsequent occupations (Julig & Mahaney, 2002). Although Lee's observations were generally quite accurate, the deposit identified as "till" is likely not glacial, but the result of non-glacial geomorphic processes considerably modified by pedogenesis (Julig & Mahaney, 2002). Mostly likely these sediments are highly oxidized and weathered nearshore or beach deposits of Lake Algonquin's Korah phase (Barnett, 2002). Distribution of artifacts throughout these shoreline deposits suggests contemporaneity of Paleoindian occupation with Korah phase water levels (Barnett, 2002).

Geoarchaeological studies are necessary to establish detailed context for archaeological assemblages, especially for sites that have been subject to complex geomorphic processes during human occupation (Julig & Mahaney, 2002). Sheguiandah is a good example, since the initial controversy surrounding interpretation of the site centred on the geomorphology of the deposits (Julig & Mahaney, 2002). Interpretations at Biloski, Simmonds and Brohm are severely hindered by a lack of sufficient geologic context. In addition, since dating archaeological sites can be difficult when no carbon or faunal remains are recovered (especially in the boreal forest), evidence of direct association with a dateable feature can be useful. Successfully demonstrating contemporaneity of a site with dateable features like strandlines must involve geoarchaeological investigations.

3.6 Paleoindian Site Distribution in the Rest of the Great Lakes

Outside of the Thunder Bay region, additional Plano sites are commonly associated with ancestral lake levels in the Huron, Erie, and Michigan basins, as well as glacial Lakes Hind and Agassiz (Fig. 3.4). This section provides a brief summary of the identified Plano sites and lithic scatters associated with proglacial lake margins. When possible, specific details regarding land use and subsistence is discussed.

3.6.1 Glacial Lake Hind

Glacial Lake Hind was one of several interconnected proglacial lakes that formed on the Canadian prairies during the period of final deglaciation (Boyd et al., 2003). Regression of glacial Lake Hind to the northern part of the basin is roughly contemporaneous with the Folsom complex (10,800-10,000 ^{14}C yrs BP) (Boyd et al., 2003). Glacial Lake Agassiz also experienced a water level drop between ~10,800-10,000 ^{14}C yrs BP, during the Moorhead phase (Boyd, 2007b), likely representing the lake elevation associated with a single Folsom point found deep in the Agassiz basin (Buchner & Pettipas, 1990). It is possible that hunters took advantage of isolated wetlands that attracted bison, using recently drained proglacial lakes (wet clay beds) to mire them (Buchner & Pettipas, 1990; Boyd et al., 2003), although this is speculation (Frison, 1998). In the early Paleoindian period, uplands surrounding the Hind basin were covered by a spruce-poplar woodland with juniper, *Artemisia*, and grass-dominated clearings while recently drained proglacial lake surfaces were quickly colonized by herbaceous wetland plant taxa (Boyd et al., 2003). Uneven spatial distribution of resources and low environmental productivity in the Lake Hind basin may have only supported very small populations of highly mobile hunter-gatherers accounting for the relative paucity of early Paleoindian materials across southern Manitoba (Boyd et al., 2003).

The Great Lakes all experienced significant low levels, although due to differential isostatic rebound these low stands are represented above the present level of Lake Superior along the northern side of the basin, and below current levels in the Huron, Erie, Ontario, Michigan, basins (Larson & Schaetzl, 2001; Slattery et al., 2007). It is likely that Paleoindian sites located along strandlines of these low lake levels are now underwater, were destroyed by fluctuating lake levels, and that some former river mouth or delta sites are now deeply buried by shifting sedimentation (e.g. Jackson, 2004).

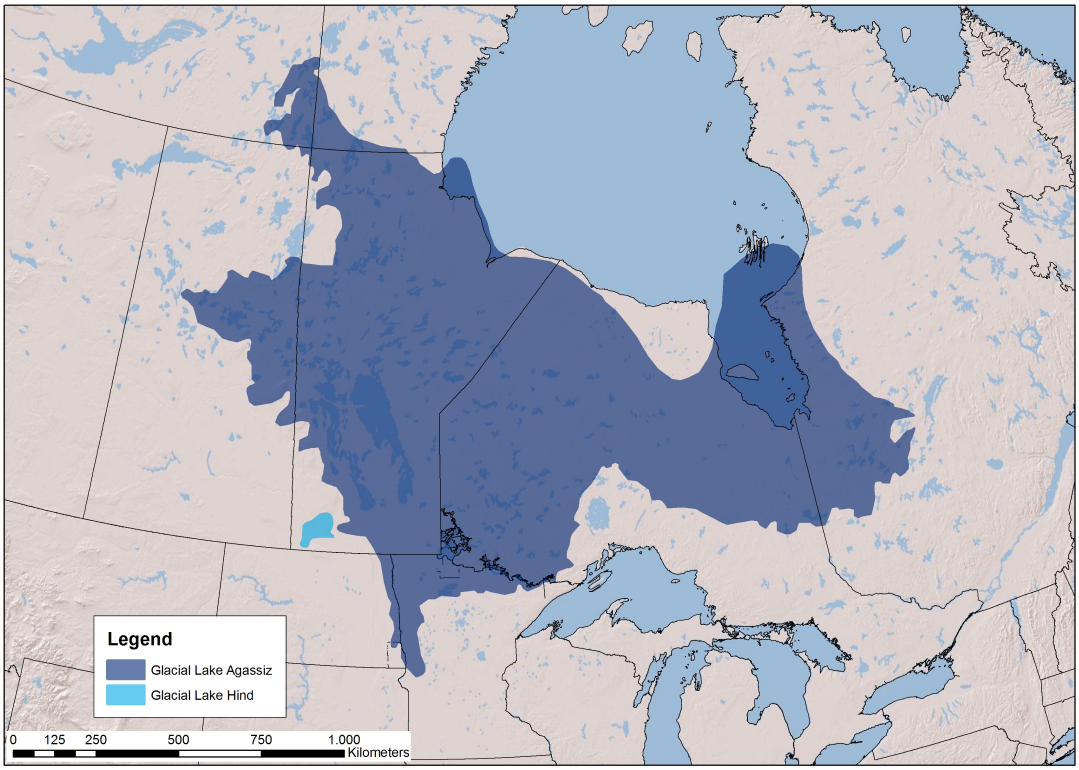

Figure 3.4. Glacial Lake Hind at its greatest extent, and the total area that Glacial Lake Agassiz occupied over its 5,000 calendar-year history. After Sun and Teller (1997) and Leverington and Teller (2003).

3.6.2 Glacial Lake Agassiz

Following the low lake level associated with the Moorhead phase, glacial Lake Agassiz rose to the Campbell level during the early Emerson phase ~10,000 ^{14}C yrs BP (Bjorck & Keister, 1983; Bajc et al, 2000; Fisher, 2003; Boyd, 2007b). The Assiniboine Delta is the largest of several late Pleistocene meltwater deltas in the Agassiz basin (2007b). At least 28 Paleoindian sites have been recorded on the delta and in the immediate vicinity, most of which are Plano and located well behind (i.e., above) the Campbell beach and other major strandlines (Boyd, 2007a). Within the Rainy River district of northwestern Ontario, four Plano sites were identified and an additional several were non-diagnostic (Haywood, 1989). Two of the Plano sites and three of the non-diagnostic sites are located on the Campbell level, while the other two Paleoindian and two non-diagnostic sites are below the Campbell strandline

(Haywood, 1989). While most Paleoindian sites are located near the former margins of glacial Lake Agassiz, the distribution of early projectile points on the Assiniboine Delta suggests that these sites tend to be located >5km behind late-glacial beaches rather than on the beaches themselves (Boyd, 2007a). A possibility for this distribution is that wetland areas inland from lake margins were more productive and perhaps better locations for occupation (Boyd, 2007a).

3.6.3 The Huron Basin

Lake level fluctuations also occurred in the Huron basin, leaving two prominent ridges representing the Warren and Algonquin strandlines (Deller, 1979; Ellis & Deller, 1986; Jackson et al., 2000). More specifically, glacial Lake Whittlesey formed at ~13,000 ^{14}C yrs BP in the Erie basin, and later coalesced with glacial Lake Saginaw in the Huron basin to form glacial Lake Warren by ~12,000 ^{14}C yrs BP (Larson & Schaetzl, 2001). According to the traditional view, lake levels in the Huron basin regressed to the Algonquin level at ~11,000 ^{14}C yrs BP with subsequent additional water level drop before transgressing up to the Nipissing level between ~5,000 and 4,500 ^{14}C yrs BP (Deller, 1979; Ellis & Deller, 1986; Jackson et al., 2000). This chronology is complicated by an opposing argument that the Main Algonquin level is much lower, and that early Paleoindian sites are actually on an upper Ardtrea strandline (for discussion on this topic, see Morgan et al., 2000; Jackson et al., 2000; Jackson, 2004). In addition, the Nipissing level is roughly at the same elevation as the Algonquin strandline, and during its beach formation sediments from the Algonquin level were effectively removed and reworked (Ellis & Deller, 1986). The relevance of understanding this chronology lies in the archaeological discoveries associated with these beach ridges; both the Warren and Algonquin strandlines have associated sites encompassing both the early and late Paleoindian time periods, discussed further below (Deller, 1979). The Barnes site is located on the Warren strandline while sites associated with the Algonquin level include Zander, Holcombe, Banting, Zander, Udora, as well as the larger Parkhill and Fisher sites (Deller, 1976; Stewart, 1984; Deller & Ellis, 1988).

The Parkhill site is said to correlate roughly with the last manifestation of Lake Algonquin, and has been dated to 10,500 ^{14}C yrs BP on the basis of overall similarities to the Folsom and Debert complexes (Roosa, 1977; Roosa & Deller, 1982). This date is extremely speculative given that a site located on a strandline does not indicate occupation at the time the beach was active, and there is no explanation for the conclusion that occupation and lake level are contemporaneous in the literature. This site however, has become the type site for the Parkhill complex (Roosa & Deller, 1982), which is represented at the Fisher site (Storck, 1983).

Extensive archaeological surveys were conducted around Holland Marsh, an embayment of Main Algonquin (Ardtrea) that evolved into a fen or marsh during the early Holocene (Stewart, 2004). Erosion and sedimentation along drainage channels may have affected site visibility, for example sites in small drainages that experienced floods or dry periods may have been removed or buried (Stewart, 2004). Seven of the 41 discovered sites contained diagnostic Paleoindian artifacts (Stewart, 2004). Occupation during the Paleoindian period focused on the southeast side of the marsh, where several channels that may have been part of a braided channel system emptied into the embayment of the glacial lake shoreline (Stewart, 2004). Other sites are located in the marsh, possibly used during periods of low water, however these were not examined in the recent surveys (Stewart, 2004). Likely, early Paleoindian groups camped on an open water embayment, while occupants in the late Paleoindian period utilized the recently abandoned strandline overlooking an emergent marsh (Stewart, 2004). Multi-component sites suggesting continuous use indicate that during the Paleoindian period, shorelines closer to the embayment head were preferred (Stewart, 2004). If migratory caribou were being pursued along the Algonquin (Ardtrea) shoreline, during the spring they would not have been able to cross the embayment due to ice and likely had to traverse the ridge and pass the concentration of sites on the southeast side of the marsh (Stewart, 2004). In contrast, the Fowler site is located at the end of a peninsula between two marsh basins and likely represents a summer or fall camp location that would have

allowed hunters to intercept swimming or landing caribou (Stewart, 2004). A higher concentration of sites at embayment heads, then, may suggest a bias towards spring oppucation that may be due to higher densities of people or activities in the spring, and move visible remains associated with spring camps (Stewart, 2004). Temporal changes in the discussed shoreline features can be explained by forest growth and the demise of migratory caribou, when a broader range of resources may have been exploited as reflected in the scattered early Archaic site distribution (Stewart, 2004).

3.6.4 The Erie Basin

In the Erie basin, glacial Lake Maumee developed ~14,000 ^{14}C yrs BP, then as mentioned previously, glacial Lake Whittlesey formed ~13,000 ^{14}C yrs BP and later transgressed to the Warren strandline while in confluence with glacial Lake Saginaw (Larson & Schaetzl, 2001). Drainage of glacial Lake Warren established glacial Lake Lundy in the Erie basin (Larson & Schaetzl, 2001). Archaeological sites have been identified on each of glacial lakes Maumee, Whittlesey, and Lundy; Caradoc site is located on the Whittlesey beach ridge, and Lux on the Lundy strandline (Deller, 1976). The Caradoc site provides evidence of ritual behaviour associated with unfluted lanceolate point assemblages consisting solely of purposefully broken artifacts (Deller & Ellis, 2001). Caradoc is situated on the remnant of a delta formed when lake levels were at Whittlesey (Deller & Ellis, 2001). Other sites associated with these strandlines between the Huron and Erie basins include Gainey phase sites: Murphy, Haunted ill, Culloden Acres, Weed, Snary (Jackson, 1996), and Bondi (Morris et al., 1993).

3.7 Land Use and Subsistence

A common theme in site interpretation at sites throughout the Great Lakes region is suitability of location for procurement of caribou. Although there is little direct evidence of Paleoindians exploiting caribou, examination of indirect

evidence such as vegetation and migration patterns indicates that caribou was a likely prey (Peers, 1985). Barren-ground caribou range over both tundra and northern boreal forest, in regions with cold winters and moderately warm summers (Peers, 1985). They tend to migrate along ridges from which they can watch for predators and take advantage of wind to keep insects at bay, as well as the rich vegetation offered by strandlines in summer months (Peers, 1985). During the winter, lichens are often sought on windswept ridgetops where snow cover is thickest, and a part of each day is generally spent on frozen lakes (Peers, 1985). Thus, vegetation along beach ridges in summer and winter months make them attractive transportation routes to caribou. Since a human group cannot keep pace with a migrating caribou herd, caribou hunters likely learned to intercept the animals at specific points along their migratory route (Peers, 1985). Nearly all of the sites along the Algonquin shoreline are situated near crossing barriers providing a natural trap that hunters likely took advantage of (Deller, 1979).

As mentioned above, glacial Lake Warren formed by ~12,000 ^{14}C yrs BP (Larson and Schaetzl, 2001), and is associated with both early and late Paleoindian sites (Deller, 1979). Since the Warren level pre-dates human occupation, presence of sites on this feature proves that Paleoindian groups were utilizing relict beach ridges, although numerous researchers in the past have claimed sites to be contemporaneous with their associated strandline despite absence of supporting evidence (e.g. Fox, 1975; Roosa & Deller, 1982). Presence of sites on raised fossil beaches and moraines likely reflects the attractiveness of high and dry ground suitable for camping. Such features likely provided transportation corridors for game such as caribou, and were also used as lookouts by hunters. If herds of caribou were migrating along the shores of Lake Minong, many sites including Brohm, Newton, Simmonds, and Boulevard are strategically located for procurement (Fox, 1976). Most campsites in the Thunder Bay region are located at the mouths of rivers and creeks that emptied into the former Norwester Bay, likely providing fish for consumption (Fox, 1976).

Proglacial lakes, however, may not have been very productive for adequate fishing. Sediments deposited in glacial Lake Agassiz commonly contain few (or no) fossils, likely the result of high sedimentation rates and associated turbidity placing limitations on the ability of phytoplankton and macrophytes to thrive (Boyd, 2007a). However, isolated wetlands on the fringe of Lake Agassiz are often associated with comparatively rich plant and invertebrate macrofossil assemblages (Boyd et al., 2003; Boyd, 2007a). This is a strong indication that although there are sites directly associated with beach ridges, it is highly likely that the productive fringes adjacent to Agassiz and other proglacial lakes were also locations of Paleoindian occupations. In contradiction, fossil mollusks have been reported in the Rainy River district of northwestern Ontario along with two species of fish (one was a sturgeon, the other unidentified) (Haywood, 1989). Recovered mollusk species indicate that water was relatively cold, there was an abundance of vegetation, and little turbidity (Haywood, 1989).

3.8 Archaeological Site Bias and Differential Visibility

Although it has been demonstrated that there is a clear association between Plano sites with paleo-shorelines, it is important to consider any potential biases when examining site distribution. Within the 2011 Standards and Guidelines for Consultants and Archaeologists written by the Ontario Ministry of Tourism and Culture, a systematic bias is placed on water sources and elevated topography as indicators of high potential areas for archaeological sites. Such pre-conceived notions lead archaeologists to concentrate on easily identifiable features such as paleo-shorelines (Hinshelwood, 2004), and could lead to neglect of other areas with site potential. The strong association of Plano sites with rivers and former shorelines may reflect this bias, although without inland regions being systematically surveyed it is difficult to prove. Beach ridges were open and high areas, with more wind and less insects (Peers, 1985) making them very attractive during the warm months of the year. However, it is difficult to believe that cold winter months were spent in open areas with high wind. It is

likely that sites located along strandlines represent spring, summer, and fall occupations as suggested by Stewart (2004), while winter campsites are inland where forest cover provided some protection from the elements. It is possible that sites only a few hundred metres from a Minong beach were protected from the elements.

Vegetation in the Boreal forest impedes surveys and creates a bias in favour of accessible locations such as modern waterways (Mulholland et al., 1997). Although there are a considerable number of archaeological sites associated with former water planes, these are prominent features that can be easily followed when conducting surveys. Slow soil accumulation in the Boreal forest makes separation of cultural layers difficult (Dawson, 1983b), but also causes artifacts to generally be close to or at surface. These two factors make site identification along strandlines easier than in areas of high sedimentation rates. Conversely, surveys in the Boreal forest must contend with thick vegetation that can inhibit adequate testing in some areas. It is difficult to conduct a stage two investigation in a blowdown area of intermingled trees, and spots with thick ground cover and roots. This makes it very difficult to systematically survey areas, and can result in wider distances between test pits causing archaeologists to obtain false negatives when a small lithic scatter is present between test pits.

In addition to site bias, the physical landscape has active and inactive landforms that must be understood to accurately interpret archaeological survey data and reconstruct settlement patterns from the spatial distribution of archaeological sites (Bettis & Mandel, 2002; Ravesloot & Waters, 2002-2004). Once archaeological sites are mapped, use of geomorphic maps and knowledge of late Quaternary history allow the investigator to determine if sites are equally preserved and visible across all landforms, or whether there are places within the study area where sites of a specific age are eroded away or buried by subsequent sedimentation (Ravesloot & Waters, 2002-2004). Utilizing this technique of overlaying site distribution on top of geomorphic maps, Ravesloot & Waters (2004) effectively demonstrate that on the Gila River in Arizona there is a

clear zonation of site types associated with landforms and that intensity of use of landforms changes through time. Similar investigations utilizing geological data of the central and eastern Great Plains demonstrate that the Holocene sedimentary record is not uniformly preserved through drainage systems (Bettis & Mandel, 2002). For example, a paucity of Archaic sites within small river valleys appears to be caused by erosion and net transport of sediment during the early and middle Holocene (Bettis & Mandel, 2002). Even though there were habitable surfaces in these valleys during the Archaic period, survival of archaeological sites is unlikely (Bettis & Mandel, 2002). In contrast, there is an abundance of Archaic sites in alluvial fans where there is exceptional preservation, revealing the importance in considering preservation potential of different landscape settings (Bettis & Mandel, 2002). Such intensive studies examining geomorphic features in order to better interpret site distribution have not been conducted in the Thunder Bay region. It is highly likely that geologic activity has created differential preservation potential and emphasizes the observed associations of Plano sites with former lake margins. Detailed descriptions of geomorphic features and associated processes influencing erosion and deposition are required for a more complete understanding of site distribution both spatially and temporally in the Thunder Bay region.

3.9 Summary

The distribution of archaeological recoveries in the Great Lakes region dating to the Plano complex shows a strong association with former lake levels in the Superior, Huron, Erie, and Michigan basins as well as with glacial lakes Agassiz and Hind. Along the northern shore of Lake Superior a series of strandlines situated above the modern water plane including the Main Minong and Post-Minong levels (Fig. 3.2). Both have yielded numerous archaeological sites, the earliest dating to the Plano complex. Although relict beach ridges throughout the Great Lakes area have been occupied by Paleoindian and Archaic groups, geoarchaeological investigations at Brohm and indicate that occupation is contemporaneous with active beach formation. This relationship

between Plano sites and beach ridges has been attributed to use of high and dry ridges for campsites as well as caribou interception points at natural crossing barriers such as streams and rivers (Deller, 1979; Peers, 1985). Due to acidic soils in the Boreal forest (MacDonald, 1971) faunal remains of caribouare not preserved, although they were likely prey for Plano hunters (Peers, 1985). This conclusion is based on inferences made from use of caribou at other Paleoindian sites, ecological data, and other factors (see Peers, 1985). Additional faunal recoveries indicate that Plano groups in the northern Great Lakes area exploited a variety of large and small game that likely included bison (Julig, 1984).

4. METHODS

Due to highway construction, archaeological work conducted within the study region included both stage four excavations, and stage two investigations. Stage four excavations take place once a site has been discovered, and the boundaries have been identified. It involves excavating the entire area of the site that will be impacted by construction. A stage two investigation was also completed along the proposed highway in areas that had not been previously examined, which resulted in the discovery of RLF.

4.1 Archaeological Sites and Exposures

Five archaeological sites examined were included in this thesis to conduct geoarchaeological studies that would complement the archaeology work, and aid with site interpretations. Ensuring that research would accomplish the primary broad goal of determining the depositional environments prior to, during, and after occupation, the study region focused on exposures near the archaeological sites. This enhanced the possibility of correlating stratigraphy between the archaeological sites and the exposures, facilitating interpretations of Paleoindian land use. All roadcut and gravel pit exposures adjacent to the archaeological sites were identified utilizing aerial photos and traverses, and all were included in this thesis because stratigraphy appeared to be intact.

In total, five archaeological sites, and seven exposures were examined. In addition, to five holes were augered to examine subsurface sediment (Fig. 4.1). The Easternmost archaeological site is Mackenzie 2, located on the East side of the Mackenzie River at an elevation of ~241m asl. One roadcut was described in addition to site stratigraphy.

On the west side of the Mackenzie River, the much more extensive Mackenzie 1 site is situated 246m above sea level (asl). Wall profiles were constructed for units displaying representative stratigraphy in the north portion of the site, the middle of the site, and the southern portion. Anomalous stratigraphic profiles revealing pit features were also described. Due to the size of the site

(roughly 10,000 m^2) and variation in stratigraphy, a 4m trench was dug for a more complete understanding of the depositional environment before, and at the time of occupation. The location of this trench was chosen because it lies to the west of artifact recoveries (therefore it would not disturb Mackenzie 1), but remains close enough to the site for stratigraphic correlations between the two.

The Construction Site is located between Mackenzie 1 and RLF laterally as well as vertically at an elevation of 236m asl. One large west-facing exposure was documented utilizing four evenly spaced profiles to accurately represent the lithofacies associations. Although the surface had been disturbed by construction in most profiles, one was documented to the natural surface.

RLF is situated lower than the Construction Site, at an elevation of 243 m asl. Stratigraphy appeared consistent throughout the site, and was documented along a north-facing trench. In addition, the southern portion of the site was examined.

Electric Woodpecker 1 and Electric Woodpecker 2 were first identified during stage three investigations in 2009. These were designated as two distinct archaeological sites due to a small stream channel that separates them. They are located on a prominent ridge that extends southwestward beyond Woodpecker 1 at an elevation of 240m asl.

Gravel Pit 1 is situated 259m asl on another prominent ridge north of the Woodpecker sites, although it is dominantly forest covered. The surface of this East-facing exposure has been disturbed by construction of a road, making it difficult to discern how far below surface the top of the exposure is. However, on the East side of the road, comparable grain-size continues to the surface where bioturbation has disturbed the stratigraphy.

Gravel Pit 2 is situated North of Gravel Pit 1 along the same road, at a lower elevation than Gravel Pit 1. A North-facing exposure was described.

The most extensive exposure is Gravel Pit 3, located Northeast of the Woodpecker sites. Removal of sediments from this gravel pit has exposed an East-facing section as well as a West-facing section, both of which were

examined. A total of eleven profiles were described for an accurate representation of stratigraphy.

Located Southwest of Mackenzie 1, the Mackenzie Roadcut exposure is located at an elevation of 240m asl. Along this roadcut, the East-facing exposure reveals four lithofacies associations, which were examined in seven profiles. In the West-facing exposure, only the stratigraphically lowest lithofacies association was apparent. Examination of this exposure was dominantly for additional paleocurrent directions as well as bedding structures.

The Mackenzie South Roadcut is located south along the same road as the Mackenzie South Roadcut, at a lower elevation of 224m asl. This is a small exposure, with water flow at its base disturbing stratigraphy.

The Southernmost exposure is Mackenzie Inn, at an elevation of 233m asl. This West-facing exposure extends to 550 cm below surface, revealing four lithofacies associations.

4.2 Archaeological Methods

Excavation at all five archaeological sites was conducted by Western Heritage, following the *Standards and Guidelines for Consulting Archaeologists (2009)*. A 1m x 1m grid was utilized with a datum of 500N 500E. The stage three assessment of each archaeological site revealed the locations of artifact recoveries, which were used as initial guides for excavation. As artifact concentrations were identified, they were excavated laterally and vertically until the units and levels became sterile (no artifacts recovered).

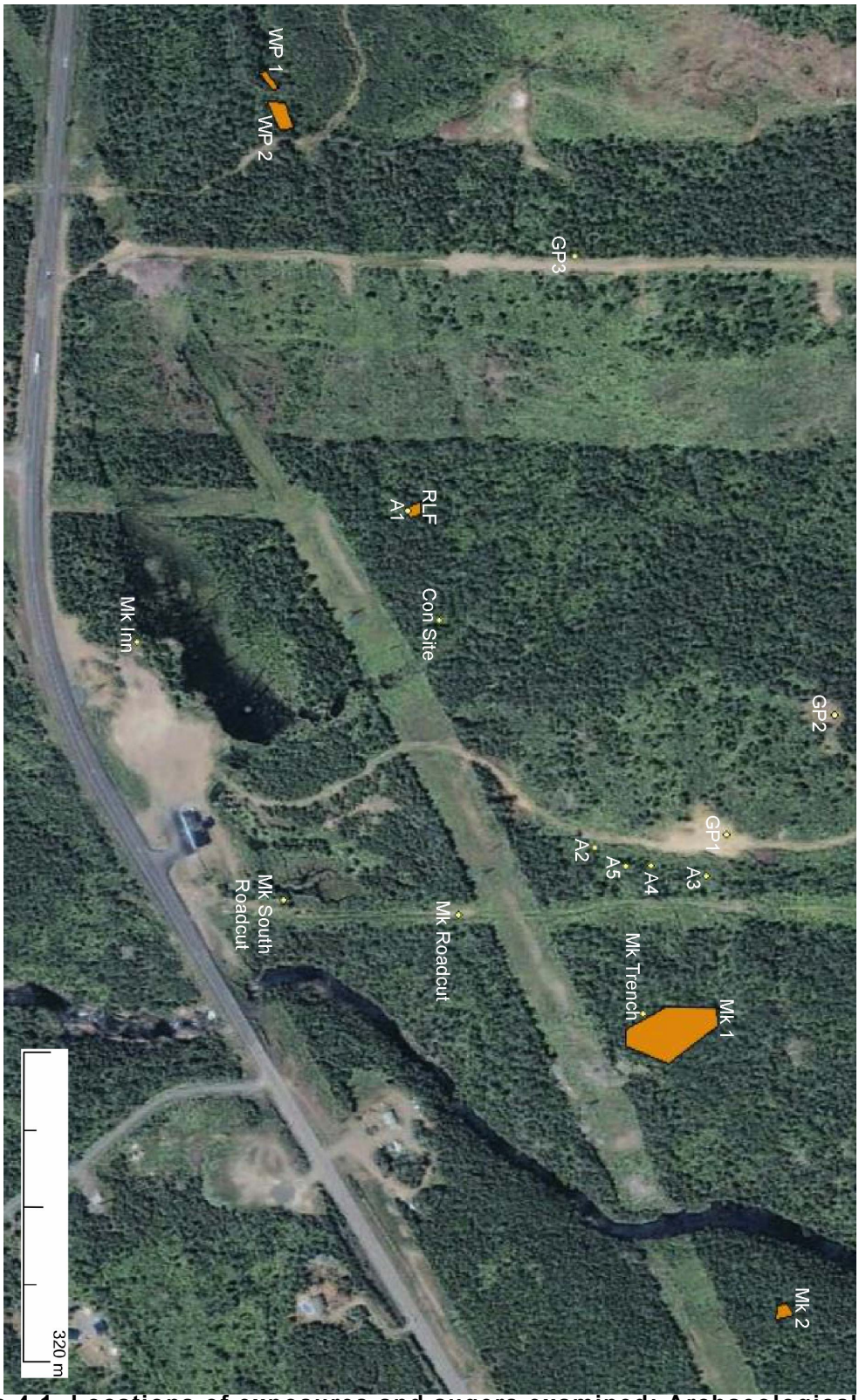

Figure 4.1. Locations of exposures and augers examined: Archaeological sites Mackenzie 1 and 1 (Mk 1 and Mk 2), Electric Woodpecker 1 and 2 (WP 1 and WP 2), and RLF; Exposures: Mackenzie Inn, Mackenzie South Roadcut, Mackenzie Roadcut, Mackenzie Trench, Construction Site (Con Site), and Gravel Pits 1, 2 and 3 (GP 1, GP 2 and GP 3); and Auger holes A1 to A5.

4.2.1 Excavation Techniques and Documentation of Artifacts

Block excavation was completed with either shovels or trowels in areas of high artifact recovery. Each 1m x 1m unit was excavated in 5cm arbitrary levels and quadrants, and line levels were used to maintain horizontal control. All sediment from each level and quadrant was screened through 6mm and 3mm mesh stacked screens. Artifacts were recorded in place whenever possible, being given a northing, easting and depth relative to the unit coordinates.

4.3 Documentation of Stratigraphy

The method utilized for documentation of stratigraphy at both the exposures and the archaeological sites is architectural element analysis, developed by Miall (1985; 1988) to promote extensive data collection. Previous techniques relied extensively on vertical profile analysis, which did not adequately represent three-dimensional variations in composition and geometry, making correct interpretations of depositional environments extremely difficult (Miall, 1985). As a result, Miall (1985; 1988) introduced the method of using photomosaics as base maps for detailed facies information, bounding surfaces, and the nature and orientation of cross-bedding.

These concepts of architectural elements and bounding surfaces have been effectively applied to the exposures described in this thesis. Architectural elements, referred to herein as lithofacies associations, were identified on the basis of grain-size, bedform composition, internal sequence, and external geometry following Miall's (1985; 1988) method. The contacts, or bounding surfaces, of each facies were also described in detail. Where possible, lithofacies associations and their contacts were examined laterally as well as vertically, and paleocurrent measurements were taken. This method ensures that the greatest amount of data possible is collected.

Stratigraphic columns created for sediments at an archaeological site have a northing and easting that corresponds to its unit coordinates within the site, as well as a direction indicating which wall of the unit is depicted. For

example, a profile of 490N 530E N wall would be a unit 10m South and 30m east of the datum, and the stratigraphic column would show the stratigraphy of the wall looking north.

4.4 Examination of Subsurface Sediments

In parts of the study area where no exposures were discovered and forest cover prevented examination of stratigraphy, auger holes were utilized to determine depth, grain-size, and colour of sediments (e.g. Overeem et al., 2003; Rommens et al., 2006). This was completed because examination of Gravel Pit 1 and the Mackenzie 1 trench (Fig. 4.1) revealed that the lithofacies associations observed at Gravel Pit 1 appeared to be the same as those ~4m below the surface of Mackenzie 1. Subsurface sediments were examined at A2 (246m asl), A3 (253m asl), A4 (249m asl), and A5 (247m asl) (Fig. 4.1) to determine whether the lithofacies associations can be connected and whether it is possibly that they represent the same depositional event.

At RLF, examination of stratigraphy in the walls of excavated units revealed that the lithofacies associations remain consistent throughout the site. However, since artifact recoveries were generally quite close to the surface a small trench was dug to expose sediments ~1m below surface, and an auger hole was utilized to determine whether and how deep a change in lithofacies associations takes place.

4.5 GIS and Air Photo Interpretation

ArcMap was utilized 1) to create an artifact size distribution map at Mackenzie 1; 2) to flood the Superior basin to known Minong levels; and 3) to examine air photos.

To create an artifact size distribution map, artifact data from the catalogue was provided by Western Heritage. Only the 2010 data was included because cataloguing of the 2011 artifacts was in progress during the completion of this thesis. Inverse Distance Weighted (IDW) was utilized in ArcMap to interpolate

cell values by averaging the values of sample data points in the neighborhood of each processing cell. The outcome is a distribution map of artifact size, with an overlying grid of units excavated in 2010.

A digital elevation model (DEM) was provided by the Lakehead University Geography Department Map Library (LUGDC, 2012a). Using known Minong elevations from identified beach deposits, the Raster Calculator in ArcMap was employed to flood the Superior basin, and to create maps to show the area of northwestern Ontario that would have been underwater during the Minong phase.

Digital air photos were provided by the Lakehead University Geography Department Map Library (LUGDC, 2012b). These were examined with the underlying DEM in an attempt to identify known strandlines and correlate them to the thesis study area.

4.6 Radiocarbon Dating and Calibration

Samples were taken from Mackenzie 1 and Woodpecker 2 by Western Heritage, and sent to Beta Analytical Radiocarbon Dating Laboratory. These were samples of organic material that appeared to be directly associated to artifacts, and therefore would date site occupation. Radiocarbon years were calibrated using the IntCal04 (Mackenzie 1) and IntCal09 (Woodpecker 2) databases with a 2 σ range, to account for variations in the ^{14}C content of the atmosphere (Reimer et al., 2004; Reimer et al., 2009).

4.7 OSL Dating

Dr. Gillilland and Dr. Adderley took sediment samples from Mackenzie 1, Woodpecker 1, and Woodpecker 2, which were submitted to The Scottish Universities Environmental Research Centre for OSL dating. These samples were subjected to laboratory preparation of sand-sized quartz, and checked for purity using a scanning electron microscope, which is outlined in detail by Kinnaird et al. (2012). Single aliquot regenerative (SAR) procedure was completed using 16 aliquots of quartz per sample (Kinnaird et al., 2012).

5. RESULTS

This chapter presents the lithofacies identified at each exposure and archaeological site. Stratigraphic columns depict the lithofacies discussed, following one legend (Fig. 5.1)

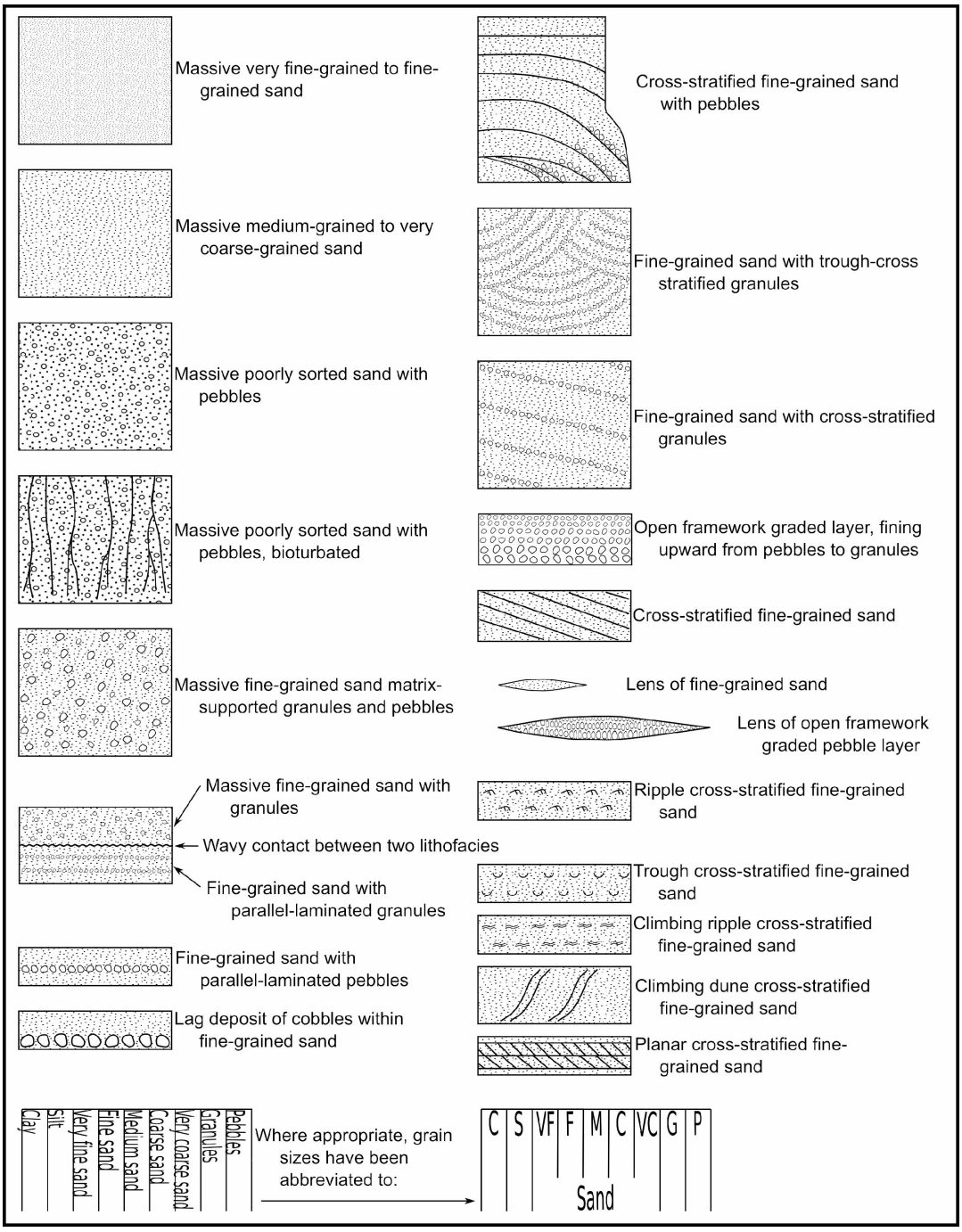

Figure 5.1. Legend for stratigraphic columns

5.1 Gravel Pit 1

Located Northwest of Mackenzie 1 (Fig. 4.1), Gravel Pit 1 is comprised of very fine-grained to fine-grained sand. The lower part of the exposure reveals climbing ripple cross-lamination, ripple cross-lamination, trough-cross bedding and thin silt-clay couplets ranging from 1mm to 5cm thick. The upper 58cm of this appears massive with colour changes. This upper massive portion of the section could represent soil formation processes and bioturbation (roots are present), or deposition of colluvium from the adjacent road, which is composed of the same sediment.

One section of parallel layers has a wavy appearance because they were draped over ripples. Ripples fill the troughs of the continuous wavy layers (Fig. 5.2). This thin layer of ripples filling troughs was eroded. Overlaying are silt-clay couplets containing roots, with the silt portion dominating in all but the basal two. A rose diagram shows the paleocurrent directions of ripples seen throughout Gravel Pit 1 (Fig. 5.3).

Normal faults were observed, the largest of which displaces layers of climbing ripple cross-lamination and trough cross-stratification (Fig. 5.4), while the second displaces a sequence of silt-clay couplets at ~55cm (Fig. 5.5). Additional disturbance was caused by root growth seen in the stratigraphic column at 45cm and 85cm (Fig. 5.5)

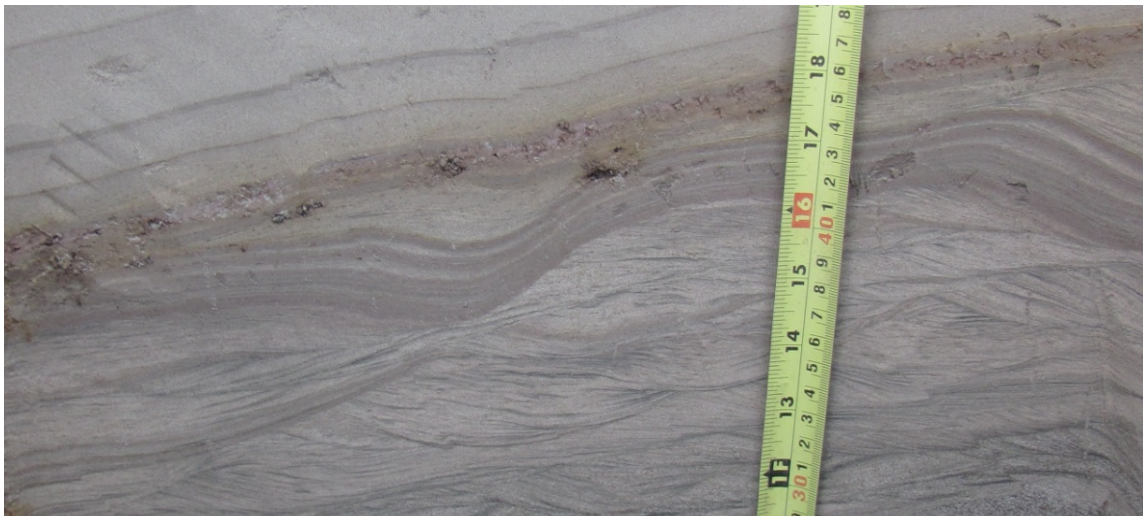

Figure 5.2. Bedforms within Gravel Pit 1

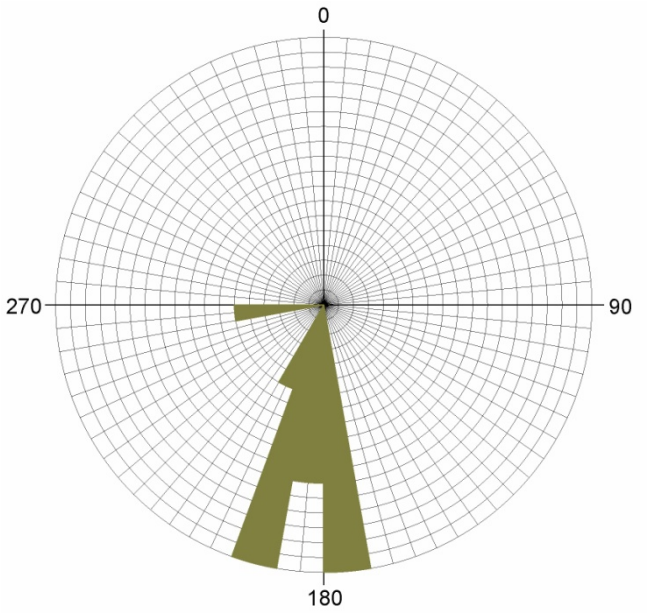

Figure 5.3. Rose diagram for Gravel Pit 1

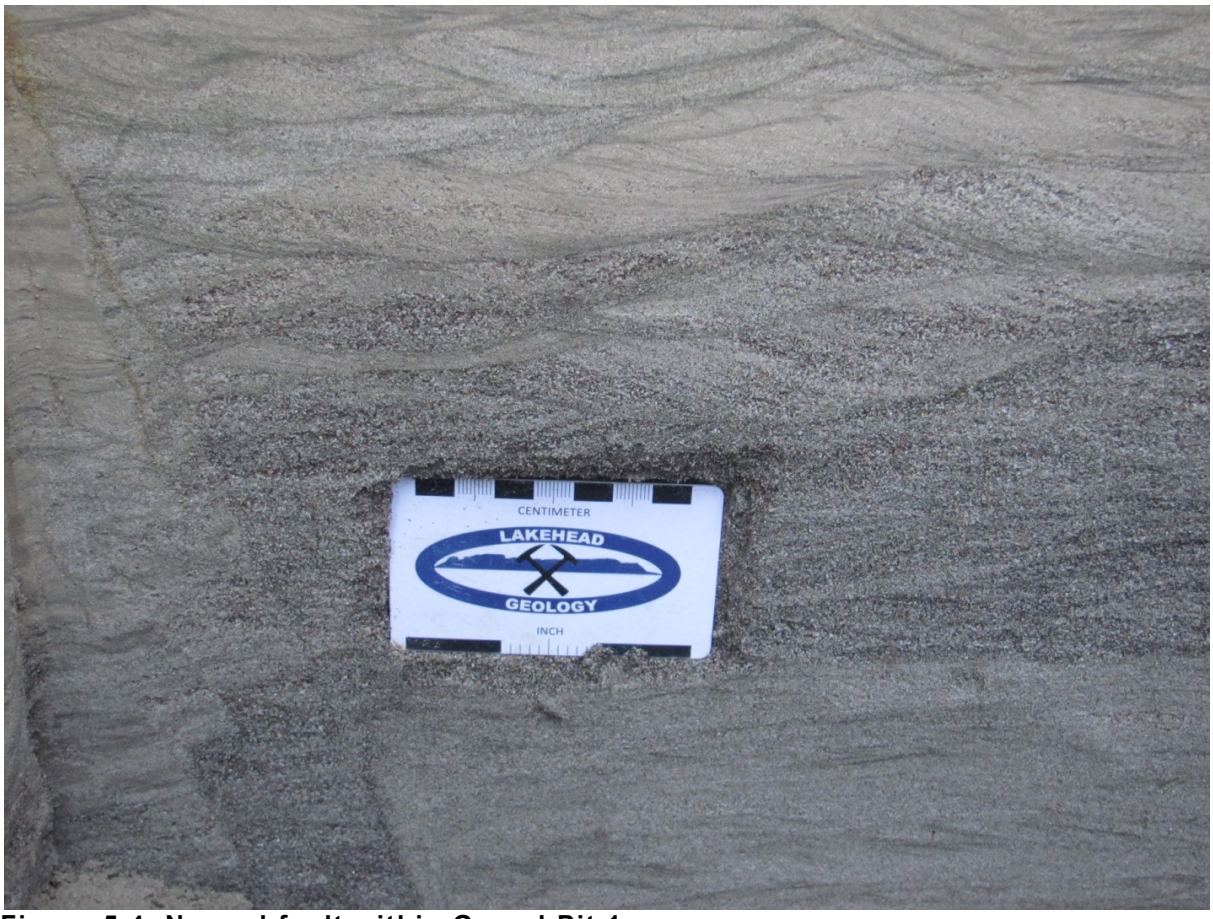

Figure 5.4. Normal fault within Gravel Pit 1

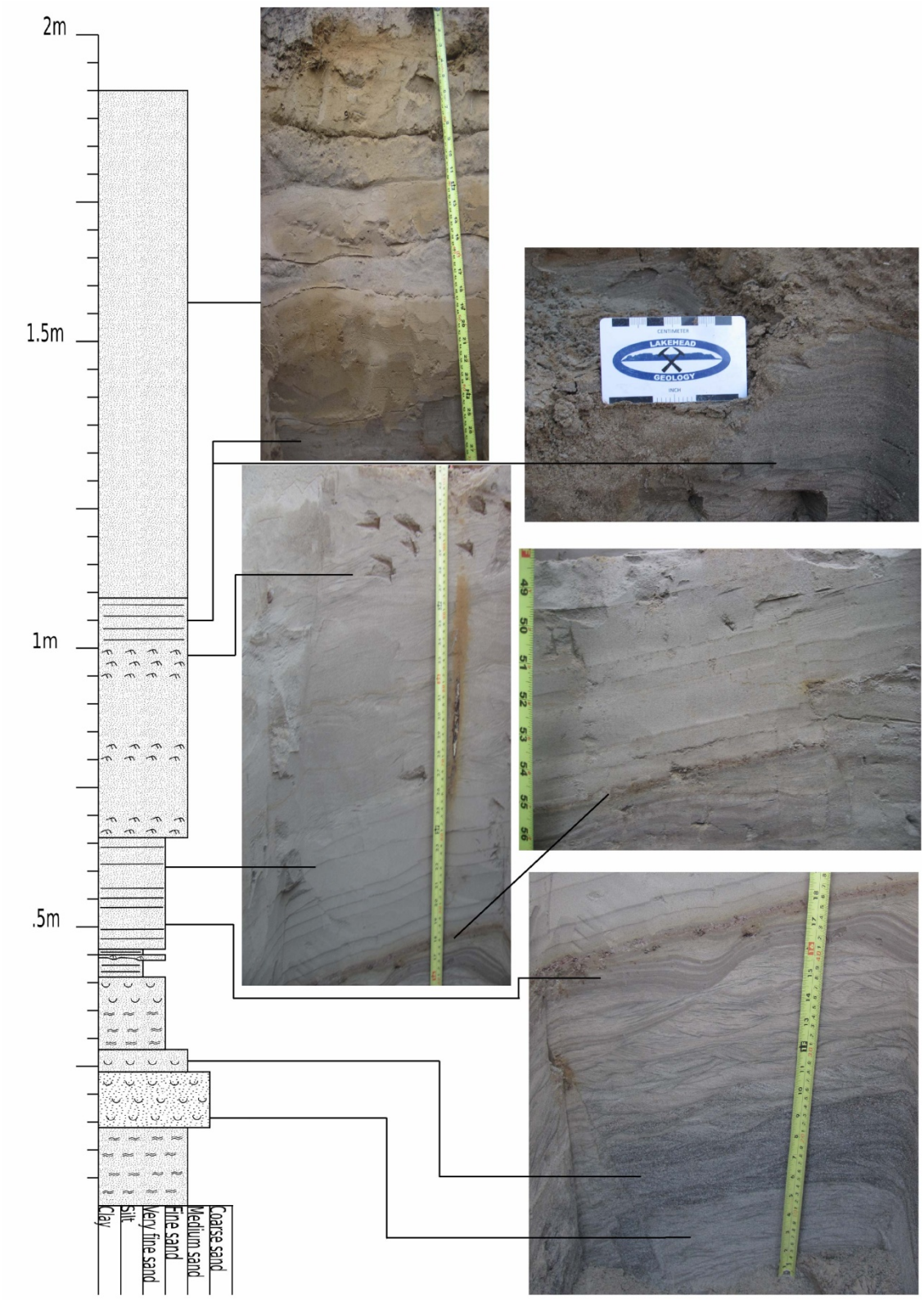

Figure 5.5. Stratigraphic column and associated photos of Gravel Pit 1

5.2 Gravel Pit 2

Located North of Gravel Pit 1 (Fig. 4.1), the north wall of this gravel pit is depicted in Figure 5.6. Lithofacies associations have been separated into eight lithofacies (Fig. 5.7 & 5.8), which are presented from the bottom to the top of the exposure. Although lithofacies 2B to 6B are not continuous eastward, they continue westward with fairly consistent thicknesses. Lithofacies 2B,3B, 4B, 5B and 6B represent the same lithofacies association. These have been separated by changes in grain-size and bedforms to aid with descriptions.

1B. Medium-Grained Sand to Pebbles

This lithofacies association is composed of cross-stratified medium-grained sand to granules and small pebbles, a maximum of 4mm in diameter, interbedded with medium-grained sand and granule matrix-supported pebbles up to ~3cm in diameter (Fig. 5.6). The contact with overlying 2B appears erosive and very abrupt. At the eastern side of the exposure, this cross-stratified bedding extends upward to lithofacies 8B with a gradational contact (Fig. 5.6 & 5.9).

2B. Very Fine-Grained to Fine-Grained Sand

Abruptly overlying the cross-stratified sand and pebbles is very fine-grained to fine-grained sand, which is also in abrupt contact with lithofacies 3, 4, and 5 (Fig. 5.7 & 5.8). The lower ~3cm of the unit has parallel-bedding ~1mm thick, with overlying ripple cross-lamination 3cm thick. The upper ~6cm of this lithofacies appears massive (Fig. 5.7). Bioturbation is apparent, represented by roots which likely destroyed bedding in the upper portion causing it to look massive.

Above the dashed line, the sand comprising lithofacies 2B (Fig. 5.7) is very well-sorted parallel-laminated fine-grained sand with layers approximately 1cm thick, however these layers are extremely difficult to see.

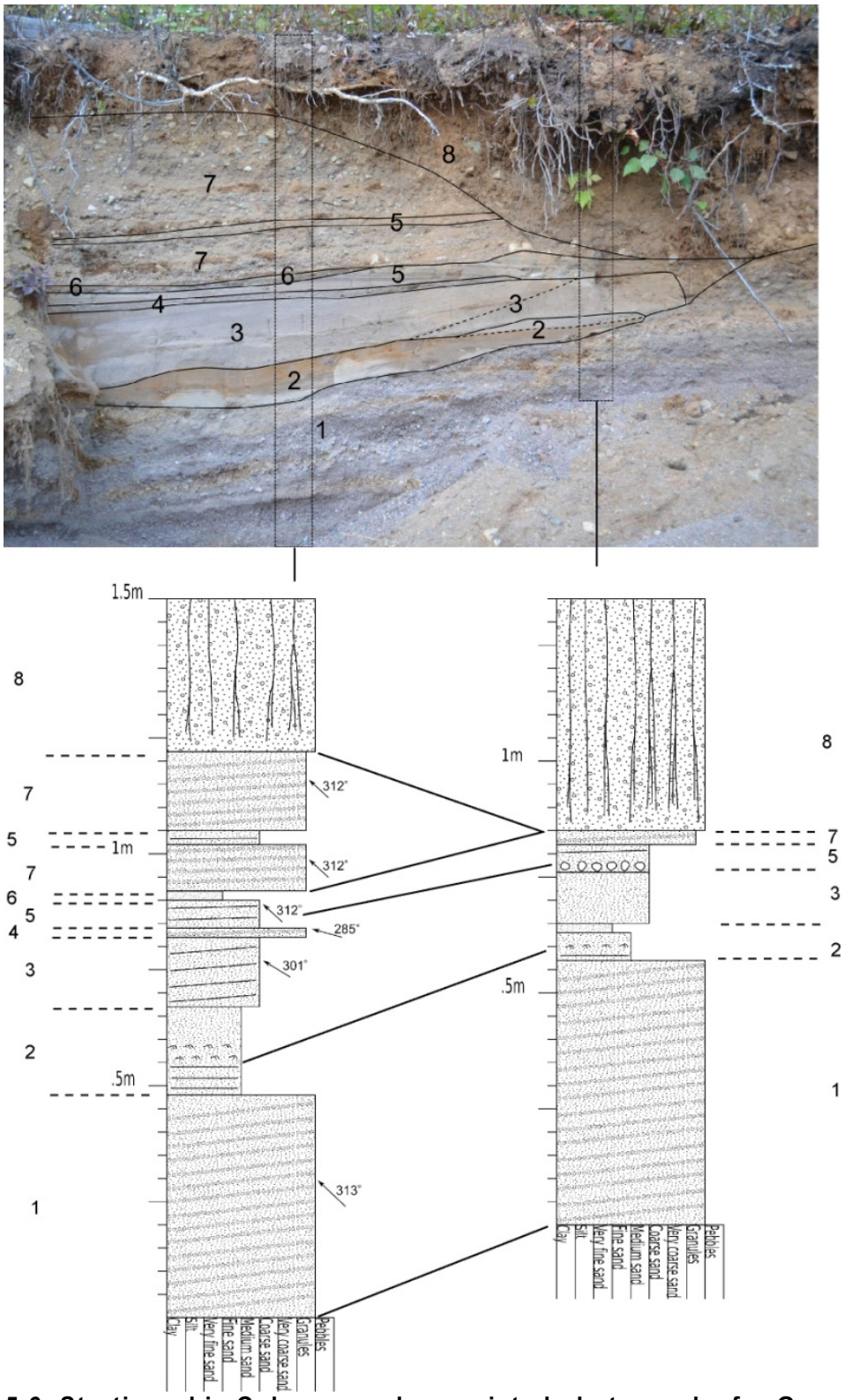

Figure 5.6. Stratigraphic Columns and associated photographs for Gravel Pit 2. On the left is the western profile, on the right is the eastern profile.

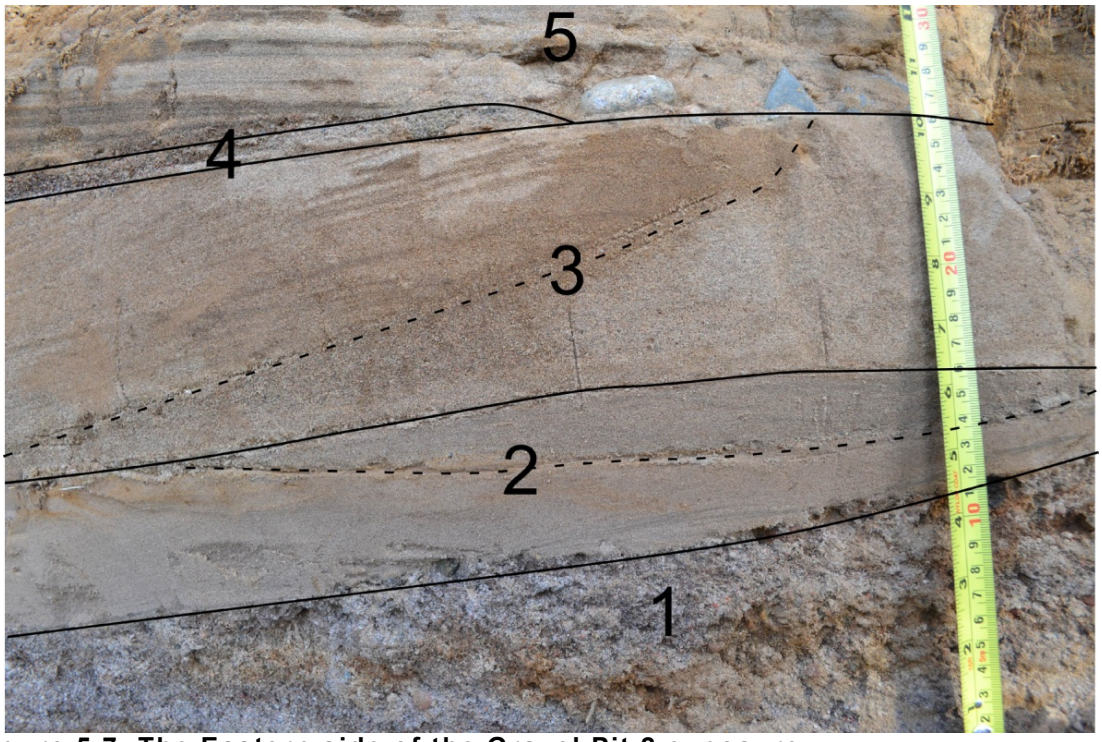

Figure 5.7. The Eastern side of the Gravel Pit 2 exposure

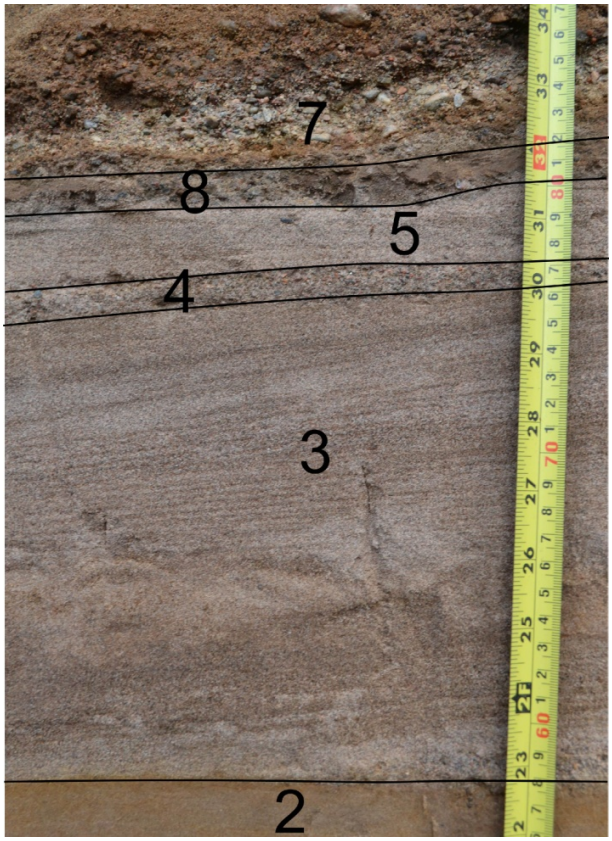

Figure 5.8. The Western side of Gravel Pit 2

Figure 5.9. Lithofacies 1B and overlying massive lithofacies 8B

Figure 5.10. Ripple cross-stratification and parallel-laminations, within unit 2

3B. Fine-Grained to Medium-Grained Sand

This lithofacies is well-sorted fine-grained to medium-grained sand (Fig. 5.7). Below the dashed line a section appears massive, while above it cross-stratification is visible (Fig. 5.7). The cross-stratified layers are generally 2 to 3mm thick, and roughly concordant to the base with convex up laminae laterally becoming concave up ones. Contacts with underlying lithofacies association 2B and overlying 4B both appear erosive and abrupt.

4B. Coarse-Grained Sand with Granules

Fairly well-sorted medium-grained to coarse-grained sand with granules up to ~3mm comprise this lithofacies. Within it, parallel-laminated beds averaging 5mm in thickness are apparent (Fig. 5.7 & Fig. 5.8). This unit appears

to grade into lithofacies 7B, with the paleocurrent direction changing from 285° in lithofacies 4B to 312° in lithofacies 7B.

5B. Fine-Grained to Medium-Grained Sand

This well-sorted fine-grained to medium-grained sand is parallel-laminated, composed of layers up to 5mm thick (Fig. 5.8). This bedding is underlain by lithofacies 3B and 4B, and overlain by 7B with abrupt lower and upper contacts (Fig. 5.7). At the contact with 3B and 4B, pebbles up to ~5cm in diameter are present (Fig. 5.7). In addition, this lithofacies association is interbedded with 7B, although the parallel-stratification is more difficult to see (Fig. 5.6).

6B. Lens of Very Fine-Grained Sand

Overlaying lithofacies 5B and underlying 9B (Fig. 5.6 & 5.11), a lens of well-sorted very fine-grained sand is apparent. At the erosive contact with underlying 5B, a few granules 1-3mm in diameter are present at some locations. The contact with overlying lithofacies 9B also appears erosive and abrupt.

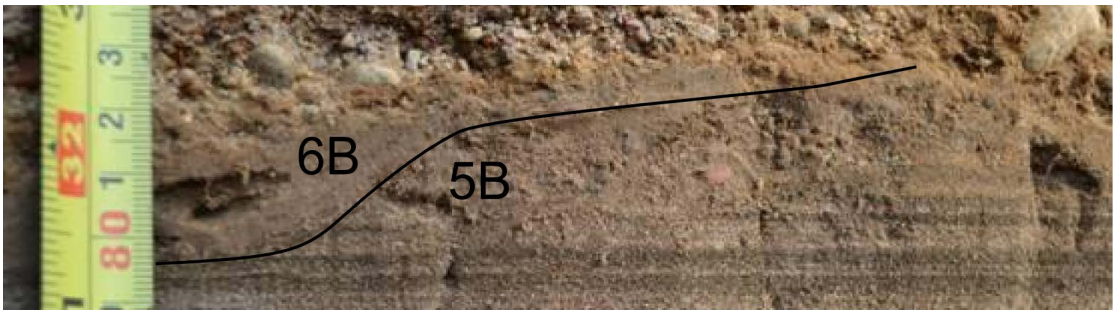

Figure. 5.11. Lithofacies 5B and overlying lens comprising lithofacies 6B

7B. Medium-Grained Sand to Pebbles

Cross-stratified medium-grained to coarse-grained matrix-supported granules up to 4mm in diameter interbedded with medium-grained to coarse-grained sand matrix-supported pebbles up to ~3cm in diameter abruptly overlie lithofacies 5B (Fig. 5.7 & 5.8). The contact with overlying 8B is gradual.

8B. Silty Sand Matrix with Pebbles

This lithofacies is strongly bioturbated with no apparent bedding (Fig. 5.9). The underlying lithofacies 7B grades into this massive lithofacies with an increase in silt content upwards, and larger pebbles, up to 5cm in diameter, than those in 7B. The diffuse boundary and consistent grain-size with lithofacies 7B indicates that these two lithofacies likely represent the same lithofacies.

5.3 Gravel Pit 3

Exposures were dug out to examine the units present along three faces of the sandy banks. As shown in Figure 5.12 (looking south), profiles along A reveal the west exposure, while faces B and C reveal the east. Face B is exposed below the road, where beds dip 1.5°northward (Fig. 5.13). Face C is exposed above the road, revealing heavily bioturbated sediments with no apparent bedding, thus only profiles along faces A and B are described.

Three lithofacies asociations were identified throughout profiles exposed at 0m, 6m, 16.5m, 23m, 28m, and 43.5m. Lithofacies 2C, 3C, 4C and 5C represent the same lithofaces association, and lithofacies 6C and 7C also represent a lithofacies association. A fence diagram correlates all of these profiles (Fig. 5.14), and a stratigraphic column with associated photos was produced for each profile (Fig. 5.15 to 5.25). These will be presented from the stratigrahically lowest lithofacies association 1, through to the highest.

Figure 5.12. Gravel Pit 3, profiles were exposed and stratigraphic columns were produced for faces A and B (Figures 6.26 to 6.36)

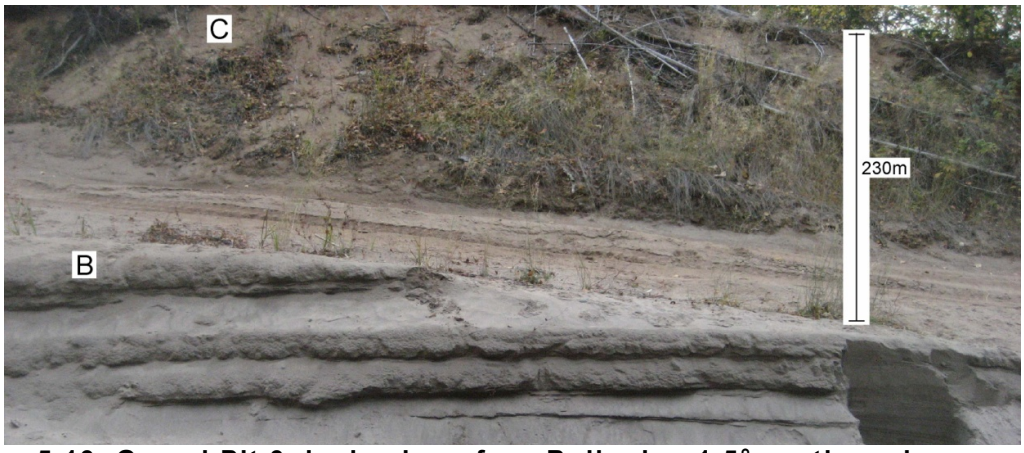

Figure 5.13. Gravel Pit 3, beds along face B dipping 1.5° northward

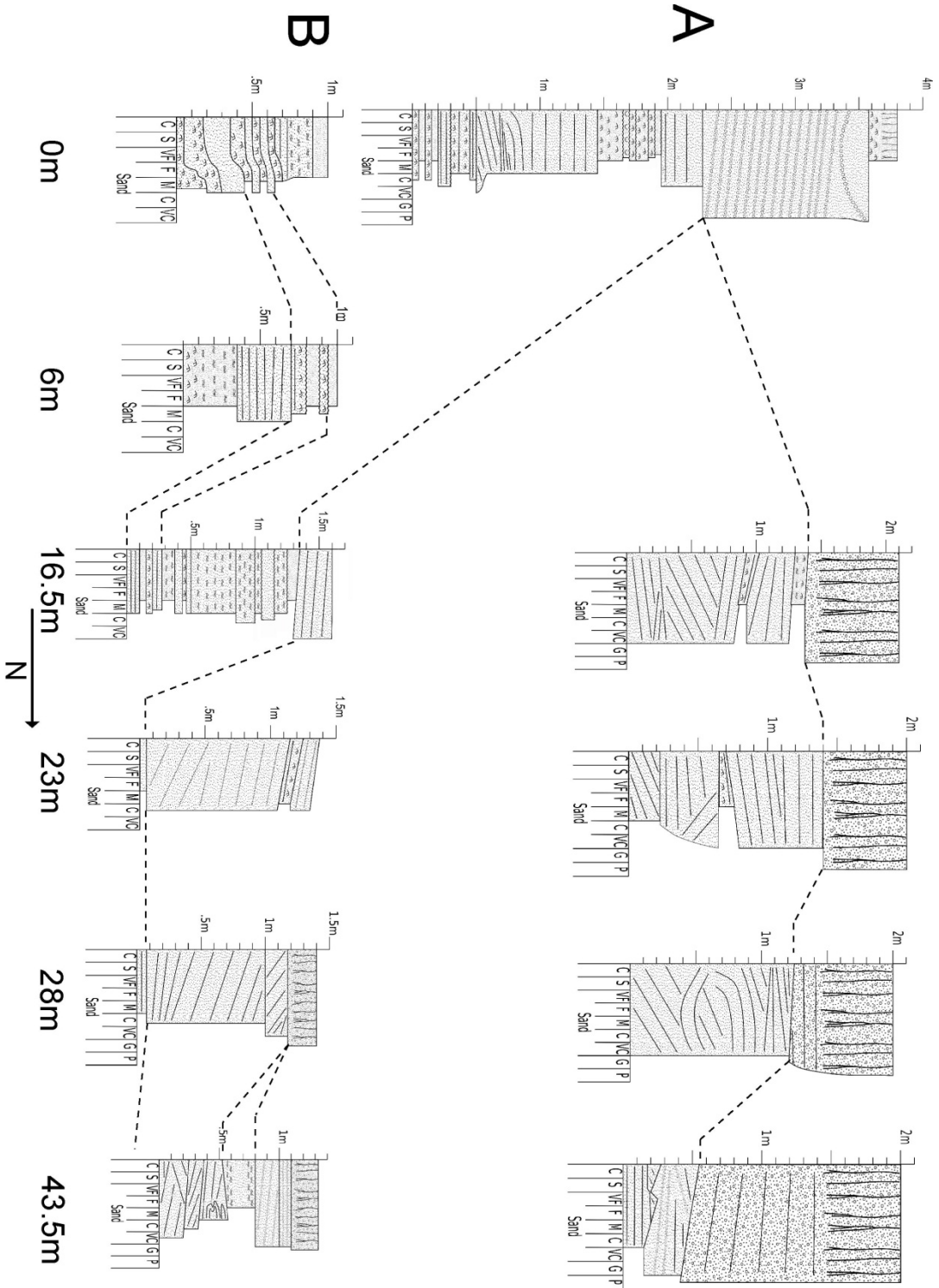

Figure 5.14. Fence diagram correlating all seven lithofacies throughout the exposed profiles at Gravel Pit 3

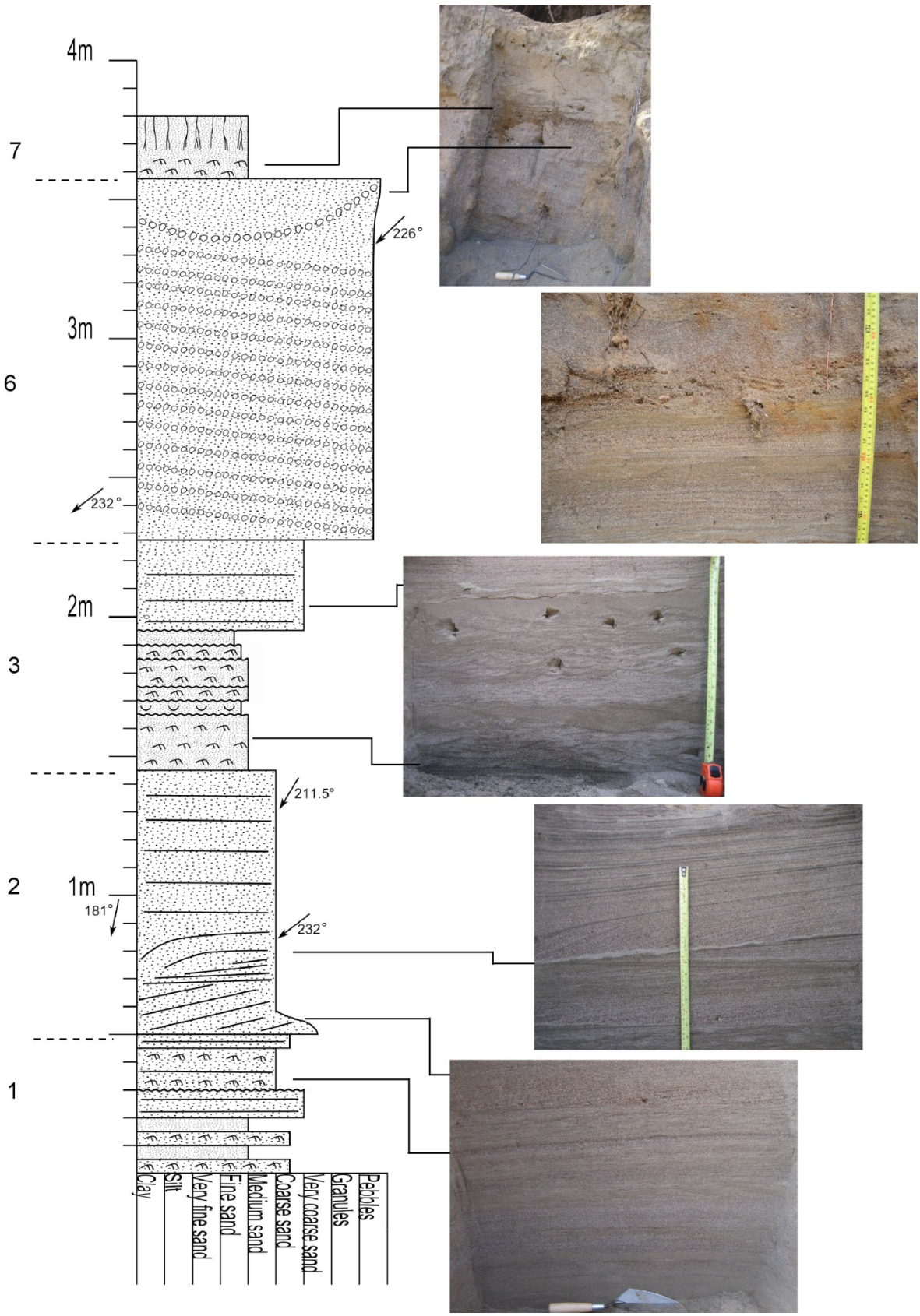

Figure 5.15. Gravel Pit 3, Profile A 0m

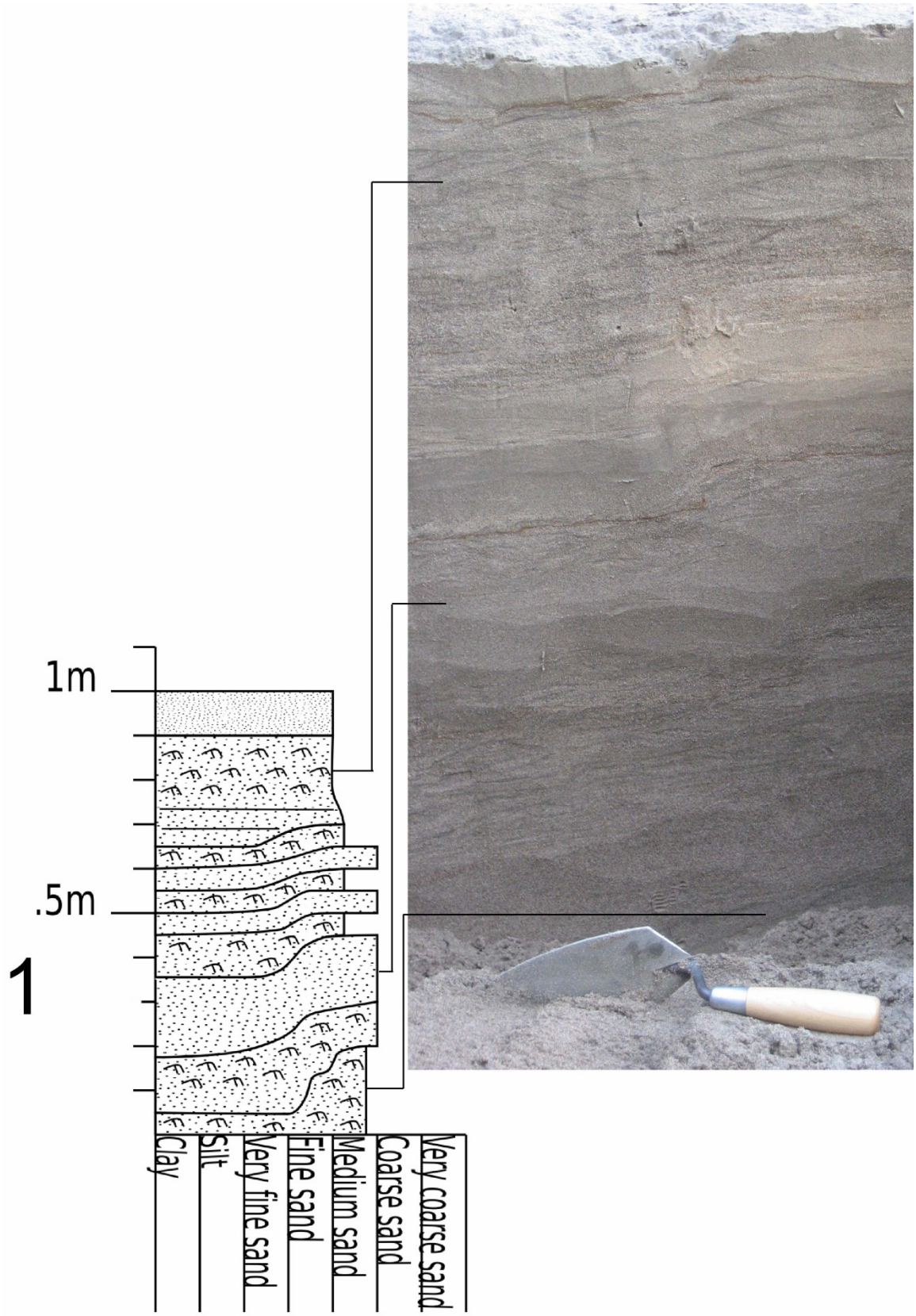

Figure 5.16. Gravel Pit 3, Profile B 0m

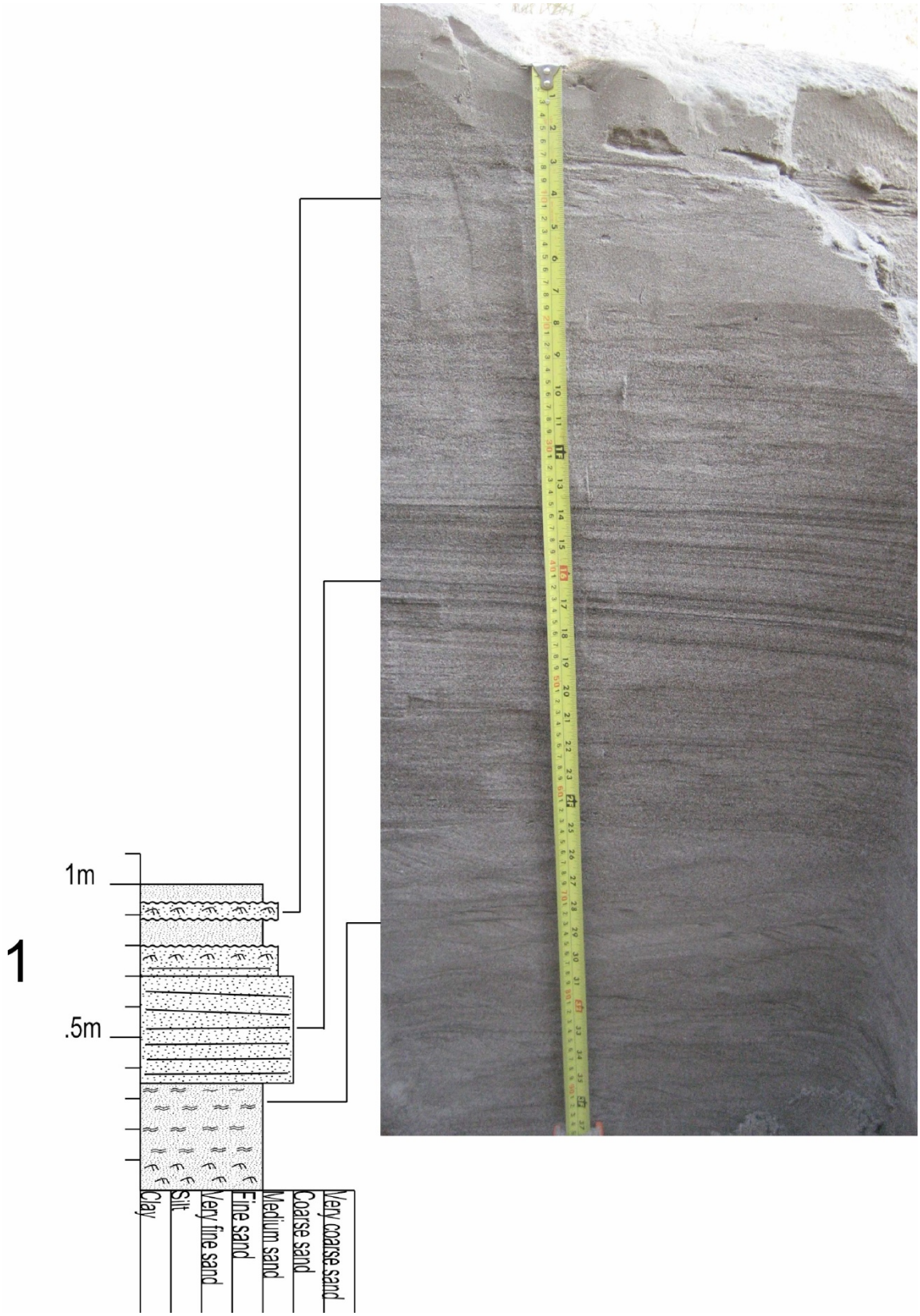

Figure 5.17. Gravel Pit 3, Profile B 6m

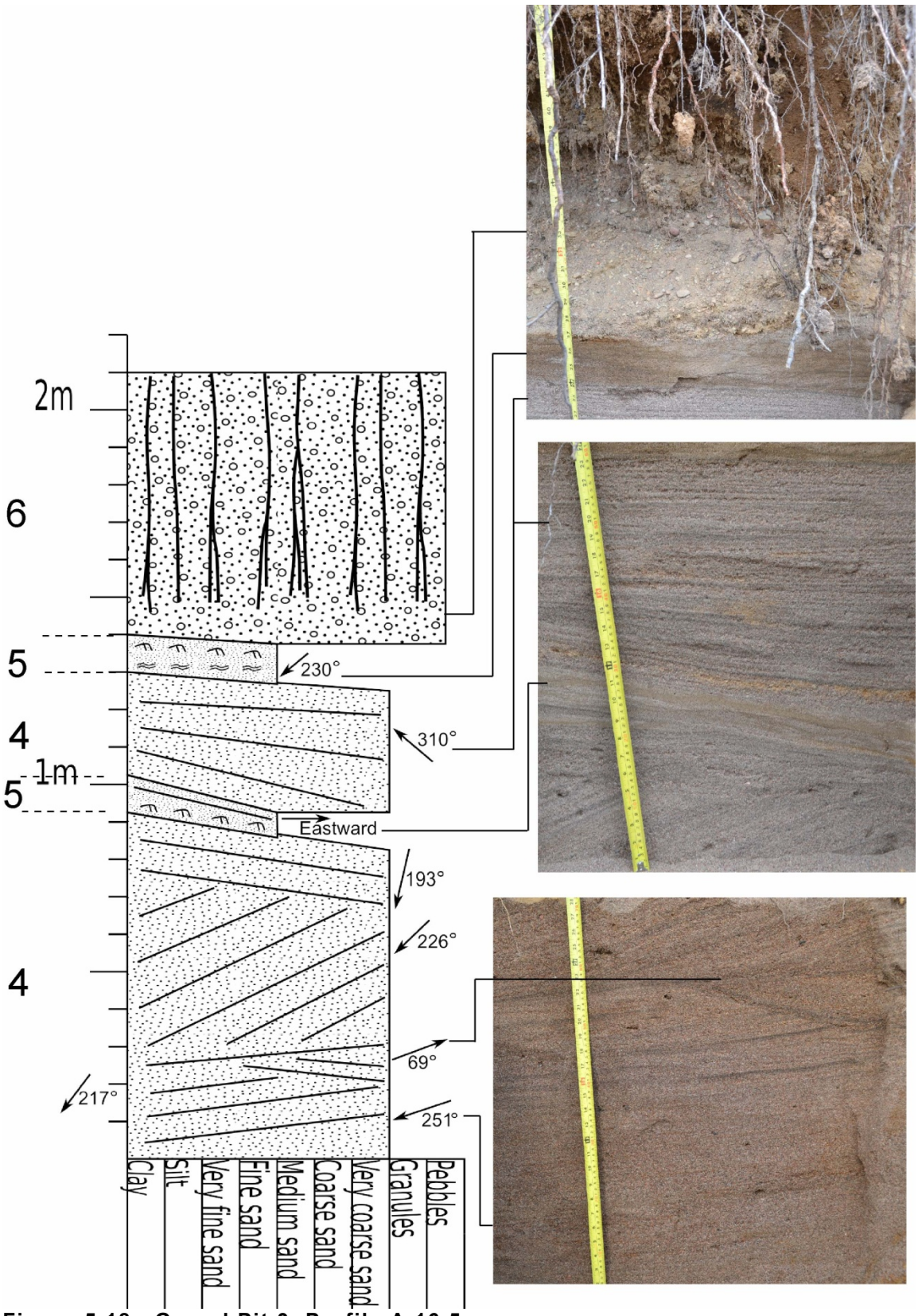

Figure 5.18. Gravel Pit 3, Profile A 16.5m

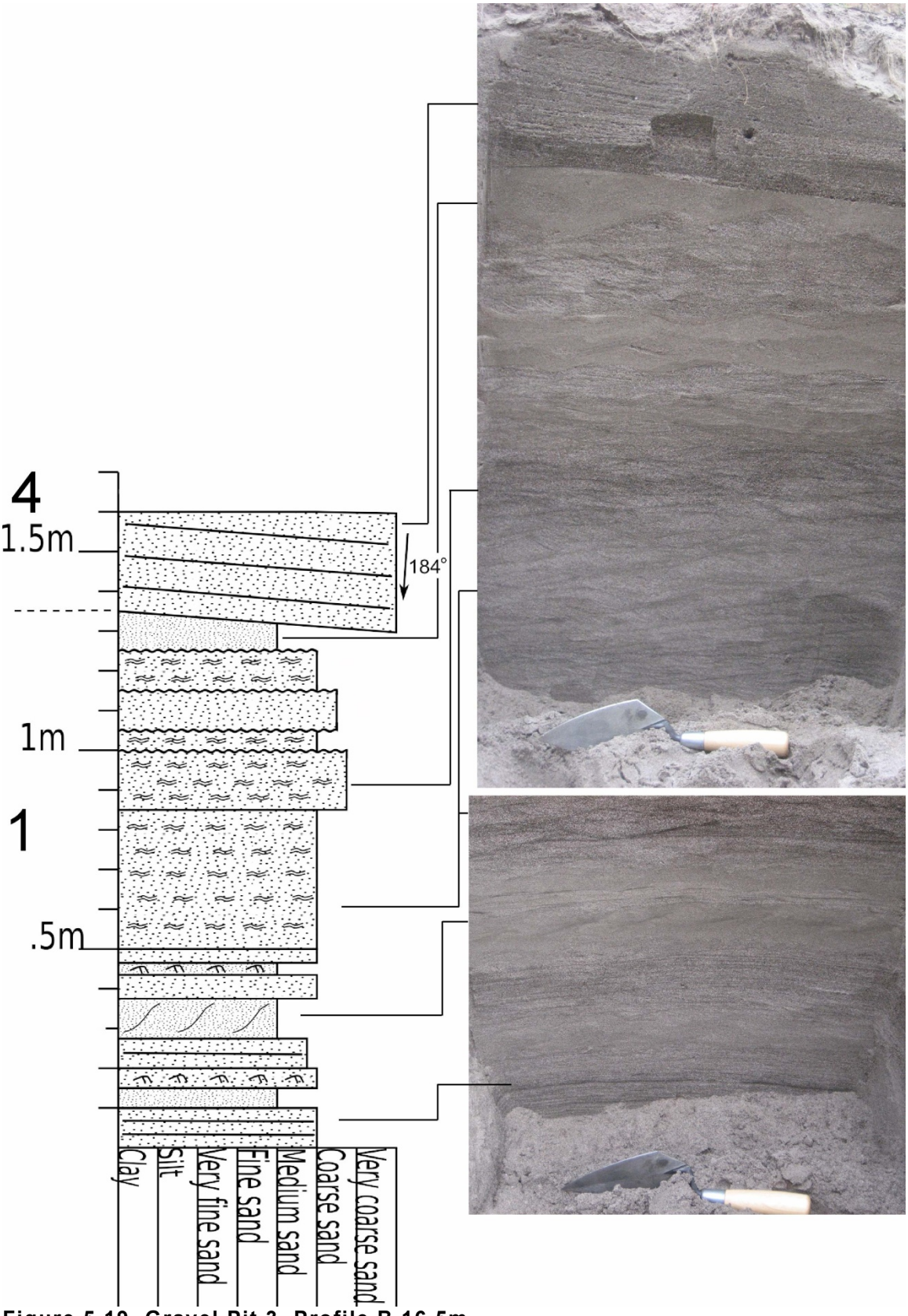

Figure 5.19. Gravel Pit 3, Profile B 16.5m

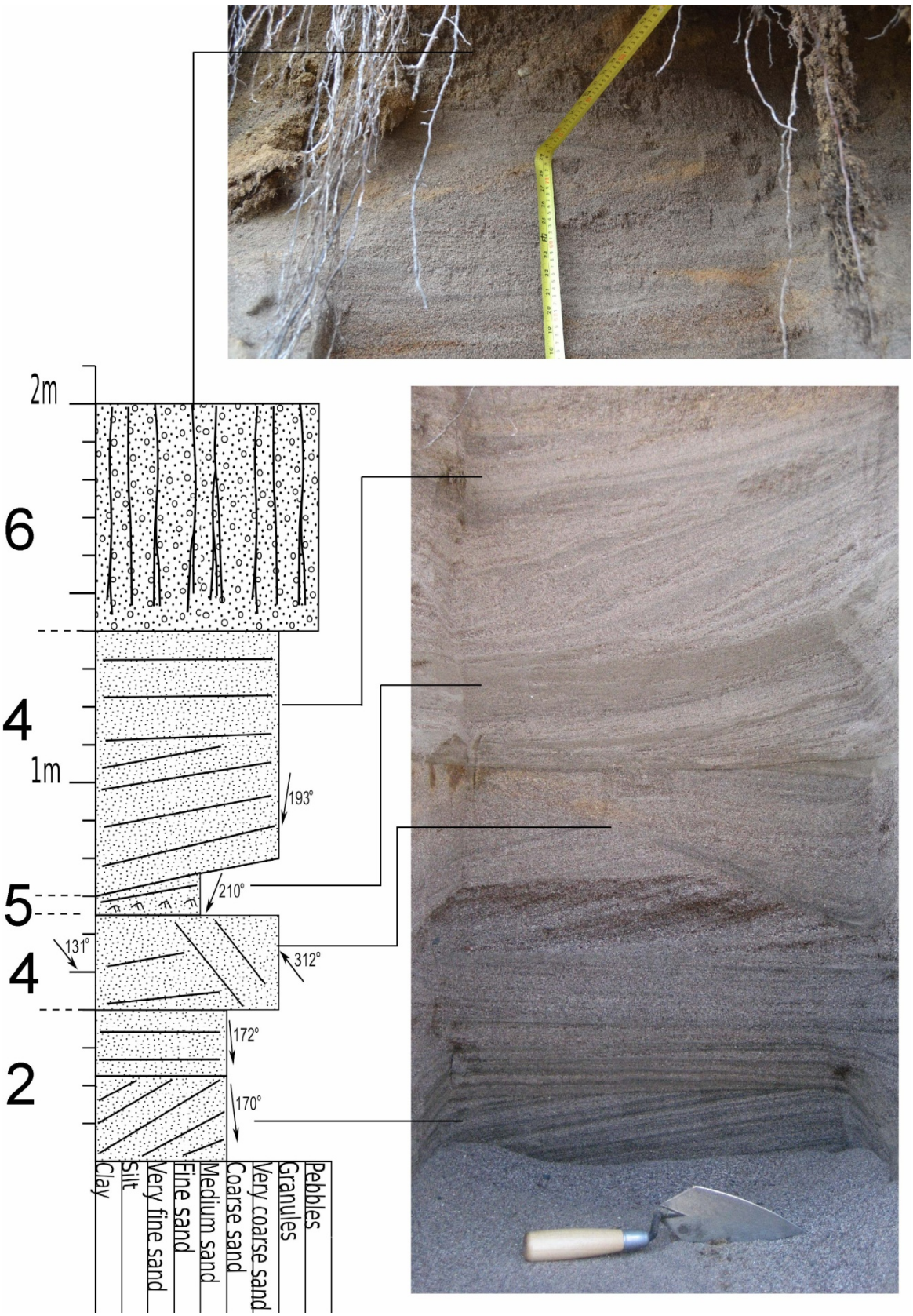

Figure 5.20. Gravel Pit 3, Profile A 23m

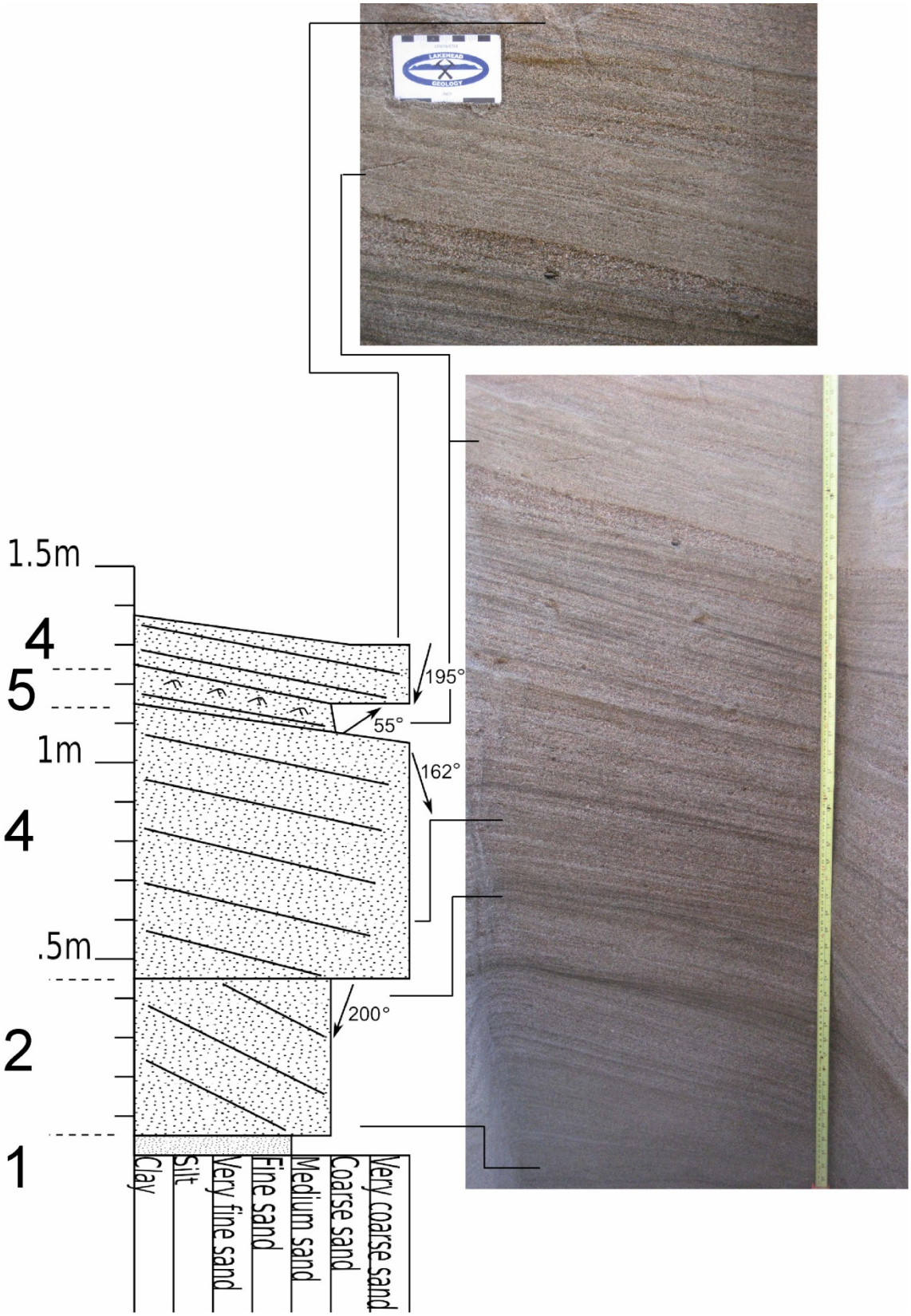

Figure 5.21. Gravel Pit 3, Profile B 23m

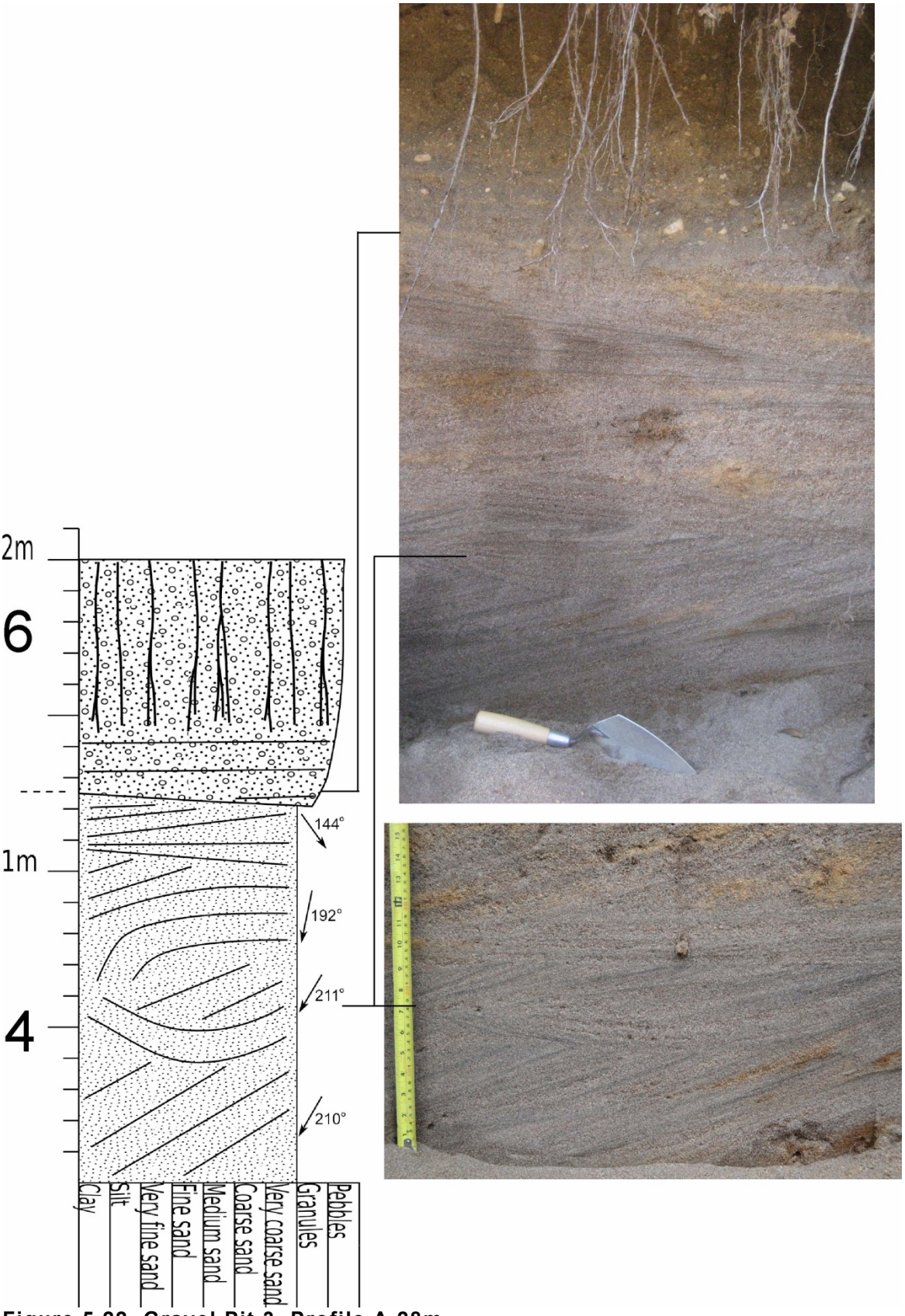

Figure 5.22. Gravel Pit 3, Profile A 28m

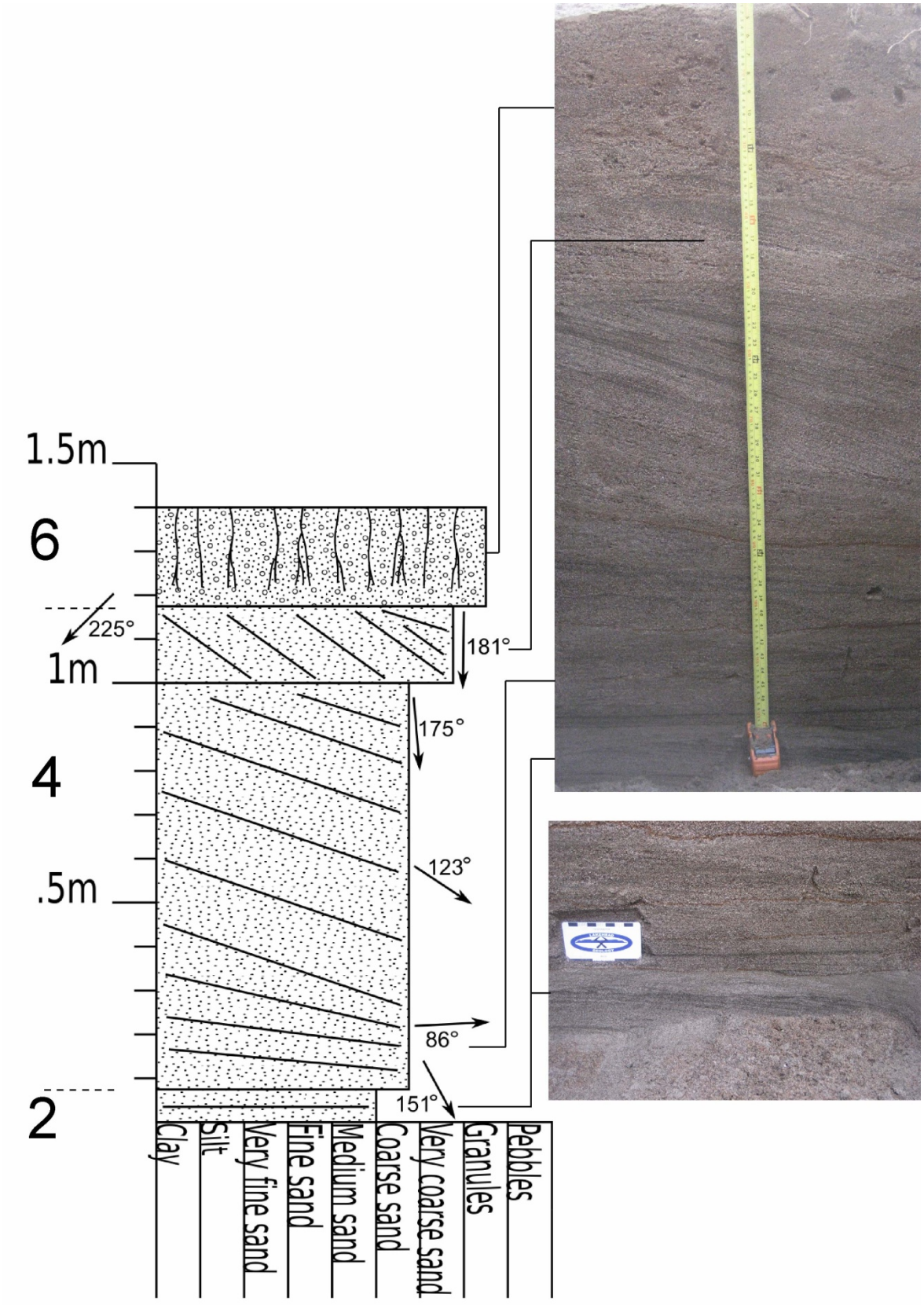

Figure 5.23. Gravel Pit 3, Profile B 28m

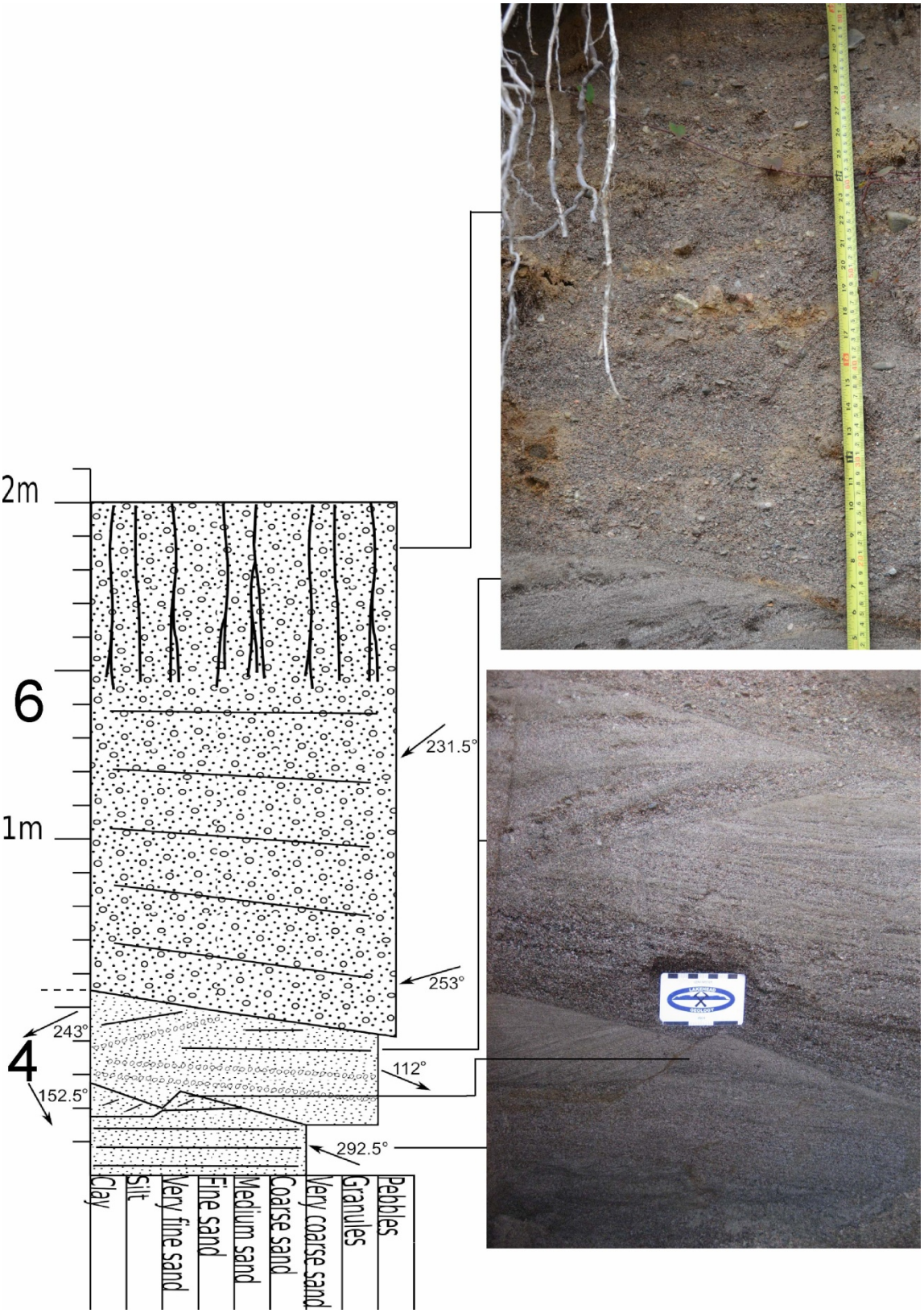

Figure 5.24. Gravel Pit 3, Profile A 43.5m

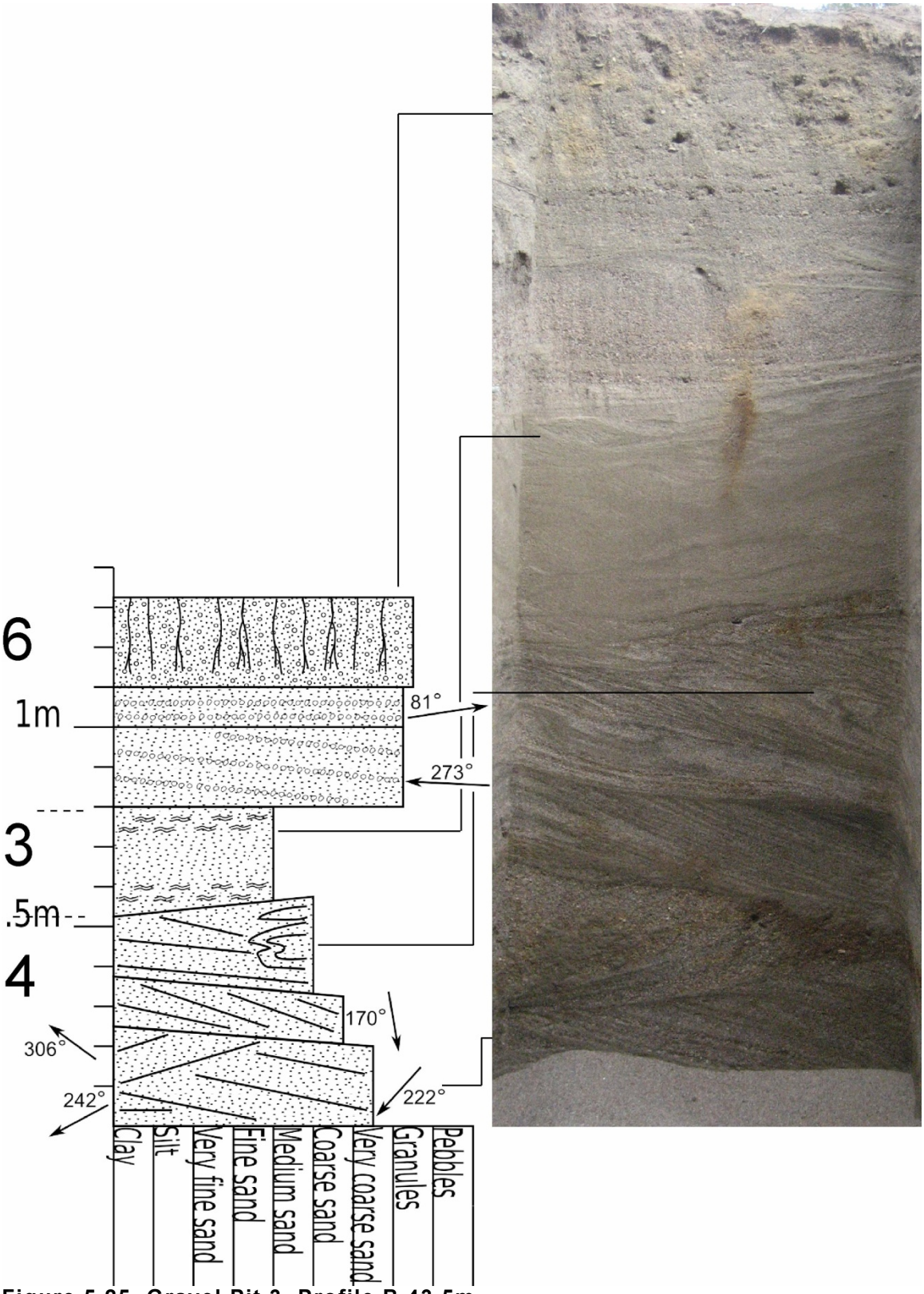

Figure 5.25. Gravel Pit 3, Profile B 43.5m

1C. Very Fine-Grained to Medium-Grained Sand

Throughout this lithofacies association, the bedforms present are ripple cross-lamination, climbing ripple cross-lamination, parallel-lamination, as well as massive layers (Fig. 5.26). The ripple cross-lamination is most commonly seen in well-sorted fine-grained sand and medium-grained sand, although they are also present within medium-grained to coarse-grained sand in profile A0m. Thicknesses of ripple bedding typically averages 2 to 3cm in thickness. The next abundant bedform, parallel-lamination, occurs in medium-grained sand, and coarse-grained sand in profile A0m. Thickness of parallel layers average 1 to 2mm. Commonly interbedded with layers of ripple cross-stratification are massive beds (e.g. B0m profile) as well as cimbing-ripple cross-lamination (e.g. B16.5m profile). Massive layers are seen in both fine-grained sand as well as medium-grained sand, and range in thickness from 3 to 9cm. Climbing ripple cross-lamination is present in medium-grained sand, with thicknesses averaging 2 to 3cm. Paleocurrent directions for this lithofacies are south to southwest (Fig. 5.27).

Figure 5.26. Ripple cross-stratification, parallel-stratification, and massive layers of lithofacies 1C

A section of this lithofacies also overlies lithofacies 2C in profile A 0m. It is comprised of very fine- to medium-grained sand, layers of ripple cross-lamination, and trough cross-stratification, as well as a massive layer in contact with unit 4 (Fig. 5.15). Contacts between layers within this unit and with overlying unit 4 are wavy, and contacts with underlying unit 2 as well as unit 4 are abrupt. Paleocurrent direction of

this section trends southwest (Fig. 5.28), which is consistent with the paleocurrent directions of ripple cross-stratification underlying lithofacies 2C (Fig. 5.27).

A section 14cm thick of this lithofacies is also apparent in profile B 43.5m between lithofacies associations 4C and 6C. Contacts with underlying 4C and overlying 6C both appear quite abrupt (Fig. 5.25). This may represent a slump event.

Contact with overlying unit 2C (profile A0m) appears gradational, whereas the contact with unit 4C (e.g. B16.5m) appears abrupt and erosive.

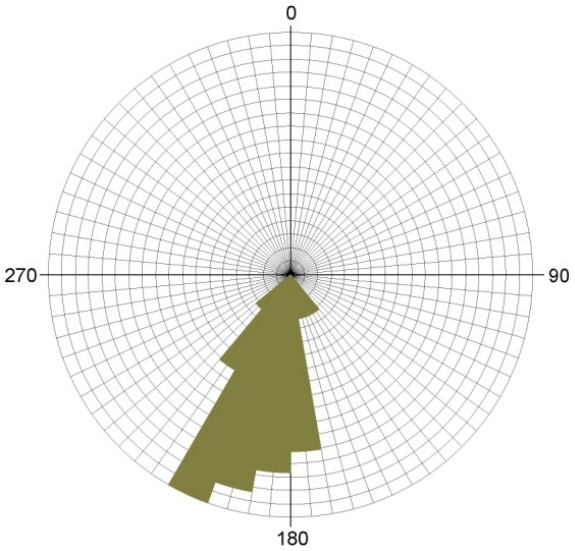

Figure 5.27. Rose diagram for lithofacies 1

2C. Very Fine-Grained to Coarse-Grained Sand

This lithofacies is dominantly composed of planar cross-stratified very fine-grained to fine-grained sand, however at the contact with lithofacies 1C (Fig. 5.15) there is coarse-grained sand as well. Planar cross-stratified layers are generally1 to 2mm thick, composed of dark laminae rich in magnetite interbedded with layers containing little to no magnetite (Fig. 5.28). In profile A 0m, overlying the stratified sands in Figure 5.28 is low-angle, planar cross-stratification, occasionally with bundled upbuilding (Fig. 5.29). This cross-stratification is present in profile A0m between lithofacies 1C and 3C (Fig. 5.15), although it is generally underlying lithofacies association 4 (e.g. profiles A 23m, B23m, and B28m). Upper and lower contacts are quite gradual.

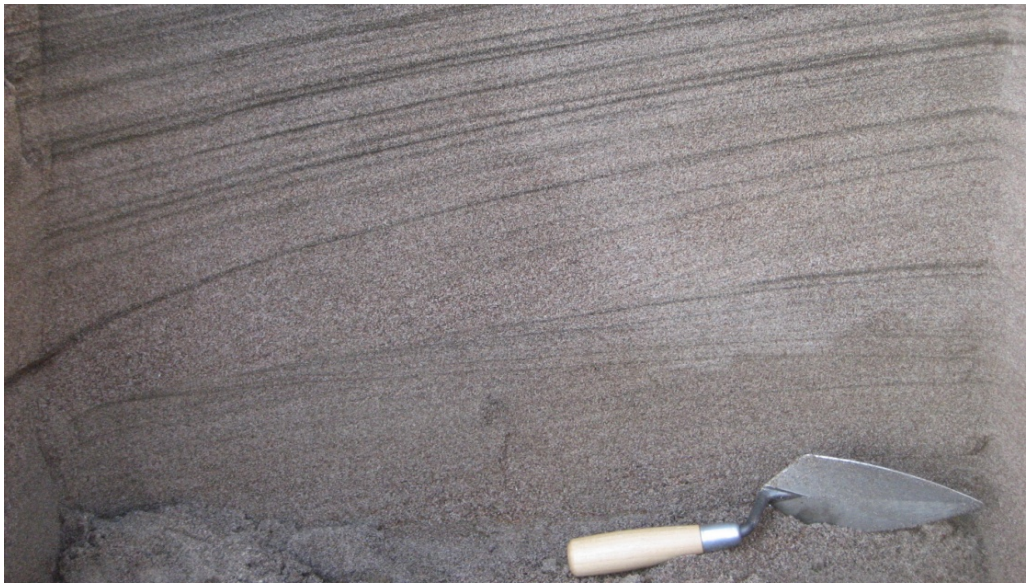

Figure 5.28. Planar cross-stratified sand comprising lithofacies 2C

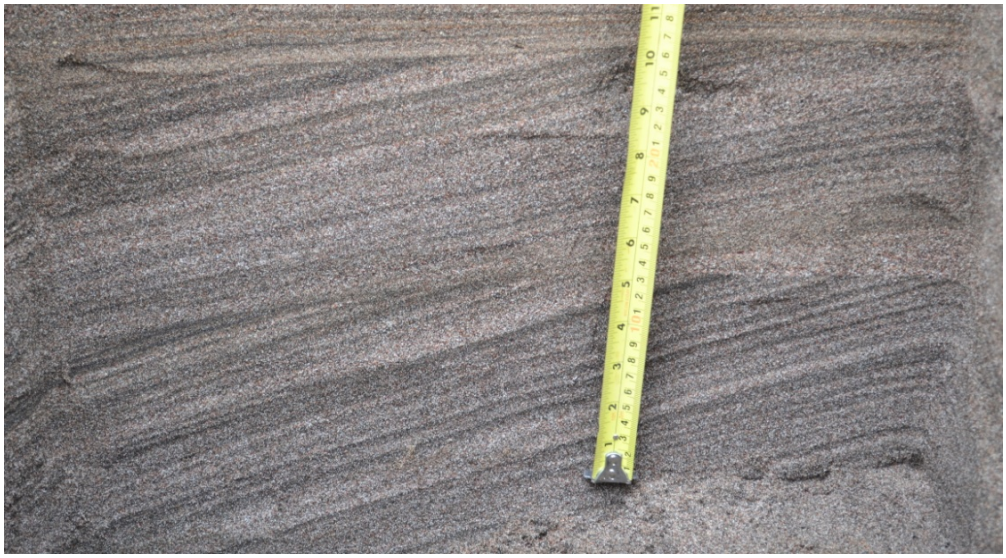

Figure 5.29. Planar cross-stratification with magnetite-rich dark laminae

3C. Very Fine-Gained to Fine-Grained Sand

This lithofacies is only seen within profile A 0m, composed of well-sorted very fine-grained and fine-grained sand. Ripple cross-lamination and trough cross-lamination is present, both bedforms average 2cm in thickness. Contact with underying lithofaces association 2C is quite abrupt, and the contact with overlying lithofacies 4C appears abrupt and wavy (Fig. 5.15). Paleocurrent directions for thislithofacies association trend south to southwest (Fig. 5.30).

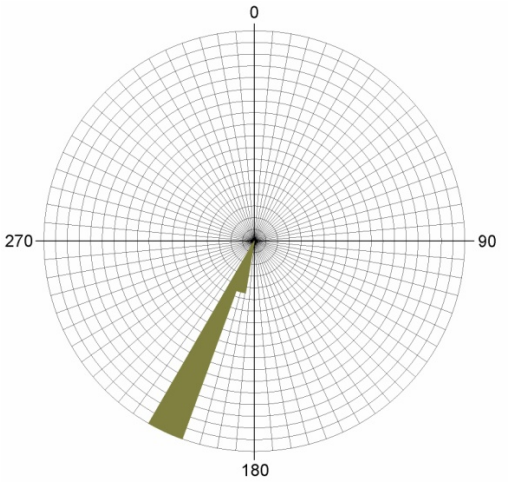

Figure 5.30. Rose diagram for section of lithofacies association 3C

4C. Medium-Grained to Coarse-Grained Sand

This lithofacies consists of dominantly planar cross-stratified layers of medium-grained to coarse-grained sand. Layer thicknesses are fairly consistent throughout all of the profiles,generally 2 to 3mm. Magnetite concentration varies throughout the unit, and occasional pebbles up to 2cm in diameter are present. There are commonly reactivation surfaces seen throughout the profiles, and a variety of paleocurrent directions (Fig. 5.31).

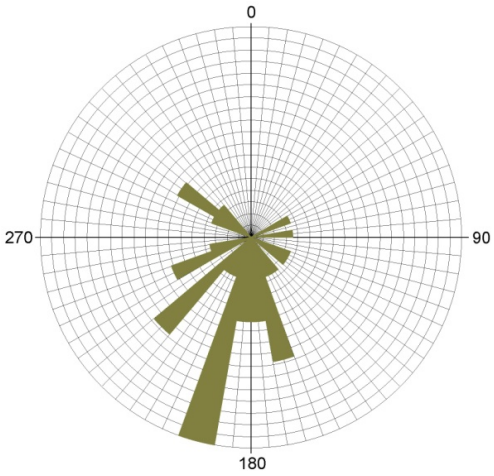

Figure 5.31. Rose Diagram for lithofacies association 4C

A normal fault displacing fine-grained to medium-grained high-angle planar cross-stratified sand beds is present within this lithofacies in profile A 43.5m (Fig. 5.32). Displacement appears to extend for 3cm, and depth is difficult to discern but likely extends to ~11cm and possible deeper. The contact with overlying low-angle planar

cross-stratified sand layers of the same lithofacies association is erosive and very abrupt.

In profile B 43.5m, the bedding in one 20 to 25cm thick section appears disturbed (Fig. 5.33). There is an abrupt contact with 1C, which may represent a slump event that disturbed the layers of this lithofacies association as it slid downslope (from left to right in Fig. 5.25).

Lastly, in profile A 28m trough cross-stratificaton is present (Fig. 5.34). This bed is ~8cm thick, and the only location trough cross-stratified layers were identified within this lithofacies throughout the profiles.

Figure 5.32. Normal fault displacing layers of lithofacies association 4C

Figure 5.33. Disturbed bedding revealed in lithofacies association 4C

Figure 5.34. Trough cross-stratification within lithfacies association 4C

5C. Fine-Grained to Medium-Grained Sand

Interbedded with lithofacies 3C are layers of ripple cross-stratification, generally 5cm thick (Fig. 5.35 & 5.36). On the basis of grain-size and stratigraphic position, this lithofacies is likely represented within profile A 0m, although ripple cross-stratification is not apparent (Fig. 5.15).

Contacts with overlying and underlying lithofacies associations appear abrupt due to the easily identified grain-size difference, however only the upper contacts are erosive.

Figure 5.35. Ripple cross-stratification within lithofacies 5C

Figure 5.36. Lithofacies 5C appearing massive

6C. Fine-Grained to Coarse-Grained Sand Matrix with Granules and Pebbles

This lithofacies is dominated by low-angle planar cross-stratified layers of matrix-supported granules and pebbles. Paleocurrent directions average 246° (southwestward). Grain-size of the matrix as well as the granule and pebble bedding varies throughout the profiles. Fine-grained to medium-grained sand matrix supported granules and pebbles averaging 1cm in diameter appear cross-stratified in profile B 43.5m (Fig. 5.37), and are massive due to bioturbation in profile B 28m. Fine-grained to medium-grained sand matrix also contain granules and pebbles up to 3cm in diameter, appearing massive in profiles A 23m, A 16m, and A 0m. Lastly, cross-stratified coarse-grained to very coarse-grained sand layers with granules and pebbles up to 3cm in diameter are seen in profiles A 43.5m (Fig. 5.38), as well as A 28m. Contacts with underlying lithofacies associations 5C and 6C appear abrupt and erosive.

Figure 5.37. Low-angle planar cross-stratification of fine-grained sand to pebbles up to 1cm in diameter, within lithofacies association 6C. Laminae dip southward.

Figure 5.38. Low-angle planar cross-stratification of coarse-grained sand to pebbles up to 3cm in diameter, seen within lithofacies association 5C

7C. Fine-Grained Sand

Abruptly overlying lithofacies 6C, this lithofacies association is composed of well-sorted fine-grained sand. The majority of this sequence contains roots, appearing strongly biourbated (Fig. 5.15). However, the lower 6cm reveal ripple cross-lamination 2cm thick.

5.4 Mackenzie Roadcut

Since the Mackenzie roadcut (Fig. 4.1) had been shored, a series of exposures were dug out along the east side of the road to trace the lithofacies associations laterally as well as vertically (Fig. 5.39). Exposures were dug roughly every 5m, or closer to capture contacts between lithofacies. A fence diagram showing stratigraphic columns for all of the profiles (Fig. 5.40), as well as stratigraphic columns and associated photos (Fig. 5.41 to 5.47) are presented below. Lithofacies 3D and 4D represent the same lithofacies association.

1D. Very Fine-Grained to Medium-Grained Sand

This lithofacies association is apparent in profiles 23m and 25m between 1 and 2m below the surface, although the only bedform identified within these profiles is ripple cross-lamination averaging 3cm in thickness. However, along the west exposure on the other side of the road this lithofacies association along the west exposure on the other side of the road extends to the surface. The west exposure reveals parallel-stratification and ripple cross-lamination within dominantly very fine-grained to fine-grained sand. Ripple cross-laminae range in thickness from 2 to 4cm while the parallel-stratified layers are typically 2 to 3mm thick. There are also massive silt laminae 1-2mm thick interbedded with cross-stratified and parallel-laminated sand layers. Paleocurrent direction of this lithofacies association trends south to southwest (Fig. 5.48).

Additional features within this lithofacies association are present, including an erosive scour and subsequent mud drape overlying ripple cross-stratification (Fig. 5.49). Another erosive scour created a wavy surface for the following deposition of ripple cross-stratification (Fig. 5.50).

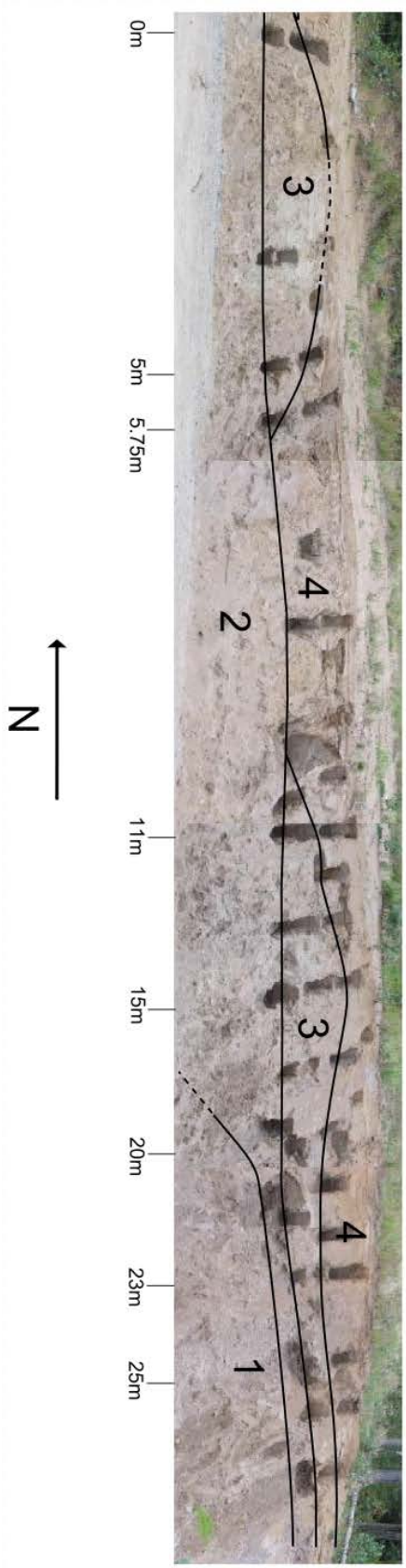

Figure 5.39. The east side of the Mackenzie Roadcut. Stratigraphic columns were created using the data collected at the distances indicated (0m, 5m, 11m, 15m, 20m, 23m, and 25m).

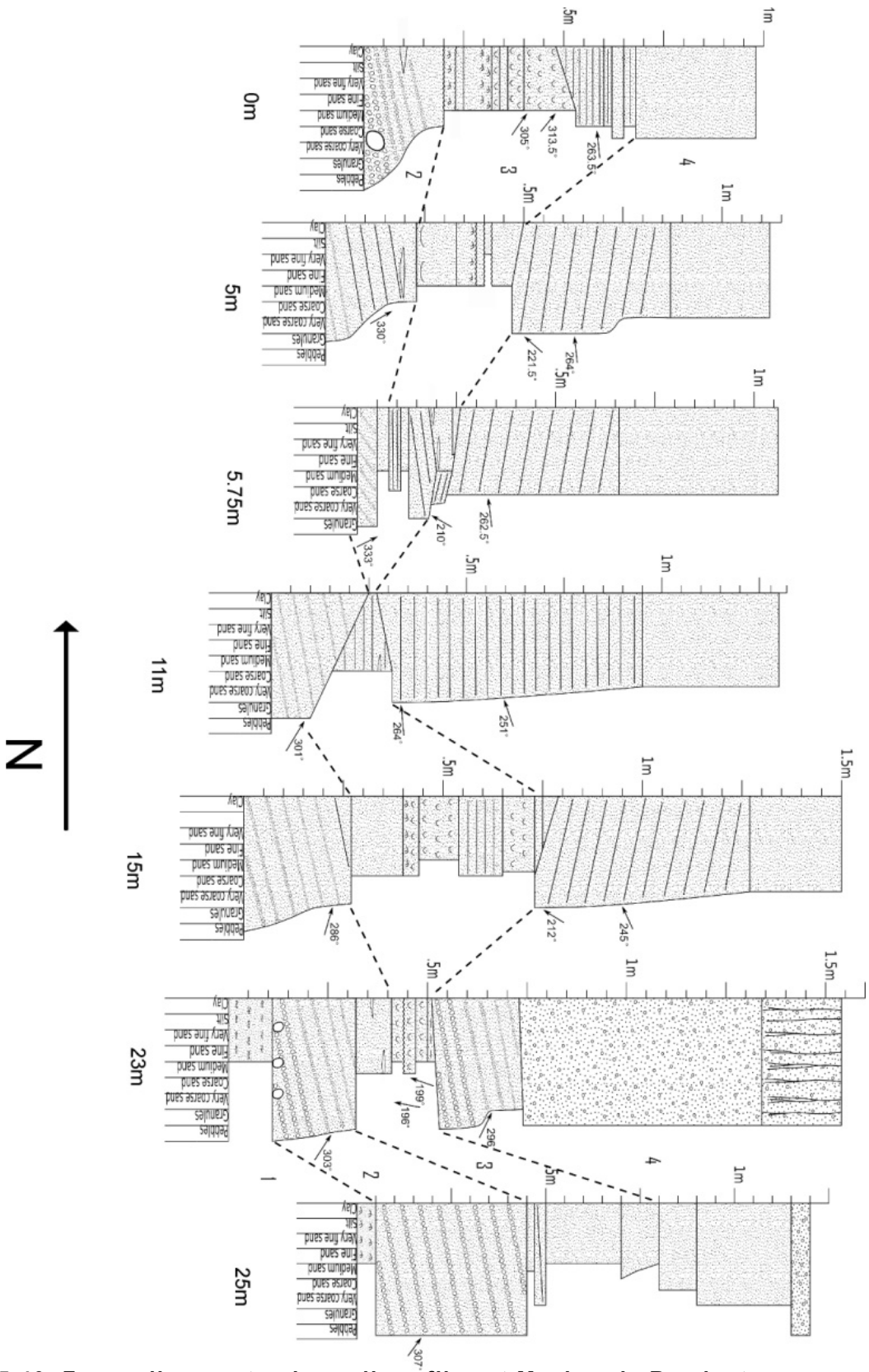

Figure 5.40. Fence diagram to show all profiles at Mackenzie Roadcut

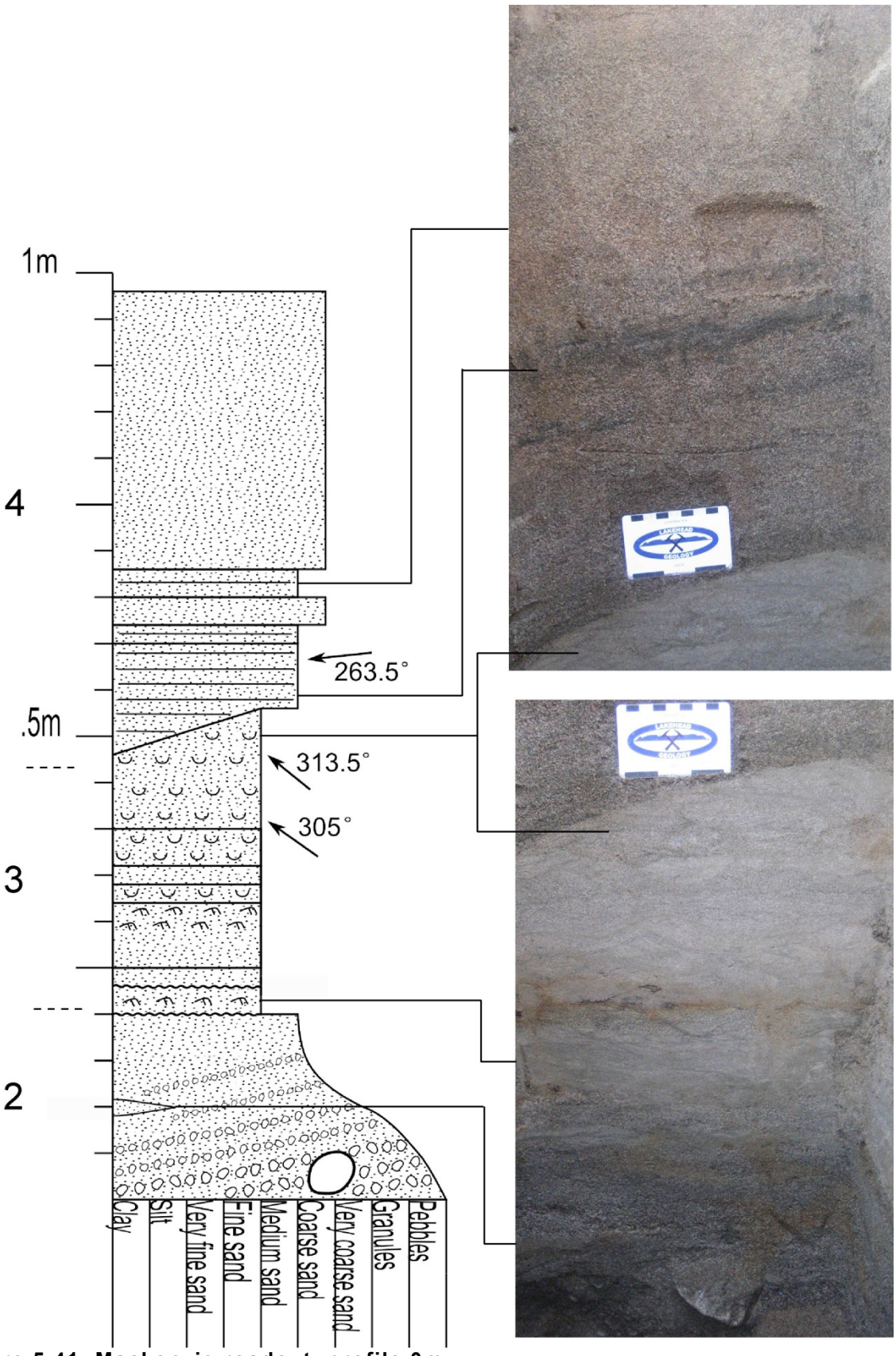

Figure 5.41. Mackenzie roadcut, profile 0m

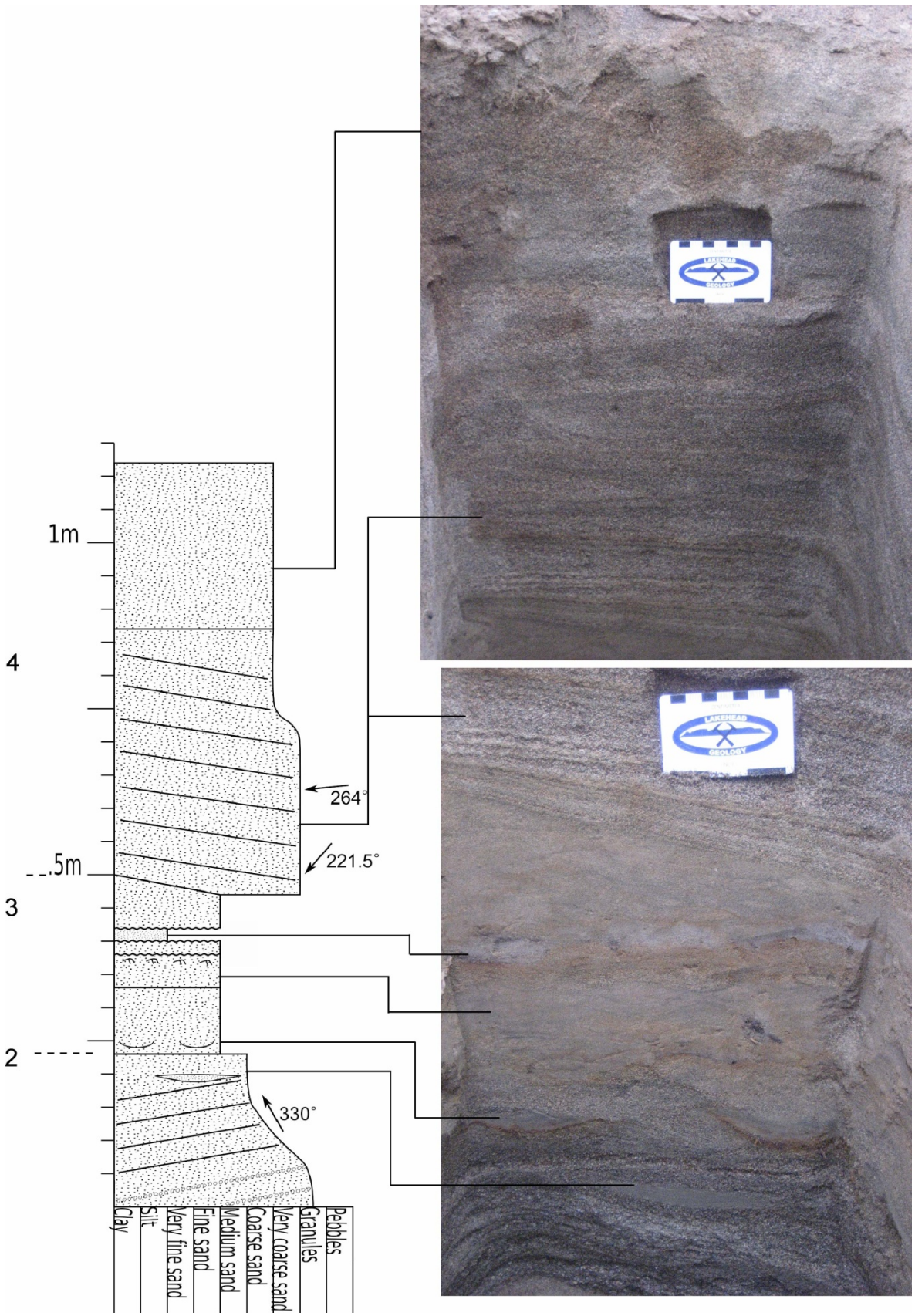

Figure 5.42. Mackenzie roadcut, profile 5m

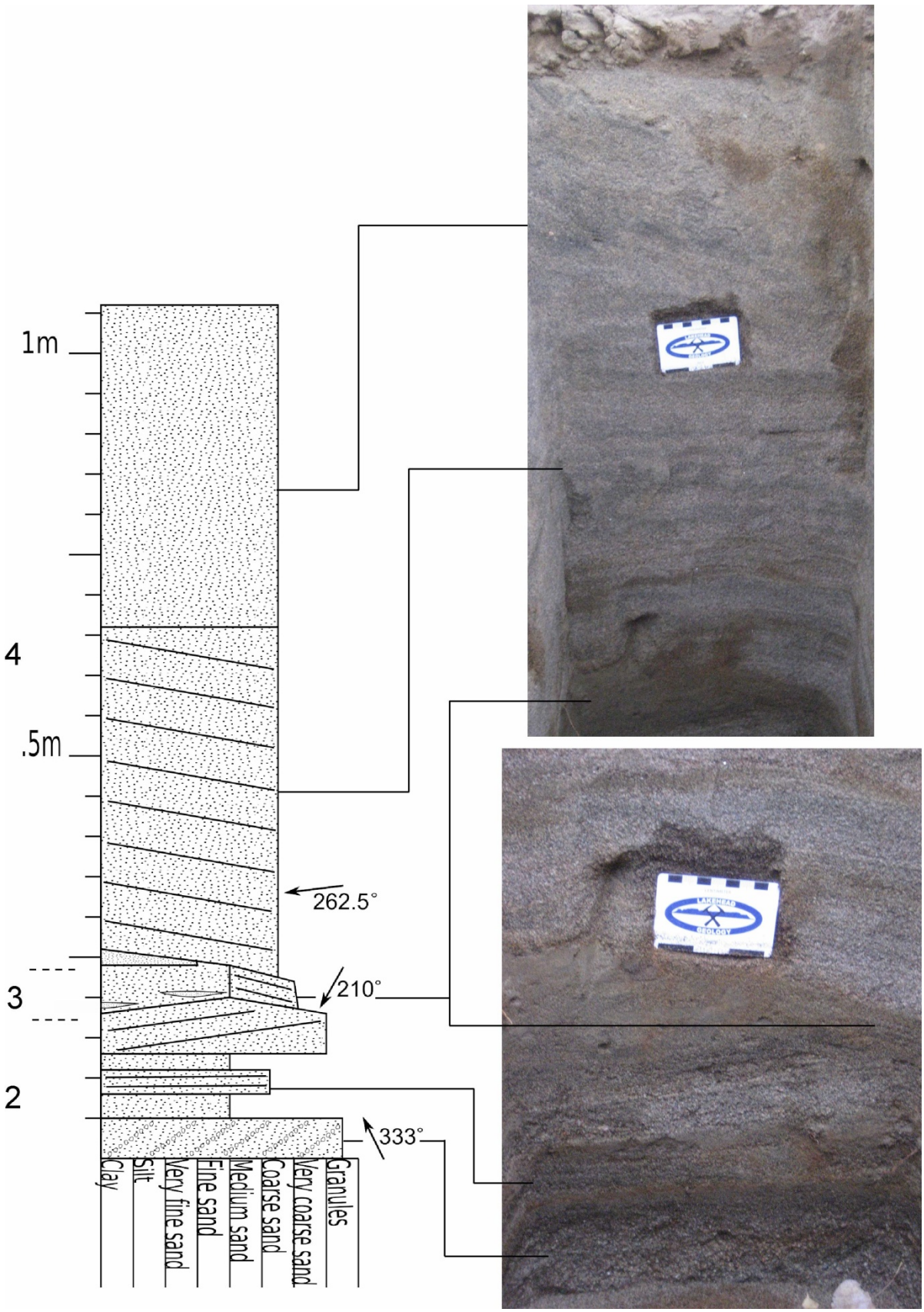

Figure 5.43. Mackenzie roadcut, profile 5.75m

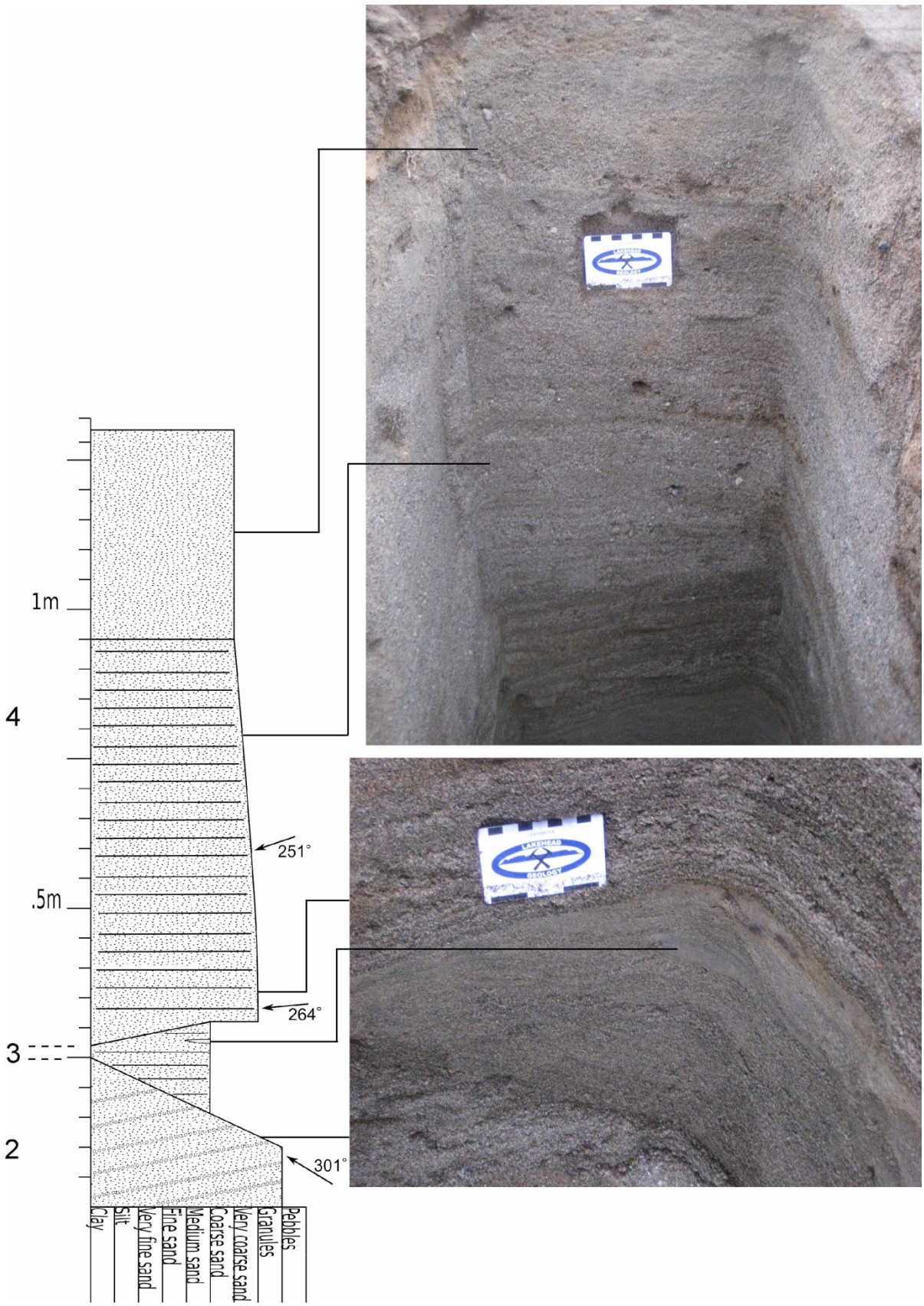

Figure 5.44. Mackenzie roadcut, profile 11m

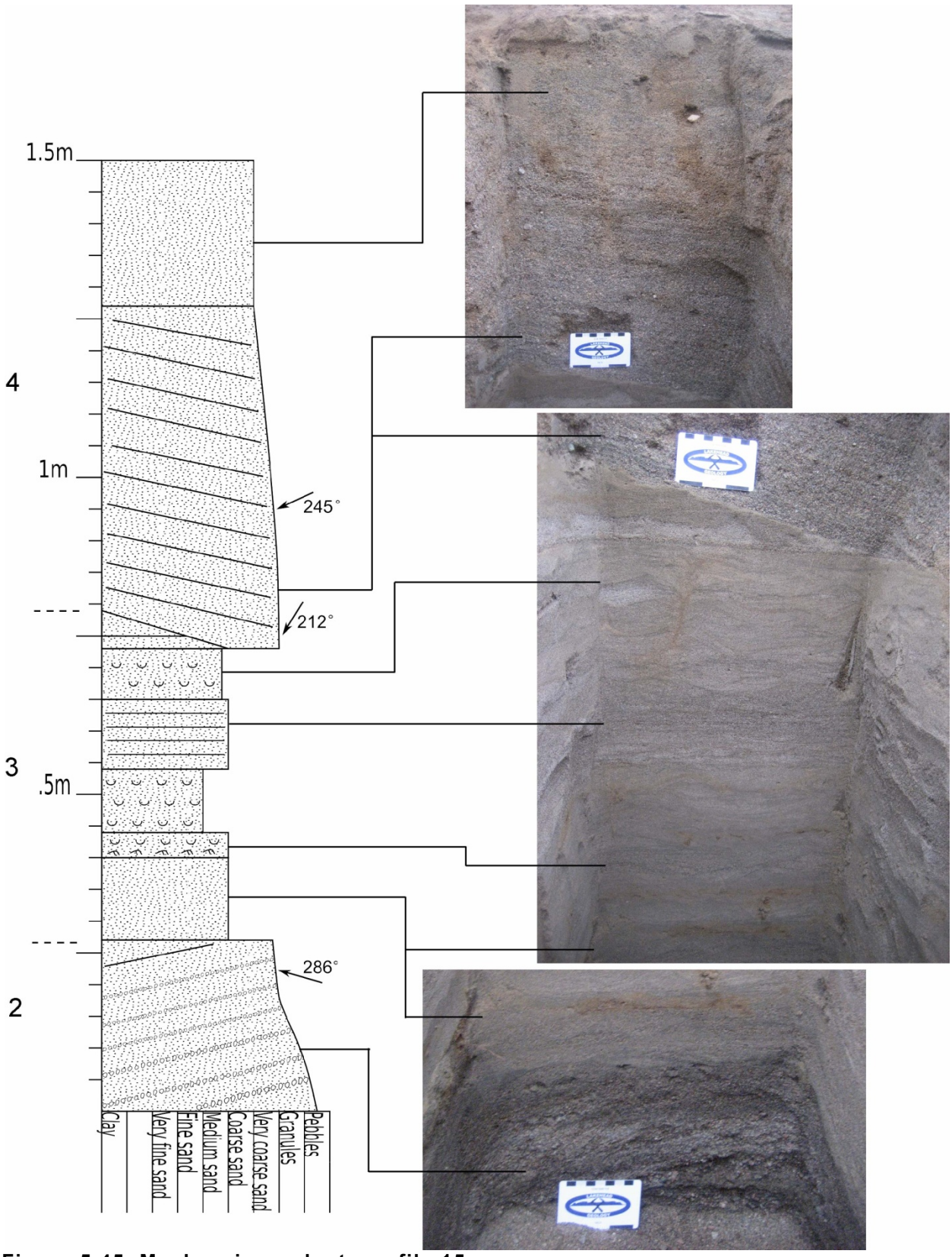

Figure 5.45. Mackenzie roadcut, profile 15m

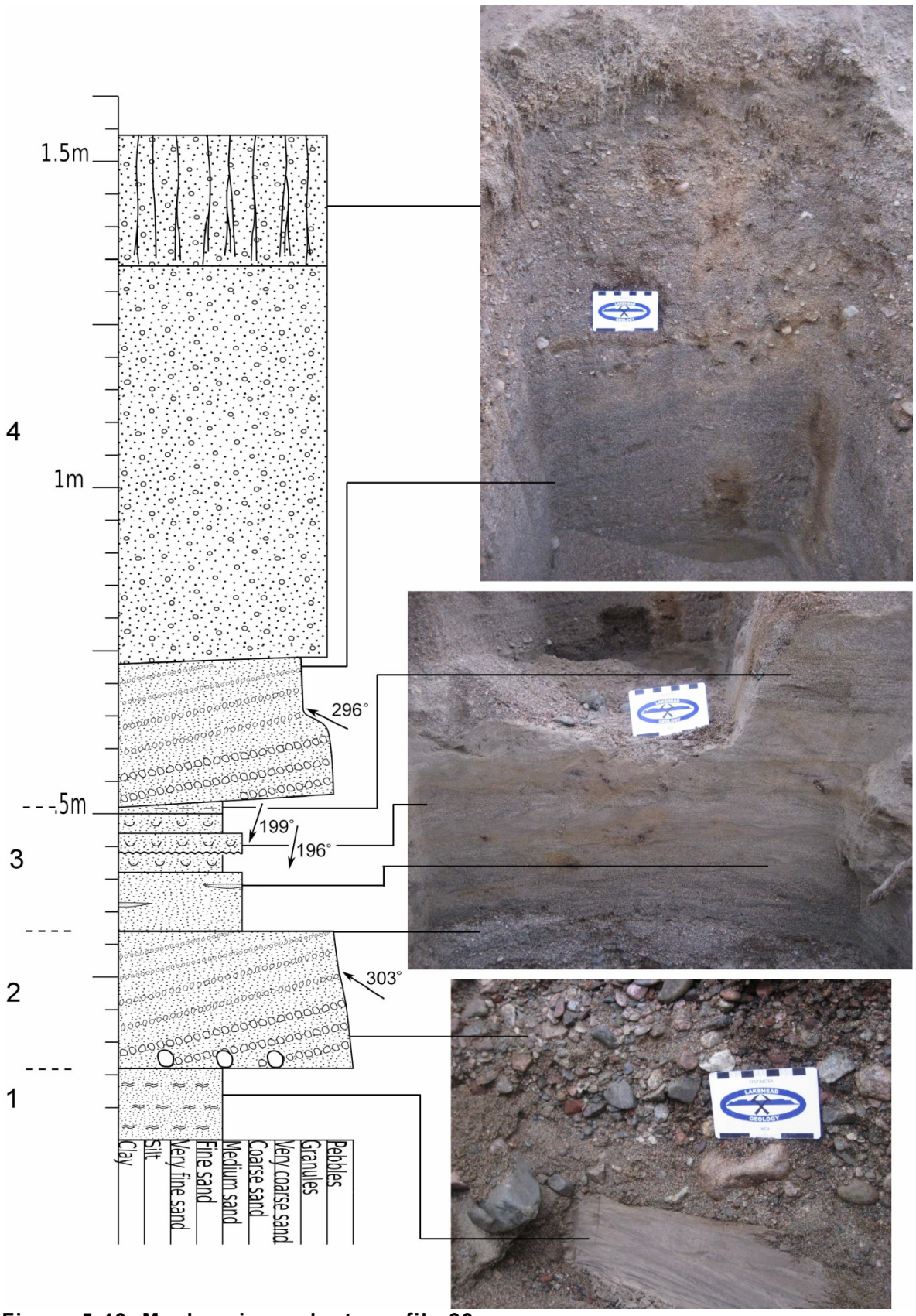

Figure 5.46. Mackenzie roadcut, profile 23m

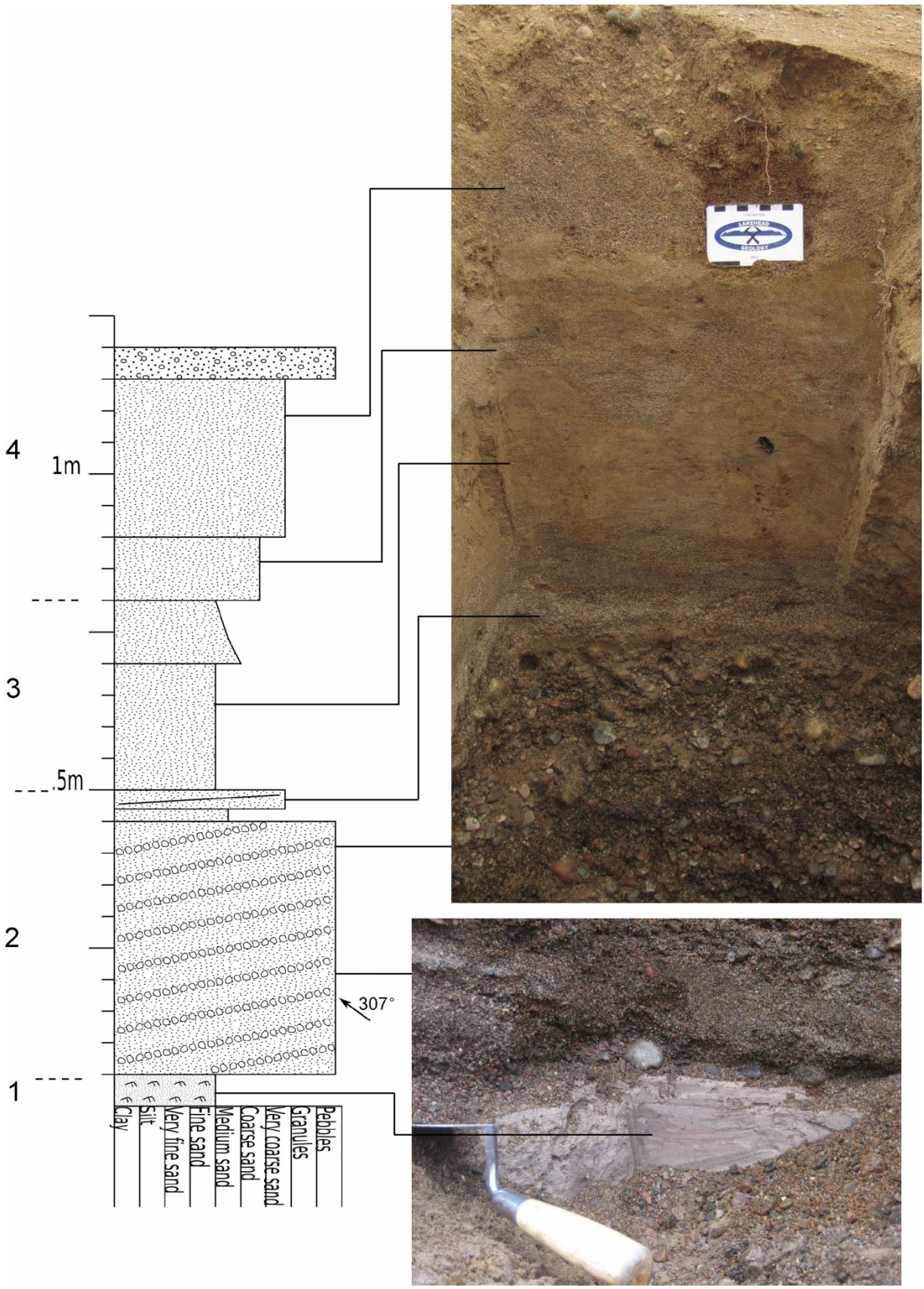

Figure 5.47. Mackenzie roadcut, profile 25m

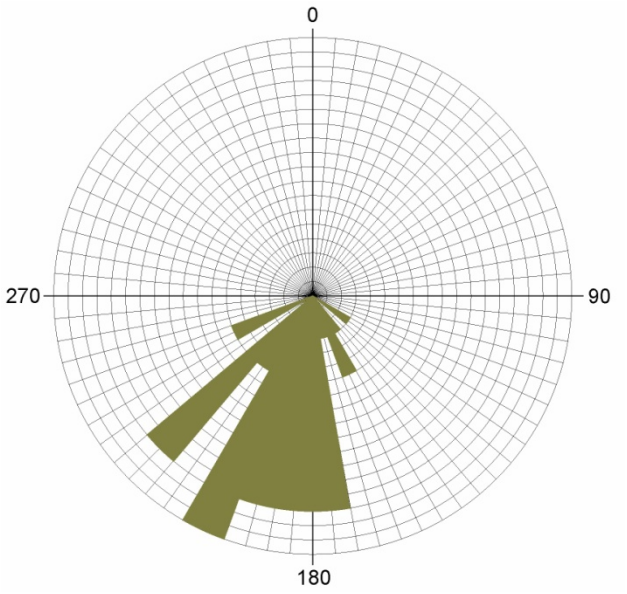

Figure 5.48. Rose diagram for lithofacies association 1D

Figure 5.49. Erosive scour and subsequent mud drape within

In the northern portion of the west exposure (around 0m to 5m in Fig. 5.50), deformation structures are also observed within this lithofacies association. One deformation structure appears to be parallel-laminated and ripple cross-stratified layers that were subsequently folded (Fig. 5.51). The fold is asymmetrical, with a fold centre pointing northward. In addition, a load structure is seen within very fine-grained to fine-grained sand (Fig. 5.52). Underlying parallel-stratification appears to be deformed into convolute bedding (Fig. 5.52).

Lastly, occasional dropstones ~6cm in diameter are present within fine-grained to medium-grained sand (Fig. 5.53).

Figure 5.50. Erosive scour followed by deposition of ripple cross-stratification

Figure 5.51. Folded parallel-lamination within lithofacies association 1D

Figure 5.52. Load Structure and Convolute Bedding within lithofacies association 1D

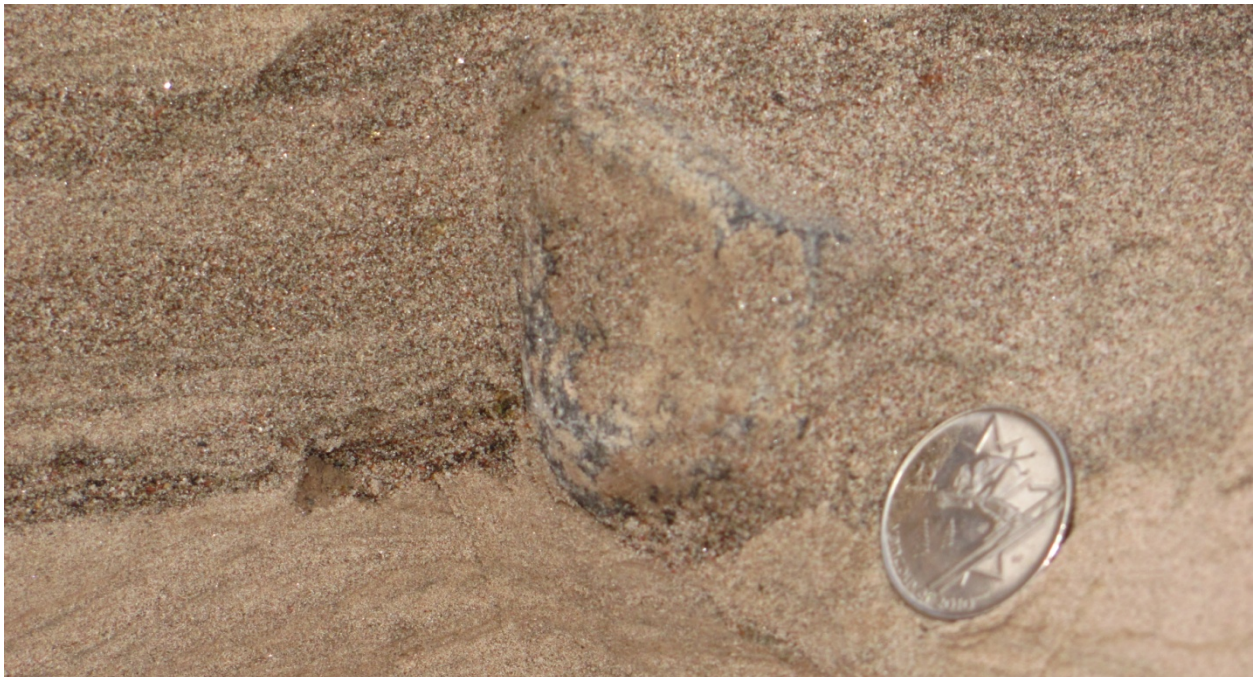

Figure 5.53. Dropstone within fine-grained to medium-grained sand of lithofacies association 1D

2D. Coarse Sand and Pebbles

The contact with lithofacies association 1D is erosive and very abrupt. Boulders up to ~25cm in diameter are present at this contact in profile 25m (Fig. 5.54). Between 15m and 20m, there was an erosive channel-shaped scour with subsequent deposition of this lithofacies association (Fig. 5.55).

At the northern end of the roadcut, only the upper and finer grains are apparent, comprising the upper 7cm of this lithofacies. This section of 2D is cross-stratified medium-grained to coarse-grained sand, with an average paleocurrent direction of 310°. The underlying sediment fines upward, from cross-stratified coarse sand and granules interbedded with pebbles up to 2cm in diameter to cross-stratified coarse-grained sand and pebbles up to 2cm interbedded with pebbles up to 8cm in diameter (Fig. 5.54). Two lenses composed of very well-sorted silt are present within the 0m and 5m profiles. Both are roughly 2cm thick and 13cm wide.

Figure 5.54. Fining upward, from pebbles and boulders up to ~25cm in diameter to medium-grained sand

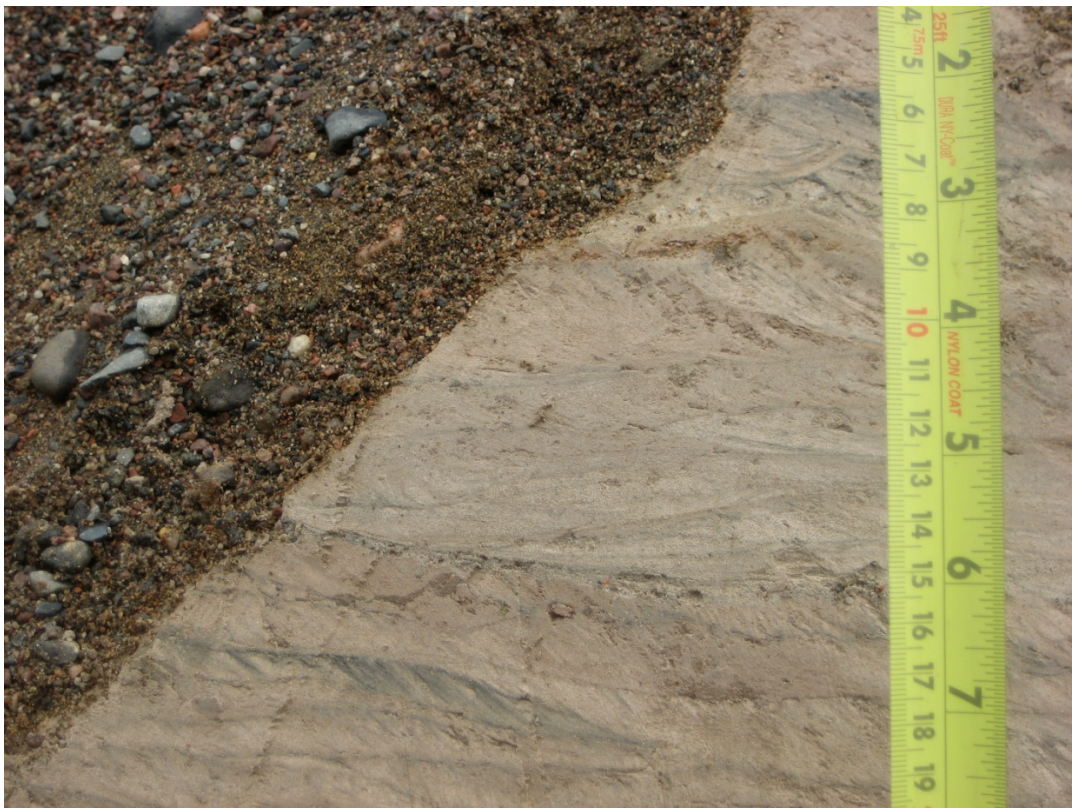

Figure 5.55. Abrupt contact of lithofacies association 1D and overlying 2D

3D. Very Fine-Grained to Medium-Grained Sand

This lithofacies is composed of well-sorted very fine-grained to medium-grained sand. Identified bedforms are trough cross-lamination, ripple cross-lamination, and parallel-stratification (Fig. 5.56). Layer thicknesses range from 2 to 10cm, thickening northward. The paleocurrent direction changes northward as well, from an average of 197° in profile 23m to 309° in profile 5m. Scallop-shaped scours are also present within this lithofacies association, infilled with silt (Fig. 5.57).

The contact with underlying lithofacies association 2D and overlying 3D appears erosive and abrupt in the majority of the profiles, although within profiles 0m and 5m, the contact appears gradual (Fig. 5.56).

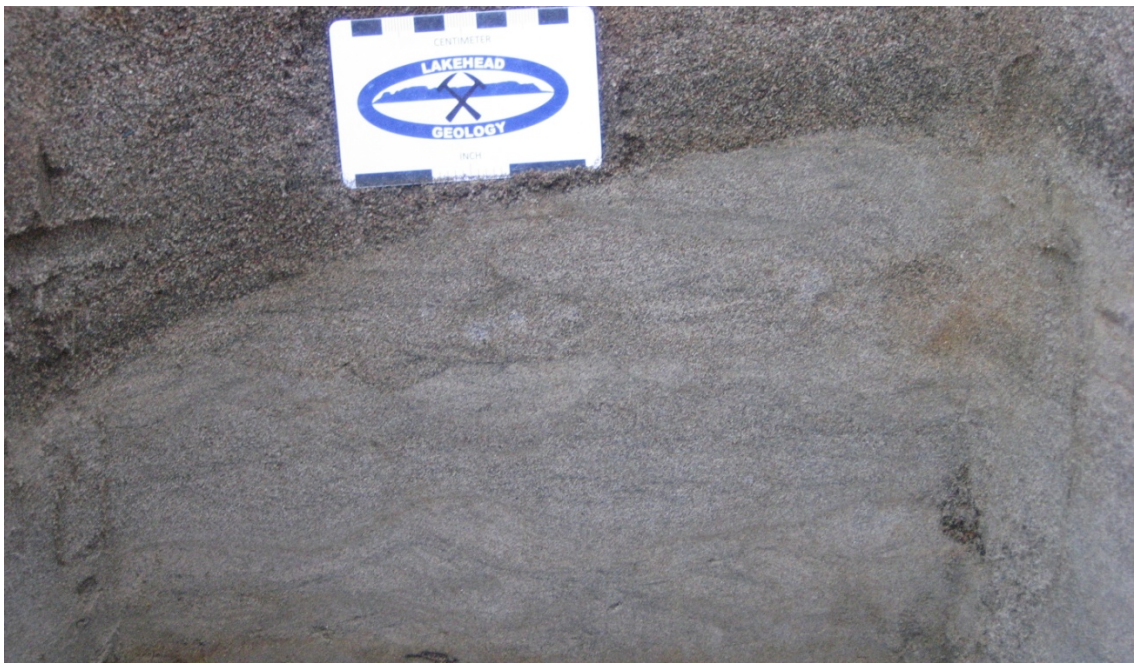

Figure 5.56. Fine-grained to medium-grained sand with trough cross-stratification and ripple cross-stratification of lithofacies association 3D

4D. Medium-Grained to Coarse-Grained Sand

The medium-grained to coarse-grained sand comprising this lithofacies is planar cross-stratified. Dark laminae are magnetite-rich, revealing low-angle and high-angle planar cross-stratification (e.g. Fig. 5.58). The thickness of these beds averages 4mm.

The upper part of this unit has been disturbed by construction, and appears to be bioturbated. The profiles south of 5.75m also reveal this lithofacies association to have occasional pebbles 1 to 2cm in diameter.

Figure 5.57. Erosive scour infilled with silt, seen in lithofacies association 3D

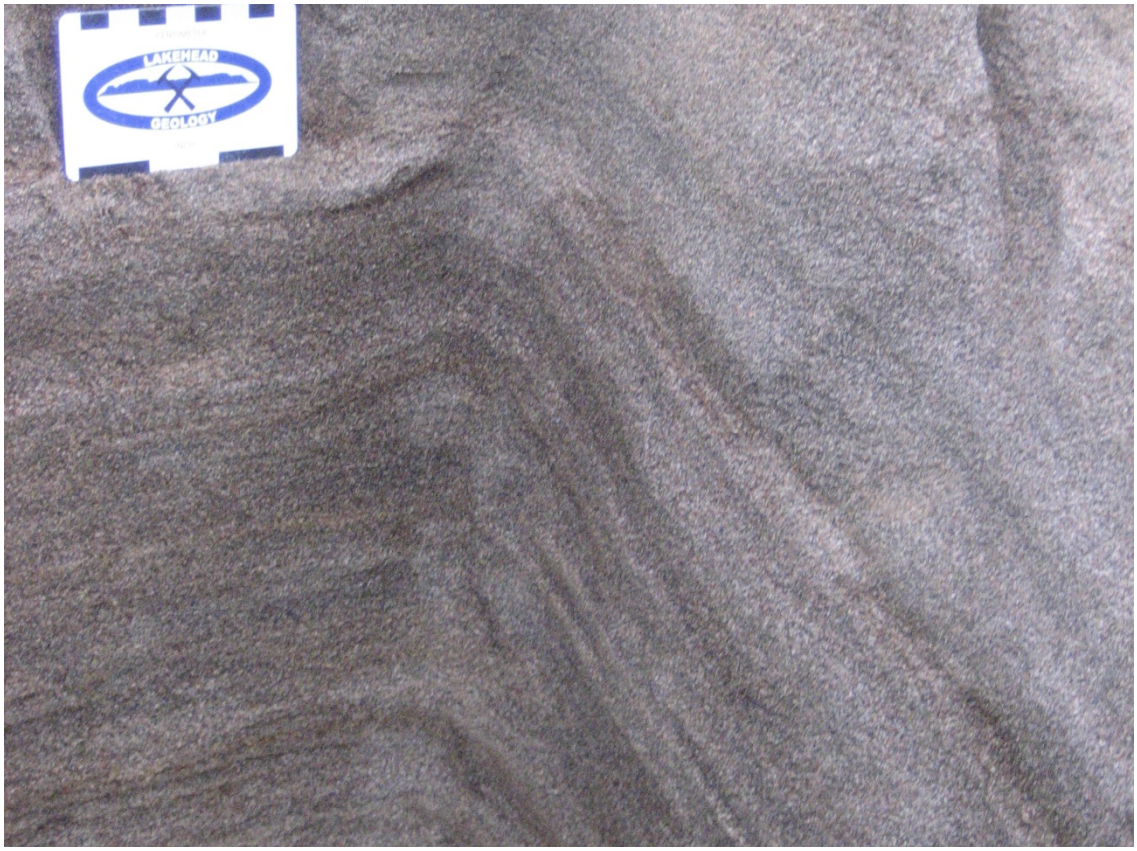

Figure 5.58. Magnetite-rich cross-stratification

5.5 Mackenzie South Roadcut

Located South of the Mackenzie Roadcut (Fig. 4.1), the South Roadcut is ~14m lower in elevation along the same road. The surface has been disturbed by both construction and bioturbation, making distance below surface difficult to measure. Stratigraphic columns and photos of the two identified lithfacies are shown in Figure 5.59.

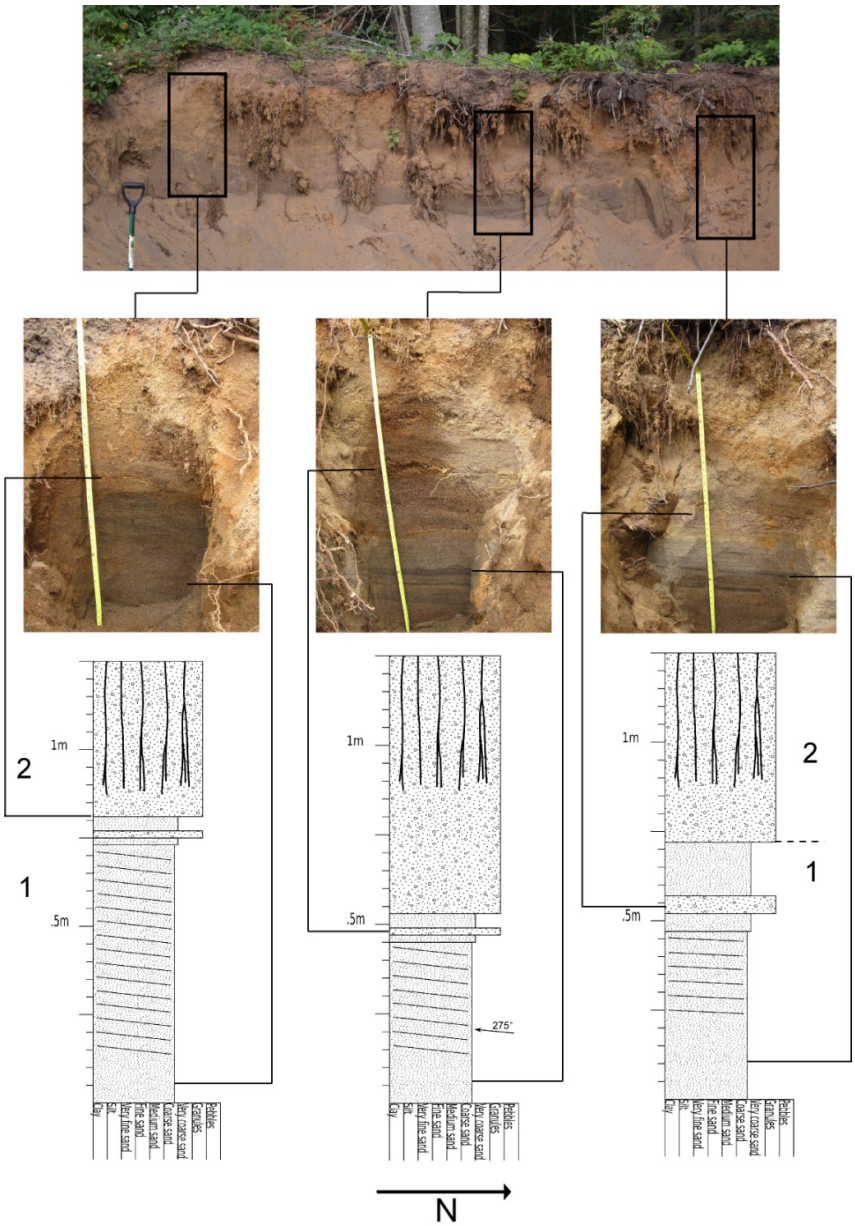

Figure 5.59. Stratigraphic column of Mackenzie South Roadcut and associated photos

1E. Fine-Grained to Granules

The lowest section of this lithofacies appears massive, likely due to disturbance by the groundwater flowing through the sand (Fig. 5.60). Overlying the massive sand is low-angle planar cross-stratified medium-grained to coarse-grained sand (Fig. 5.61). Planar cross-stratified layers average 1cm in thickness, and contain magnetite-rich dark laminae. Within this lithofacies association is a layer of medium-grained to coarse-grained sand containing few granules, thinning southward from 6cm to 2cm in thickness (Fig. 5.59).

Figure 5.60. Planar cross-stratified sand overlying massive sand comprising lithofacies 1E

Figure 5.61. Low-angle planar cross-stratified sand composing lithofacies association 1E

2E. Medium-Grained Sand to Pebbles

This lithofacies is composed of medium-grained to coarse-grained sand layers interbedded with coarse sand to sub-angular pebbles up to 1cm in diameter (Fig. 5.62). Bioturbation has severely affected the upper section, causing it to appear massive.

Figure 5.62. Pebble layers within medium-grained to coarse-grained sand composing lithofacies association 2E

5.6 Mackenzie Inn Exposure

Located west of the Mackenzie South roadcut (Fig. 4.1), the Mackenzie Inn exposure extends to 550cm below surface and reveals four lithofacies associations (Fig. 5.63). Stratigraphic columns were created for this exposure with accompanying photos of each lithofacies (Fig. 5.64 and 5.65). Lithofacies 2F and 3F represent the same lithofacies association

1F. Reverse Graded Clayey-Silt to Fine-Grained Sand

Reverse graded beds comprise this lithofacies association, ranging in grain-size from clayey-silt to fine-grained sand (Fig. 5.66 & 5.67). The most abundant reverse graded layers are very fine-grained to fine-grained sand ranging in thickness from 3 to 6cm. Thinner reverse graded layers of clayey silt to very fine-grained sand are next in abundance, and average 1cm in thickness (Fig. 5.66). Contacts of clayey silt or silt layers with the underlying graded layer are commonly wavy (Fig. 5.67).

2F. Massive Layers of Medium-Grained Sand to Granules

The contact of this lithofacies with the underlying lithofacies association 1F appears gradational. Overlying the uppermost graded layer of lithofacies association 1F is a 5cm thick layer of massive fine-grained to medium-grained sand matrix containing coarse-grained sand grains and granules (Fig. 5.68). There also appears to be loading of coarser sand grains and granules from lithofacies 2F into the underlying massive layer.

The remainder of this lithofacies may appear to be graded, however these are massive layers with loading and infiltration. Layers composed of very coarse-grained sand with granules and few pebbles are interbedded with massive medium-grained sand to coarse-grained sand. The finer sand grains have infiltrated the empty spaces between larger grains of underlying beds, and also been loaded by overlying coarser grains (Fig. 5.68). The finer layers composed of medium-grained sand to coarse-grained sand range from 1 to 3cm in thickness, and the coarser layers are dominantly 2 to 3 cm thick, composed of very coarse-grained sand with granules and a few pebbles.

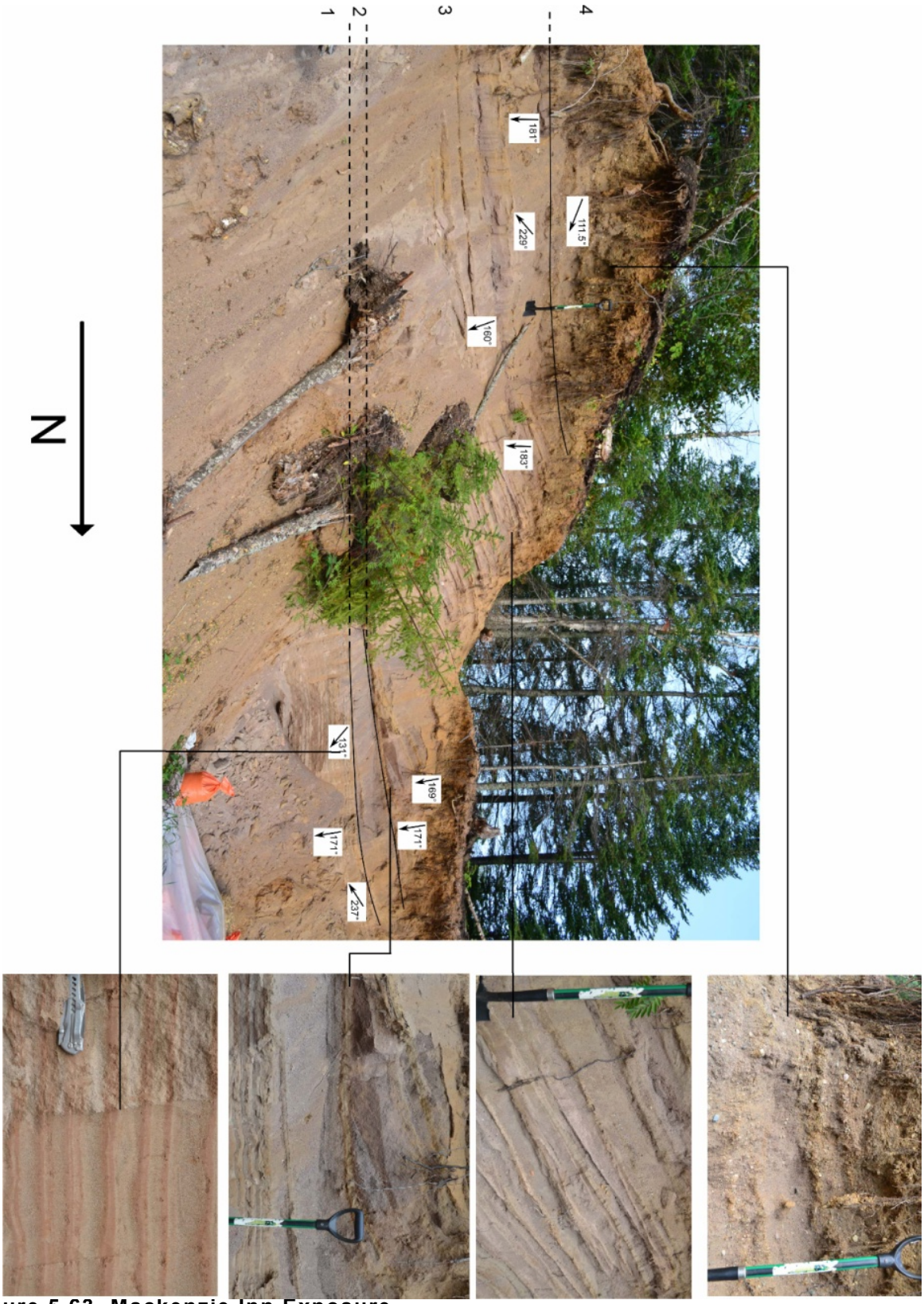

Figure 5.63. Mackenzie Inn Exposure

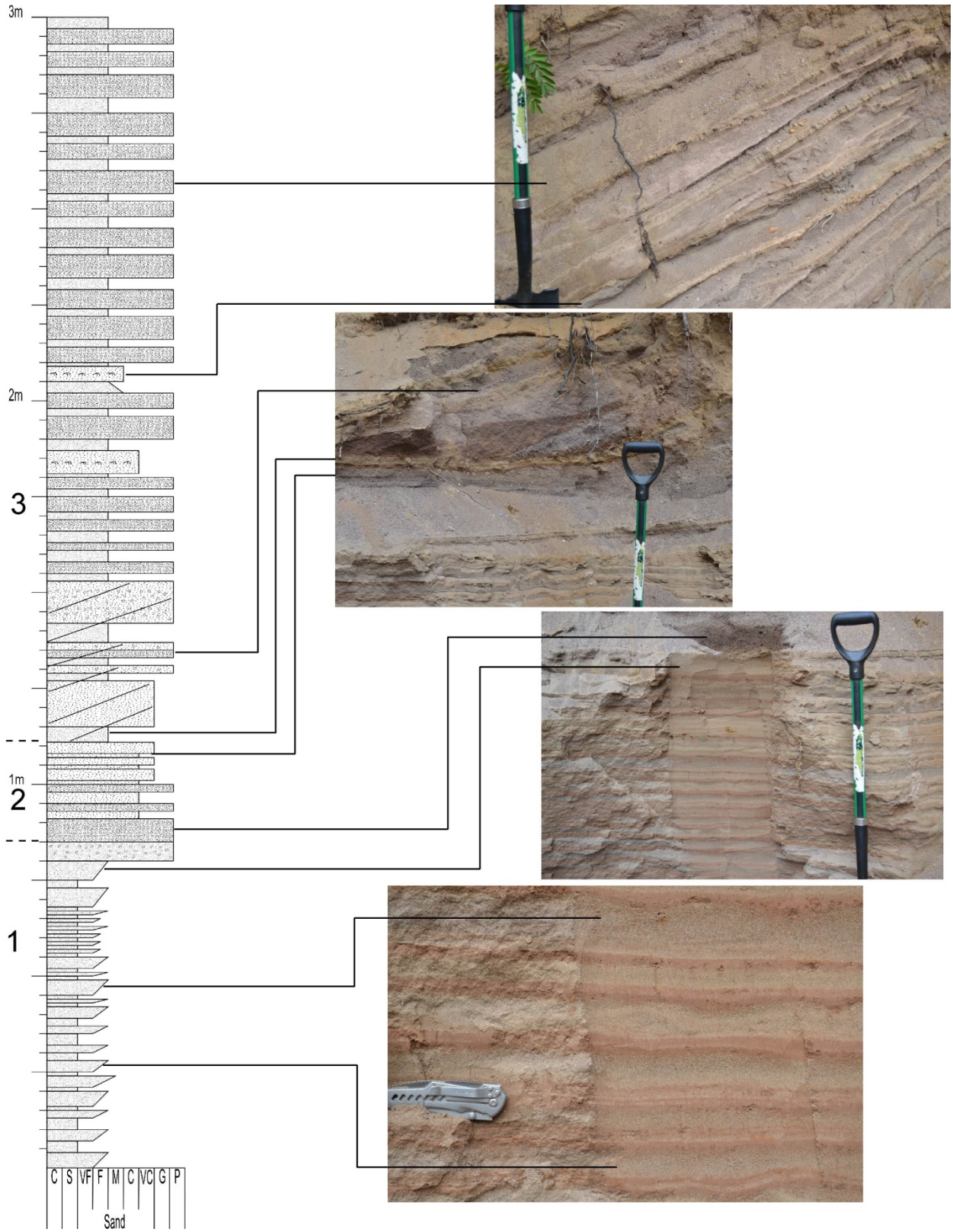

Figure 5.64. Lower section of the Mackenzie Inn Exposure, showing lithofacies associations 1F, 2F and 3F

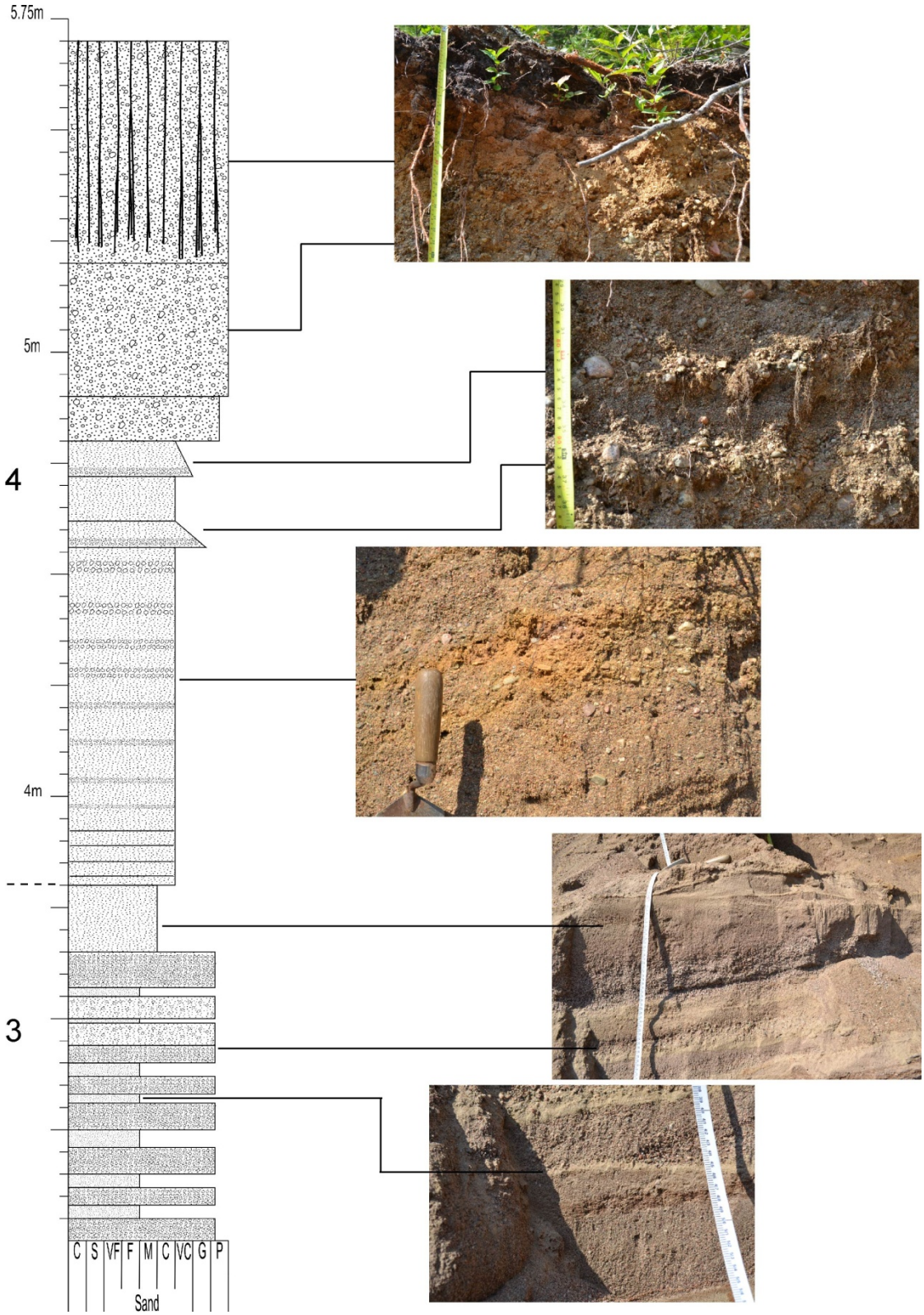

Figure 5.65. Upper section of Mackenzie Inn exposure, showing lithofacies associations 3F and 4F

Figure 5.66. Thin reverse graded layers within lithofacies association 1F

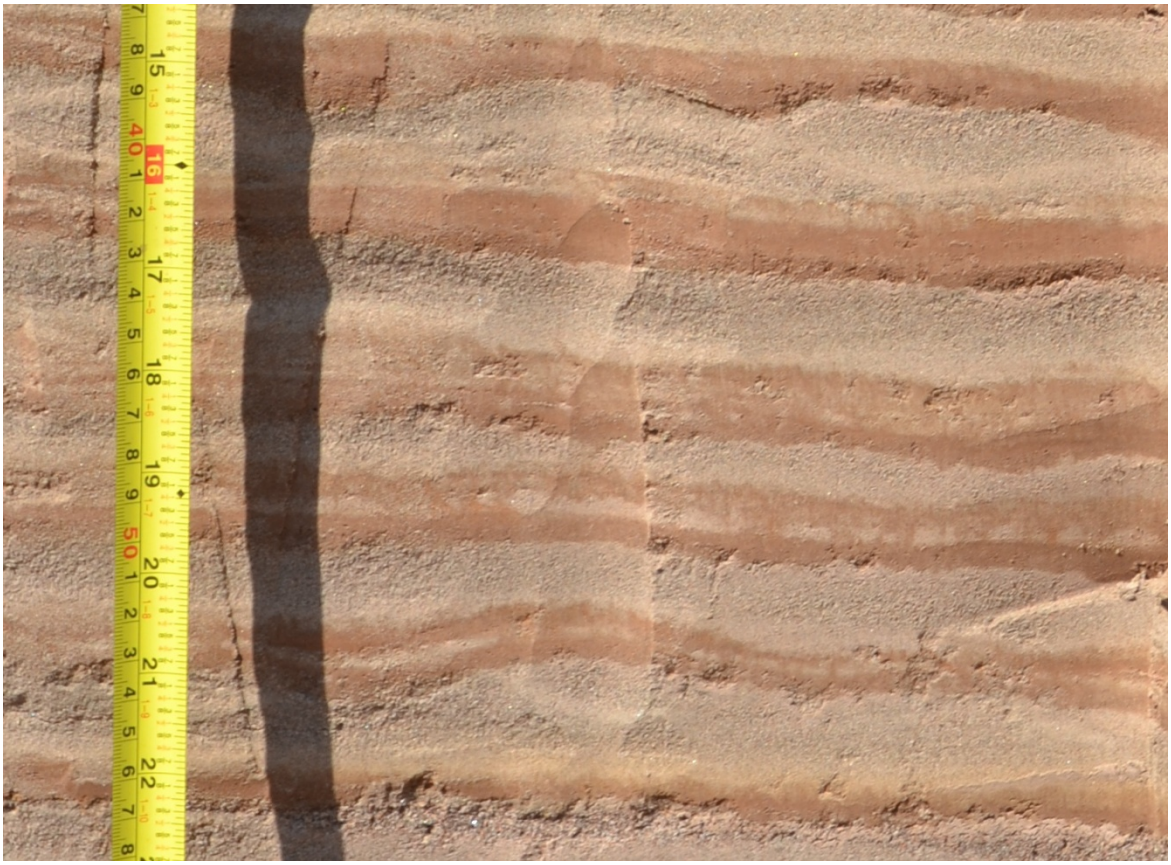

Figure 5.67. Wavy contacts of layers within lithofacies association 1F

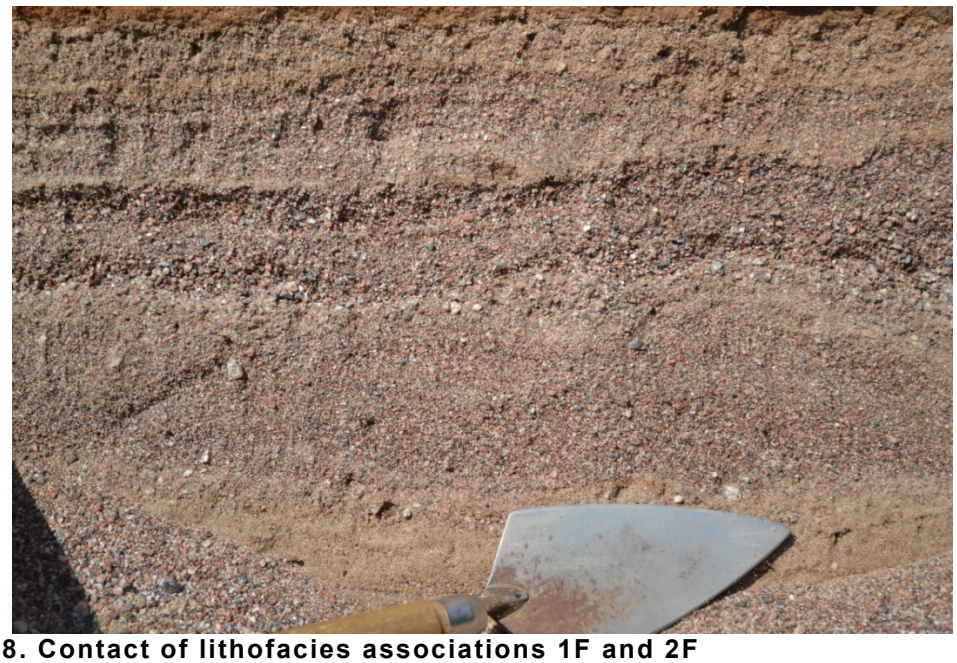

Figure 5.68. Contact of lithofacies associations 1F and 2F

3F. Cross-Stratified Fine-Grained Sand and Coarse-Grained Sand to Granules

Abruptly overlying 2F is large-scale low-angle planar cross-stratification (Fig. 5.65 & 5.69), dominated by well-sorted fine-grained sand layers 2 to 6cm thick interbedded with massive poorly-sorted layers. Poorly-sorted layers are composed of massive very coarse-grained sand to granules in layers ranging in thickness from 2 to 12cm.

Figure 5.69. Cross-stratification of lithofacies association 3F

Present although uncommon within this lithofacies association are layers containing ripple cross-lamination. One rippled layer of fine-grained to medium-grained sand is 4cm thick. It is overlain by a layer of fine-grained sand 2cm thick and underlain by a reverse graded layer of medium-grained sand to fine-grained sand (Fig. 5.70). The second example is seen within a layer of medium-grained sand to coarse-grained sand (Fig. 5.71).

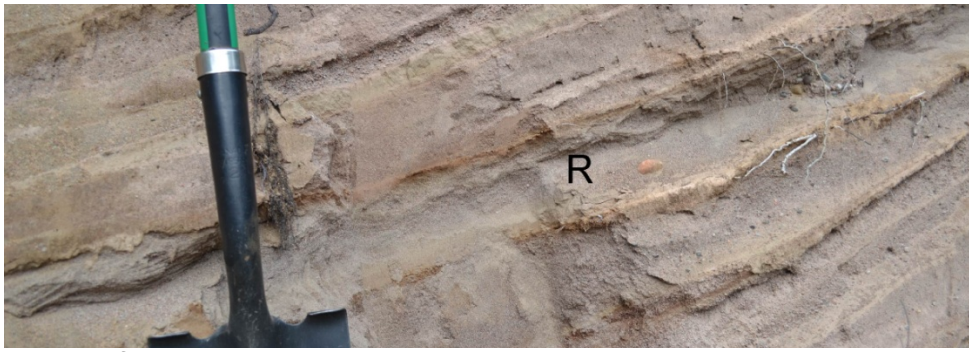

Figure 5.70. Lithofacies association 3F, containing ripple cross-lamination (R)

Figure 5.71. Ripple cross-lamination within lithofacies association 3F

The last feature identified within this lithofacies association is scallop-shaped scours that are infilled with fine-grained sand (Fig. 5.72). Layers of fine-grained sand average 2cm in thickness.

Figure 5.72. Lithofacies association 3F, revealing erosive scours (outlined in black) infilled with fine-grained sand

4F. Medium-Grained to Coarse-Grained Sand Matrix with Pebbles

At the abrupt contact with 3F, bedding is composed of medium-grained to coarse-grained sand matrix with irregular granule and pebble layers persisting for ~80cm (Fig. 5.65). Overlying this, near the surface, are two graded layers of granules to coarse-grained sand separated by a layer of fairly well-sorted very coarse-grained sand (Fig. 5.65). The remaining upper section of this lithofacies association is composed of massive granules and small pebbles within a medium-grained to coarse-grained sand matrix. This upper ~1m appears strongly bioturbated, which has likely disturbed visible stratigraphy.

5.7 Construction Site

The Construction Site is located between Mackenzie 1 and RLF (Fig. 4.1), revealing three lithofacies associations seen in four profiles (Fig. 5.73). A fence diagram is provided, along with stratigraphic columns and photos for each profile (Fig. 5.74 to 5.78).

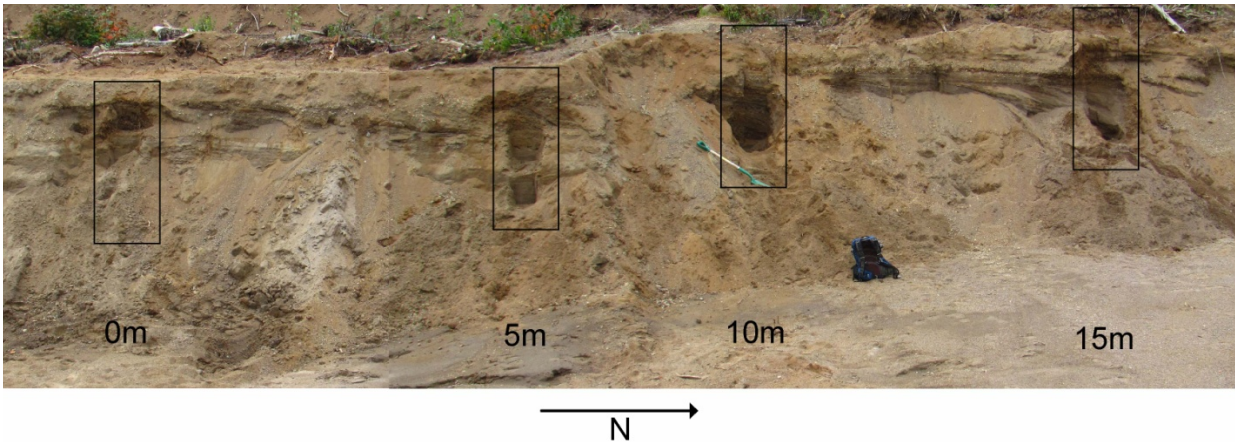

Figure 5.73. Profiles documented at Construction Site

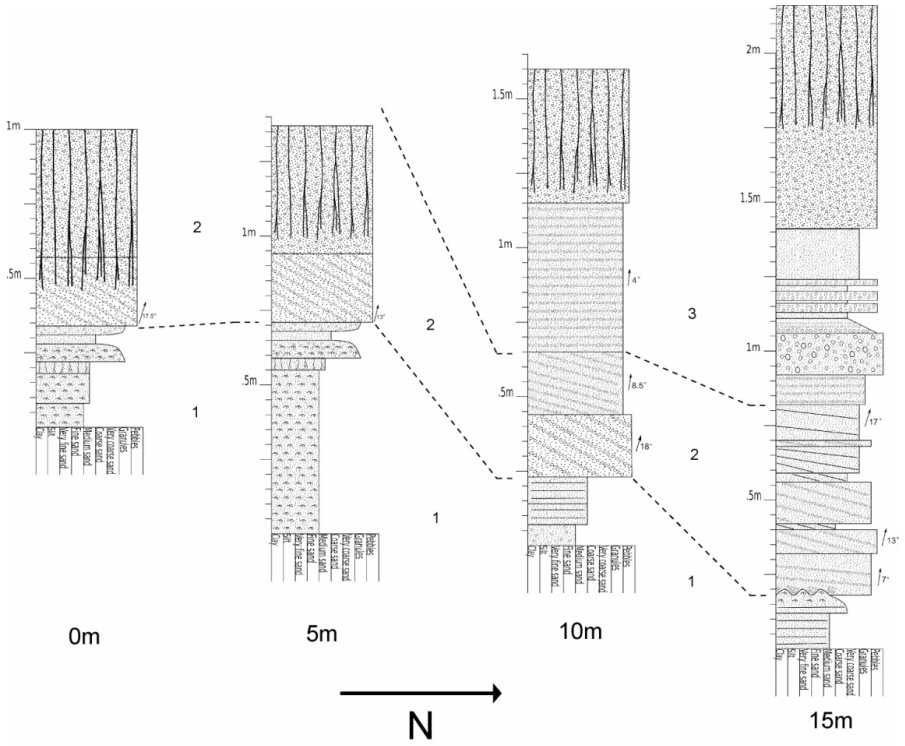

Figure 5.74. Fence diagram correlating lithofacies associations identified at Construction Site

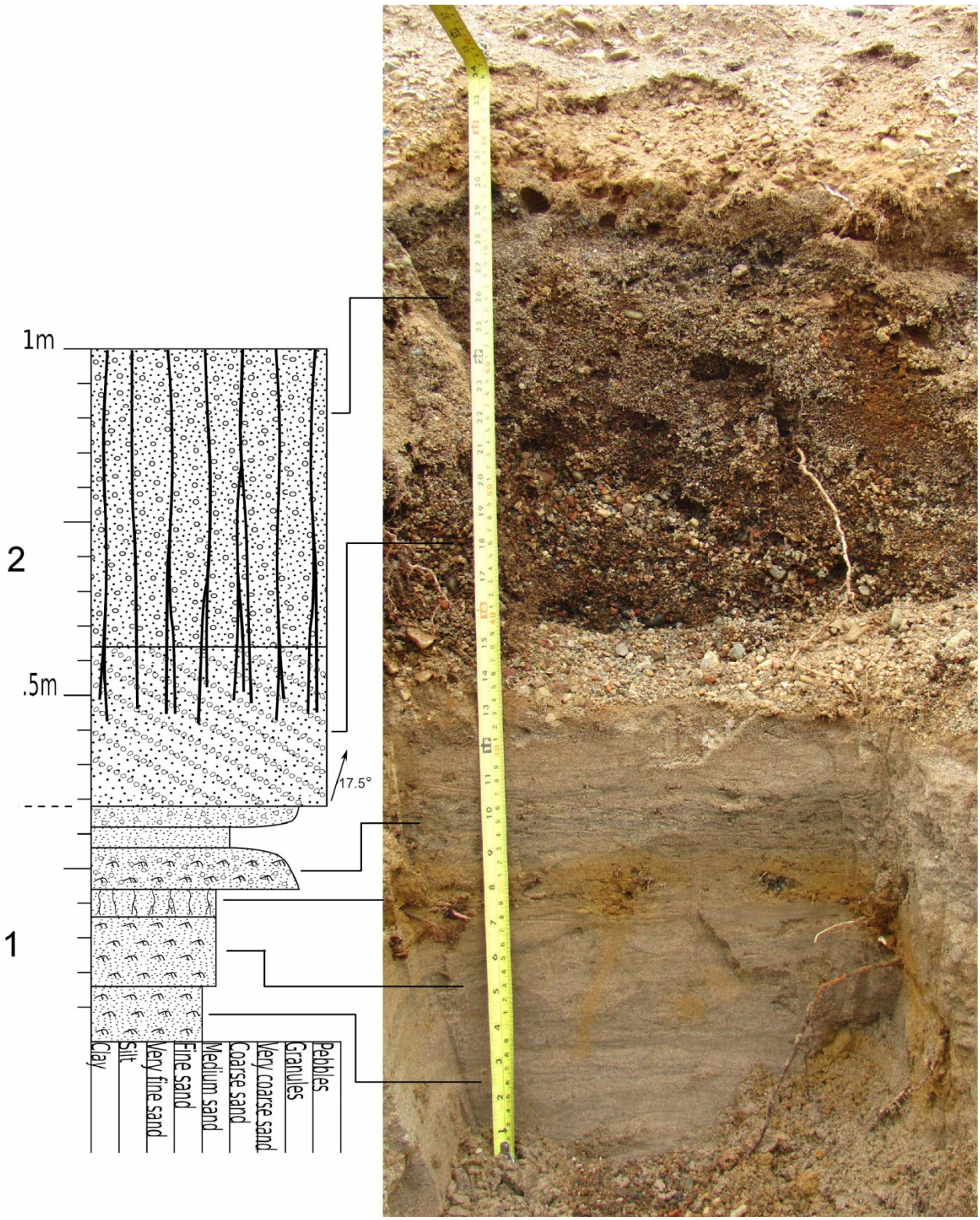

Figure 5.75. Construction Site, profile 0m

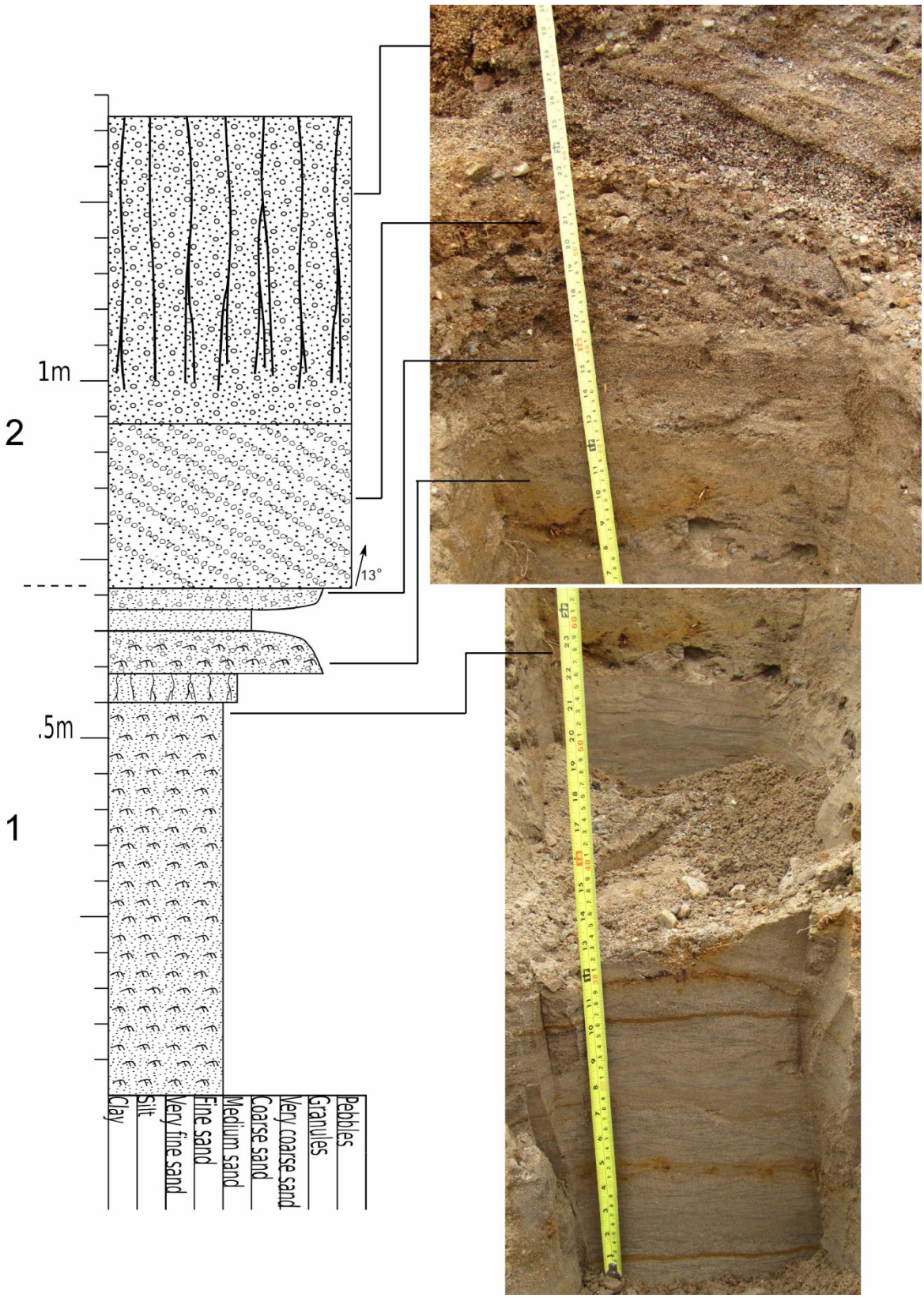

Figure 5.76. Construction Site, profile 5m

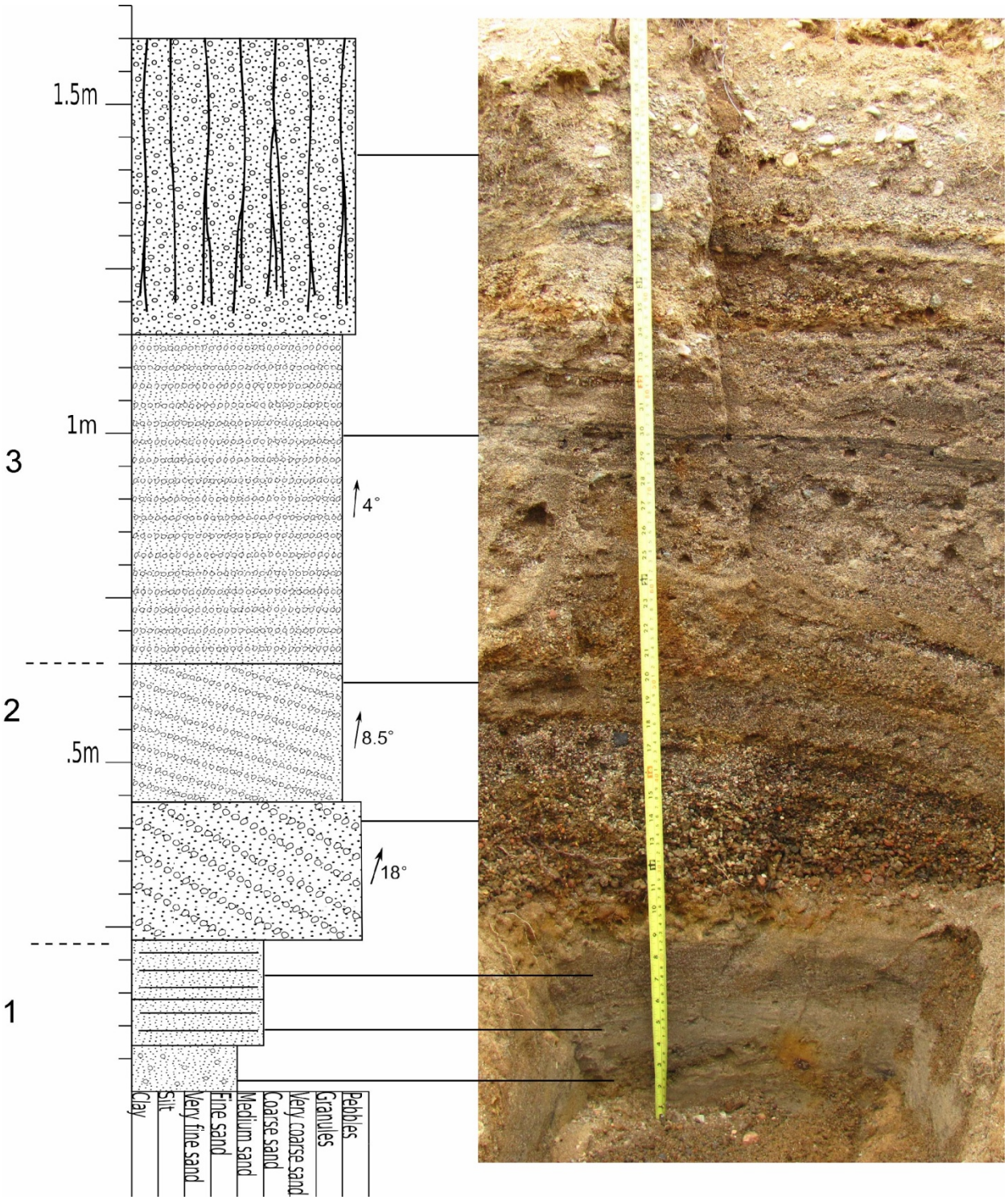

Figure 5.77. Construction Site, profile 10m

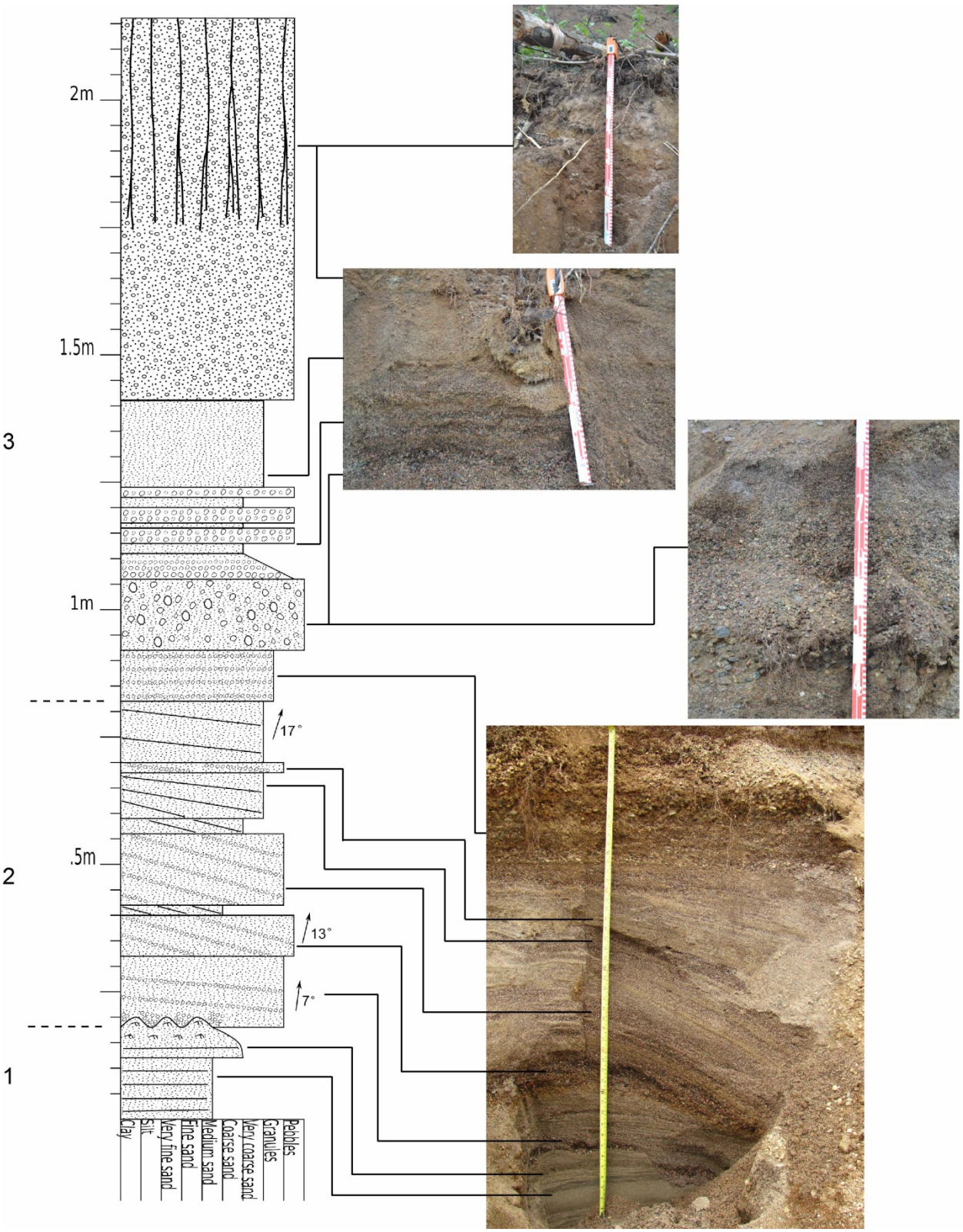

Figure 5.78. Construction Site, profile 15m

1G. Fine-Grained to Medium-Grained Sand

Ripple cross-lamination with layers averaging 2cm in thickness dominate this lithofacies association (Fig. 5.79), as seen in stratigraphic profiles for 0m, 5m, and 10m. Also present are parallel layers of iron-rich fine-grained sand, apparent in Figure 5.79. Ripple cross-lamination is also observed in the 15m profile, although this layer is about 3cm in thickness, directly underlying lithofacies association 2G (Fig. 5.80). Paleocurrent directions for lithofacies association trend northwest (Fig. 5.81).

Figure 5.79. Ripple cross-lamination within lithofacies association 1G

The next most abundant bedform is parallel-stratificiation. Seen in the medium-grained sand of profile 10m and fine-grained to medium-grained sand of profile 15m, these layers average 2mm in thickness. Some parallel-stratified laminae are dark and contain magnetite (Fig. 5.80). Within the parallel-bedding of profile 15m, are two scallop-shaped scours (labeled 1 and 2). Contact with overlying lithofacies association 2G is wavy (Fig. 5.80 and Fig. 5.82), with an erosive scour present in Figure 5.80.

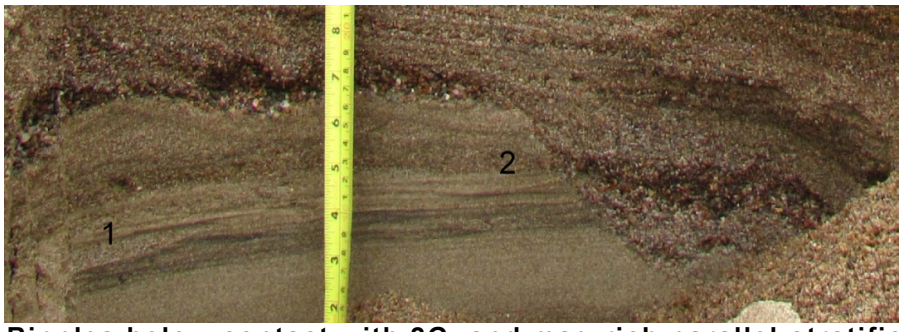

Figure 5.80. Ripples below contact with 2G, and mag-rich parallel-stratification. Two scallop-shaped scours are also present, indicated by 1 and 2

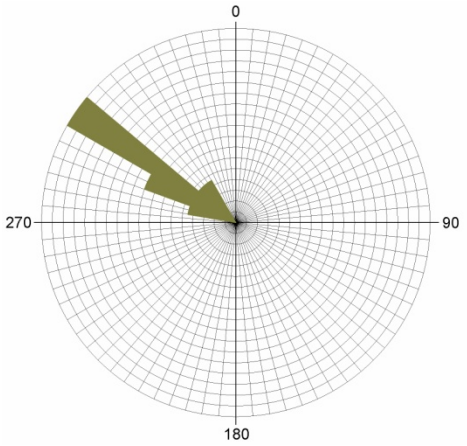

Figure 5.81. Rose diagram of lithofacies association 1G

Figure 5.82. Wavy contact of lithofacies associations 1G and 2G

2G. Planar Cross-Stratified Medium-Grained Sand to Pebbles

At the contact with 1G (Fig. 5.80 & 5.82), medium-grained sand to granules are planar cross-stratified with the coarsest clasts infilling the troughs of the wavy contact. This wavy contact is not visible in the other three profiles.

This lithofacies association is dominated by large-scale planar cross-stratification composed of layers averaging 1 to 2cm in thickness. Grain-size varies from coarse-grained sand to pebbles, to medium-grained sand to granules. The lower ~40cm of cross-stratification in profile 15m appears concave down (Fig. 5.83), although the

majority of this lithofacies association is planar cross-stratified (Fig. 5.83). The uppermost sections of profiles 0m and 5m also reveal this lithofacies association, however due to bioturbation and likely disturbance during construction, stratigraphy is not visible. Paleocurrent directions for lithofacies association 2G trend northeast (Fig. 5.74 to 5.77).

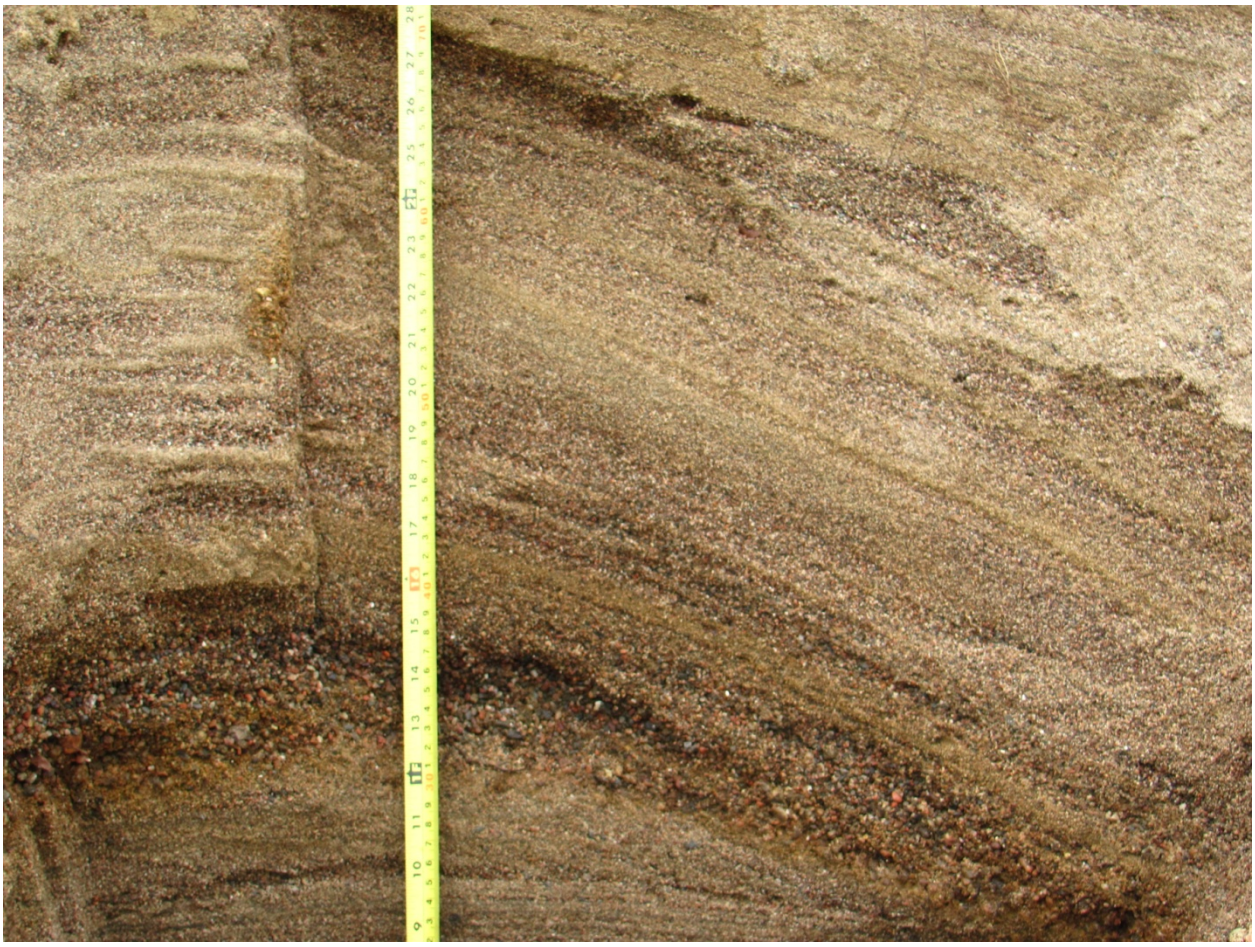

Figure 5.83. Concave downward cross-stratification overlain by planar cross-stratification

3G. Parallel-Stratified Medium-Grained Sand to Pebbles

Overlying the planar cross-stratification, the same grain-size of medium-grained sand to pebbles is parallel-laminated (Fig. 5.84). However, in the 10m profile, this parallel-laminated section of the lithofacies association has a higher concentration of medium sand matrix with fewer granules and pebbles in the bedding (Fig. 5.85) which is

comparable to lithofacies 2G in the 5m profile. Also within the 10m profile, medium-grained magnetite-rich parallel layers 2mm thick are present.

The sediments overlying the parallel-stratification are only observed in profile 15m. Massive layers of poorly-sorted medium-grained sand to pebbles are present, generally generally averaging 4cm in thickness, although one bed is 14cm thick. Interbedded with these massive layers are layers of well-sorted coarse-grained sand averaging 3cm thick, as well as one layer grading from granules to coarse-grained sand 5cm thick. Overlying the uppermost massive poorly-sorted layer is a well-sorted very coarse-grained sand layer 17cm thick, although this bed may appear massive due to disturbance by bioturbation. The upper ~1.75m of this lithofacies association is strongly bioburbated silty medium-grained sand matrix with pebbles.

Figure 5.84. Planar cross-stratifiaction of lithofacies association 2G and parallel-stratification of 3G

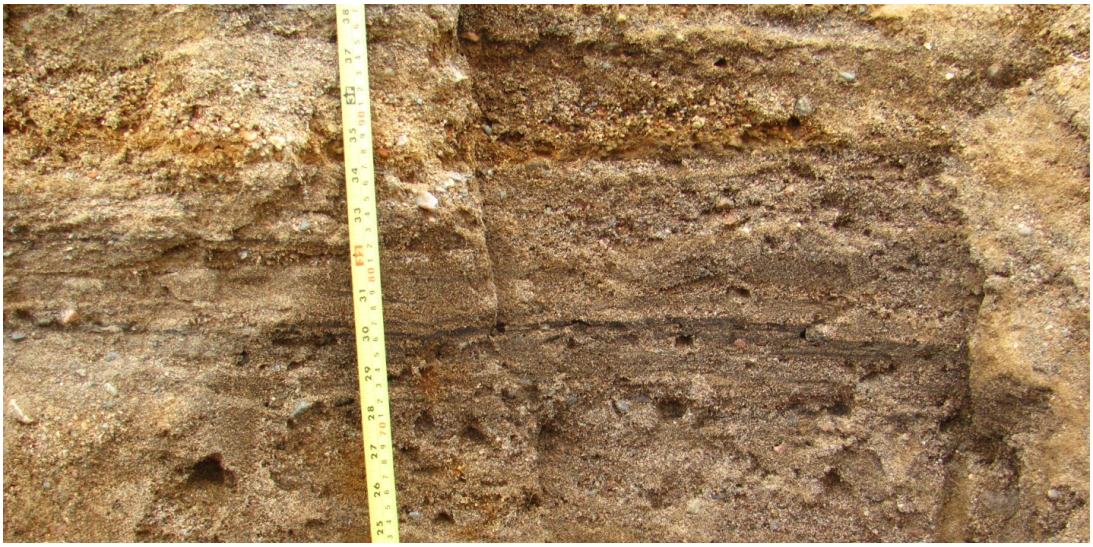

Figure 5.85. Parallel-stratified medium-grained sand with fewer granules and pebbles within lithofacies association 3G

5.8 Trench

A trench was dug on the west side of the Mackenzie 1 archaeological site facing ~345°, extending to 4m below surface. This allowed six lithofacies to be seen in the West, North, and East walls of the trench (Fig. 5.86). A stratigraphic column was produced from measurements taken from the east wall Fig. 5.87.

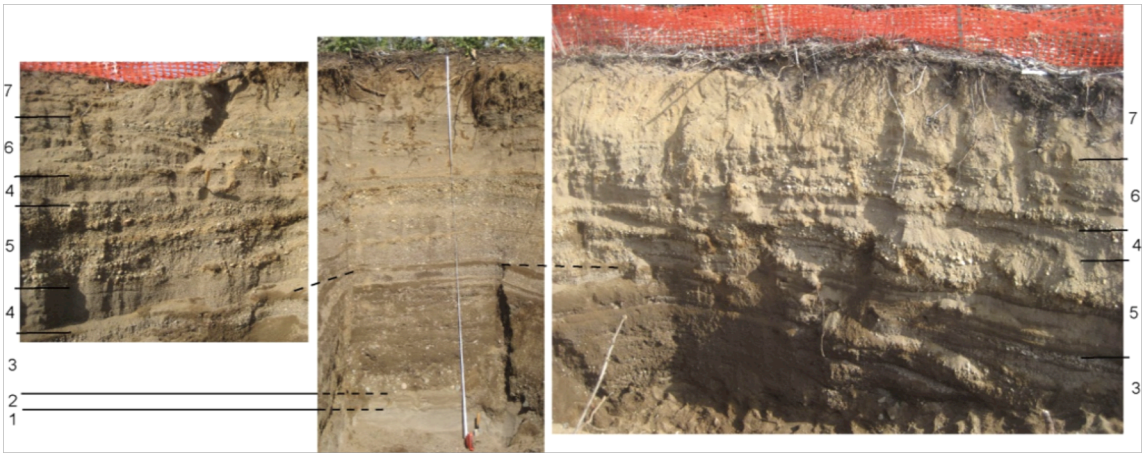

Figure 5.86. The Mackenzie 1 trench, ~4m in depth. Shown are three photos: the West wall on the left; the North wall in the middle; and the East wall on the right. Lithofacies associations are numbered and described below.

1H. Fine-Grained to Medium-Grained Sand

At the bottom of the trench there is a section ~18cm thick of large scale climbing ripples within fine-grained to medium-grained sand. Some of the lee side laminae observed within this lithofacies appear to be contorted, overturned slightly in the direction of current flow.

2H. Very Fine-Grained to Fine-Grained Sand

Abruptly overlaying the climbing ripples, this lithofacies is composed of very fine-grained to fine-grained sand. Ripple cross-lamination is apparent within this upper fine-grained sand, in layers averaging 3cm in thickness. As well, parallel-stratified very fine-grained to fine-grained sand layers are present, generally overlying ripples making the parallel-stratified layers appear wavy.

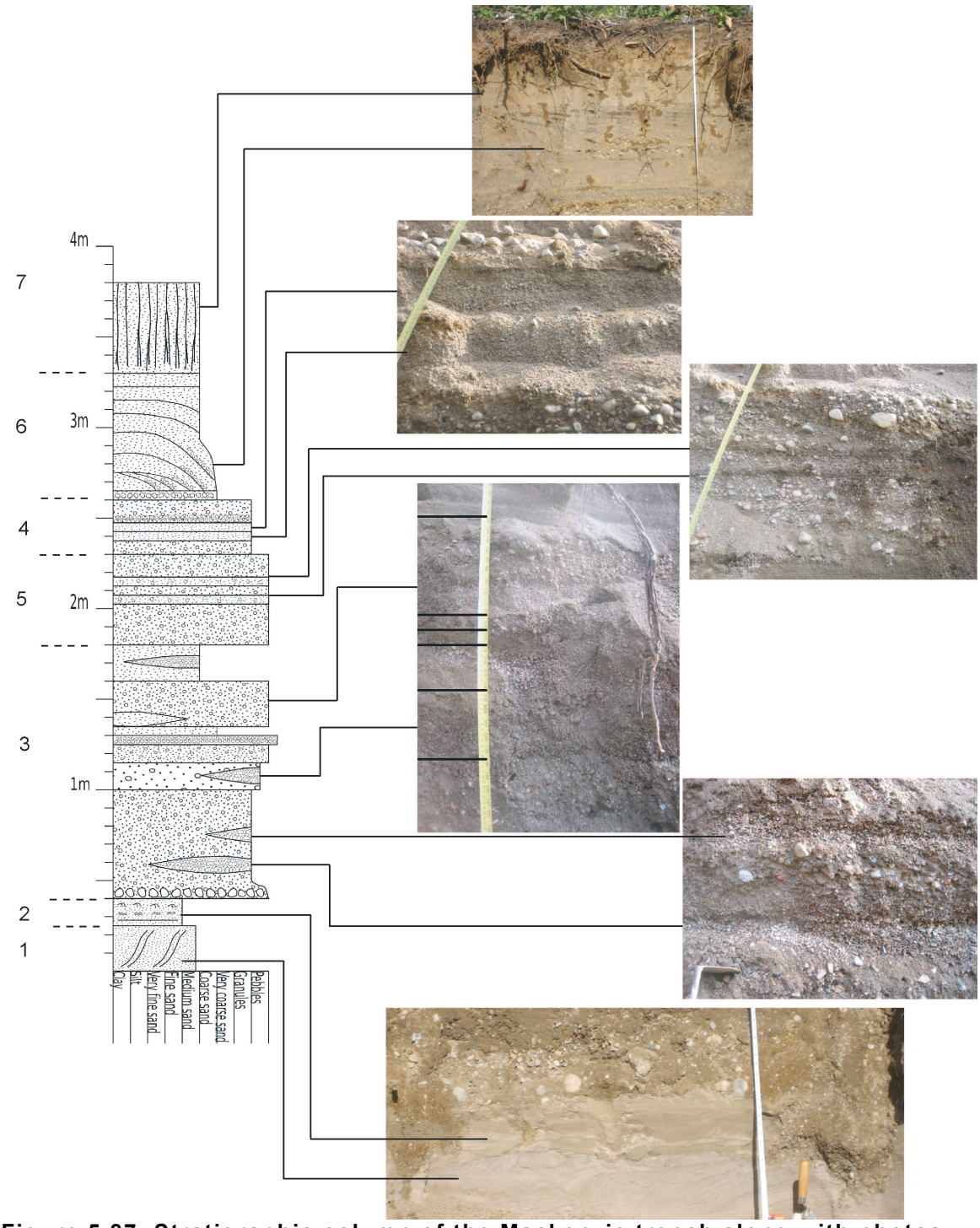

Figure 5.87. Stratigraphic column of the Mackenzie trench along with photos

3H. Sand and Gravel

Abruptly overlying the very well-sorted sands is a layer of subrounded cobbles ~10cm in diameter within a medium-grained to coarse-grained sand

matrix (Fig. 5.88). Above the cobble layer, medium-grained and coarse-grained sand with pebbles up to ~4cm in diameter generally appear massive, although some medium-grained to coarse-grained sand layers are interbedded with coarse-grained sand to pebbles. Sand layers thicken upwards from 2 to 6cm in thickness, while coarser pebbly layers thicken upward from 3cm to 10cm in thickness.

Figure 5.88. Lag deposit overlying lithofacies association 1H

Within the massive to bedded sand and gravel unit in the eastern wall of the trench, lenses of open framework small pebbles are present (Fig. 8.89). These lenses grade from small pebbles with few medium pebbles to small pebbles with granules. Lenses average 4cm in thickness, and are up to 30cm in length.

Figure 5.89. Graded lens within lithofacies association 2H

4H. Well-Sorted Medium-Grained to Coarse-Grained Sand

In the North wall, a well-sorted medium-grained sand to coarse-grained sand layer with some magnetite is ~5cm thick. Interbedded between two sections of this lithofacies is 4H, cross-stratified sand and gravel (Fig. 5.90). The bottom of both well-sorted sand sections dips down in a southward direction, although the upper contact has relatively no dip causing the unit to thicken southward.

Within the well-sorted sand, best identified in the west wall of the trench, are layers one or two pebbles thick averaging 2cm in thickness. The pebble layers within sell sorted sand underlying lithofacies 4H dip down southward at roughly the same angle as the sand and gravel unit, although in the well-sorted sand overlying the cross-stratified sand and gravel, the pebble layers do not dip.

Figure 5.90. Lithofacies association 4H interbedding lithofacies 3H

5H. Cross-Stratified Sand and Gravel

In the northern wall, layered between two well-sorted sand beds, the sand and gravel unit appears parallel-stratified. However, the west wall of the trench reveals that the pebbly medium- to coarse-grained sand is planar cross-stratified (Fig. 5.90). Paleocurrent direction is south to southeast. The bottom of the sequence between well-sorted sand beds has no observable dip, abruptly

overlying the well-sorted sand unit, although the top dips at an angle of 15° towards the south.

6H. Magnetite Rich Cross-Stratified Sand and Gravel

Overlying the upper well-sorted sand lithofacies is a layer one pebble thick of medium to large pebbles averaging 2 to 3cm in diameter within medium-grained sand (Fig. 5.91). Overlying the pebble layer, best identified in the western and northern walls, is cross-stratified medium pebbles within magnetite rich medium-grained sand (Fig. 5.91). Exposure within the west wall reveals that horizontally stratified sand and gravel gradually becomes cross-stratified planar cross-stratified with progradation in a north to northeast direction, almost opposite the paleocurrent direction of the underlying cross-stratified sequence.

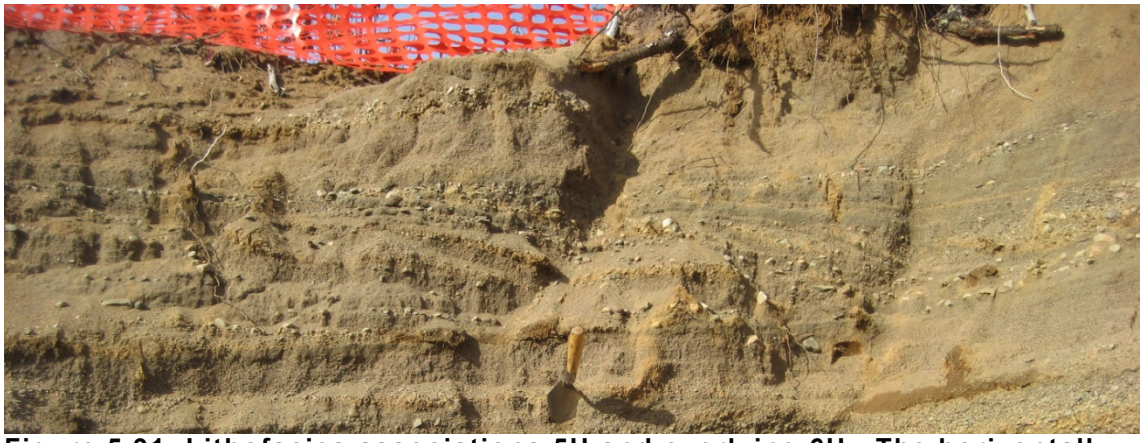

Figure 5.91. Lithofacies associations 5H and overlying 6H. The horizontally-straitifed sand and gravel comprising lithofacies association 6H gradually becomes planar cross-stratified.

7H. Massive Silty Sand with Pebbles

This lithofacies is 25cm thick, appearing massive and separated from the underlying cross-stratified unit by a thin pebble layer composed of pebbles 15cm in diameter. It is composed of well-sorted silty fine-grained to medium-grained sand with pebbles. Some magnetite was present, although the magnetite concentration appears lower than within in the underlying cross-stratified sand and gravel bedding. Discontinuous pebble layers up to ~5cm thick are observed within this massive sand.

5.9 Mackenzie 1

The Mackenzie 1 archaeological site is roughly 10,000m^2, located on the west side of the Mackenzie River (Fig. 4.1). Lithofacies identified at Mackenzie 1 are described for representative profiles of excavated units in the northern portion of the site, the southern portion and the central portion. In addition, profiles are provided for an anomalous linear feature as well as three pit features.

Units 549N 517E, 548N 517E, and 549N 516E

1I. Well-Sorted Medium-Grained to Coarse-Grained Sand with few Pebbles

The stratigraphy seen in the northern portion of Mackenzie 1 is quite different from the rest of the site. The lithofacies is dominantly medium- to coarse-grained sand with occasional granules, pebbles averaging 2-3cm in diameter and pebble layers generally one pebble thick (Fig. 5.92 & 5.93).

Figure 5.92. South walls of excavated units 549N 516E and 549N 517E

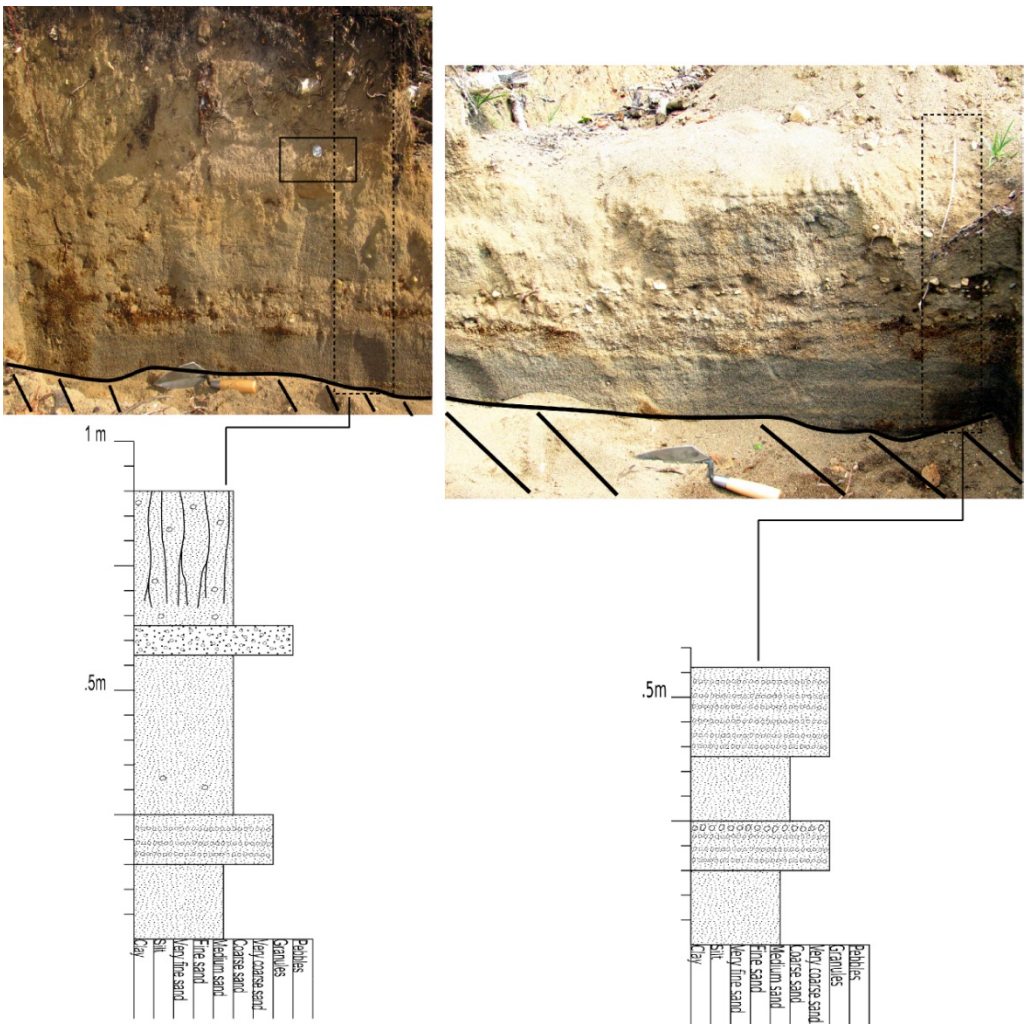

Figure 5.93. East walls of excavated units 549N 517E and 548N 517E. The box around the quarter of 549N 517E is shown in Figure 6.93.

The lower section of these wall profiles is composed of very well-sorted fine-grained to medium-grained sand. This appears to be parallel-bedded layers of magnetite-rich sand interbedded with non magnetite-rich sand, averaging 1cm in thickness. This bedding dips northeast.

The overlying sand varies in grain-size from medium-grained to coarse-grained, occasionally with matrix-supported pebbles and pebble layers, also dipping northeast. Along the south wall of excavated units 549N 516E and 549N 517E, a pebble layer is seen to curve around tree roots (Fig. 5.92).

The East wall of unit 549N 517E (under the quarter in Figure 5.93) also reveals a bed 6cm thick of coarse-grained sand, granules and few pebbles ~1cm in diameter (Fig. 5.94). This massive layer abruptly overlies well-sorted medium-grained sand.

The upper ~25cm of this profile is comprised of the same medium-grained to coarse-grained sand with few pebbles, however it also contains roots and appears to be bioturbated.

Figure 5.94. Massive Layer within lithofacies 1

Units 496N 508E and 497N 508E

The east and south walls of excavated unit 496N 508E, as well as the west wall of unit 497N 508E are described because they reveal the representative lithofacies observed throughout much of Mackenzie 1 (Fig. 5.95 & 5.96).

4l. Magnetite-Rich Cross-Stratified Coarse-Grained Sand to Granules

The stratigraphically lowest lithofacies is seen in the west wall of unit 497N 508E (Fig. 5.95). Composed dominantly of magnetite-rich planar cross-stratified coarse-grained to very coarse-grained sand layers interbedded with layers of granules containing few pebbles, this lithofacies is capped by a silt layer ~1cm thick. Paleocurrent direction from this lithofacies indicates progradation in a northeastward direction.

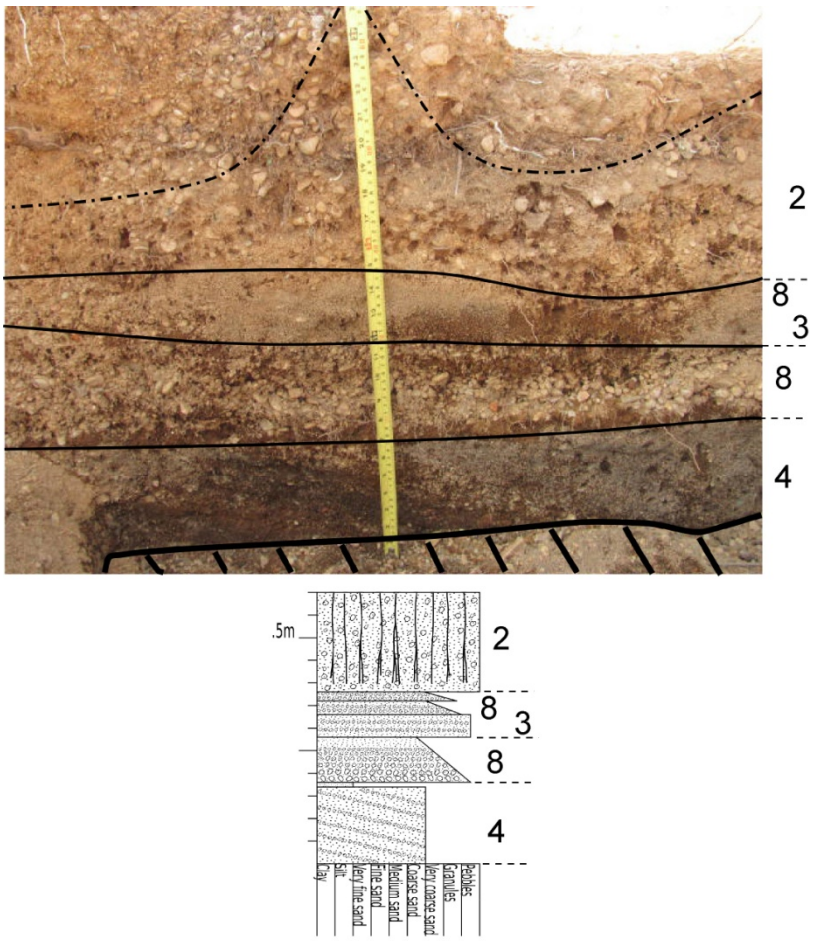

Figure 5.95. West wall of unit 497N 508E

8I. Graded layer of Pebbles to Coarse-Grained Sand

Abruptly overlying the silt layer of lithofacies 5I is a layer 7cm thick of pebbles up to 3cm in diameter, grading to granules within in coarse-grained sand matrix. The upper portion of this graded layer is also seen at the bottom of unit 496N 508E (Fig. 5.96).

Two additional graded layers are also present juxtaposed between lithofacies 3I and 2I (Fig. 5.95 & 5.96). These are 3cm in thickness, grading from granules with few pebbles to medium-grained and coarse-grained sand.

3I. Coarse-Grained Sand Interbedded with Granules and Pebbles

This lithofacies is layered between two graded beds (lithofacies 8I) (Fig. 5.95 & 5.96). It is composed of parallel-stratified coarse-grained sand interbedded with open

framework granules and pebbles up to 3cm in diameter. Layers are well-sorted, and contacts with the underlying and overlying graded layers are easily identified due to the presence of parallel beds.

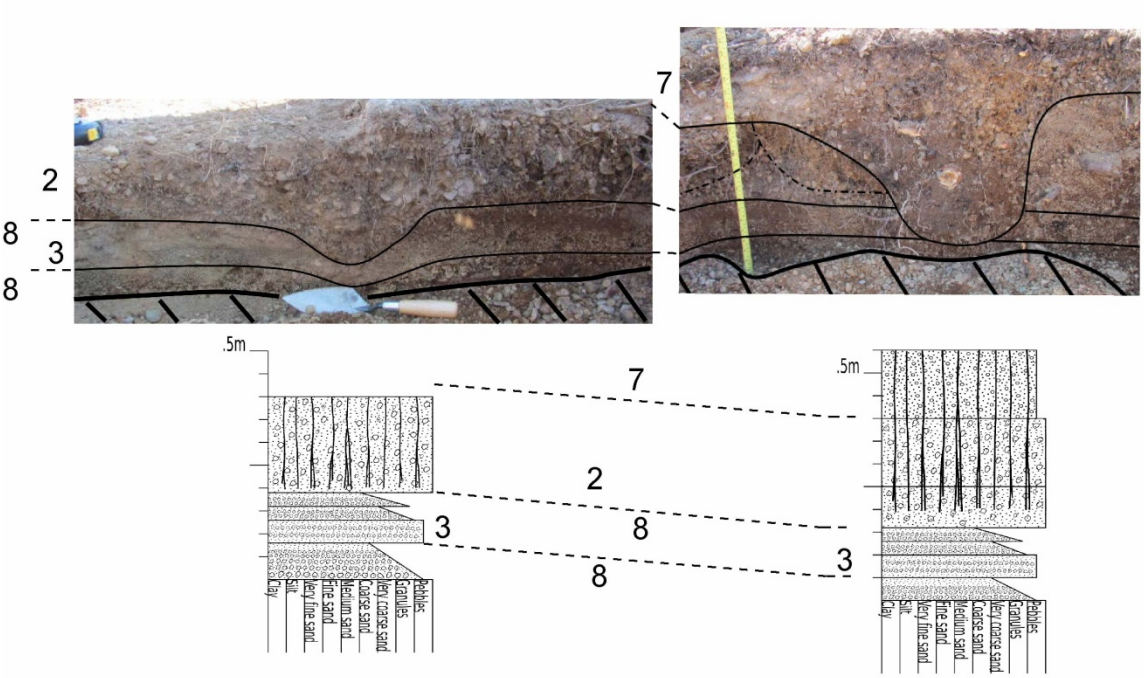

Figure 5.96. East wall (left), and South wall (right) of unit 496N 508E

2l. Pebbles within a Sand and Granule Matrix

This lithofacies is composed of pebbles averaging 3cm in diameter within a matrix of medium-grained sand to granules. Although this lithofacies is generally matrix-supported pebbles (e.g., Fig. 5.96), it is occasionally clast-supported with very little to no matrix (e.g., Fig. 5.95).

Bedding appears massive in the east wall of unit 496N 508E (Fig. 5.96), however pebble imbrication is present in the south wall of unit 496N 508E and the west wall of unit 497N 5058E (Fig. 5.96). Pebble imbrication is shown with dashed lines, appearing to represent successive channel cut and fill structures.

7l. Silty Medium-Grained to Coarse-Grained sand with Pebbles

This is dominantly the uppermost lithofacies identified throughout Mackenzie 1 (except in the northern portion of the site described above). It also represents the occupation layer(s) of the site, where all artifacts were recovered. Composed of

massive and poorly-sorted silty medium-grained to coarse-grained sand with pebbles, there are always associated tree roots of varying sizes. The massive nature of the lithofacies is likely the result of bioturbation that may have been an active process even during deposition and occupation of the archaeological site.

Unit 459N 528E

Located in the southern part of Mackenzie 1, the west wall of unit 459N 528E reveals the same lithofacies as those described above.

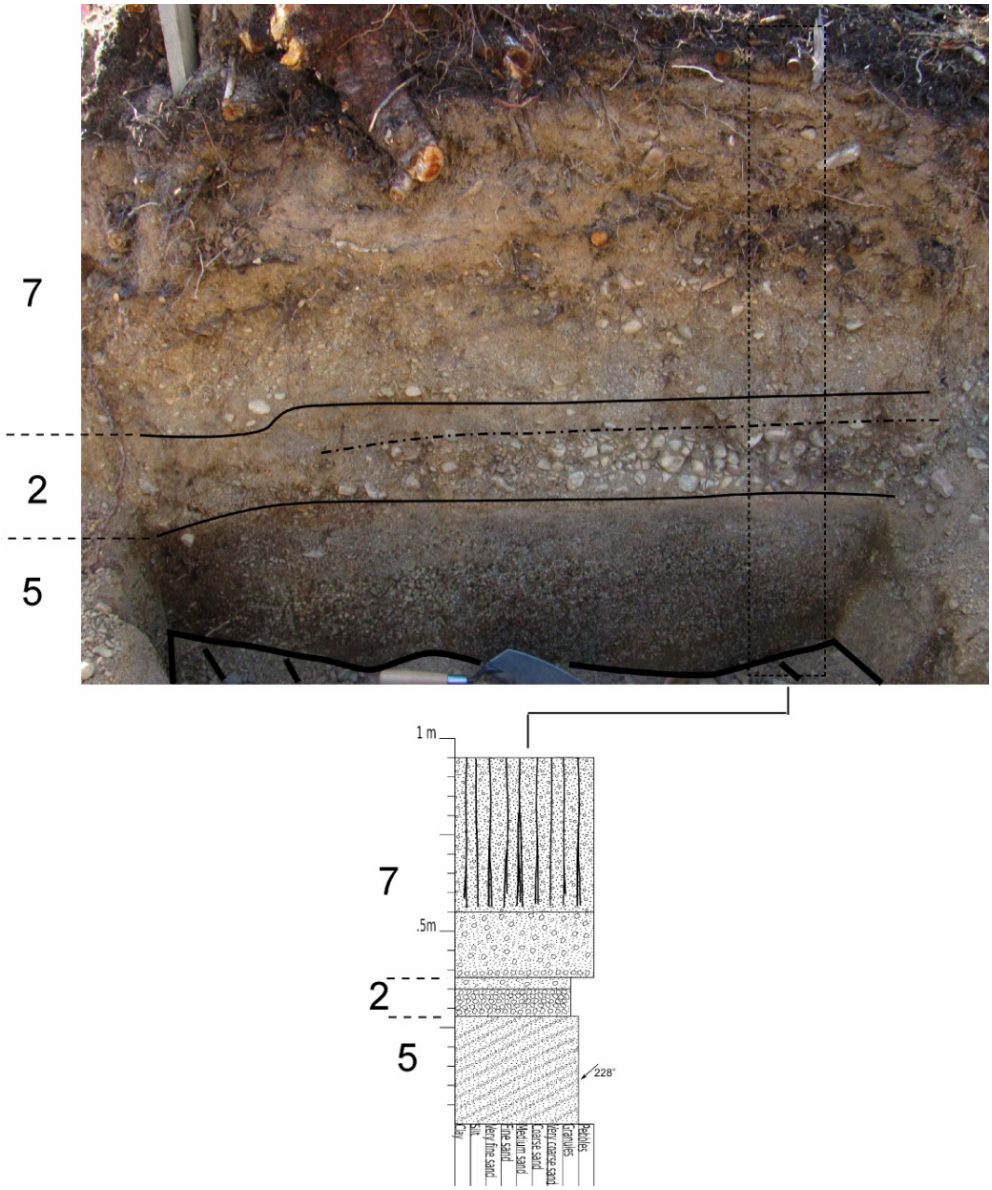

Figure 5.97. West wall of excavated unit 459N 528E

5I. Cross-Stratified Coarse-Grained Sand to Granules

This lithofacies is composed of planar cross-stratified coarse-grained to very coarse-grained sand layers interbedded with layers of granules containing few pebbles (Fig. 5.97). Individual layers are well-sorted, open framework, and dip slightly at about 10°. Paleocurrent direction of unit 459N 528E indicates progradation in a southwest direction. This is abruptly overlain by lithofacies 2I.

2I. Pebbles within a Sand and Granule Matrix

The bottom 7cm of this lithofacies (defined by a dashed line) is composed of pebbles averaging 3cm in diameter within a matrix of medium-grained sand to granules, although there is a significant lateral change in the concentration of matrix to pebbles (Fig. 5.97). At the northern end of the wall, there are more pebbles than matrix. However, southward the amount of pebbles decreases until there are very few. There is no apparent pebble imbrication.

The upper section of this lithofacies is dominantly coarse-grained sand to granules containing few pebbles, similar to the underlying sediment at the southern end of the wall (Fig. 5.97). This section appears massive and poorly-sorted.

7I. Silty Medium-Grained to Coarse-Grained sand with Pebbles

At the contact with lithofacies 2I is a layer of pebbles averaging 2cm in diameter, one pebble thick. The remainder of the lithofacies appears massive, composed of silty medium-grained to coarse-grained sand with pebbles. There is an upward increase in silt content, and the upper 40cm is strongly bioturbated.

Linear Feature

In the southern part of Mackenzie 1, there is a linear feature of silty sand with pebbles similar to lithofacies 7I although containing a finer matrix (Fig. 5.98). This feature varies in depth, and is strongly associated with a high concentration of artifacts. Two units revealing representative lithofacies are described.

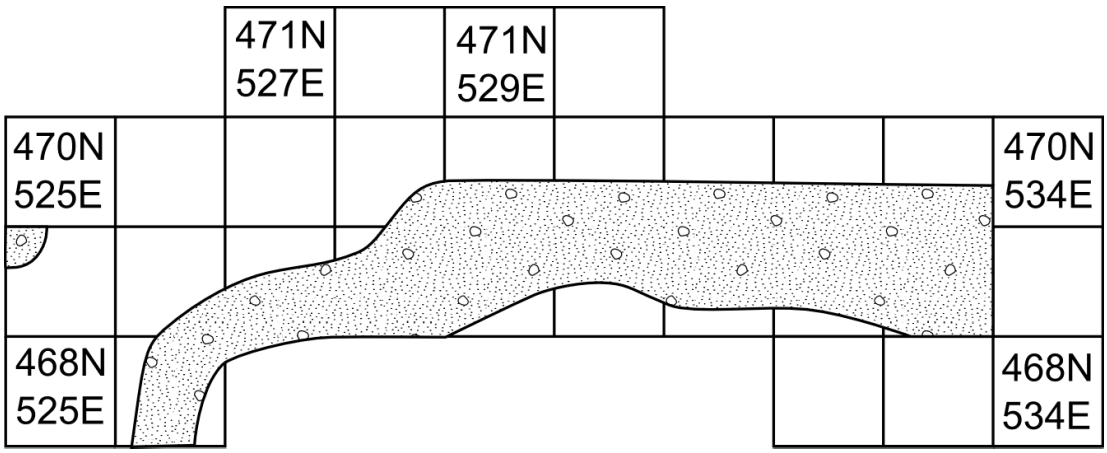

Figure 5.98. Plan View of the linear feature at Mackenzie 1

Units 470N 528E and 468N 526E

3I. Coarse-Grained Sand Interbedded with Granules and Pebbles

This lithofacies is composed of parallel-bedded coarse-grained sand interbedded with granules and pebbles up to 3cm in diameter, although the grain-size varies (Fig. 5.99 & 5.100). The east wall of unit 470N 528E and the east wall of unit 468N 526E reveal three grain-sizes: the coarsest is very coarse-grained sand interbedded with pebbles up to 2cm in diameter; underlying this is coarse–grained sand very coarse-grained sand interbedded with granules; and the finest is coarse-grained sand interbedded with very coarse-grained sand and few granules.

7I. Silty Medium-Grained to Coarse Grained sand with Pebbles

In these profiles, lithofacies 7I abruptly overlies 3I. In the east wall of unit 470N 528E there are more pebbles than generally seen within the silty sand (Fig. 5.99), more typically like the lithofacies seen in the east wall of profile 468N 526E (Fig. 5.100).

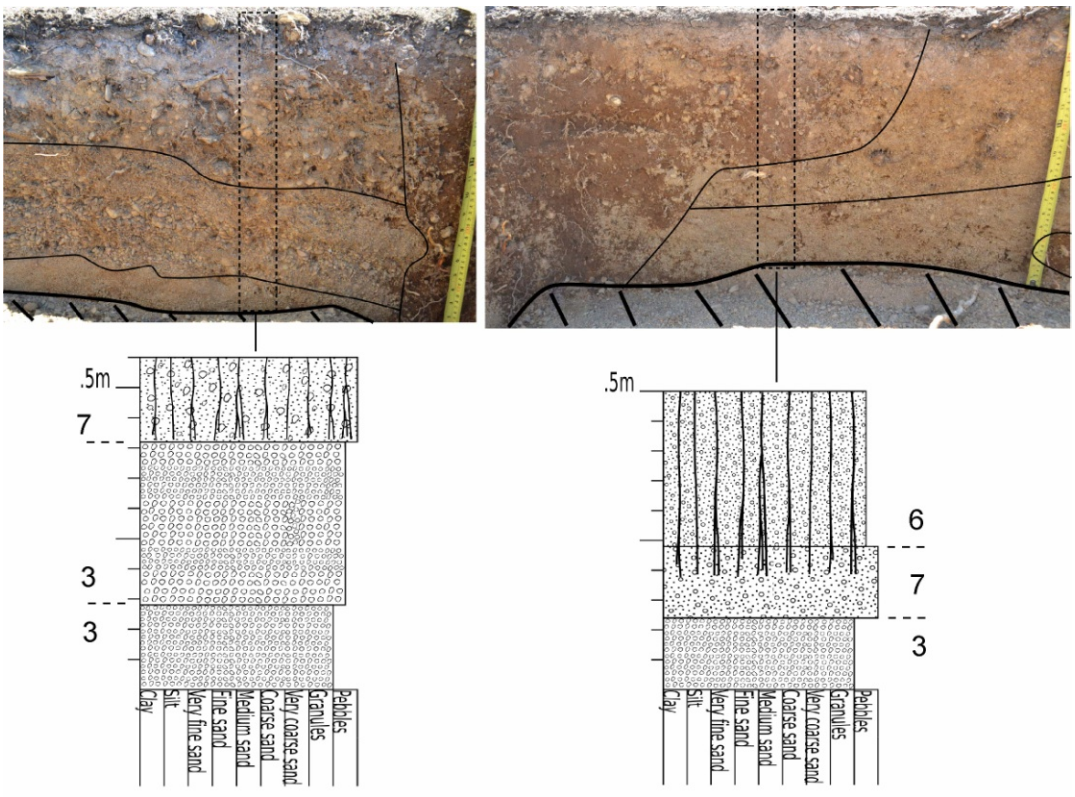

Figure 5.99. East and south walls of excavated units 470N 528E

6I. Silty Medium-Grained Sand with Pebbles

Composed of poorly-sorted silty medium-grained sand with pebbles, this lithofacies varies in depth from ~25cm to ~50cm below surface. There is no apparent bedding, and the contacts are always abrupt. In the east wall of unit 470N 528E (Fig. 5.99), this silty massive sediment truncates intact stratigraphy vertically. Contacts with lithofacies 7I and 3I in the south wall of 470N 528E and the east wall of unit 468N 526E (Fig. 5.99 & 5.100) also appear erosive, although these are truncated at a slope as well as horizontally.

This lithofacies is only present along the units indicated in Figure 5.98, within two pit features (described below), and along the south wall of the 455N line of units (455N 529E eastward to unit 455N 534E) (e.g. Fig. 5.101). The south wall of these excavated units reveals disturbed sediment, as evidenced by the organic layers mixed into lithofacies 6I (Fig. 5.102). Additional support that this southernmost section of Mackenzie 1 is disturbed is the presence of a shoe insole discovered during excavation ~20cm below surface.

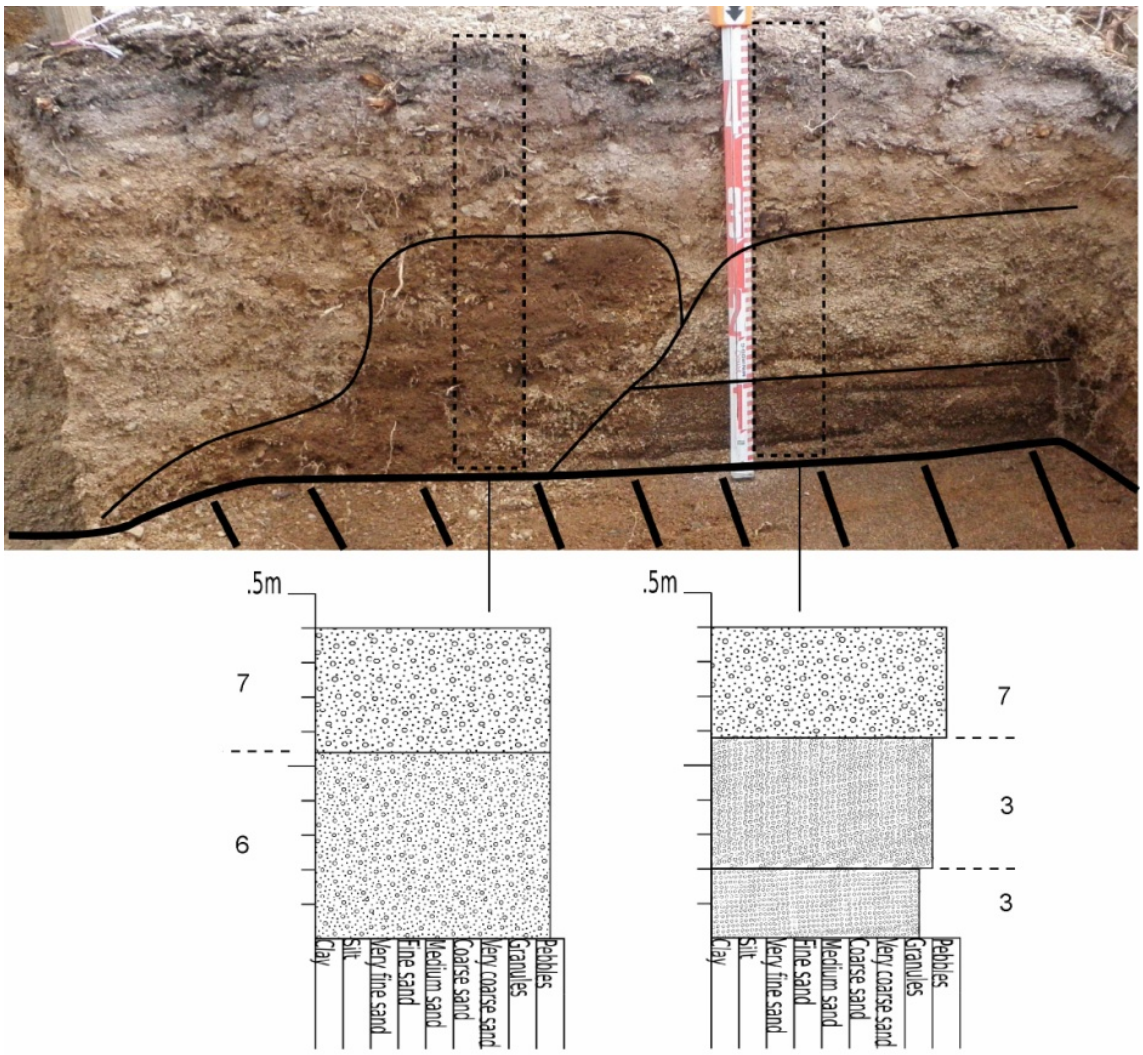

Figure 5.100. East wall of unit 468N 526E

Figure 5.101. South wall of unit 455N 530E, revealing lithofacies 6l

Figure 5.102. Disturbance in the south wall of unit 455N 528E

Pit Features

Three anomalous pit features were identified within the southern portion of Mackenzie 1, important to site interpretation because they all contain a high concentration of artifacts. Two of these contain lithofacies 6I as seen within the walls of excavated units 478N 518E and 462N 529E (Figs. 5.103 & 5.106). The third pit featuere, exposed in the east wall of unit 497N 506E, is composed of lithofacies 7I. These features are not linear, commonly extending about 1m laterally and vertically. The two pit features filled with lithofacies 6I were not identified until after the adjacent units were excavated; the profiles created for these (Figs. 5.103 & 5.106) reveal the stratigraphy underlying excavated units.

Unit 478N 518E

In addition to the stratigraphic analysis conducted for this thesis, this pit was profiled by soil scientists Dr. Paul Adderley (Department of Biological and Environmental Sciences, University of Stirling) and Dr. Krista Gilliland (Western Heritage). Field profiling techniques were employed to select horizons most suitable for micromorphology studies as well as Optically Stimulated Luminescence (OSL) dating (Gilliland, 2012; Kinnaird et al., 2012). Preliminary micromorphological results and OSL dates obtained by these other researchers are reported in Kinnaird et al. (2012), Gilliland (2012) and Gilliland et al. (2012). In Chapter 7, I briefly evaluate these dates in relation to new stratigraphic data reported in this thesis.

3I. Coarse-Grained Sand Interbedded with Granules and Pebbles

In this profile, 5I is composed of horizontally-stratified coarse-grained to very coarse-grained sand layers interbedded with layers of granules containing few pebbles (Fig. 5.103). The beds within this lithofacies dip slightly to the southwest, and there appear to be magnetite free layers interbedded with layers of higher magnetite concentration. Abruptly underlying this lithofacies is open framework pebbles appearing massive (Fig. 5.104), overlying there is an abrupt contact with lithofacies 1.

1I. Silty Medium-Grained Sand

Abruptly overlying cross-stratified sand and granules, there is a layer 2cm thick of silty medium-grained sand. This appears comparable to the upper portion of lithofacies 1I located in the northern portion of Mackenzie 1, seen in units 548N 517E, and 549N 516E (Fig. 5.92 & 5.93).

3I. Coarse-Grained Sand Interbedded with Granules and Pebbles

Abruptly overlying the thin layer of silty medium-grained sand, there is parallel-stratified coarse-grained sand interbedded with granules and pebbles up to 3cm in diameter (Fig. 5.103 & 5.104). This layer may appear to be reverse graded, however close examination reveals that the lower portion is composed of coarse-grained sand interbedded with dominantly granules, while the upper 3cm is composed of coarse-grained sand interbedded with pebbles and few granules. The upper contact with overlying lithofacies 2I is gradational.

This lithofacies is also present in the west wall, although it is not laterally continuous and is dominantly coarse-grained sand interbedded with granules. Contacts in this wall with lithofacies 8I and 2I appear abrupt.

Figure 5.103. South and west walls of unit 478N 518E

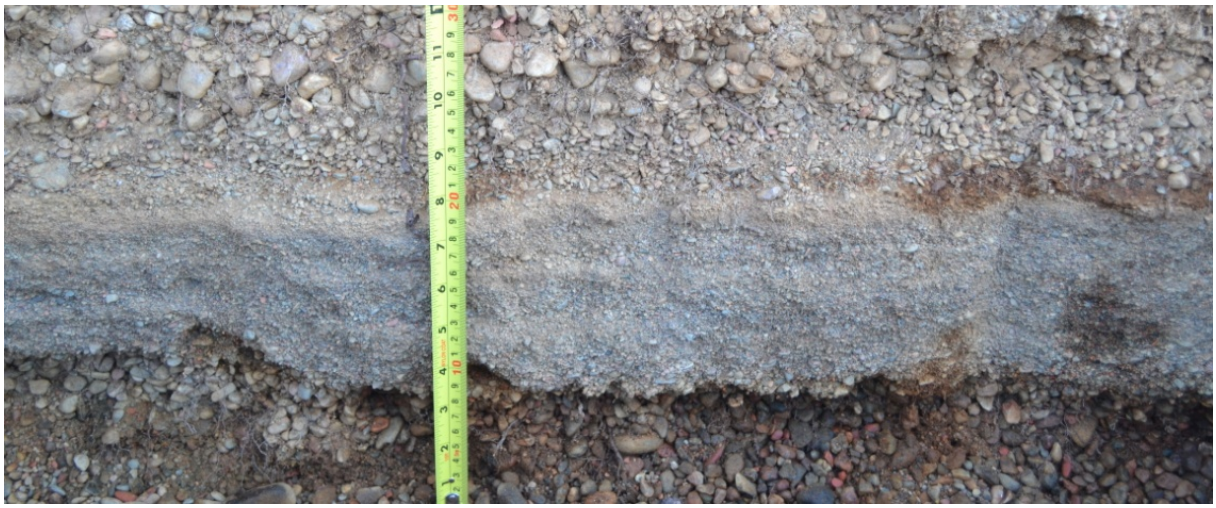

Figure 5.104. Lithofacies 3 underlain by massive open framework pebbles, overlain by a thin silt layer (lithofacies 1) and lithofacies 3 at the top.

2I. Pebbles within a Sand and Granule Matrix

In the south and walls, this lithofacies is composed of pebbles averaging 2-3cm in diameter within a matrix of medium-grained sand to granules (Fig. 5.103). There is no apparent bedding within either of these deposits. The south wall reveals a contact with the underlying lithofacies that is gradational, however there is a very abrupt and vertical contact with lithofacies 7I in the west wall.

7I. Silty Medium-Grained to Coarse-Grained sand with Pebbles

Typically only comprising the upper ~30cm of the sediment at Mackenzie 1, this profile reveals silty medium-grained sand to coarse-grained sand with pebbles extending to 65cm b.s. This lithofacies appears massive, with vertical and horizontal contacts that are all abrupt (Fig. 5.103).

8I. Graded layer of Pebbles to Very Coarse-Grained Sand

The west wall of unit 478N 518E reveals vertical layers that are graded laterally from pebbles up to 3cm to very coarse-grained sand (Fig. 5.103 and 5.105). Contact with adjacent lithofacies 7I is gradational.

6I. Silty Medium-Grained Sand with Pebbles

Within unit 478N 518E, this lithofacies is silty medium-grained sand with pebbles and appears consistent with exposure in other excavated unit walls. The silty medium-grained sand erosively truncates the lithofacies seen in the south wall almost vertically, and abruptly contacts lithofacies 7I in the west wall (Fig. 5.103).

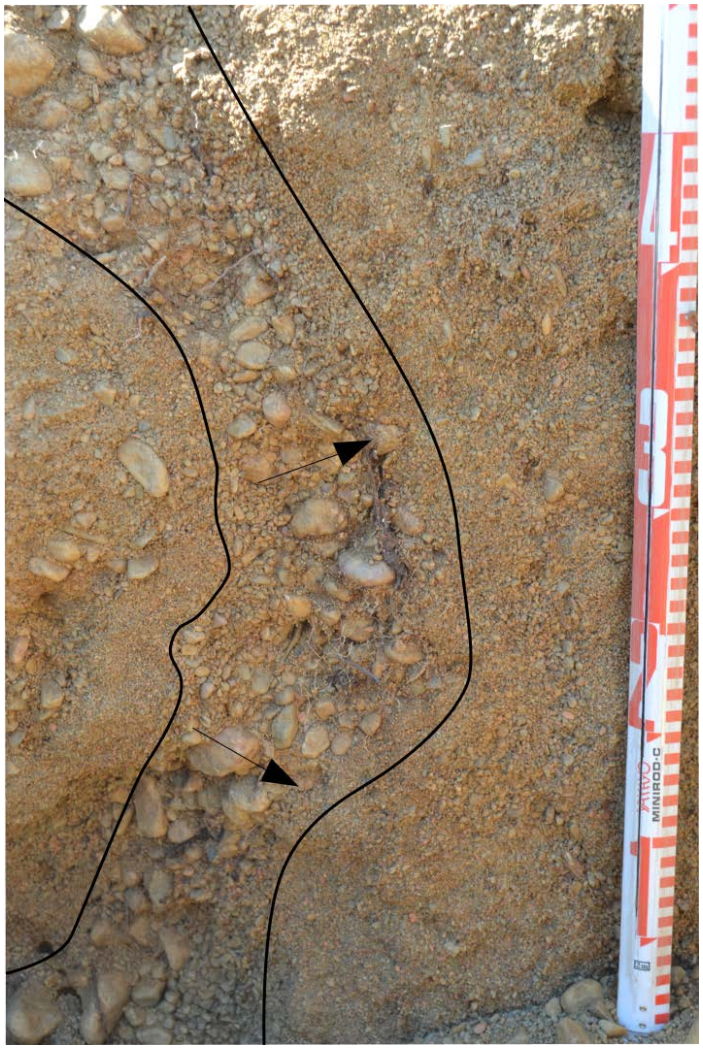

Figure 5.105. Laterally graded layers within the west wall of unit 478N 518E. Arrows indicate the direction of grading.

Unit 462N 529E

3I. Coarse-Grained Sand Interbedded with Granules and Pebbles

In this profile, the lithofacies is composed of coarse-grained sand interbedded with granules (Fig. 5.106). There are no pebbles within this bedding. This is abruptly overlain by lithofacies 8I.

8I. Graded layer of Pebbles to Very Coarse-Grained Sand

Abruptly overlying lithofacies 3I is a layer 8cm thick of pebbles up to 3cm in diameter, grading to granules within in coarse-grained sand matrix (Fig. 5.106). Unlike the contact with lithofacies 6I in the previous units, this graded layer is not truncated. Instead, this layer thins westward, and appears to line lithofacies 6I.

7I. Silty Medium-Grained to Coarse-Grained sand with Pebbles

Abruptly overlying the graded layer, there is a layer of poorly-sorted silty sand with granules and pebbles. There are few roots present, which indicates that the massive appearance of this lithofacies could be the result of bioturbation. The contact with overlying lithofacies 6I is gradual; the difference is based solely on grain-size difference.

6I. Silty Medium-Grained Sand with Pebbles

In this profile, the silty medium-grained sand has more pebbles than seen in other unit walls. The contact with underlying lithofacies, does not appear to be erosive. Within this exposure, the lithofacies contains roots providing evidence that the massive appearance is the result of bioturbation.

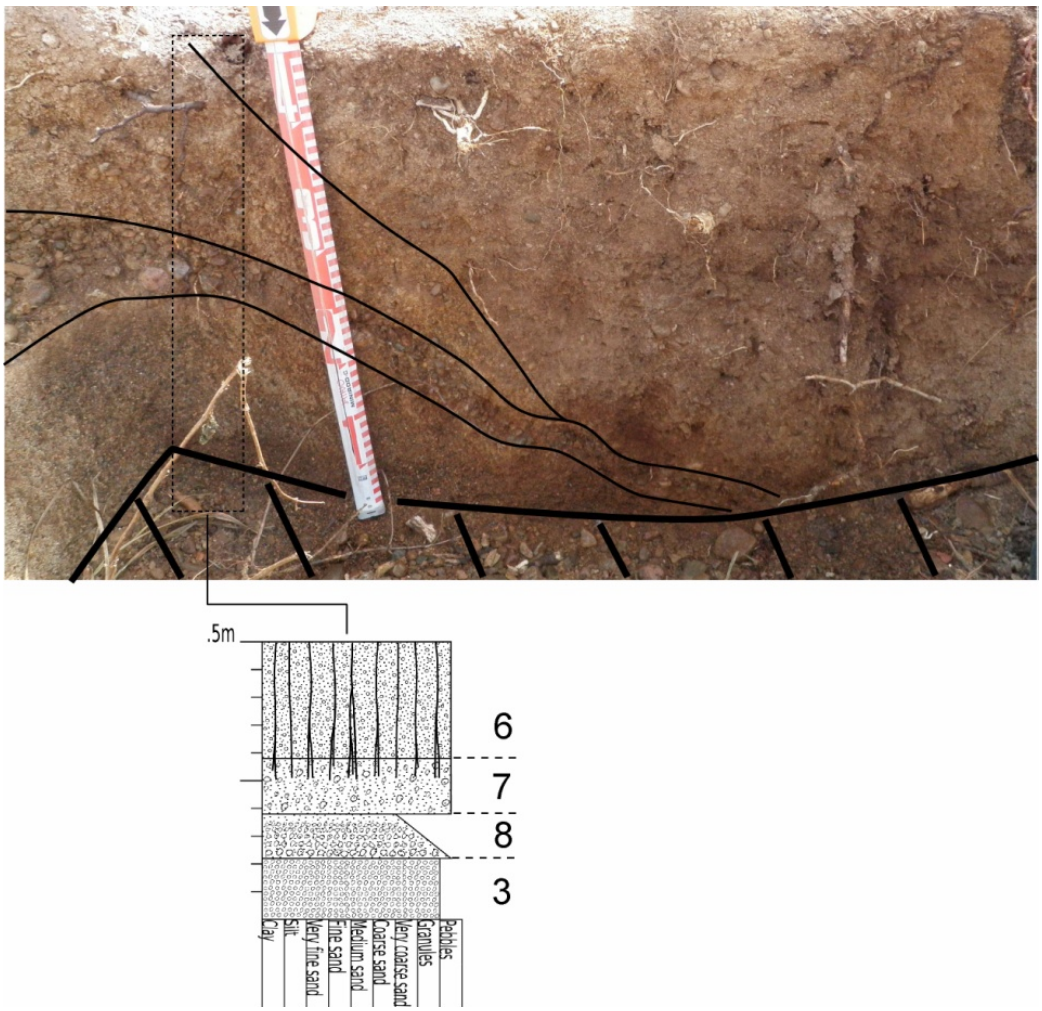

Figure 5.106. South wall of unit 462N 529E

Unit 497N 506E

3l. Coarse-Grained Sand Interbedded with Granules and Pebbles

The stratigraphically lowest lithofacies, seen in the east wall of unit 497N 506E is a layer of coarse-grained sand interbedded with granules (Fig. 5.107). This bed has an abrupt contact with overlying lithofacies 5l. Higher in the profile, there is another layer of coarse-grained sand interbedded with granules, although this is also contains some pebbles up to 1cm in diameter. This layer curves around lithofacies 7l, and is almost vertical as it grades into lithofacies 2l.

In the south wall, this lithofacies abruptly lies between lithofacies 8l and 2l. It is dominantly coarse-grained sand interbedded with granules and few pebbles. However,

there are also thin beds of coarse-grained sand with very coarse-grained sand and few to no granules, as well as a pebble layer one pebble thick.

4I. Magnetite Rich Cross-Stratified Coarse-Grained Sand to Granules

In this profile, 5I is composed of planar cross-stratified coarse-grained to very coarse-grained sand layers interbedded with layers of granules containing few pebbles (Fig. 5.107). Paleocurrent direction indicates progradation in a northeast direction. This is abruptly overlain by lithofacies 2I and 8I.

2I. Pebbles within a Sand and Granule Matrix

In the south and walls, this lithofacies is composed of pebbles averaging 2-3cm in diameter within a matrix of medium-grained sand to granules (Fig. 5.107). This lithofacies generally appears matrix supported, however in the southeast corner it is clast supported. In this southeast corner as well as the western portion of the south wall, pebble imbrication is shown with dashed lines, appearing to represent successive channel cut and fill structures (Fig. 5.107) similar to the south wall of unit 496N 508E and the west wall of unit 497N 5058E (Fig. 5.96).

8I. Graded layer of Pebbles to Very Coarse-Grained Sand

Abruptly overlying the planar cross-stratification in the south wall of unit 497N 506E is layer grading from pebbles averaging 2cm in diameter to coarse-grained sand (Fig. 5.107). This graded bed is overlain abruptly by lithofacies 2I.

7I. Silty Medium-Grained to Coarse-Grained sand with Pebbles

In unit, lithofacies 7I abruptly overlies lithofacies 3I, and also lies adjacent to it as a nearly vertical contact. There are more pebbles than typically seen within this lithofacies (e.g. Fig. 5.99 & Fig. 5.100).

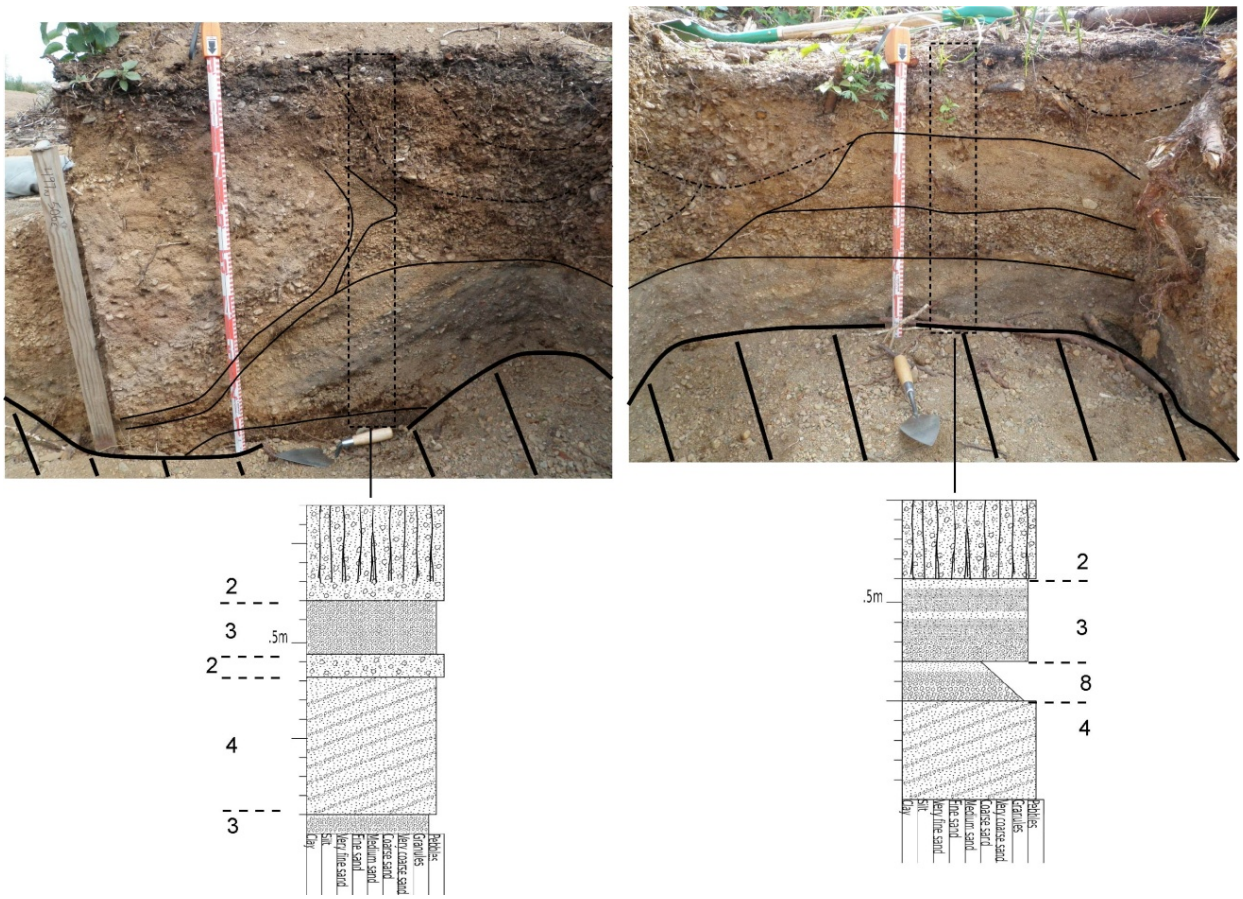

Figure 5.107. East and south walls of unit 497N 506E

5.9.1. Artifacts at Mackenzie 1

In the northern portion of Mackenzie 1, artifacts were recovered from lithofacies 1l (well-sorted medium-grained to coarse-grained sand with few pebbles). The southern portion of Mackenzie 1 contained artifacts in lithofacies 7l (silty medium-grained to coarse-grained sand with pebbles), and within the pit features in lithofacies 6l (silty medium-grained sand with pebbles). Artifact placement varied throughout the site, although they were typically recovered from surface to ~50cm, the majority of which came from within 15-30cm below surface. The only exceptions to this are the pit features, which generally contained artifacts to the bottom of them.

5.10 Mackenzie 2

Mackenzie 2 is a small archaeological site located on the east side of the Mackenzie River (Fig. 4.1). All artifacts were recovered at this site within the upper 40cm within sediment that varies little throughout the site. Description of a roadcut north of Mackenzie 2 is also provided.

Roadcut

The surface of the roadcut has been removed, however bioturbation near the top of the exposure indicates that it is likely close to the natural surface (Fig. 5.108).

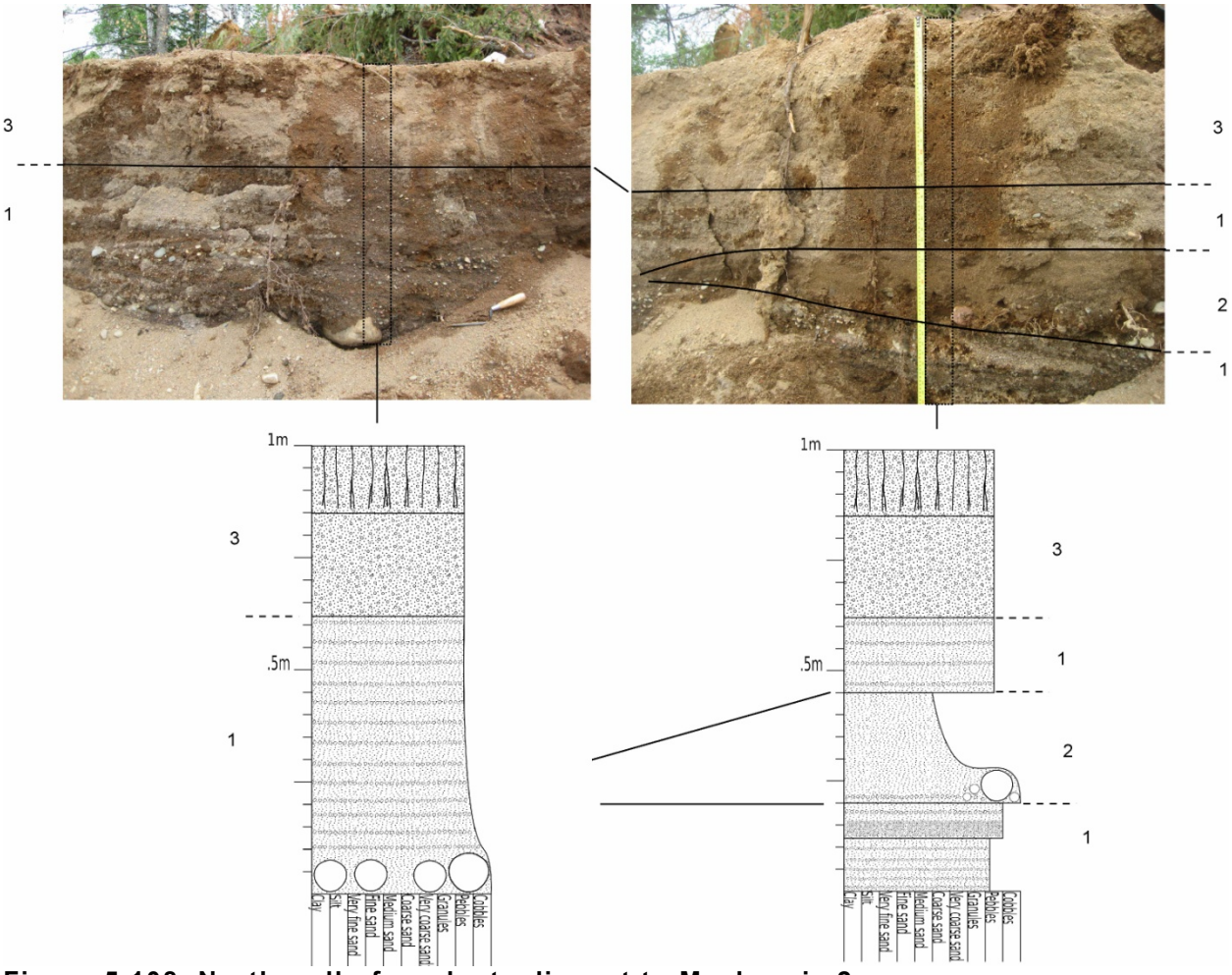

Figure 5.108. North wall of roadcut adjacent to Mackenzie 2

1J. Cross-Stratified Medium-Grained Sand to Small Pebbles

The stratigraphically lowest lithofacies seen in the roadcut is parallel-stratified medium-grained to coarse-grained sand matrix supported granules and pebbles up to 4cm in diameter (Fig. 5.108). The upper 10cm of this lithofacies is slightly coarser, containing more pebbles than granules within the sand matrix. Layers throughout this lithofacies thicken as they coarsen westward, from 2cm in thickness to 5cm. Upward, these layers are increasingly difficult to see as this cross-stratification becomes massive. The contact with overlying lithofacies 2J appears erosive.

2J. Fine-Grained to Medium-Grained Sand with Lag Deposit

The contact with underlying lithofacies 1J appears to be erosive, and contains a lag deposit of matrix supported pebbles and cobbles up to 5cm in diameter (Fig. 5.108). The remainder of this lithofacies is composed dominantly of well-sorted fine-grained to medium-grained sand, with pebbles gradually disappearing and absent completely in the upper 15cm.

3J. Silty Medium-Grained Sand to Pebbles

Layers within underlying lithofacies 1J gradually become indistinguishable (Fig. 5.108). Lithofacies 3J is composed of silty medium-grained to coarse-grained sand with granules and pebbles. It likely represents the same lithofacies association as 1J, however due to bioturbation the bedding appears massive.

Unit 520N 515E

4J. Medium-Grained Sand to Very Coarse-Grained Sand

This lithofacies is seen throughout the Mackenzie 2 site, and always indicates a sterile level (no artifacts). It is dominantly composed of well-sorted medium-grained sand with no apparent bedding. The south wall of unit 520N 515E reveals a gradual transition to underlying coarse-grained to very coarse-grained sand (Fig. 5.109). This layer also appears to be massive.

3J. Silty Medium-Grained Sand to Pebbles

Abruptly overlying well-sorted sand is the same silty medium-grained sand to coarse-grained sand with granules and pebbles seen in the roadcut (Fig. 5.109). This is the lithofacies always associated with artifacts at Mackenzie 2. It is strongly bioturbated, appearing massive.

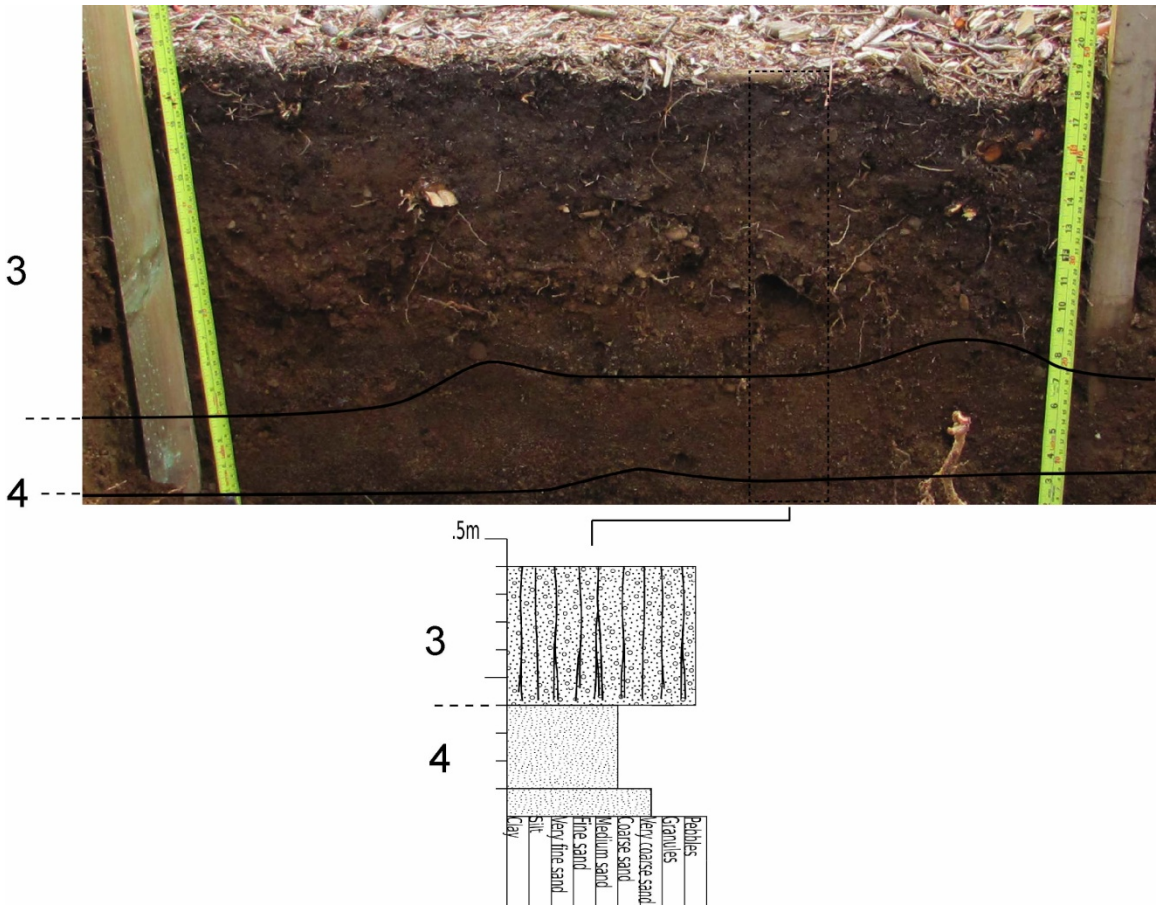

Figure 5.109. South wall of unit 520N 515E at Mackenzie 2

5.10.1. Artifacts at Mackenzie 2

At Mackenzie 2, artifacts were concentrated from surface to 15cm below surface, within the bioturbated lithofacies 3J (silty medium-grained sand to pebbles). Throughout the site, artifact amounts generally decreased gradually until 35cm below surface.

5.11 RLF

The RLF archaeological site is located between Mackenzie 1 and the Woodpecker sites (Fig. 4.1). Stratigraphy throughout is fairly consistent, although the southern portion is coarser grained. Descriptions of two representative unit walls are provided (Fig. 5.110 & 5.111).

Units 497N 455E and 485N 451E

The lithofacies seen in the north wall of unit 497N 455E are laterally continuous, extending from 497N 456E eastward to 497N 449E.

1K. Very Fine-Grained Sand to Fine-Grained Sand with Pebble Layer

Identified in the northern portion of the site, this lithofacies association is composed of low angle parallel-stratified very fine-grained sand to fine-grained sand. A trench was dug along the 497N line, about 5cm deep and 7m wide. Interbedded with the very well-sorted sand, one massive layer and one pebble layer are present, and both are laterally continuous throughout the trench exposure (Fig. 5.110). The upper section of this lithofacies seen in 497N 455E is bioturbated and appears massive.

2K. Fine-Grained Sand to Medium-Grained Sand with Pebble Layers

Seen throughout the southern portion of RLF, this lithofacies association is low angle horizontally-stratified, although most layers are less sorted than lithofacies association 1K. The parallel-stratification is dominantly composed of fine-grained sand to medium-grained sand layers interbedded with medium-grained sand containing granules and few pebbles up to 1cm in diameter (Fig. 5.111). Magnetite-rich layers are also present; these are well-sorted medium-grained sand and interbedded with non magnetite-rich layers. Rare planar cross-stratification is also present (Fig. 5.112).

A graded layer of small pebbles to coarse-grained sand is present within the west wall of unit 485N 451E (Fig. 5.111). The pebbles are clast-supported,

fining upward through granules with a sand matrix to medium-grained sand. The upper contact is diffuse.

3K. Silty Medium-Grained Sand with Pebbles

A small tapered concave up feature about 30cm wide and 40cm deep is present within the west wall of unit 485N 451E, with a diffuse boundary. Infilling the feature is massive silty medium-grained sand, containing matrix-supported pebbles as well as roots. In the southern portion of the RLF site, this lithofacies is present throughout, extending from the surface to about 25cm below surface.

Figure 5.110. North wall of excavated unit 497N 455E

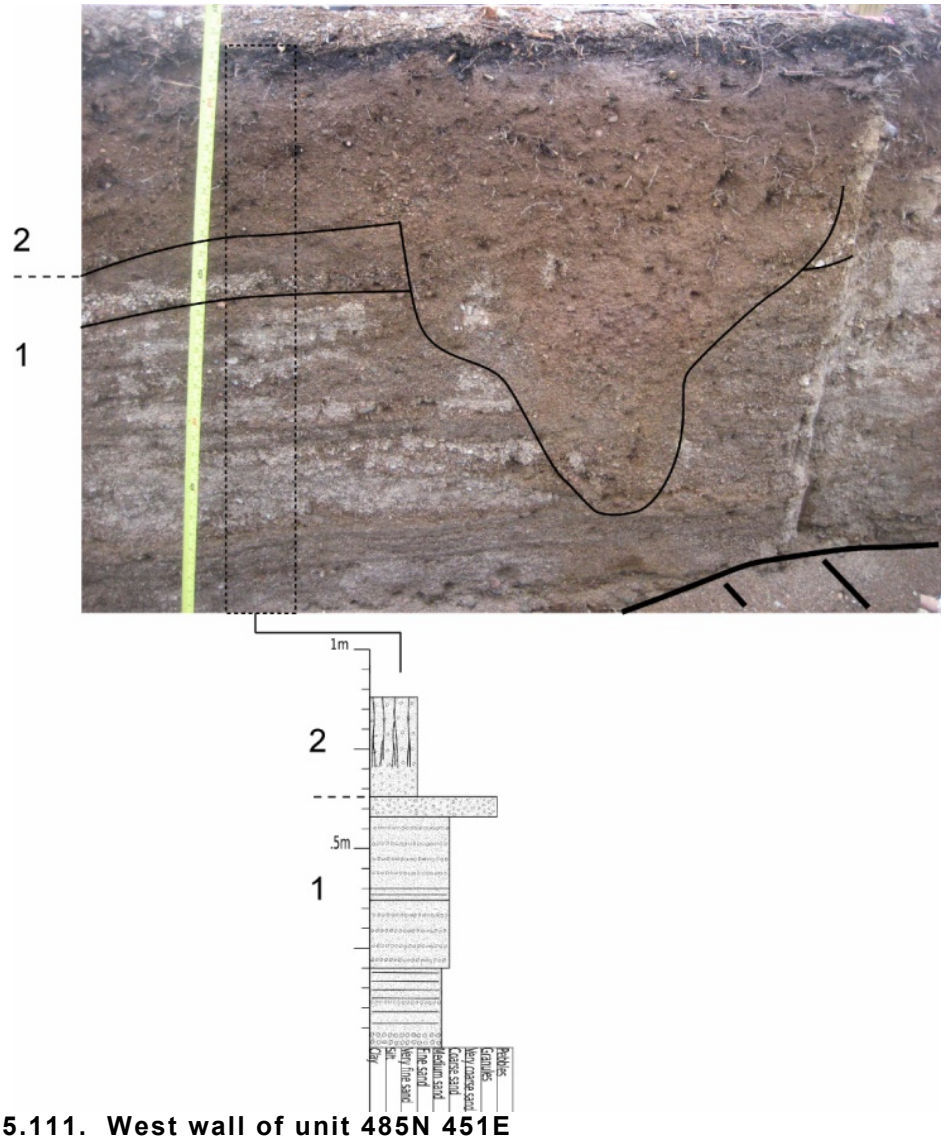

Figure 5.111. West wall of unit 485N 451E

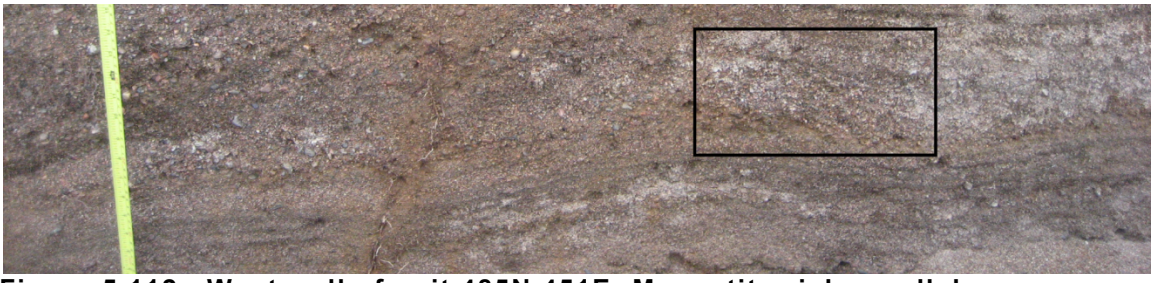

Figure 5.112. West wall of unit 485N 451E; Magnetite-rich parallel-stratification as well as planar cross-stratified sand (outlined in black).

5.11.1 Artifacts at RLF

Throughout the RLF site, artifacts were typically concentrated from surface to 15cm below surface. In the northern portion of the site, artifacts were within the bioturbated lithofacies 1K (very fine-grained to fine-grained sand with pebble layer), and within the southern portion of the site they were associated with lithofacies 2K (fine-grained to medium-grained sand with pebble layers), and 3K (silty medium-grained sand with pebbles). The amount of artifacts decreased gradually until 25cm or 30cm below surface.

5.12 Electric Woodpecker 1 and Electric Woodpecker 2

The most western archaeological sites within the study area are the Woodpecker sites (WP) (Fig. 4.1), located on a prominent ridge (Fig. 5.113). First identified in 2009, artifacts recovered from these sites appear contemporaneous, however, two site designations were given because they are bisected by a stream channel (Fig. 5.114).

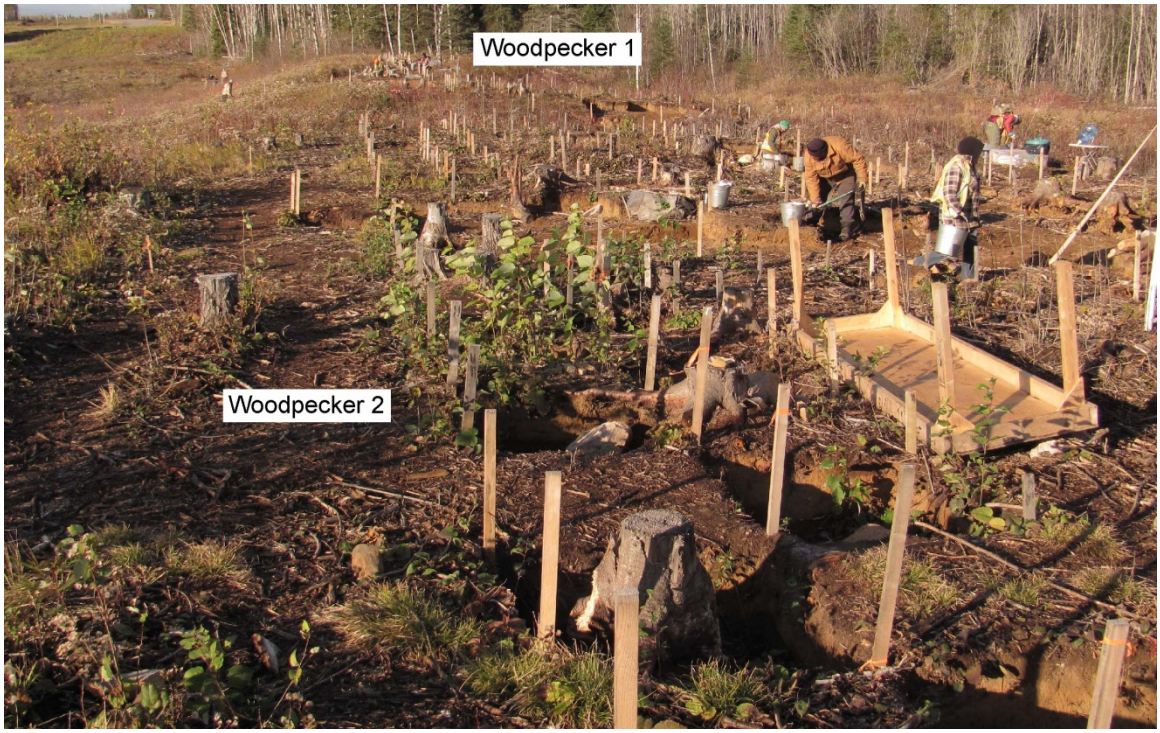

Figure 5.113. Electric Woodpecker sites, looking westward

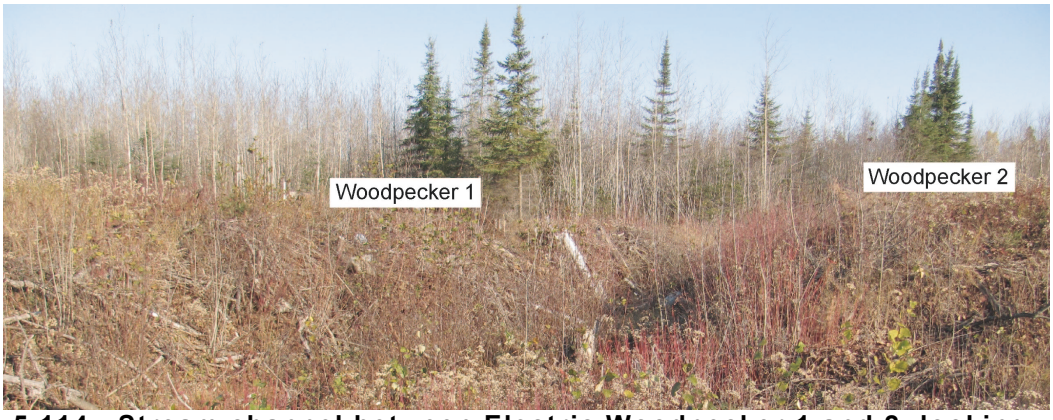

Fig. 5.114. Stream channel between Electric Woodpecker 1 and 2, looking northward

During excavation at WP 1, a large pit feature was identified. Within this pit feature, there are no apparent bedforms, although charcoal and red staining are present (Figs. 5.115 & 5.116). The pit fill (lithofacies 5L) in units 503N 469E and the northern portion of 502N 469E contained artifacts. However, units 501N 469E and the southern portion of 502N 469E were sterile below lithofacies 4L (Figs. 5.115 & 5.116). Due to the depth of artifact recoveries, and presence of charcoal with associated red staining, the west walls of units 499N 498E to 503N 498E (Figs. 5.114 & 5.116) are described in addition to the south wall of unit 499N 468E (Fig. 5.117). This pit was also profiled by soil scientists (Gilliland, 2012), and sampled for micromorphology studies (Gilliland et al., 2012) and OSL dating (Gilliland, 2012; Kinnaird et al., 2012).

1L. Fine-Grained to Medium-Grained Sand

The stratigraphically lowest lithofacies identified throughout these units is a well-sorted bed of fine-grained to medium-grained sand. This always appears to be massive, abruptly underlying lithofacies 2L as well as lithofacies 6L (the pit fill sediment). Throughout the profiles, the contact with lithofacies 2L is always horizontal with both lithofacies 1L and 2L appearing laterally continuous. However, in the west wall of unit 503N 468E (Fig. 5.116), the well-sorted sand intrudes into lithofacies 6L.

2L. Medium-Grained sand with few Granule and Pebble Layers

This lithofacies abruptly overlies well-sorted sand, revealing lateral changes in bedforms throughout the unit walls described (Figs. 5.115, 5.116, & 5.117). At the contact with lithofacies 1L, there is generally a granule and pebble layer within a matrix of well-sorted medium-grained sand (Figs. 5.116 & 5.117). In Figure 5.118, this granule and pebble layer is overlain by planar cross-stratification within medium-grained sand. Planar cross-stratified beds are 2 to 3cm thick. The uppermost section of this lithofacies is dominantly composed of parallel-bedded granules and pebbles within a medium-grained sand matrix (e.g. Fig. 5.118).

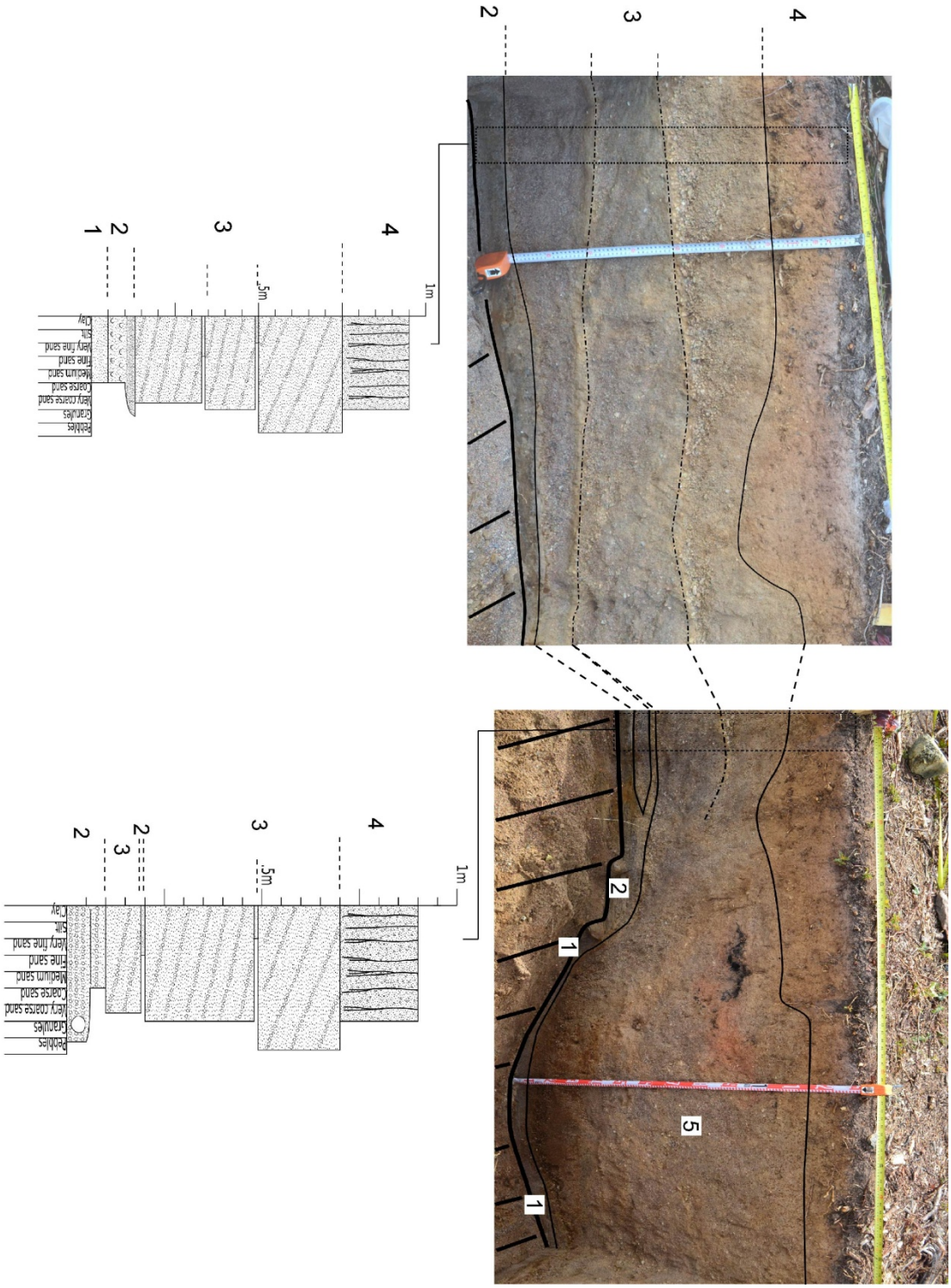

Figure 5.115. WP 1 pit feature, shown in West walls of units 501N 469E, 502N 469E, and 503N 469E

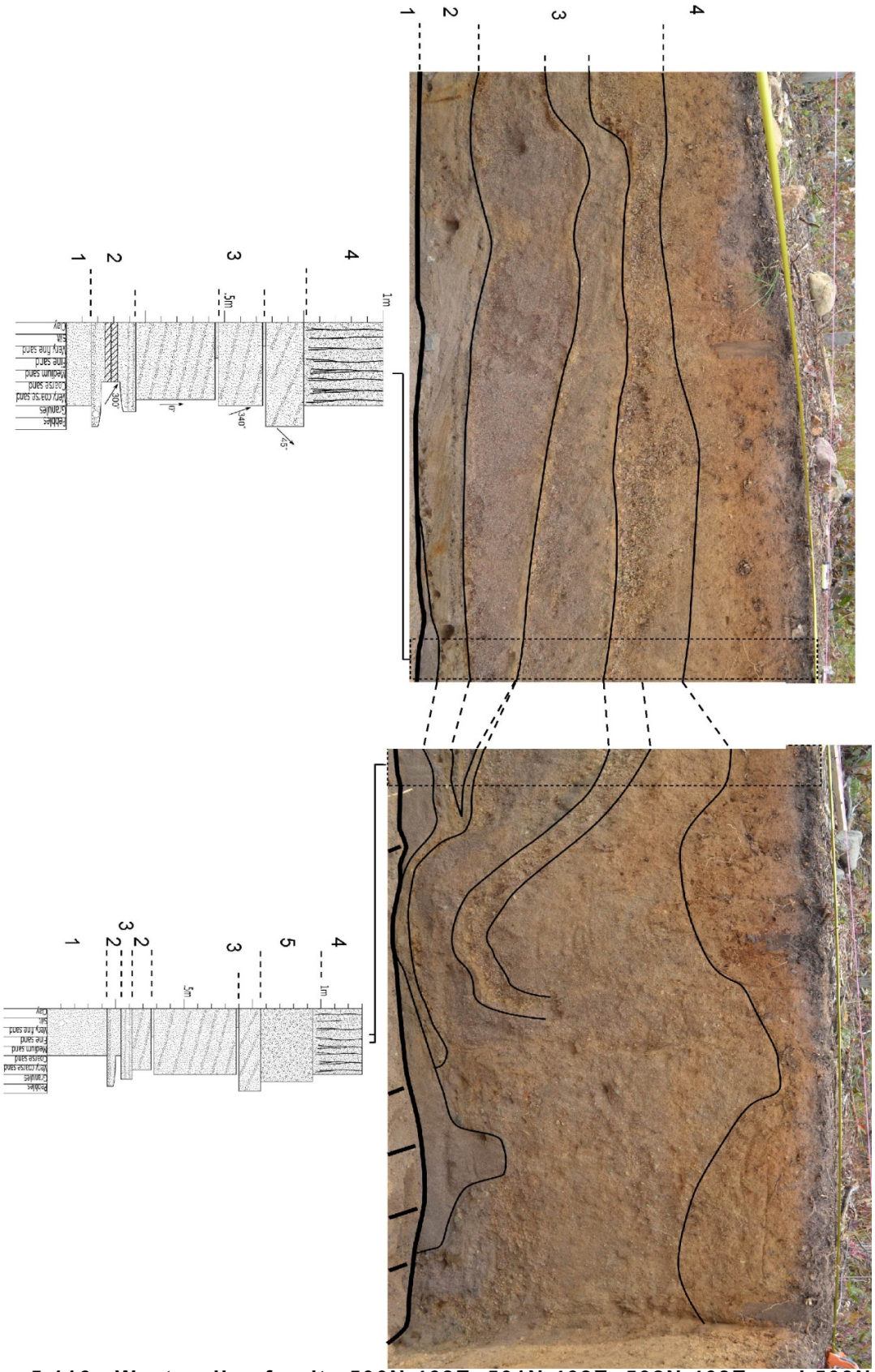

Figure 5.116. West walls of units 500N 468E, 501N 468E, 502N 468E, and 503N 468E at WP 1

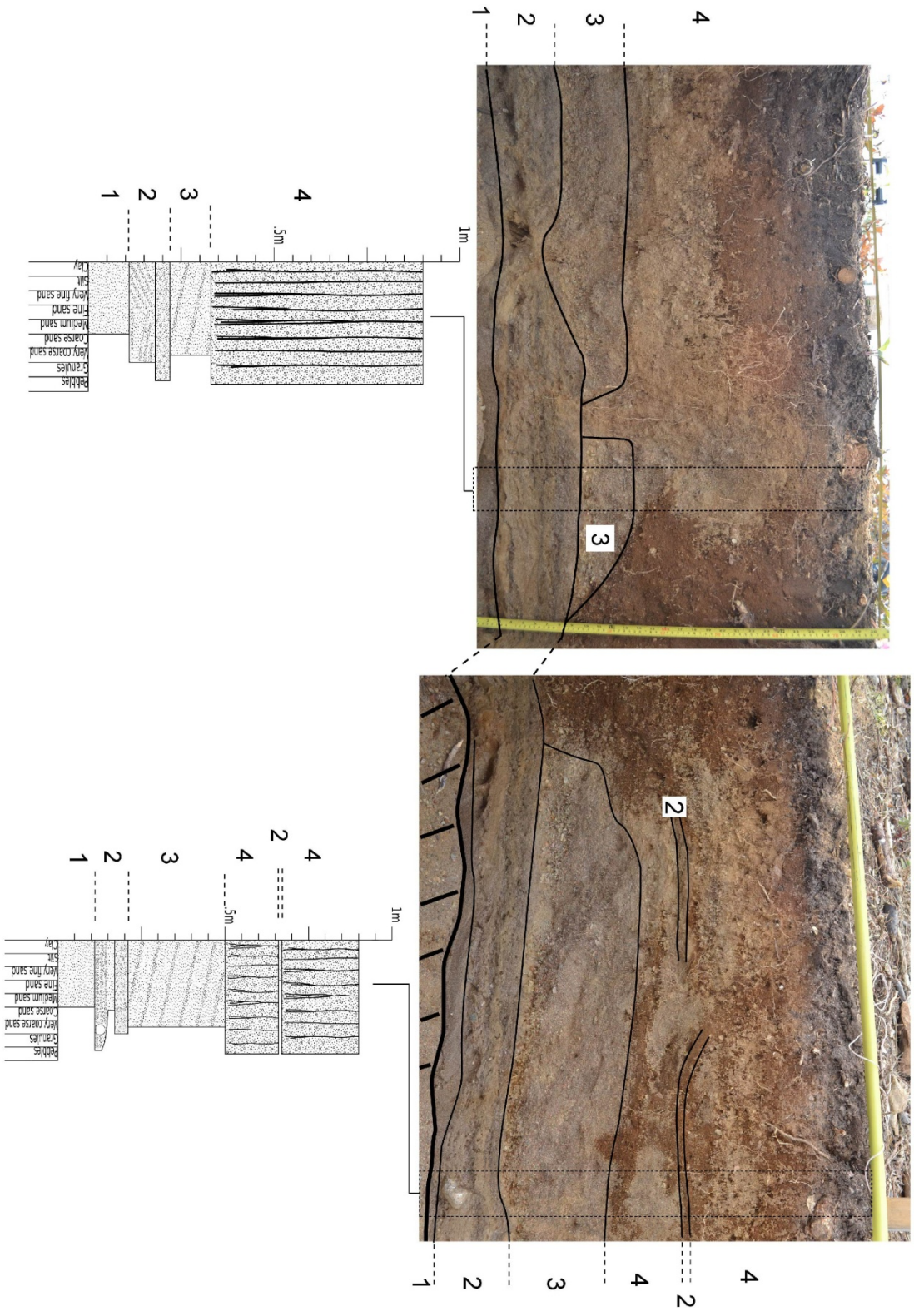

Figure 5.117. South wall of 499N 468E on the left, and West wall of 499N 468E on the right, at WP 1

However, Figure 5.119 reveals trough cross-stratified medium-grained sand at the contact with 1L. Trough cross-stratified sand beds 5cm thick are overlain by another layer of trough cross-stratified sand, in which beds are only 2 to 3cm in thickness. Overlying the trough cross-stratified medium-grained sand is parallel-stratified granules to pebbles within a medium-grained sand matrix (Fig. 5.118).

Figure 5.118. Planar cross-stratification within lithofacies association 2L

Figure 5.119. Trough cross-stratification within medium-grained sand of lithofacies association 2L

Trough cross-stratification is also present within the matrix supported granule to pebble layer that is dominantly parallel bedded. Figure 5.118 shows a pebble to granule layer at the contact with underlying lithofacies 1L. Overlying this is medium-grained sand containing trough cross-stratified granules with few pebbles. These trough cross-stratified beds average 4cm in thickness, and are overlain by parallel bedded granules to pebbles within the same medium-grained sand matrix (Fig. 5.118).

The granule to pebble layer that is commonly present at the contact with lithofacies 1L is also directly overlain by the parallel-stratified granules to pebbles within a medium-grained sand matrix that typically represents the uppermost section of this lithofacies (Fig. 5.119). Figure 5.121 demonstrates this, showing that there is no layer of cross-stratified medium-grained sand interbedding the parallel layers of matrix supported granules and pebbles.

Figure 5.120. Trough cross-stratified medium-grained sand with granules, within lithofacies association 2L

Figure 5.121. Parallel-stratified medium-grained sand to pebbles within lithofacies association 2L

Adjacent to the pit feature (Figs. 5.115 & 5.116), there is also a laterally discontinuous layer of lithofacies 2L (Fig. 5.122). Lithofacies 3L represents progradation, and is overlain by a parallel-bedded layer of what appears to be the same medium-grained sand underlying lithofacies 3L. The parallel bedding averages 3mm in thickness, and slopes at a same angle as the top of underlying lithofacies 3L. This layer of medium-grained sand thins laterally from 4cm thick as it becomes massive, fining southward into a silt layer only 2cm thick (Fig. 5.116).

Figure 5.122. Lithofacies associations 1L, 2L and 3L

3L. Cross-Stratified Medium-Grained sand to Pebbles

This lithofacies is composed of planar cross-stratified medium-grained sand to pebbles, comprising three stacked beds (differentiated by dashed lines) that differ in grain-size (Figs. 5.115 & 5.116). Paleocurrents from these three beds indicates progradation in a northward direction (Fig. 5.116). The stratigraphically lowest planar cross-stratified bed is composed of coarse-grained sand to pebbles up to 1cm in diameter, and overlain by a layer averaging 2cm thick of silt to parallel bedded medium-grained sand (lithofacies 2L). Overlying the silt to medium-grained sand layer is a second bed of cross-stratified medium-grained sand to pebbles up to 1cm in diameter. This bed is slightly finer grained the one underlying it, and is overlain by a layer of silt generally 2cm thick. The uppermost bed comprising this lithofacies is the coarsest, composed of planar cross-stratified medium-grained sand to pebbles up to 3cm in diameter. Within this bed, the layers appear to be graded due to the coarser grains (pebbles) rolling downslope.

4L. Silty Medium-Grained to Coarse-Grained Sand with Pebbles

This generally comprises the uppermost lithofacies observed throughout the Woodpecker sites. Contact with the underlying cross-stratified sand to pebbles is seen grading into silty medium-grained to coarse-grained sand with granules and pebbles (Figs. 5.115 & 5.116). Although the south and west walls of unit 499N 468E appears to have a much finer matrix, this is the result of higher moisture content from a slightly higher concentration of clay and silt. This poorly-sorted lithofacies always contains roots, and appears to be strongly bioturbated.

5L. Silty Fine-Grained Sand to Coarse-Grained Sand with Pebbles

This lithofacies has a concave-up base, composed of poorly-sorted silty fine-grained sand to coarse-grained sand and pebbles. The pit feature appears to be massive, and infilled with sediment that is adjacent to it. Lithofacies 3L continues into this lithofacies, resulting in one massive layer composed of medium-grained sand with pebbles (Fig. 5.116).

Unit 511N 591E

Located on the west side of the stream channel, this unit is within the WP 1 archaeological site and reveals different lithofacies than those seen above (Fig. 5.123).

6L. Cross-Stratified Medium-Grained sand to Pebbles with Reactivation Surface

This lithofacies is composed of planar cross-stratified medium-grained to coarse-grained sand with few pebbles up to 7mm in diameter (Fig. 5.123). A reactivation surface indicates there was a change in velocity. The lower bed of planar cross-stratification contains no pebbles and layers averaging 5mm thick, while the upper bed shows that an increase in velocity allowed pebbles to be mobilized by the current and deposited in layers that are up to 1cm in thickness. Paleocurrent direction indicates a northeastward direction of flow (Fig. 5.123).

7L. Cross-Stratified Silt to Pebbles

Abruptly overlying lithofacies 6L, festoon cross-stratified beds are composed of silt to medium-grained sand matrix containing granules and pebbles (Fig. 5.123). Layers generally average 4cm in thickness.

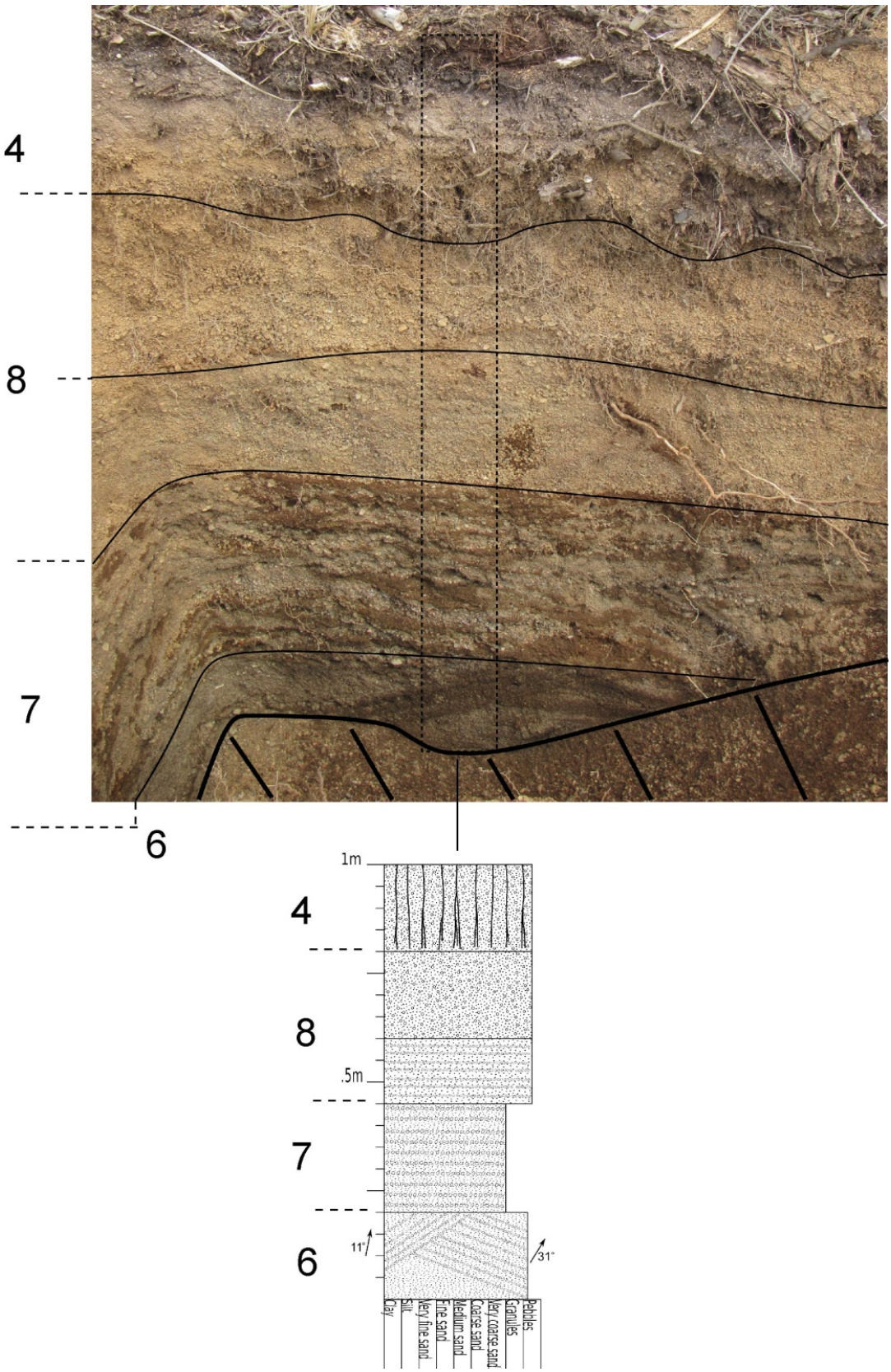

Figure 5.123. East wall of unit 511N 591E

7L. Cross-Stratified Medium-Grained Sand to Pebbles

Abruptly overlying the festoon cross-stratification is low angle cross-stratified medium-grained sand to very coarse-grained sand with granules and pebbles 1 to 2cm in diameter (Fig. 5.123). This lithofacies is slightly bioturbated, and no layers are prominent enough to determine a paleocurrent direction. A line separates two beds of this lithofacies because the upper section is more bioturbated and appears massive, although consistent grain-size and a very diffuse contact indicate that they represent the same lithofacies (Fig. 5.123).

4L. Silty Medium-Grained to Coarse-Grained Sand with Pebbles

There is a very gradual and diffuse contact with the underlying massive and bioturbated lithofacies 3L (Fig. 5.123). However, this lithofacies contains more silt and fewer pebbles, consistent with lithofacies 4L identified in the walls of units described above.

510N 505E

On the east side of the stream channel, this unit is considered to be within the WP 2 archaeological site.

1L. Fine-Grained to Medium-Grained Sand

Seen at the bottom of unit 510N 505E there are two beds of well-sorted fine-grained to medium-grained sand (Fig. 5.124), which appear to be the same as the sand underlying the large pit feature (Fig. 5.124). The lower bed appears massive, and is abruptly overlain by lithofacies 9L. At this contact, one large cobble and a large pebble are seen to be within the well-sorted sand although these are part of lithofacies 9L (Fig. 5.124). Abruptly overlying lithofacies 9L, another bed of well-sorted fine-grained to medium-grained sand is parallel-stratified with layers averaging 5mm in thickness.

9L. Massive Fine-Grained Sand to Cobbles

This lithofacies is composed of poorly-sorted medium-grained to coarse-grained sand containing granules, pebbles ranging from 1cm to 4cm in diameter, as well as a cobble 10cm in diameter (Fig. 5.124). The upper and lower contacts with lithofacies 1L are quite abrupt, although a cobble and large pebble are seen to lie within the underlying well-sorted sand. The pebbles within this poorly-sorted lithofacies do not appear to be imbricated.

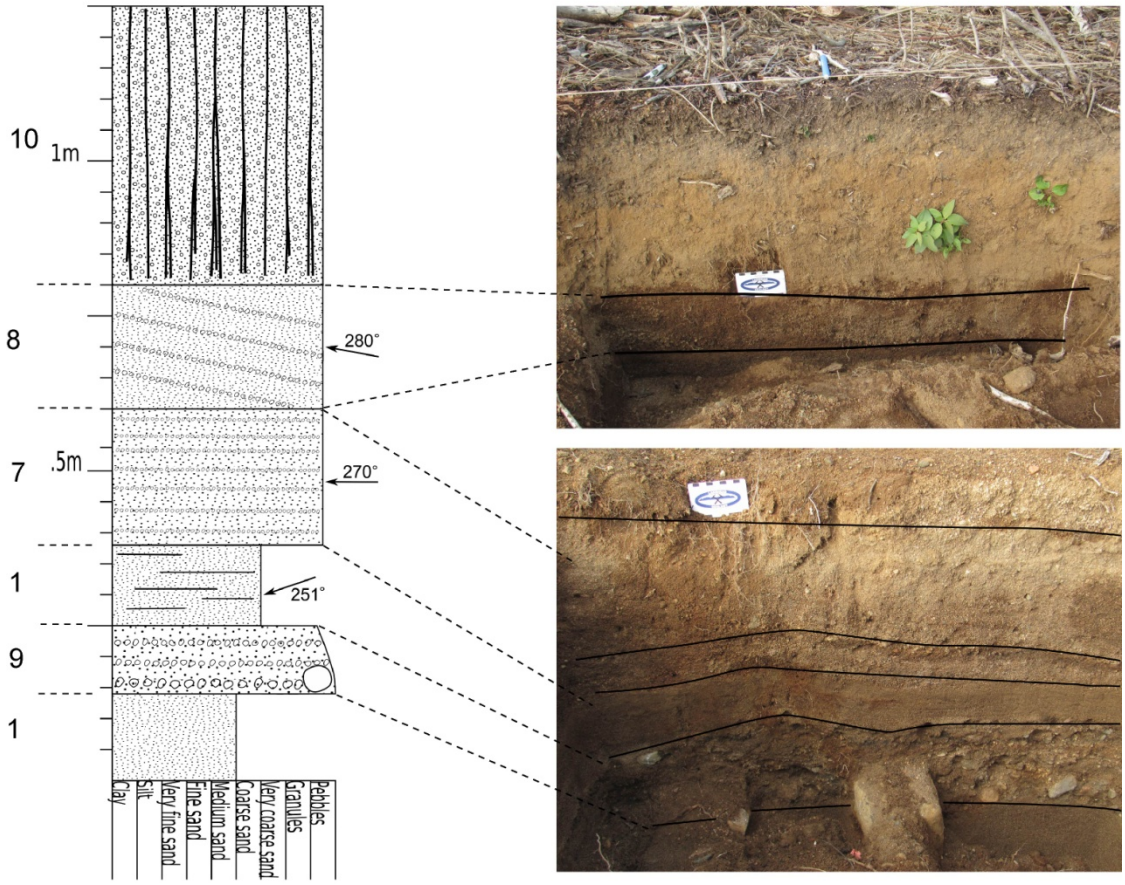

Figure 5.124. West wall of unit 510N 505E

7L. Cross-Stratified Silt to Pebbles

Seen in the east wall of unit 510N 505E (Fig. 5.124), this lithofacies is much thinner than where it is exposed in unit 511N 591E of WP 1 (Fig. 5.124) and appears to be planar cross-stratified instead of festoon cross-stratified. There is only one silt-rich layer within this bed, thus the grain-size of this lithofacies and lithofacies 8L in the stratigraphic column are the same.

8L. Cross-Stratified Medium-Grained Sand to Pebbles

Abruptly overlying the silty planar cross-stratified lithofacies 7L is medium-grained sand to very coarse-grained sand with granules and pebbles 1 to 2cm in diameter (Fig. 5.124). The paleocurrent is due west, changing slightly to northwest above the line separating two beds of this lithofacies (Fig. 5.124). There is a very gradual change upward to lithofacies 10L.

10L. Silty Fine-Grained to Medium-Grained Sand with Few pebbles

Composed of silty fine-grained sand to medium-grained sand containing few pebbles, this lithofacies appears massive and strongly bioturbated (Fig. 5.124). There are fewer pebbles within a much finer matrix than lithofacies 4L, which extends to the surface at WP 1 (Fig. 5.124).

Unit 512N 529E

The last unit of WP 2 described is quite different from what is observed throughout the majority of the site (Fig. 5.125). These lithofacies were only identified to the west of the road bisecting WP.

11L. Clay-Rich Very Fine-Grained Sand

This lithofacies is composed dominantly of clay-rich very fine-grained sand, however one large cobble 15 to 20cm in diameter is seen as well (Fig. 5.125). Roots are present within this lithofacies, and no bedforms are apparent.

12L. Fine-Grained to Medium-Grained sand with few pebbles

Abruptly overlying the massive clay-rich sand is fine-grained to medium-grained sand containing few pebbles that vary in size from 3cm to 10cm in diameter (Fig. 5.125). Also seen within the sand are small amounts of charcoal (circled in Fig. 5.125), and roots. This lithofacies grades into overlying lithofacies 13L.

13L. Silty Fine-Grained Sand with Pebbles

This lithofacies is very badly bioturbated, containing numerous roots (Fig. 5.125). It is composed of silty fine-grained sand with pebbles ranging from 1cm to 10cm in diameter, appearing massive.

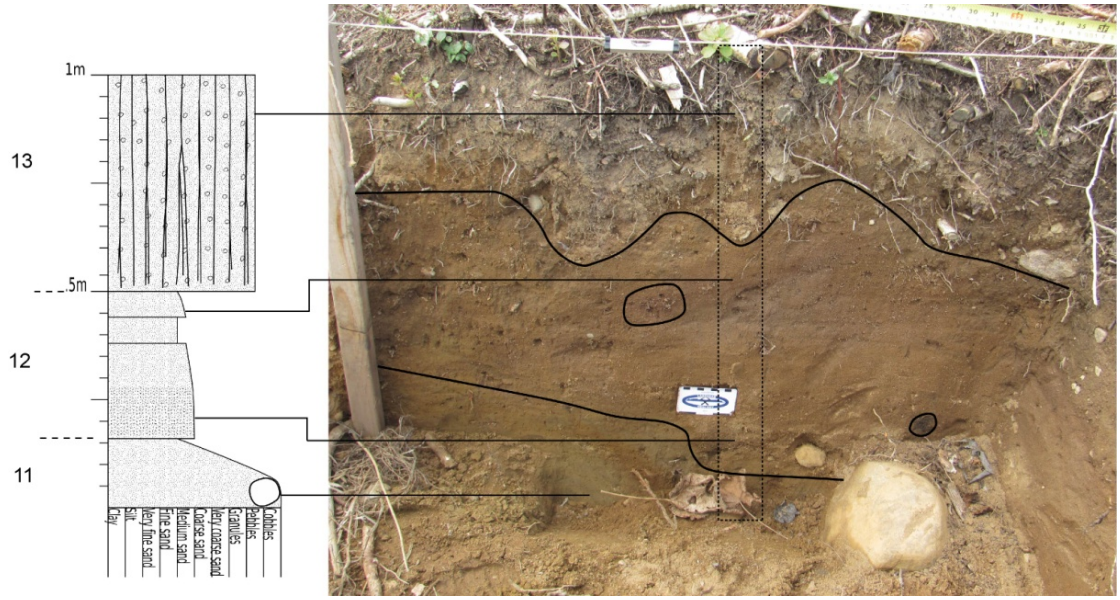

Figure 5.125. Circles indicate presence of charcoal.

Unit 530N 565E

Excavations in the summer of 2012 were conducted in the eastern portion of the Woodpecker 2, and revealed additional lithofacies (Fig. 5.126). One wall profile is presented here, although the lithofacies are laterally continuous and additional photos are provided.

2L. Medium-Grained sand with few Granule and Pebble Layers

This lithofacies appears to be the same as the one identified adjacent to the large pit at Woodpecker 1, with similar variability. Within the north wall of unit 530N 565E, there is poorly-sorted and horizontally-stratified fine-grained sand to coarse-grained sand containing granules and pebbles up to 7mm in diameter (Fig. 5.126). Upward the matrix appears to remain the same but the pebbles are slightly larger, up to 2cm in diameter. This section of the lithofacies is also massive, with no apparent horizontal-stratification or imbrication.

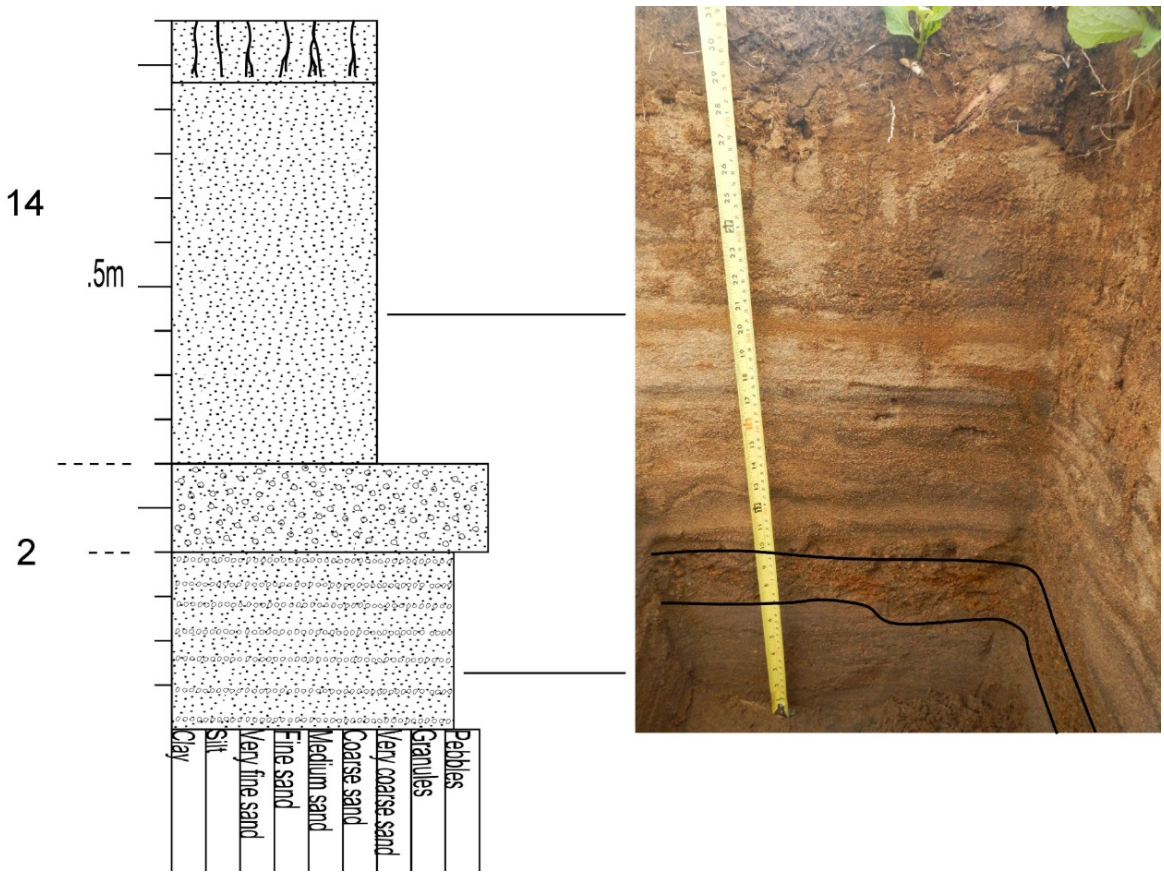

Figure 5.126. North wall of unit 530N 565E

Within the west wall of unit 525N 558E, the stratigraphically lowest portion is composed of fine-grained sand with planar cross-stratification. Overlying, there are layers of parallel-stratified granules to pebbles within a fine-grained to medium-grained sand matrix (Fig. 5.127). Additional bedforms include horizontally-stratified layers of fine-grained to medium-grained sand, as well as one reactivation surface (Fig. 5.127). A similar sequence is also present within the units 525N 558E, 511N 535E, and 527N 552E indicating that it is quite laterally continuous on the east side of the stream channel.

The lithofacies sequence in unit 527N 552E is dominantly consistent with the one described for unit 525N 558E, although at the bottom of the profile there are cobbles (Fig. 5.128). This poorly-sorted fine-grained sand with granules and pebbles appears very similar to lithofacies 8L.

Figure 5.127. Lithofacies 2L within unit 525N 558E

Figure 5.128. Lithofacies 2L within the wall profile of unit 525N 552E

14L. Well-Sorted Fine-Grained to Coarse-Grained Sand

This lithofacies is composed of well-sorted low-angle cross-stratified layers that vary slightly in grain-size. Layers are dominantly fine-grained sand or medium-grained sand, and occasionally coarse-grained sand. These are also magnetite-rich layers interbedded with non magnetite-rich layers. Artifacts were recovered from within this lithofacies (Fig. 5.129).

Units along the road reveal lithofacies 15, which is also present 20 to 30 metres away throughout the eastern portion of the site. Absence of modern soil

in the profiles along the road (Fig. 5.130) indicates that the surface of the road was removed, likely when it was graded. A profile of the ridge adjacent to the road is dominantly composed of massive fine-grained to medium-grained, overlying lithofacies 13L (Fig. 5.131). The massive portion of the profile also contains roots, and is likely bioturbated.

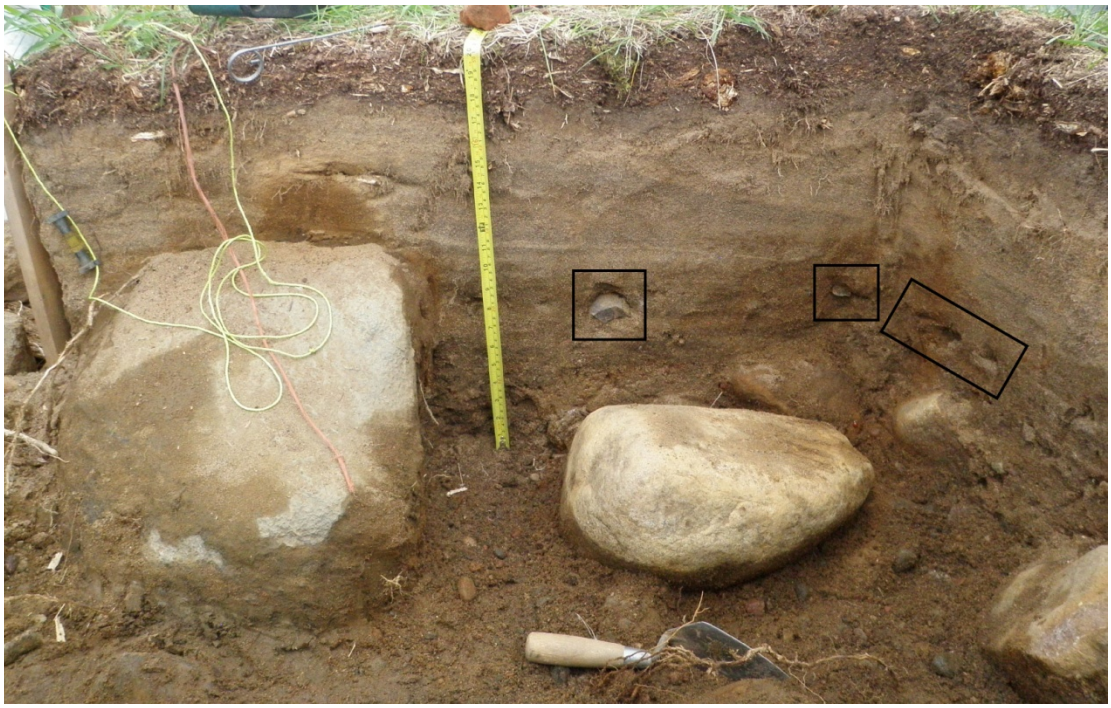

Figure 5.129. Artifacts recovered from within lithofacies 13L at Woodpecker 2. Artifact locations are outlined in black.

Figure 5.130. Unit directly under the road at Woodpecker 2 revealing lithofacies 13L with no overlying modern soil

Figure 5.131. Profile of ridge adjacent to the road

Also within lithofacies 13L are small linear trails that appear silver-coloured within the red sediment (Fig. 5.132). These are about 5mm in diameter, and extend from the wall profile to the floor of unit 510N 450E.

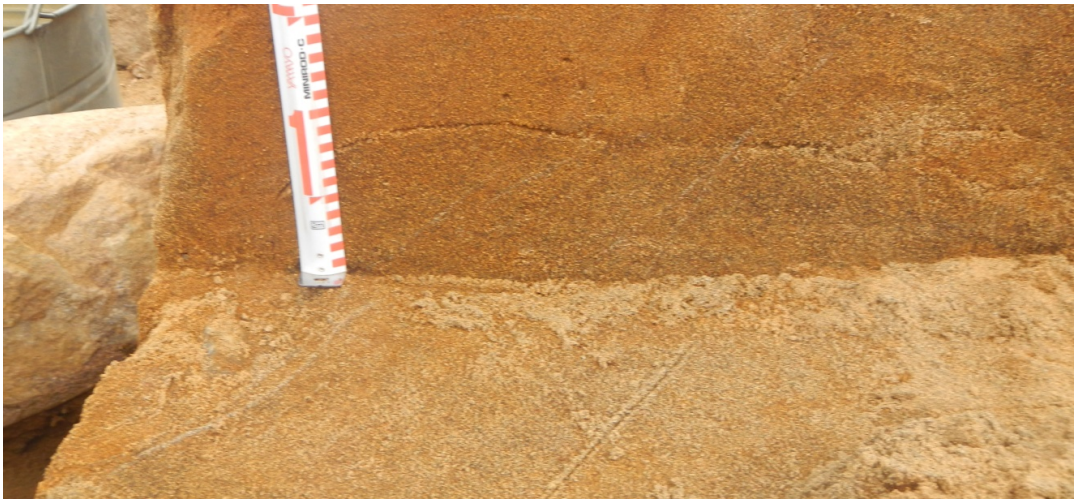

Figure 5.132. Linear trails within unit 510N 450E

5.12.1. Artifacts at the Woodpecker Sites

Artifacts were recovered from variable depths and lithofacies throughout the Woodpecker sites, although dominantly in bioturbated sediments with no identifiable stratigraphy. In general, artifacts were found from surface to 50cm or 60cm below surface within lithofacies 4L (silty medium-grained to coarse-grained sand with pebbles). However, artifacts were recovered from surface to the bottom of the pit feature at Mackenzie 1 within lithofacies 5L (silty fine-grained to coarse-grained sand with pebbles). In one portion of the site, artifacts were found within lithofacies 11L (clay-rich very fine-grained sand), 12L (fine-grained to medium-grained sand with few pebbles), and 13L (silty fine-grained sand with pebbles). Lastly, one excavated unit revealed artifacts within lithofacies 13L (silty fine-grained sand with pebbles). This is the only instance of artifacts being associated with identifiable stratigraphy.

5.13 Auger Holes

Lithofacies 1A, 1C, 1D, 1G, and 1H (located at Gravel Pit 1, Gravel Pit 3, the Mackenzie Roadcut, the Construction Site, and the Mackenzie 1 Trench respectively) appear to represent the same lithofacies association (Fig. 4.1). Paleocurrent directions within lithofacies 1A trend southward, which is also the paleocurrent direction seen within lithofacies 1C and 1D. Lithofacies association 1G is northwest, and there are no paleocurrent directions for 1H. Holes were augered to determine whether lithofacies 1A extends to the Mackenzie Roadcut and Mackenzie Trench.

A1

At the RLF archaeological site, the auger hole indicates that lithofacies 1K extends to ~160cm b.s. At about this depth, there are large rocks (over 5cm in diameter) that inhibit utilizing the auger. Below this layer of rocks, well-sorted very fine-grained to fine-grained sand is present. At 200cm b.s. there appears to be parallel-stratified beds averaging 3mm in thickness within the fine-grained sand, however the majority of this lithofacies extending to 345cm b.s. appears massive.

A2, A3, A4, and A5

A2 is downslope from Gravel Pit 1 (Fig. 4.1), and the upper 35cm of sediment within the auger hole is very fine-grained to fine-grained sand. This likely represents colluvium, as evidenced by the organic layer 35cm b.s., which is possibly the natural surface. Underlying the organic layer is medium-grained to coarse-grained sand with pebbles, likely representing the lithofacies identified at Mackenzie 1 however no bedforms are visible in the augered sediment. At ~130 cm b.s. there is either bedrock or a layer of pebbles. This was encountered within three auger holes, and it was not possible to auger deeper. Since it is possible that a pebble layer represents the same lag deposit identified at A1 within the Mackenzie 1 Trench, additional holes were augered.

Similar to the sediment identified in A2, the sediment observed in A3, indicates colluvium represents the upper 67cm. Underlying there is no observable organic layer, however medium-grained to coarse-grained sand with pebbles is present. This sediment extends to surface within augers A4 and A5. At 180cm b.s. in A3, and 130cm in A4 large pebbles were present, through which augering is not possible.

The hole at A5 reveals medium-grained to coarse-grained sand with pebbles that extends to 95cm b.s. Underlying this, black organic-rich fine-grained sand with granules is present. This is water saturated, which inhibited augering deeper than 115cm.

6. INTERPRETATIONS

This chapter is divided into two sections, beginning with lithofacies interpretations. Once the depositional environments within the study area are established, the paleogeographic interpretations are discussed.

Previous work (Zoltai, 1965; Julig, 1984; Julig et al., 1990; Phillips & Fralick, 1994b) has demonstrated that sediments deposited in the Thunder Bay region at this time are likely related to glacial, lacustrine, deltaic, fluvial, or aeolian environments. Within the study area, seven separate lake levels were identified (Fig. 6.1), as presented in this section. Figure 6.1 depicts the vertical association of these lake levels.

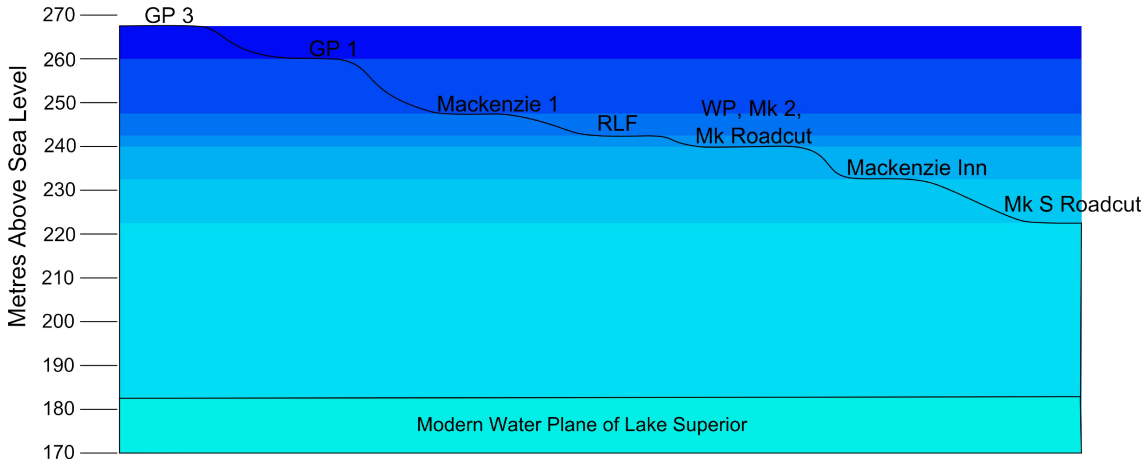

Figure 6.1. Strandlines identified within the study area. Elevations discussed below are shown.

6.1 Lithofacies Interpretations

Interpretations of each exposure are provided in this chapter. The processes of deposition for each lithofacies and lithofacies association are outlined and the overall depositional environment of each sequence is discussed. This has been completed through comparison with other similar deposits that are described in the literature.

6.1.1 Gravel Pit 1

Lithofacies 1A. Very Fine-Grained to Medium-Grained Sand

Only one lithofacies association was identified at Gravel Pit 1, located at the top of a prominent ridge that continues north of Mackenzie 1. It is composed of very fine-grained to fine-grained sand with ripple cross-lamination, climbing ripple cross-lamination, parallel-stratification and massive layers.

Ripple lamination results from density underflows of sediment-laden meltwater flowing into a glacial lake (Jopling & Walker, 1968). The climbing ripples identified within lithofacies association 1A are type A (Jopling & Walker, 1968), composed entirely of climbing sets of lee side laminae with no preservation of stoss side laminae. Ripple amplitude does not decrease gradually upward. The absence of stoss side laminae implies that fall out from suspension was not rapid enough to bury the grains moving on the bed (Jopling & Walker, 1968). Suspension deposition is therefore not rapid enough to preserve stoss side lamination, indicating that the suspension/traction ratio is very low for the formation of climbing ripples (Jopling & Walker, 1968).

Parallel-stratified massive layers are likely the result of sedimentation from suspension (c.f. Pickering, 1982; Ashley et al., 1982). Continued fallout of sediment from suspension occurs after ripple migration has ceased or nearly ceased (Ashley et al., 1982). Draped laminae (Gustavson et al., 1975), deposited from suspension and draping ripple cross-lamination occasionally appear wavy.

Sequences of ripple cross-stratification overlain by parallel-stratification and capped by ripple cross-stratification are present within this lithofacies association. This indicates that flow of the river entering the Superior basin was variable (Myrow et al., 2008).

The bedforms and grain-size characteristics identified at Gravel Pit 1 are consistent with similar lithofacies associations interpreted to represent the prodelta sequence of a glacial deltaic system (e.g. Smith & Eriksson, 1979; Gustavson et al., 1975). The rippled beds are interpreted as deposition by density underflows entering a glacial lake, while the flow was in contact with the

lake bottom (Jopling & Walker, 1968). Parallel-stratification was deposited by interflows or overflows, while the current was not in contact with the lake bottom (Pickering, 1982; Sturm & Matter, 1978).

Within this prodelta sequence, small-scale normal faults are present. These are similar to features identified in other exposures, within sands that have been displaced on the scale of milimetres to centimetres (e.g. Visser et al., 1984; Vanneste et al., 1999). This small-scale faulting is a semi-brittle type of soft sediment deformation, which could be developed by sudden stress when pore water pressure was raised (not sufficiently to reach liquefaction), or when the sand was frozen (Vanneste et al., 1999).

6.1.2 Gravel Pit 1 Summary

Gravel pit 1 is consistent with a prodelta sequence deposited in the lakeward portion of a delta. It is located at a modern elevation of 259m asl, which is about 13m higher than any known lake margin in the Superior basin. Although it is not possible to determine the level of the proglacial lake this sequence represents, it likely does not represent a high stand in the Superior basin. Elevation indicates that the prodelta sequence more likely represents a late stage of Lake Beaver Bay (Stuart, 1993; Phillips & Fralick, 1994b), discussed further below.

Gravel Pit 1 is located on a prominent ridge (Fig. 6.1), which likely represents a wave-cut shoreline (e.g. Meldahl, 1995; Drake & Bristow, 2006) consistent with Minong beach terraces in the Thunder Bay region (e.g. Julig et al., 1990). The shoreline elvation is consistent with a known Minong strandline (Phillips & Fralick, 1994b).

6.1.3 Gravel Pit 2

Lithofacies 1B, 7B, and 8B. Medium-Grained Sand to Pebbles

Lithofacies 1B and 7B likely represent the same lithofacies association. This conclusion is based on similarities observed in grain-size as well as bedforms. Lithofacies 1B and 7B are both composed of medium-grained sand to pebbles while lithofacies 8B contains silt and roots which have bioturbated the stratigraphy. However, lithofacies 8B is likely a continuation of the same lithofacies association. Where bedding is apparent, laterally continuous planar cross-stratified medium-grained sand to pebbles a maximum of 5cm in diameter is present.

The planar cross-stratified medium-grained to coarse-grained sand with matrix-supported pebbles are similar to conglomerates from the Cardium Formation (Western Canadian Sedimentary Basin) interpreted as river-mouth sediments (Hart & Plint, 2003). Poorly developed clast segregation and laterally continuous foreset to bottomset bedding (e.g. Fig. 5.8) is consistent with an inertia-dominated river-mouth environment (Wright, 1977). This type of river outflow is generally associated with steep gradient streams entering deep fresh-water lakes, although it may occasionally prevail at newly created river-mouths along the open coast (Wright, 1977). The section examined at Gravel Pit 2 is interpreted to be the bar front of a river-mouth where a river entered a deep lake, with no observable wave re-working (Clifton, 1973; Wright, 1977; Hart & Plint, 2003).

Lithofacies 2B. Very Fine-Grained to Fine-Grained Sand

The base of this lithofacies is concave up, indicating that it represents a channel fill sequence (Ramos & Sopena, 1983). Bedforms within the very fine-grained to fine-grained sand are ripple cross-lamination and parallel-stratification. These bedforms result from sub- to super-critical river flows, generally representing the infilling of small channels (Ramos et al., 1986). Ripple cross-lamination occurs in the shallowest parts of a channel (Bridge et al., 1986), and

during high flow velocity ripples can be completely flattened as they transition to upper plane bed parallel-stratification (Van Den Berg & Van Gelder, 1993).

Lithofacies 3B. Fine-Grained to Medium-Grained Sand

This lithofacies is composed of cross-lamination roughly concordant to the base with convex up laminae laterally becoming concave up, similar to facies identified within braided stream systems (Allen, 1983b; Ramos et al., 1986). These have been interpreted as river bars, in which laminae were deposited generally at an angle to the erosional surface over which the bar was travelling, but never on a slope steep enough to have caused avalanching (Allen, 1983b). This process results in a gently inclined slope underlain by plane-bedded sand, consistent with a long and narrow lobe-shaped bar (Allen, 1983b).

Lithofacies 4B. Coarse-Grained Sand with Granules

Within the sand and granules comprising this lithofacies, parallel-laminated beds averaging 5mm in thickness are apparent. A higher velocity flow likely eroded the base of this lithofacies, and was capable of transporting the coarser grains comprising it. The top of the lithofacies is convex up, similar to flat-bedded facies occurring as very thin units. Ramos et al. (1986) interpreted similar deposits as an upper-regime bedform developed at the beginning of an episode of increasing energy, as a result of a change in flow stage.

Lithofacies 5B. Fine-Grained to Medium-Grained Sand

This lithofacies is parallel-laminated, composed of layers up to 5mm thick, and contains pebbles at the contact with lithofacies 3B and 4B. The plane bedded sand underlain by pebbles is consistent with a river bar within the braided river system (Allen, 1983b). However, this could also represent a river channel. The pebbles at the base of the lithofacies may represent a lag deposit, resulting from the winnowing of finer clasts when the current is strongest (Allen, 1963), and the parallel-lamination would represent upper plane bed conditions (Van Den Berg & Van Gelder, 1993).

6B. Lens of Very Fine-Grained Sand

Two lenses composed of silty very fine-grained sand with an erosive base and top comprise this lithofacies. These likely represent one layer, which has been eroded into by overlying river-mouth gravels. The scoured base indicates that it represents an erosive channel, which is lined with fine-grained sediment (c.f., Ramos & Sopena, 1983).

6.1.4 Gravel Pit 2 Summary

This sequence appears to represent a river-mouth depositional environment, with north to northwestward progradation. Lithofacies 1B likely represents the bar front of a river-mouth, and overlying lithofacies 2B to 6B were deposited within the braided river of this system. The braided river was on the scale of metres wide, as indicated by the lateral continuity of the channel and river bar deposits. The lag deposit within lithofacies 5B, and scours infilled with silty very fine-grained sand indicates that the river current fluctuated. This may represent seasonal changes.

6.1.5 Gravel Pit 3

Lithofacies 1C. Very Fine-Grained to Medium-Grained Sand

This lithofacies association is composed of ripple cross-lamination, climbing ripple cross-lamination, and massive parallel-stratification. Ripple cross-lamination and climbing ripple cross-lamination can be caused by density underflows entering a glacial lake (Jopling & Walker, 1968; Sharpe et al., 1992; Boyd, 2007). The climbing ripple cross-stratification present here is dominantly Type A, deposited when sediment was transported mainly by traction, with small input from a suspended load (Jopling & Walker, 1968). Less commonly seen are sinusoidal ripples, deposited when the suspension/traction ratio is relatively high (Jopling & Walker, 1968). Sinusoidal ripples are interbedded with parallel-stratification, which are deposited by grains falling out of suspension when the flow is not in contact with the bottom (e.g., Pickering, 1982; Ashley et al., 1982).

This appears to represent a prodelta sequence within a glacial deltaic system (e.g. Gustavson et al., 1975; Smith & Eriksson, 1979), as seen in lithofacies association 1A.

Lithofacies 2C. Very Fine-Grained to Coarse-Grained Sand

The low angle planar cross-stratification comprising this lithofacies association is characteristic of beach foreshore deposits (Thompson, 1937). Laminae within this lithofacies association are defined by alternating layers of magnetite-rich (identified with a magnet) and magnetite-poor sand. This distinctive lamination results from grain segregation within bed flow during wave backwash (Clifton, 1969). Waves and littoral currents are capable of sorting and uniformly spreading sediment in individual laminae, although currents can vary greatly and produce contiguous laminae of well-sorted material of markedly differing grain-sizes (Thompson, 1937). An incoming wave transports a consistent particle size, dependent on specific gravity to the slope of the beach, depositing the grains that cannot be transported by the backwash flow (Thompson, 1937). The backwash tends to erode deposits of the swash zone more deeply at the lower than at the upper surface of the beach, resulting from the erosive power of the backwash increasingly downslope (Thompson, 1937). The magnetite-rich layers result from their high specific gravity, which makes magnetite grains more difficult to transport (Thompson, 1937). As a wave carries both smaller high-density and low-density grains, the heavy smaller grains tend to settle to the bottom of the deposited lamina. Then the subsequent backwash transports the low-density grains and leaves the high-density grains resulting in a magnetite-rich layer (Thompson, 1937).

Lithofacies 3C. Very Fine-Gained to Fine-Grained Sand

This lithofacies association is only present in profile A 0m, and is composed of ripple cross-stratified and trough cross-stratified fine-grained sand overlain by horizontally-stratified coarse-grained sand with few granules. Paleocurrent direction of the ripple cross-stratification averages 204°, which was

toward the large lake. This sequence may represent a ridge and runnel system. Ridges form on the upper shoreface after storm events under conditions of asymmetric oscillatory flow, and actively migrate landward (Dabrio, 1982). On the landward side of these ridges, a trough develops comprising the runnel environment, where ripples form due to wave and longshore currents (Dabrio, 1982). As the ridge continues to prograde, it will migrate over the runnel deposits and weld onto the beach berm (Dabrio, 1982). Water spilling over the ridge due to wave action will flow parallel to the shore, and eventually enter rip channels where it travels seaward as a rip current (Davis et al., 1971). Rip channels located along coastlines that are not significantly influenced by tides will generally last only days, until there is sufficient longshore current caused by wave swash to fill the rip areas (Davis et al., 1971). The lakeward direction of ripples identified in profile A 0m may represent a rip channel common to ridge and runnel systems, with overlying horizontally-stratified sand representing the ridge as it migrated over the channel.

Lithofacies 4C. Medium-Grained to Coarse-Grained Sand

Planar and rare trough cross-stratified sand comprises this lithofacies association, with common reactivation surfaces and a variety of paleocurrent directions. These features are similar to those observed in coastal dunes (Bigarella et al., 1969). Aeolian dunes are commonly associated with the backbeach environment, controlled by nearshore processes as well as the beach slope (Sherman & Bauer, 1993).

The internal structure of coastal dunes has been well defined by Bigarella et al. (1969). High angled foreset beds are common, with high dip angles where conditions of regional moisture facilitate cohesion of the sand grains (Bigarella, 1969). Reactivation surfaces are dominantly horizontal or dip downwind at a low angle (Bigarella, 1969). However, high angled reactivation surfaces do occur on the downwind part of large dunes (McKee, 1966). Cross-stratification is dominantly planar, although trough cross-stratification is also frequent (Bigarella et al., 1969). Another common feature is penecontemporaneous deformation,

characteristic of the upper slipface. Contorted bedding occurs due to gravity at the time of or shortly after deposition (Bigarella, 1969).

Lithofacies 5C. Fine-Grained to Medium-Grained Sand

Interbedded with the aeolian dune lithofacies are rippled layers, generally about 5cm in thickness. These appear to be wind ripples, which are common in dry interdune deposits (Kocurek, 1981). Interdune environments are flat or gently sloping areas between dunes, where the wind is more directionally variable due to eddying around the upwind dune (Fryberger et al., 1983). Rapid erosion often occurs in interdune areas due to storage of drifting sand by the dune immediately upwind (Frygerger et al., 1983), which is likely why this lithofacies is not common within Gravel Pit 3. Wind ripples will not form on a damp surface (Kocurek, 1981), thus these interdune ripples likely formed on a dry surface.

Lithofacies 6C. Fine-Grained to Coarse-Grained Sand Matrix with Pebbles

This lithofacies association is similar to lithofacies 1B and 7B and is composed dominantly of planar cross-stratified fine-grained to coarse-grained sand with pebbles. The lower section was likely deposited at the bar front of a river-mouth (Clifton, 1973; Hart & Plint, 2003; Wright, 1977). Absence of sorting indicates that wave re-working was not significant (Clifton, 1973; Hart & Plint, 2003). The trough cross-stratification identified at the top of this lithofacies association likely represents dune migration within the channel of the river-mouth environment (Steel & Thompson, 1983).

Lithofacies 7C. Fine-Grained Sand

The upper portion of this lithofacies association contains roots and appears strongly bioturbated, making an interpretation difficult. Only a small section near the base reveals bedding, where ripple cross-lamination is apparent. The underlying erosive contact with a river-mouth deposit provides some evidence that this likely represents a channel. Ripple cross-lamination would be

the result of low-regime river flows (Ramos et al., 1986), in the shallowest part of the channel (Bridge et al., 1986).

6.1.6 Gravel Pit 3 Summary

The lithofacies identified at gravel pit 3 represent a prograding sequence beginning with a prodelta. Paleocurrent directions comparable to lithofacies 1A and 1D indicate that they may all represent the same delta. The overlying shoreface sequence was likely deposited after the water level rose since there is no evidence of wave action in the prodelta. It is not possible to discern the amount of water level rise. It is likely that the shoreface prograded southward. Overlying this is a rip channel common to runnel systems. It is only present in one of the profiles at gravel pit 3 because they form solely near the berm. The dune and interdune deposits represent the backbeach area, where sediment is transported from the beach shoreface by the wind. The overlying river-mouth may indicate another slight rise in water level, when the migrating river that previously supplied sediment to the prodelta region was in confluence with the lake margin. However, it is more likely that the stream channel was simply flowing through the dune field. The uppermost lithofacies 7C likely represents the channel of the river, where there was no wave action.

The uppermost lithofacies (2C to 6C) represent a shoreline (Fig. 6.1) at an elevation consistent with Lake Minong.

6.1.7 Mackenzie Roadcut

Lithofacies 1D. Very Fine-Grained to Medium-Grained Sand

Ripple cross-lamination, sinusoidal ripple lamination, and parallel-stratified massive layers comprise this lithofacies association. These bedforms have been discussed for lithofacies associations 1A and 1C. This sequence was likely deposited by density underflows entering a glacial lake (e.g., Gustavson et al., 1975; Smith & Eriksson, 1979) when the sediment was dominantly transported in suspension (Jopling & Walker, 1968; Pickering, 1982; Ashley et al., 1982).

Deformation structures observed within this prodelta sequence are folded laminae, load structures, and convolute bedding. The folded laminae could have been deformed at the front of an advancing glacier (Aber, 1982), however the deformation is not laterally continuous as you would expect and it is unlikely the subaqueous prodelta region would have been deformed in this manner. It is more likely that the folded laminae are involutions (Boyd et al., 2012). These structures may indicate permafrost degradation when high porewater pressures caused loading and injection along sedimentary boundaries (Harris et al., 2000). However, no other cryoturbation features have been identified within this lithofacies association. More likely, given the subaqueous depositional environment of a prodelta and the absence of additional evidence of cryoturbation, these deformation structures were not deformed due to permafrost conditions. These deformation structures are interpreted as soft sediment deformation contemporaneous with or closely following deposition, similar to those identified by Rossetti (1999).

The four main mechanisms that may cause soft sediment deformation are gravity forces acting on layers underlying more dense sedimentary layers, liquefaction of sediment, slumping, and shear stress exerted on recently deposited sediment by a flow moving above it (Blatt et al., 1980). Liquefaction and fluidization are related process that account for several deformation features, due to vertical gravitational compaction expressed on low cohesion, metastable sands with excess pore pressure (Mills, 1983). Liquefaction occurs homogeneously throughout the bed, whereas fluidization is more brief and local, with fluid movement restricted to vertical pipes or conduits (Mills, 1983).

Folding and contortion of interbedded muds and sand results from vertical displacement, or vertical and lateral movement due to shear stress (Mills, 1983). The load structures observed in this lithofacies association likely formed due to sediment with a relatively higher density overlying sediment with a lower density (Owens, 1996). Load structures form when the lower layer loses strength and the overlying layer sinks into it (Owens, 1996). The convolute bedding underlying the dish structures in this lithofacies association, likely evolved by

progressive deformation of parallel-stratification due to liquefaction with vertical displacement, maybe with horizontal shear stress (Lowe & LoPiccolo, 1974; Mills, 1983).

One dropstone is present within this prodelta lithofacies association, within parallel-stratified sand. This dropstone would have been deposited when the dominant sedimentation process was suspension fall-out (Pickering, 1982; Ashley et al., 1982). Ice rafting likely carried outlying clasts to the prodelta environment (Ovenshine, 1970), and may have been from lake ice or an iceberg. This is similar to the observed dropstones within a glacial-marginal Arctic lake (Smith, 2000).

Lithofacies 2D. Coarse Sand and Pebbles

This lithofacies is composed of planar cross-stratified sand and gravel, and has an erosive concave up base. Although the paleocurrent direction is consistent throughout all of the profiles (north-northwest), the grain-size varies. The coarsest layers are composed of boulders and pebbles, and these grade northward into coarse-grained sand with pebbles. Commonly, the exposures also reveal a fining upward sequence.

This lithofacies is similar to large channels filled with large trough cross-sets of gravel interpreted to be the result of bankfull discharge, when the entire valley acted as a channel (Ramos & Sopena, 1983). The variation in grain-size observed would be the result of different flow velocities in the channel as depth varied (Ramos & Sopena, 1983).

Small lenses identified in two profiles likely represent thin fine-grained drapes, which have been identified within laterally accreting conglomerates (Ramos & Sopena, 1983).

Lithofacies 3D. Very Fine-Grained to Medium-Grained Sand

Within profiles 0m and 5m, the contact with underlying lithofacies 2D appears gradual. The rest of the profiles reveal a contact that is quite abrupt, and appears erosive. Bedforms within the fine-grained to medium-grained sand

are trough cross-laminated, ripple cross-laminated, and parallel-stratified. Although these bedforms develop within braided streams during low water stages (Miall, 1977), reactivation surfaces and scallop-shaped scours are also present within this lithofacies association. Although coarser grained, similar lenses have been identified within a shallow water lacustrine environment (Hwang & Chough, 1990). Wave motions at the sediment surface involve a brief landward-directed surge, and a longer but weaker lakeward-directed return flow (Reading & Collinson, 1996). Breaking waves generate the surf zone, where coarse sediment is transported landward while finer sand and silt are suspended briefly in bursting clouds (Reading & Collinson, 1996). At the landward limit of wave penetration, in the swash zone, each wave produces a shallow and high velocity, landward-directed swash flow followed by a shallower, seaward-directed backwash (Reading & Collinson, 1996). Plane bed or antidune conditions predominate this swash zone (Reading & Collinson, 1996), and within the foreshore to shoreface environment the most common bedforms are horizontal-stratification and trough cross-stratification (Reading & Collinson, 1996). This is consistent with lithofacies association 3D, which is interpreted to represent a shallow shoreface to foreshore environment. The scallop-shaped scours and reactivation surfaces discussed were likely deposited by wave-induced currents producing dunes, ripples and horizontally-stratified layers.

Lithofacies 4D. Medium-Grained to Coarse-Grained Sand

The well-sorted nature of this lithofacies association, and alternating magnetite-rich layers with magnetite-poor layers are consistent with a beach foreshore environment, discussed for lithofacies association 2C (Thompson, 1937; Clifton, 1969). However, the lower portion of some exposures reveals layers that dip at a steeper angle than would be expected on a beach. These are similar to lithofacies associations interpreted as spit platforms (Nielsen et al., 1988; Makinen & Rasanen, 2003). A spit platform is a large-scale structure formed by sediment transport along the coastline, attached to the land mass at one end and terminating in open water at the other (Nielsen et al., 1988). The

inclined bedding comprising the lower portion of this lithofacies association likely formed when sorted glacial deposits were intensely reworked by littoral processes, representing the platform foresets of a prograding spit-platform sequence (e.g., Makinen & Rasanen, 2003). Overlying layers with little to no dip likely represent a beach foreshore environment, with pebble layers representing storm deposition (Thompson, 1937; Clifton, 1969). This sequence is likely the result of a prograding spit platform becoming a beach foreshore, which is the common progression of these lithofacies.

6.1.8 Mackenzie Roadcut Summary

The prodelta sequence at the Mackenzie roadcut likely represents the same delta or delta complex as gravel pit 1 and lithofacies 1C. One dropstone was identified providing evidence that icebergs may have been actively involved in deposition. The abrupt contact and concave up base of the overlying lithofacies indicates that there was subsequent erosion, likely within a channel. However, the deposit infilling the channel is the result of bankfull discharge, which was likely subaqueous. Abruptly overlying the channel-fill sequence, the stratigraphy indicates the swash zone of a prograding beach shoreface. The convex-up shape of this lithofacies suggests that two offshore bars were formed, and influenced by wave action. A spit platform, evidenced by high-angle cross-stratification, prograded lakeward over the bars and gradually became the low-angle cross-stratification of a beach shoreface.

The prodelta sequence was likely deposited within proglacial Lake Beaver Bay, which likely dissipated as the Superior lobe retreated from northwestern Ontario. The channel could have been eroded during this low stand, before proglacial Lake Minong rose and provided the subaqueous conditions required for the bankfull discharge. Subsequent beach sediments likely reflect a Minong level in the Superior basin (Fig. 6.1). This sequence is discussed below.

6.1.9 Mackenzie South Roadcut

Lithofacies 1E. Fine-Grained to Granules

The low angle planar cross-stratification comprising this lithofacies association is characteristic of beach foreshore deposits, discussed for lithofacies association 2C (Thompson, 1937; Clifton, 1969). The alternation of light and dark laminae result from swash and backwash currents sorting grains by size and density (Thompson, 1937). Coarser and less well-sorted layers within this lithofacies association were likely deposited on the foreshore during a storm (Thompson, 1937).

Lithofacies 2E. Medium-Grained Sand to Pebbles

This is likely the same lithofacies association as 1E, however presence of roots indicate that bioturbation has destroyed some stratigraphy. This lithofacies is well-sorted, and contains layers of pebbles likely deposited during a storm event, which is consistent with a beach foreshore environment (Thompson, 1937).

6.1.10 Mackenzie South Roadcut Summary

Located at an elevation of 224m asl, this beach shoreface sequence likely represents another Minong level in the Superior basin (Fig. 6.1). The slope from Mackenzie Roadcut to Mackenzie South Roadcut is consistent with Minong beach terraces identified in the Thunder Bay region (e.g. Julig et al., 1990).

6.1.11 Mackenzie Inn

Lithofacies 1F. Reverse Graded Clayey-Silt to Fine-Grained Sand

This lithofacies is composed of reverse graded very fine-grained sand to fine-grained sand layers interbedded with silt layers. The massive silt layers, averaging 1cm in thickness, likely represent deposition from suspension (Pickering, 1982; Ashley et al., 1982).

Normal and reverse graded layers commonly occur in deltaic and lake bottom depositis (Gustavson et al., 1975). Reverse graded layers have been interpreted as interflows and overflows (Aario, 1972; Sturm & Matter, 1978), as well as underflows (Sallenger, 1979). Deposition from interflows or overflows is explained by currents of increasing velocity, with fine-sediment supply ceasing during the following deceleration phase (Aario, 1972). Grain-flows have also been utilized to explain reverse graded layers, summarized by Bagnold (1954) in which dispersive pressure in concentrated flows of sand-size and larger particles is higher on larger grains since shear stress is constant, which causes larger grains to migrate towards the surface of the flow into zones of less shear stress (Sallenger, 1979). In contrast, some researchers prefer kinetic sieving as an explanation for reverse grading in grain-flows because Bagnold's (1954) conclusions are based on a concept, which only has statistical validity, and should not be applied to individual grains within a flow (Middleton, 1970). When kinetic sieving takes place, small particles fall through the open pore spaces that temporarily open in an agitated granular mass more easily than large ones (Makse et al., 1997; Middleton, 1970).

Grain-flows are commonly composed of medium-grained to coarse-grained sand or larger clasts, and layers tens of centimetres thick (e.g., Muto & Steel, 1997), therefore it is more likely that these reverse graded layers are the result of accelerating interflows and overflows (Aario, 1972; Sturm & Matter, 1978). These are interbedded with massive layers representing deposition by fallout from interflows and overflows (Jopling & Walker, 1968).

Lithofacies 2F. Massive Layers of Medium-Grained Sand to Granules

Layers in this lithofacies are composed of medium-grained sand to granules, appear massive, and dip at a very low angle. These are similar to massive sandstones found at the lower reaches of a Gilbert-type delta foreset slope (Muto & Steel, 1997). The absence of internal structure indicates that these layers were deposited as subaqueous sandy debris flows (Muto & Steel, 1997). Debris flows are rheological plastics, and they freeze once shear stresses

can no longer overcome internal shear strength. This mechanism causes their massive appearance (Stow et al., 1996).

Lithofacies 3F. Cross-Stratified Fine-Grained Sand and Coarse-Grained Sand to Granules

Beds within this lithofacies association are planar cross-stratified, commonly composed of silt to fine-grained sand layers interbedded with coarse-grained sand to granule layers. Silty sand layers likely represent deposition from suspension (Pickering, 1982; Ashley et al., 1982). Sand layers are dominantly massive, although some ripple cross-stratification is also present. Given the observable decrease in slope, and similarity to foreset beds within a Gilbert type delta (Muto & Steel, 1997), this lithofacies likely represents a deltaic foreset environment. A similar sequence composed of graded layers were interpreted as grain-flows, which result from steep slopes common to the foreset beds of a Gilbert type delta (Muto & Steel, 1997). Although grain-flows commonly form reverse graded layers (Stow et al., 1996) not observed within this lithofacies association, reverse grading is not always present within them. This lithofacies association most likely represents grain-flows deposited on the delta foreset slope.

Rare normal grading and ripple cross-lamination within the sand layers may indicate the operation of turbulence as a major factor in these flows, aiding in the suspension of particles and their deposition with waning eddy velocities. The upward components of turbulent fluid motion provide the main grain support mechanism of highly turbulent currents, commonly forming graded layers (Stow et al., 1996).

Erosive scours are present within this lithofacies association. A fully turbulent sandy high-density turbidity current may be locally erosive, resulting in lenticular deposits and scours (Lowe, 1982). The observed erosive scours are always overlain by a massive silty sand layer, which is subsequently overlain by a grain-flow or turbidity current deposit.

Lithofacies 4F. Medium-Grained to Coarse-Grained Sand Matrix with Pebbles

The medium-grained sand to coarse-grained sand with pebbles comprising this lithofacies association is parallel-stratified. Although the matrix grain-size is consistent throughout this lithofacies association, there is a coarsening upward sequence from parallel-stratified sand to matrix-supported granules, and at the top are matrix-supported pebble layers. Considering its stratigraphic position overlying a delta foreset sequence, this may represent the upper portion of a prograding delta. The lower sequence in this lithofacies association may represent the subaqueous delta top, and as the delta prograded it became a river-mouth environment. As the river-mouth prograded, the coarser sediments were deposited closer to the mouth of the river, adjacent to the channel (Wright, 1977).

The graded layers identified at the top of this lithofacies association may represent channel mouth-bars within a braided stream channel (Fralick & Pufahl, 2006). Between these graded layers is a layer of well-sorted sand, which is indicative of wave re-working that preferentially winnowed sand from a previously deposited mixture of sand and pebbles (e.g., Clifton, 1973).

6.1.12 Mackenzie Inn Summary

The sequence exposed to the west of the Mackenzie Inn appears to represent the bottomset, foreset, and topset beds of a delta. The bottomset bed is composed of overflow and interflow deposits, overlain by the prograding lower reaches of a foreset slope with common debris flows. The steep slope of the foreset bed is present above, with overlaying subaqueous delta top deposits. Subsequent river-mouth sediments indicate that there is another shoreline at ~233m asl (Fig. 6.1). This likely represents one of the lowest levels of Lake Minong (c.f. Phillips & Fralick, 1994b).

6.1.13 Construction Site

Lithofacies 1G. Fine-Grained to Medium-Grained Sand

This lithofacies association is composed dominantly of ripple cross-lamination with some parallel-stratified massive layers. Given the overlying foreset and topset beds, this likely represents the bottomset beds of a Gilbert-type delta. Initial work on these deltaic systems was completed by Gilbert (1885; 1890), and consists of subaerial topset beds and subaqueous foreset and bottomset beds (Reading & Collinson, 1996). Bottomset beds are deposited from a mixture of suspended load and gravity flows (Reading & Collinson, 1996). Ripples identified within this lithofacies association likely formed when the river current entering a glacial lake was in contact with the prodelta, and parallel-stratification was deposited by fall-out from suspension (Jopling & Walker, 1968; Pickering, 1982; Ashley et al., 1982; Smith & Eriksson, 1979; Gustavson et al., 1975).

Lithofacies 2G. Planar Cross-Stratified Medium-Grained Sand to Pebbles

The large-scale planar cross-stratification comprising this lithofacies association appears to be the foreset of a Gilbert-type delta. Foreset bedding in the upper portions of deltas consists of cross-stratified sand and gravel inclined as much as 30 degrees, forming where bedload, dropped at a river mouth, continues down the delta front as grain-flows or frictional debris-flows (Gustavson et al., 1975). The contact between foreset and topset beds in glaciolacustrine deltas is erosional and records the position of the channel bottom of the stream that supplied sediment to the delta, which is always some distance below the actual lake level (Gustavson et al., 1975).

3G. Parallel-Stratified Medium-Grained Sand to Pebbles

Horizontally-stratified sand and gravels comprising this lithofacies association is consistent with the topset bed of a Gilbert-type delta. Topset beds are generally good examples of gravel bar deposition consisting mostly of crude plane beds and rare cross-beds (Gustavson et al., 1975). The delta topsets are

generally fluvial sediments, dependent on the same conditions that produce characteristic sedimentary structures in fluvial deposits (Gustavson et al., 1975). The coarse-grained nature and very low angle bed dip seen in this lithofacies association is very similar to topset beds interpreted to represent a Scott type braided river (Clemmensen & Houmark-Nielson, 1981). However, sediments in these braided river systems consist mainly of longitudinal bar gravels with sand lenses formed by infill of channels (Miall, 1977). It is more likely that this topset bed was deposited subaqueously, in a river-mouth environment. Poorly developed clast segregation and laterally continuous foreset to bottomset bedding (e.g., Fig. 5.72) is consistent with an inertia-dominated river-mouth environment (Wright, 1977).

6.1.14 Construction Site Summary

Similar to the Mackenzie Inn exposure, this sequence likely represents a prograding delta. However, paleocurrent directions at the Construction Site indicate northward flow. The prodelta bed is abruptly overlain by the large-scale cross-stratification characteristic of a delta foreset slope. The topset bed was likely subaqueous.

This prograding delta was likely deposited within Lake Beaver Bay, when water was flowing off the Superior lobe causing northward flow (c.f. Phillips & Fralick, 1994b). This sequence could have been preserved because it was either below wave base during subsequent Minong levels, or subaerial.

6.1.15 Mackenzie Trench

Lithofacies 1H. Fine-Grained to Medium-Grained Sand

This lithofacies is composed of climbing dunes, formerly called large-scale climbing ripples by Allen [1968] and Williams (1970). Climbing dunes were defined by Allen (1968) as those with chords (wavelength) exceeding 60cm and heights exceeding 4cm, forming in medium-grained to very coarse-grained sand (Williams, 1970). They appear to be generated by high-stage flow, which

explains their presence in medium-grained sand (Williams, 1970). The climbing dunes observed at the bottom of the Mackenzie Trench reveal an absence of stoss side laminae comparable to the smaller Type A climbing ripples seen in lithofacies association 1A (Jopling & Walker, 1968). Therefore, the climbing dunes are likely the result of a high velocity flow in which very little fall-out from suspension supplied sediment allowing preservation of lee side laminae (Jopling & Walker, 1968; Williams, 1970). Very little of this lithofacies was exposed making it difficult to determine the depositional environment. Given the overlying finer-grained lithofacies, it is possible that this sequence represents a time when flow velocity increased allowing transportation of coarser materials and formation of climbing dunes.

The bedding at the top of this lithofacies association appears to be slightly deformed (Fig. 5.86); speficially, it is overturned in the direction of current movement. This is comparable to deformation identified in a subaqueous outwash deposit, interpreted as folding that resulted from shear stress exerted during deposition of the succeeding bed (Rust & Romanelli, 1975).

Lithofacies 2H. Very Fine-Grained to Fine-Grained Sand

This lithofacies is composed of parallel-stratification and ripple cross-stratification. An accurate interpretation is difficult because this sequence is only 8cm thick. However, given the fine grain-size and identified bedforms, this is likely an offshore environment similar to the prodelta environments already described for lithofacies 1A. This fine-grained sediment would have been transported lakeward, with parallel-stratification resulting from suspension fallout and ripple cross-lamination forming when the current was in contact with the bed (Jopling & Walker, 1968; Pickering, 1982; Ashley et al., 1982).

Lithofacies 3H. Sand and Gravel

This lithofacies association is composed of massive sand and pebbles, with lenses of well-sorted open framework pebbles. This bedding is consistent with proglacial braided stream deposits (e.g. Church & Gilbert, 1975; Steel &

Thompson, 1983). Proglacial fluvial deposits in proximal environments are characterized by nearly featureless or diffuse parallel bedding, resulting from rapid deposition of material from transport (Church & Gilbert, 1975). Initial deposition of very coarse materials leads to discontinuous, horizontal bedding, while subsequent entrapment of finer sediment tends to obscure any structure the original deposits may have had and renders stratification less visible (Church & Gilbert, 1975). This is consistent with proglacial braided stream conglomerates identified in England (Steel & Thompson, 1983).

Within this braided stream environment are concave up lenses of open framework gravels that fine upward. The concave up shape indicates that they are small channels, which may fill with stratified gravels depending on flow conditions (Ramos & Sopena, 1983; Ramos et al., 1986). Material carried near the bed would have been deposited in the channel during waning flows (Church & Gilber, 1975). More specifically, the channel fill was likely deposited in a manner similar to the open framework gravels, which occasionally form river bars. During high flows, sand would have been carried in suspension above the gravels, which were deposited in small channels (Ramos & Sopena, 1983). As flow decreased, finer gravels were deposited above the larger ones (Ramos & Sopena, 1983) resulting in a graded lenticular bedform.

Lithofacies 4H. Well-Sorted Medium-Grained to Coarse-Grained Sand

The well-sorted sand comprising this lithofacies is uncharacteristic of a braided stream environment, and likely has been wave re-worked, similar to a sandstone dominated shoreface (Clifton, 1973; Hart & Plint, 2003). The pebble layers may reflect coarser sediment supply during storm events (Hart & Plint, 2003).

Lithofacies 5H. Cross-Stratified Sand and Gravel

The stratigraphic column produced for the Mackenzie Trench (Fig. 5.86) reveals parallel-stratified sand and pebbles. However, the west wall reveals these layers from a different perspective, in which cross-stratification is apparent.

This planar cross-stratification is very similar to coarse-grained braided river transverse bars, shown to form when a river current transports a mixed load of sand and gravel (e.g. Miall, 1977; 1978; Bluck, 1979; Allen, 1983). As both sand and gravel roll up the stoss side, it accumulates at the top of the bar and avalanches down the lee side (Bluck, 1979; Allen, 1983). The direction of progradation of the bar comprising this lithofacies association is southward.

Lithofacies 6H. Magnetite Rich Cross-Stratified Sand and Gravel

This lithofacies association is composed of well-sorted medium-grained sand with a high magnetite concentration containing matrix-supported pebbles. The sand and gravel is horizontally-stratified to planar cross-stratified. The magnetite-rich and well-sorted sand comprising this lithofacies likely resulted from wave reworking in a beachface environment, in a process described for lithofacies 2C (Thompson, 1937). The parallel-stratified to cross-stratified sand and gravel prograding northward, or landward, is similar to a facies interpreted to be backshore deposits (Nishikawa & Ito, 2000). More specifically, in this context the horizontal-stratification would represent a berm top while the northward dipping planar cross-stratification represents the landward portion of a berm ridge (Hine, 1979).

Lithofacies 7H. Massive Silty Sand with Pebbles

This lithofacies is poorly-sorted silty sand with granules and pebbles, always appearing massive. Presence of roots indicates that the massive appearance likely due, at least in part, to bioturbation (Wood & Johnson, 1978).

6.1.16 Mackenzie Trench Summary

Although lithofacies 1H and 2H are thin deposits, they are consistent with a prodelta environment where the current is occasionally in contact with the lake bottom. Overlying is a sequence composed of beach and river sediments that indicate a river-mouth. As the river in confluence with a lake margin migrated over the landscape, it transported sand and gravel to the beach. The river-mouth deposits indicate that the shoreline was river-dominated, as evidenced by the

braided river sequence and river bar, or wave-dominated which resulted in well-sorted sand.

6.1.17 Mackenzie 1

A topographical map with the excavation grid of the Mackenzie 1 archaeological site produced by Dr. Scott Hamilton (Department of Anthropology, Lakehead University) is provided to show the location of units discussed (Fig. 6.2).

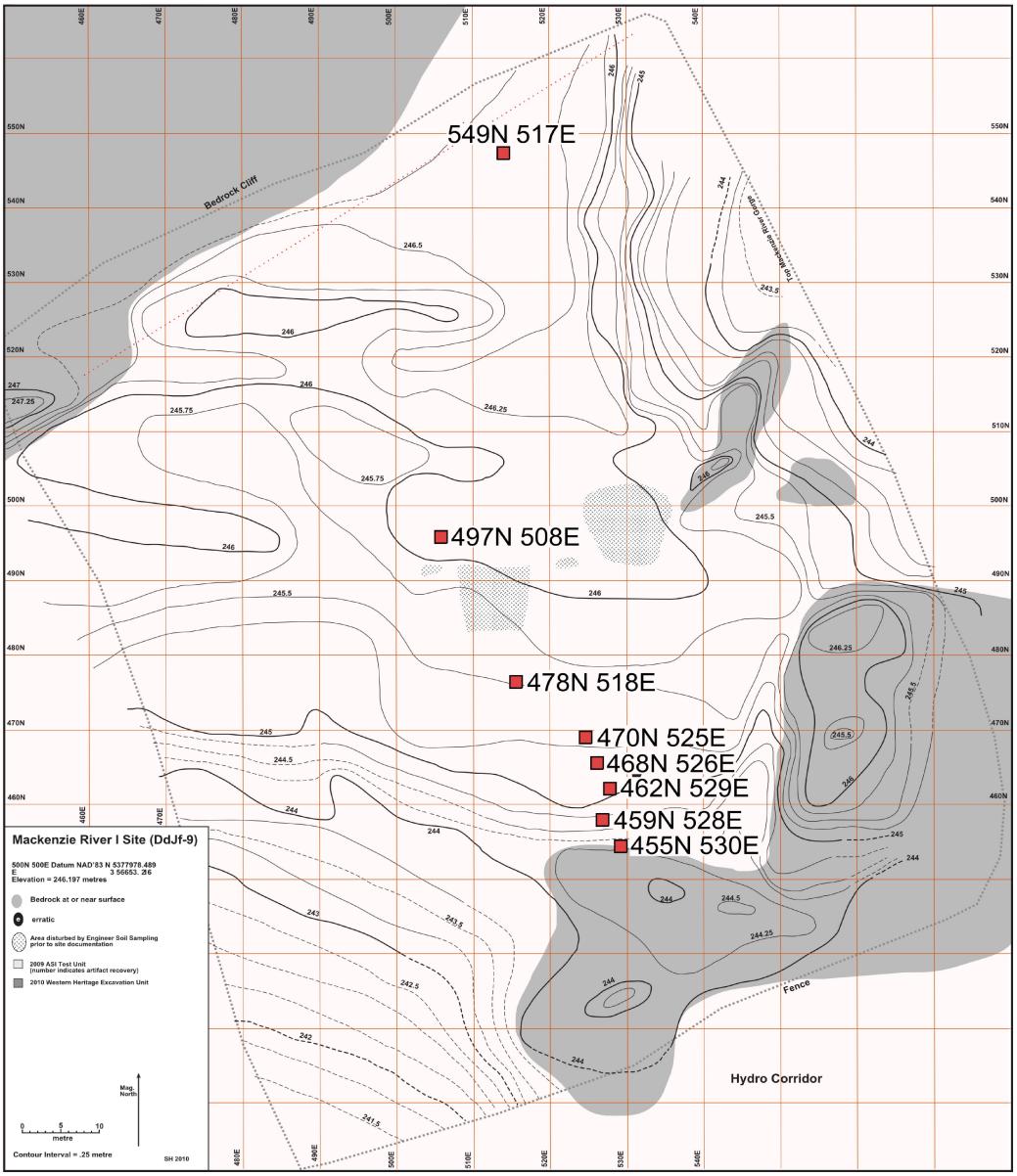

Figure 6.2. Site map of Mackenzie 1 showing profiled units

Lithofacies 1I. Well-Sorted Medium-Grained to Coarse-Grained Sand with few Pebbles

This lithofacies association is only present in the northern portion of the Mackenzie 1 site, and is composed of laterally continuous low angled parallel-stratified magnetite-rich layers interbedded with non magnetite-rich layers. Within these, there are occasional pebble layers and one layer 5cm thick of massive sand with granules and few pebbles. This is interpreted to be a beachface environment, with characteristic grain-size sorting and high concentrations of magnetite already discussed for lithofacies association 2C (Thompson, 1937). The pebble layers and massive layer are likely the result of storm events, when higher energy waves were capable of transporting coarser grains to the shoreface.

The upper portion of this lithofacies association appears massive, likely resulting from bioturbation as evidenced by the presence of roots. A consistency in grain-size indicates that the northern portion of the site remained a beach shoreface until water level declined and deposition ceased.

Lithofacies 2I. Pebbles within a Sand and Granule Matrix

This lithofacies is composed dominantly of clast-supported pebbles with some granule matrix, although the upper portion of some sequences is matrix-supported. Throughout this lithofacies, successive channel cut and fill structures are apparent within the clast-supported sections. This was likely the result of a similar process to sithofacies 3H. During high flows, sand would have been carried in suspension above the gravels, which were deposited in small channels (Ramos & Sopena, 1983). A granule or sand matrix would then indicate a waning flow, which would have caused deposition of gradually smaller grains (Ramos & Sopena, 1983). Where this lithofacies appears to be matrix-supported, roots are present. Likely, these sections have been bioturbated.

The wall profile of unit 459N 528E reveals this lithofacies, although laterally and vertically, the matrix-supported pebbles gradually become medium-

grained sand with few granules. This likely represents a waning flow, with successive deposition of the coarser to finer material.

Within unit 497N 506E, artifacts were recovered from within this lithofacies association. Absence of size sorting and evidence of rounding on these artifacts indicates that they do not represent occupation contemporaneous with the river sediments. Instead, it is likely that they were left by occupants after the river sequence deposited, and subsequent bioturbation caused vertical and/or horizontal displacement.

This lithofacies is also present within the west wall of unit 459N 528E, revealing matrix-supported pebbles within medium-grained sand. However, the morphology of the deposit is quite different and likely does not represent channel fill. The flat base and convex down top is consistent with a river bar (Ramos & Sopena, 1983), as is the massive appearance of bimodally transported sand and pebbles (Steel & Thompson, 1983). This was likely deposited within a high water discharge flow with relatively high sediment concentration within a braided river (Steel & Thompson, 1983).

Lithofacies 3I. Coarse-Grained Sand Interbedded with Granules and Pebbles

This lithofacies is seen throughout the southern portion of the Mackenzie 1 site, and is composed of well-sorted open framework layers that vary in grain-size. Layers are always low-angle, parallel-stratified. Most commonly, they are composed of coarse-grained sand interbedded with granules and pebbles. A high degree of sorting and pronounced horizontal-stratification is typical of wave-dominated shoreface conglomerates (Hart & Plint, 2003), which is likely the environment this lithofacies represents. The variation in grain-size likely resulted from differences in wave energy (Thompson, 1937)

Lithofacies 4I. Magnetite-Rich Cross-Stratified Coarse-Grained Sand to Granules

This lithofacies is composed dominantly of magnetite-rich planar cross-stratified coarse- sand layers interbedded with layers of granules containing few pebbles. Paleocurrent direction indicates northeastward progradation. Although

little of this lithofacies is exposed, the high concentration of magnetite, landward dipping stratification, and lateral continuity of at least three metres indicates that it could be a berm deposit (Hine, 1979; Nishikawa & Ito, 2000), similar to lithofacies 6H.

Lithofacies 5I. Cross-Stratified Coarse-Grained Sand to Granules

This lithofacies is composed of planar cross-stratified sand and gravel with a southwest paleocurrent direction. This is consistent with migration of transverse bars identified within low sinuosity streams (Ramos & Sopena, 1983). These bars with well-defined foresets may reflect a lower water and sediment discharge than longitudinal bars (Ramos & Sopena, 1983). However, the well-sorted nature of the layers, and low dip angle is also consistent with a beach lower shoreface environment (Clifton, 1973; Postma & Nemec, 1990). This lithofacies is only identified southward of the shoreface deposits at Mackenzie 1, and may also represent the subaqueous lakeward portion of lithofacies 3I.

Lithofacies 6I. Silty Medium-Grained Sand with Pebbles

This lithofacies is composed of poorly-sorted to massive silty sand with pebbles. It is only found in the pit and linear features of the southern portion of Mackenzie 1. Artifacts were always associated with this lithofacies. Possible formation processes for the pit features are discussed first, and followed by analysis of the linear feature.

The pit features are all about 1m in length and depth, and filled with poorly-sorted unstratified sediments. One natural process that can produce massive and poorly-sorted sediments are debris flows (Stow et al., 1996) discussed for lithofacies 2F. However, a debris flow would not account for the erosive concave up base of these features. In addition, a debris flow deposit would likely be identified elsewhere at the archaeological site.

Mechanical mixing of sediments can occur during tree fall, when uprooted trees bring masses of earth to the surface (Wood & Johnson, 1978). The natural falling of trees may leave shallow depressions where roots and adhering rock

and soil are torn up, although larger depressions may result from wind thrown live trees (Wood & Johnson, 1978). Modern tree falls are common within the boreal forest. However, a 1m depression seems unlikely to result. Pollen studies indicate that tree species roughly contemporaneous with the late stages of Lake Minong include spruce, pine and birch (Julig et al., 1990), which are consistent with modern boreal forest species (Kemp, 1991). Vertical rooting patterns of trees in the boreal forest are generally restricted to the upper 30 to 50cm of the soil profile, while horizontally, large roots are aggregated around the stem, and small roots are interspersed more evenly throughout the stand (Brassard et al., 2009). Given the very abrupt contact of this lithofacies with adjacent ones, and the size of the pit features, it seems unlikely that they are the result of tree falls.

Another interpretation for these pit features is buried ice melt. Depressions observed in predominantly sandy sediments of river deposits can result from buried ice melt due to collapse during escape of meltwater (Collinson, 1971). These collapse depressions are relatively rare in comparison with features formed by grounded ice, although they are much more likely to be preserved since they penetrate below the surface (Collinson, 1971). Within a river system, as water stage rises due primarily to melting of snow, the ice is lifted and breaks up until the whole width of a river can be covered by blocks of moving ice (Collinson, 1971). Since the Mackenzie 1 site appears to represent a river-mouth depositional environment, it is also possible that ice originated at the shoreline of proglacial Lake Minong. For example, during sub-freezing temperatures spray produced in the surf zone is blown onto the foreshore and frozen (Zumberge & Wilson, 1953). Whatever the source, collapse depressions have been observed, and commonly range from 2 to 3m across and up to 50cm deep (Collinson, 1971), which is consistent with the pit features found at Mackenzie 1.

One pit feature, located in unit 478N 518E, has a very abrupt contact that bisects the adjacent lithofacies. For the buried ice melt scenario to be plausible, the ice would have been adjacent to the shoreface deposits (lithofacies 1l, 2l,

and 3I) while they were deposited. Micromorphology of this pit reveals that the bottom of the pit contains a relatively high abundance of organics and silty clay coatings, which may indicate cultural fill (Gilliland et al., 2012). Presence of microscopic taconite, the most abundant lithic material recovered at Mackenzie 1, was also interpreted to indicate cultural pit fill (Gilliland et al., 2012). In addition, OSL profiling results suggest that the pit fill is oldest at the bottom and youngest at the top (Gilliland et al., 2012). These findings do not discredit the buried ice theory. It is possible that the site was occupied while the ice block was in place, and as it melted the cultural sediments sunk to fill in the depression. In this scenario, the pit fill would not have been exposed to sunlight and would therefore still provide an OSL date contemporaneous with occupation.

The west wall of excavated unit 478N 518E is adjacent to a pit feature, and reveals near-vertical layers that grade laterally from pebbles to coarse-grained sand (Fig. 6.102). These layers are comparable to near-vertical massive layers interpreted as clastic dykes (Rijskijk et al., 1999). In a proglacial permafrost environment, formation of dykes in permeable gravels is explained by groundwater driven by a glacier being prevented from rising by the frozen surface layer (Rijskijk et al., 1999). The high water pressure generated exceeds the overburden pressure, causing pressurized groundwater to escape through gaps in the permafrost along with fluidized sediments (Rijskijk et al., 1999). It has been hypothesized that downward-infilled hydrofractures form underneath ice sheets, and adjacent to an ice sheet margin hydrofractures are upward-filled (Boulton & Caban, 1995; Van der Meer et al., 1999). The near-vertical layers identified at Mackenzie 1 may have been formed by this hydrofracture upward-filling process. Although opinions vary as to whether the sediments need to be frozen during dyke formation, there must have been an aquiclude or impermeable layer to hydraulically confine water and create pressurized water conditions (Rijskijk et al., 1999). If the buried ice that allowed the pit feature to form melted during warm temperatures, and the ground subsequently froze during cold months, the frozen surface sediments could have been the impermeable layer that caused the ice meltwater to escape through gaps in the

frozen ground. This scenario accounts for the pit feature within unit 478N 518E, as well as the near-vertical layers adjacent to it.

The wall profile of unit 462N 529E reveals a pit feature lined with a massive pebble layer. The proximity of this feature to the disturbed sediment identified in the southern portion of site (where a shoe insole was recovered during excavations), indicate that this is most likely the result of recent disturbance. Soil sampling was conducted at Mackenzie 1 with excavators, as a part of the engineering survey. The pit could be the result of an excavator bucket removing sediment, followed by pebbles rolling into the depression and being covered by adjacent sediment to fill it in. The linear feature, also close to the southern portion of the site with recent disturbance, could also be the result of recent disturbance with heavy machinery. Roots are commonly found within the linear feature, although adjacent and seemingly intact stratigraphy has no presence of organics (e.g., Figs. 5.98 and 5.99). This is very similar to the modern disturbance produced at Woodpecker 2 adjacent to road, discussed below.

The pit feature within unit 497N 506E is also lined with a layer. This pit feature is the largest, and can be explained by both modern disturbance during soil sampling as well buried ice melt.

Lithofacies 7I. Silty Medium-Grained to Coarse Grained sand with Pebbles

This lithofacies is poorly-sorted silty sand with granules and pebbles, always appearing massive, and commonly comprising the upper 25 to 50cm of Mackenzie 1. Artifacts at the Mackenzie 1 site are dominantly associated with this lithofacies. Presence of roots indicates that the massive appearance of this poorly-sorted lithofacies is likely due, at least in part, to bioturbation (Wood & Johnson, 1978). With the exception of silt, the grain-sizes within this lithofacies are consistent with those seen in the other lithofacies, deposited in a beachface, berm, or channel environment.

Lithofacies 8l. Graded layer of Pebbles to Coarse-Grained Sand

Graded layers were identified throughout the Mackenzie 1 site. Grain-size varied from pebbles to coarse-grained sand as well as granules to coarse-grained sand. These graded layers dominantly overly and/or underlie beach shoreface deposits (lithofacies 3l). Similarly graded facies have been identified within beachface deposits, interpreted to represent migration of gravel sheets (Hart & Plint, 2003) as well as offshore-directed storm generated currents (Zonnefeld & Moslow, 2004). Graded layers could have been deposited by the migration of megaripples and sand waves within a sand sheet, or due to the waning energy of a storm event (Figueiredo et al., 1982).

Alternatively, these graded layers may represent abandonment of channel mouth bars (Fralick & Pufahl, 2006). During high flows, the finer grains (sand and occasionally granules) were carried in suspension as the coarser grains were deposited (Ramos & Sopena, 1983). As flow decreased, the finer grains were deposited above the larger ones, filling pore spaces but generally not reaching the lowest beds (Ramos & Sopena, 1983). This process would produce a lower open framework gravel or granule and an upper sand filled gravel or granule layer (Ramos & Sopena, 1983).

6.1.18 Mackenzie 1 Summary

The northern portion of the Mackenzie site appears to represent a Minong shoreline (Fig. 6.1), while the southern portion is consistent with a river-mouth environment. During deposition of the beach shoreface in the northern portion of the site, ~3 metres higher than the southern portion, there is no evidence of fluvial action. Likely, as water level lowered (or isostatic rebound raised the land relative to the lake) to the southern portion of the site, glacial meltwater was spilling into Lake Minong at the Mackenzie 1 Site.

The large amounts of artifacts recovered from the Mackenzie 1 site likely reflect successive occupations over an extended period of time.

6.1.19 Post-Depositional Processes Affecting Mackenzie 1

At Mackenzie 1, a few artifacts were recovered from within a lithofacies interpreted to represent fluvial deposition. This could be the result of fluvial reworking at the site, river systems contemporaneous with occupation that were used as refuse dumps, or bioturbation. Since fluvial reworking would have significant implications for site interpretation (e.g., artifact distribution for activity areas), an artifact size distribution map was created by the author. Unpublished data, property of Western Heritage (Gjende Bennett 2011, pers. comm.) was utilized for this. By creating a shapefile with one point for every artifact recovered, a distribution map of artifact size was created (Fig. 6.2). If a fluvial system reworked artifacts at the site, linear features of size sorting would likely be displayed.

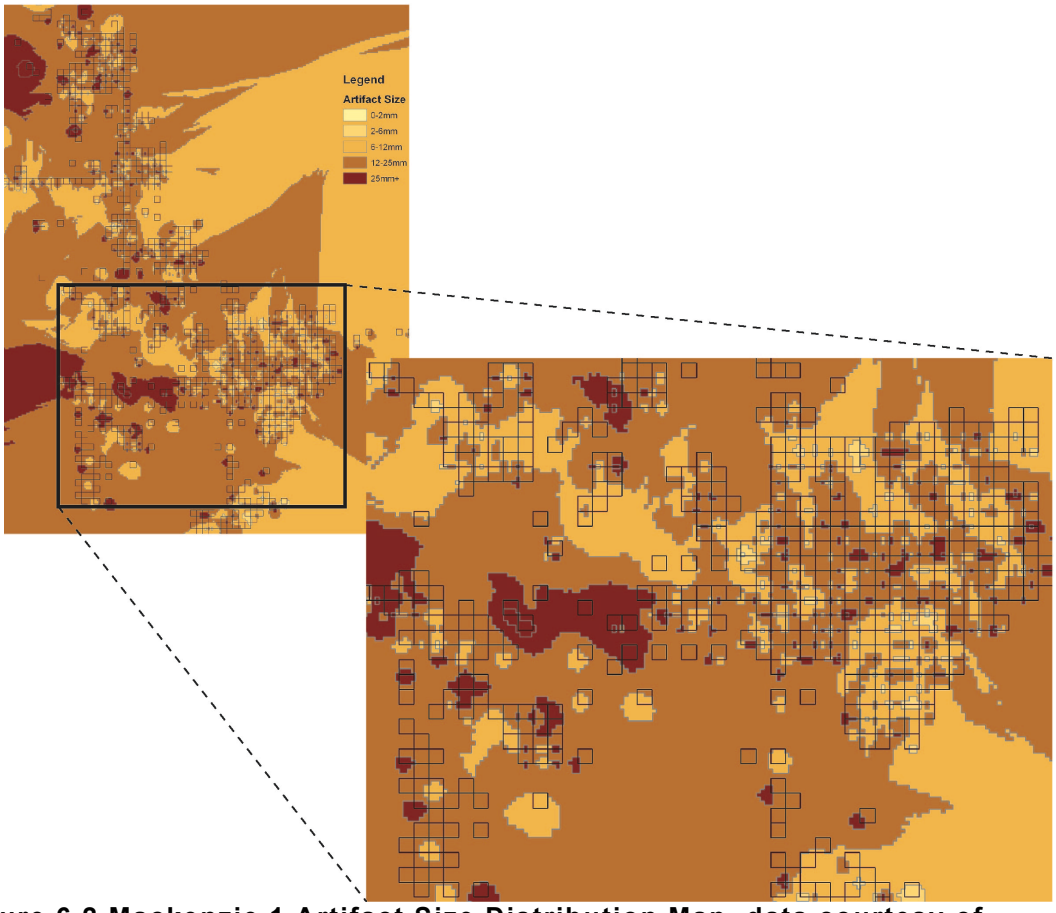

Figure 6.2 Mackenzie 1 Artifact Size Distribution Map, data courtesy of Western Heritage

The excavation grid system is overlain on the distribution map, each square represents a 1m x 1m unit excavated in 2010 (areas with no units were excavated in 2011 and the data was not incorporated). There does not appear to be any evidence of artifact sorting. The southern portion of the site, where lithofacies below occupation layer(s) represent a river-mouth depositional environment, is shown larger to demonstrate absence of sorting. This map, coupled with a lack of evidence to indicate post-occupation fluvial action suggests that the artifacts at Mackenzie 1 were not river re-worked.

Additional disturbance features at Mackenzie 1 were likely caused more recently by burrowing animals, and heavy machinery. No photos were taken, however small holes (~10 cm in diameter) filled with modern soil and organics are most likely caused by burrowing animals. The disturbance created during construction-related soil sampling was identified by massive sand and pebbles with presence of modern soil and roots (Fig. 5.100 and 5.101). This disturbance likely only impacted a small section within the southernmost portion of the site, and may have produced two of the pit features.

6.1.20 Mackenzie 2

Lithofacies 1J. Cross-Stratified Medium-Grained Sand to Small Pebbles

This lithofacies is parallel-stratified medium-grained to coarse-grained sand matrix supporting granules and pebbles up to 4cm in diameter. A layer with few cobbles up to 9cm in diameter comprises the lowest portion of this lithofacies. Layers throughout this lithofacies thicken as they coarsen westward, from 2cm in thickness to 5cm. Upward, these layers become increasingly diffuse and difficult to identify. The absence of sorting, and horizontal-stratification is consistent with a braided stream environment (Steel & Thompson, 1983; Hart & Plint, 2003). The sand matrix supports the larger clasts, which indicates that the sand and cobbles were likely deposited more or less simultaneously, from a flow of high sediment concentration and rapid deposition (Steel & Thompson, 1983).

The cobbles at the bottom of the lithofacies may represesent a channel lag deposit, representing the coarsest material available to the river (Allen, 1963).

These clasts are only shifted during high stages when the current is strongest, and through winnowing they have been sorted from the more readily transported finer clasts (Allen, 1963).

Lithofacies 2J. Fine-Grained to Medium-Grained Sand with Lag Deposit

The contact with underlying lithofacies 1J appears to be erosive, and contains a lag deposit of matrix supported pebbles and cobbles up to 5cm in diameter. The remainder of this lithofacies is composed dominantly of well-sorted fine-grained to medium-grained sand, with pebbles gradually disappearing and absent completely in the upper 15cm. The upper boundary of this fine-grained to medium-grained sand is convex up, indicating that this lithofacies represents a river bar (Ramos & Sopena, 1983). The upward and lateral decrease then absence of pebbles likely represents a waning flow, as the river bar was abandoned as discussed for lithofacies 8I (Fralick & Pufahl, 2006).

Lithofacies 3J. Silty Medium-Grained Sand to Pebbles

This lithofacies is composed of massive silty medium-grained to coarse-grained sand with granules and pebbles, as well as roots. It likely represents the same lithofacies as 1J, evidenced by the gradual change from parallel-stratified sand and gravel to massive sand and gravel. It is likely that bioturbation caused the bedding to appear massive.

Lithofacies 4J. Medium-Grained Sand to Very Coarse-Grained Sand

This lithofacies is dominantly composed of well-sorted medium-grained sand with no apparent bedding. Although throughout Mackenzie 2 the grain-size varies to very coarse-grained sand, this lithofacies is always well-sorted. This sorting may be the result of wave re-working, similar to a sandstone dominated shoreface (Clifton, 1973; Hart & Plint, 2003). However, it may also represent a high flood stage when water was not confined to incised channels (Ramos & Sopena, 1983). The flood water would have spread from the main channels across bar surfaces and abandoned channel deposits, flowing with high velocity

across all sediments and forming horizontal or low-angle bedding (Ramos & Sopena, 1983). The lateral continuity of this lithofacies throughout the archaeological site indicates that the mostly likely interpretation is wave re-working.

6.1.21 Mackenzie 2 Summary

The lithofacies present at Mackenzie 2 suggest channel deposition and bar abandonment within a braided river system. Well-sorted sand likely indicates the wave re-working of a nearshore environment. The elevation of this exposure is 241m asl, consistent with a Minong lake level (Fig. 6.1). It likely represents the same shoreline as the Woodpecker Ridge and the Mackenzie Roadcut sediments.

6.1.22 RLF

Lithofacies 1K. Very Fine-Grained Sand to Fine-Grained Sand with Pebble Layer

The northern portion of RLF is composed of well-sorted fine-grained sand with a pebble layer and a massive layer, and the southern portion contains medium-grained sand with pebble layers. This is consistent with a beach environment (Thompson, 1937), as summarized for lithofacies association 2C. The well segregated grain-size the result of wave re-working on a shoreface while the massive and pebble layers were likely deposited during storm events (Thompson, 1937).

Lithofacies 2K. Fine-Grained Sand to Medium-Grained Sand with Pebble Layers

In this lithofacies, few magnetite rich layers of well-sorted medium-grained sand are interbedded with non-magnetite rich layers. These layers are consistent with a beachface environment, where sediment sorting and concentration of magnetite layers result from wave re-working (Thompson, 1937). This lithofacies association also contains less well-sorted low angle horizontally-stratified layers composed of fine-grained sand to pebbles. These massive layers are likely the

result of storm events, when higher energy waves were capable of transporting coarser grains to the shoreface.

Similar to lithofacies 8I, the graded layer likely represents shoreface deposition since there is no evidence of fluvial deposition. The grading could represent the migration of a gravel sheet (Hart & Plint, 2003), or offshore directed storm generated currents (Zonnefeld & Moslow, 2004).

Lithofacies 3K. Silty Medium-Grained Sand with Pebbles

The tapered concave up feature identified in the southern portion of RLF is composed of massive silty medium-grained sand with pebbles. The grain-size is consistent with the underlying beach deposit although also containing silt. The feature is about 30cm wide and 40cm deep, with roots present throughout and a diffuse contact with adjacent parallel-stratifiaction. This size is consistent with the rooting patterns of trees in the boreal forest (Brassard et al., 2009), and may therefore represent bioturbation.

6.1.23 RLF Summary

Excavations at the RLF site reveal beach shoreface deposits at an elevation of 243m asl, consistent with Minong lake levels (Fig. 6.1). During preliminary examinations of the artifacts recovered from RLF, potential rounding was identified by Western Heritage employees. It is possible that the Paleoindian occupation at this site was contemporaneous with active beach formation of this possible Minong lake level, although absence of identifiable stratigraphy associated with the artifacts does not allow this relationship to be clearly established.

6.1.24 Woodpecker 1 and 2

Lithofacies 1L. Fine-Grained to Medium-Grained Sand

This lithofacies is composed of well-sorted massive fine-grained to medium-grained sand, and extends below the excavated depth. Similar to lithofacies 4J, this could be wave re-worked sediment in a beach environment (Clifton, 1973; Hart & Plint, 2003) or overflow deposits from a high flood (Ramos & Sopena, 1983).

Lithofacies 2L. Medium-Grained sand with few Granule and Pebble Layers

The bottom and top of this lithofacies at Woodpecker 1 is composed of low-angle horizontally-stratified matrix supported granules and pebbles up to 1cm in diameter within medium-grained sand. Between these granule and pebble layers, sorted medium-grained sand is planar cross-stratified and trough cross-stratified, and medium-grained sand with granules and pebbles is trough cross-stratified as well as parallel-stratified. These bedforms develop within braided streams during low water stages (Miall, 1977), and upper flow regime (Van Den Berg & Van Gelder, 1993). However, this could also be produced in the swash zone of a beach shoreface, similar to lithofacies 3D. In the swash zone, each wave produces a shallow and high velocity, landward-directed swash flow followed by a shallower, seaward-directed backwash (Reading & Collinson, 1996). Plane bed or antidune conditions predominate this swash zone (Reading & Collinson, 1996), and within the foreshore to shoreface environment the most common bedforms are horizontal-stratification and trough cross-stratification (Reading & Collinson, 1996).

Within this beach shoreface environment, there is also an explanation for the boulders and large cobbles. In the James Bay area of subarctic Quebec, large boulders common to glacial and glaciofluvial deposits are also present on sandy beaches (Dionne, 1979). These likely represent ice transportation and ice push. During sub-freezing temperatures spray produced in the surf zone is blown onto the foreshore and frozen (Zumberge & Wilson, 1953), producing lake

ice. The poorly-sorted layers that comprise lithofacies 2L can be attributed to ice push supplying a variety of grain-sizes to the nearshore environment. Either minimal wave reworking, net deposition, or a combination of these two factors could produce the poorly-sorted but laterally continuous layers within this lithofacies.

Lithofacies 3L. Cross-Stratified Medium-Grained sand to Pebbles

This lithofacies association is composed of three beds, all planar cross-stratified medium-grained sand to pebbles although the grain-size varies slightly. Stratigraphically, the lowest bed is composed of coarse-grained sand to pebbles 1cm in diameter and capped by a silt layer averaging 2cm in thickness. Overlying this is the second bed, with medium-grained sand to pebbles up to 1cm in diameter and also capped by a silt layer averaging 2cm in thickness. The uppermost bed is composed of medium-grained sand to pebbles up to 3cm in diameter.

These may represent three coarse-grained braided river bars similar to lithofacies 5H. They have been shown to form when a river current transports a mixed load of sand and gravel (e.g. Bluck, 1979; Allen, 1983). As both sand and gravel roll up the stoss side, it accumulates at the top of the bar and avalanches down the lee side (Bluck, 1979; Allen, 1983), which causes the appearance of graded layers. However, the paleocurrent directions indicate that a river flowing northward deposited these river bars. As discussed below, this scenario is reasonable only if the LIS lay to the south of the site at this time, and the landscape sloped northward allowing meltwater to be directed north as the glacier retreated. However, washover lobes are more consistent with the other river-mouth and beach sequences at the Woodpecker sites. Coastlines with little to no tidal currents and a lagoon in the backbeach area commonly experience wave run-up that eventually scours the most landward berm of the beach (Schwartz, 1982). This is called a blowout (e.g. Wroblewski, 2009), where planar cross-stratification dipping landward is common (Schwartz, 1982). The coarse-

grained sediment likely reflects the river input also indicated by the river-mouth deposits of lithofacies 5L, 6L, and 7L.

Lithofacies 4L. Silty Medium-Grained to Coarse-Grained Sand with Pebbles

This poorly-sorted lithofacies composed of medium-grained sand to pebbles always contains roots, and appears to be strongly bioturbated. It generally comprises the uppermost sequence at the Woodpecker sites and is dominantly associatiated with recovered artifacts. Root growth has likely caused mechanical mixing of soil and sediment, obliterating stratigraphy (Wood & Johnson, 1978).

This lithofacies is present within unit 499N 468E, extending to ~55m below surface. The contact with an underlying spillover lobe appears to be erosive, and is similar to the Mackenzie 1 linear feature. This may have been caused by modern disturbance with heavy machinery, or by buried ice melt.

Lithofacies 5L. Silty Fine-Grained Sand to Coarse-Grained Sand with Pebbles

River systems within cold environments can experience ice activity during the spring flood when the water stage changes (Collinson, 1971). Examination of a modern river system revealed that ice blocks become grounded as they move into shallow water, for example moving over a river bar or due to a fall in water stage (Collinson, 1971). Grounded ice produces flow separation and erosion caused by water scouring around and under the ice, resulting in horseshoe-shaped scour (Collinson, 1971). Depressions observed in predominantly sandy sediments were interpreted as buried ice melt, caused by collapse during escape of meltwater (Collinson, 1971). These collapse depressions are relatively rare, however they are much more likely to be preserved since they penetrate below the surface (Collinson, 1971).

Results of OSL profiling conducted within this pit feature reveal OSL signals that vary throughout (Gilliland et al., 2012), with relative dates that are not chronological (Gilliland et al., 2012). This likely indicates that the sediment was re-deposited, and is consistent with the ice melt scenario.

Lithofacies 6L. Cross-Stratified Medium-Grained sand to Pebbles with Reactivation Surface

This lithofacies is composed of planar cross-stratified medium-grained to coarse-grained sand, with a reactivation surface and overlying sediments comprised of medium-grained sand to coarse-grained sand matrix supported pebbles up to 7mm. The paleocurrent directions for two beds are northeast (11° and 31°), providing evidence that both were deposited by unidirectional flow. A comparable lithofacies was identified in the Battery Point Sandstone in Quebec, composed of large-scale planar-tabular cross-bedded sandstones in sets averaging 60cm in thickness (Cant & Walker, 1976). The large-scale stratified sands were interpreted to be large bedforms deposited within a braided stream channel (Cant & Walker, 1976), similar to the conglomerate transverse bars that form within channels (Ramos & Sopena, 1983). Within lithofacies 5L, the increase in proportion and size of pebbles above the reactivation surface could be due to river migration, or an increase in flow velocity.

Lithofacies 7L. Cross-Stratified Silt to Pebbles

Abruptly overlying lithofacies 5L, festoon cross-stratified layers are composed of silt to medium-grained sand matrix containing granules and pebbles. Festoon is a variety of trough cross-stratification first applied by Knight (1929), consisting of elongate semi-ellipsoidal troughs that crosscut each other so that only a portion of each layer is preserved (McKee & Weir, 1953). Festoon cross-stratification results from the filling of channels by crossing currents from a convex bank (Doeglas, 1962). This occurs in shallow cross channels of braided river systems, as cobbles are deposited when they roll into deeper water and finer particles travel further but settle rapidly as the current moves above them (Doeglas, 1962). The material which fills these cross channels is derived from the upstream adjacent bar, which will be slightly lowered and flattened (Doeglas, 1962).

Lithofacies 8L. Cross-Stratified Medium-Grained Sand to Pebbles

This lithofacies is composed of low angle cross-stratified medium-grained sand to very coarse-grained sand with granules and pebbles 1 to 2cm in diameter. These layers are slightly bioturbated, and none are prominent enough to determine a paleocurrent direction. The upper portion of this lithofacies in unit 511N 591E is more bioturbated and appears massive, although consistent grain-size and a very diffuse contact indicate that they represent the same lithofacies. There is a gradual change from horizontal layers to low-angle cross-stratification seen in the 510N 505E profile. Absence of pebble segregation makes it unlikely that this lithofacies is wave re-worked (Clifton, 1973; Hart & Plint, 2003). Although finer grained than the gravel bars examined by Eynon and Walker (1974), this lithofacies may represent the initial stage of longitudinal bar formation during or immediately after flood stage. As the flood flow was reduced, a bar developed with horizontal-stratification, and the gradual upward change to low-angle cross-stratification in profile 510N 505E represents avalanching at the bar front (Eynon & Walker, 1974).

Lithofacies 9L. Massive Fine-Grained Sand to Cobbles

This lithofacies is only present in one profile, composed of poorly-sorted medium-grained to coarse-grained sand containing granules, pebbles ranging from 1cm to 4cm in diameter, as well as a cobble 10cm in diameter. The upper and lower contacts with lithofacies 1L are quite abrupt, and pebbles within this poorly-sorted lithofacies do not appear to be imbricated. Similar to lithofacies 2F, the absence of internal structure indicates that this layer was deposited as a subaqueous debris flow (Muto & Steel, 1997). Debris flows are rheological plastics, and they freeze once shear stresses can no longer overcome internal shear strength, which causes their massive appearance (Stow et al., 1996).

Lithofacies 10L. Silty Fine-Grained to Medium-Grained Sand with Few pebbles

Composed of silty fine-grained sand to medium-grained sand containing few pebbles as well as roots, this lithofacies appears massive and strongly

bioturbated. The consistent grain-size with underlying lithofacies 7L indicates that it likely represents the same depositional environment, however without identifiable stratigraphy this cannot be demonstrated.

Lithofacies 14L. Well-Sorted Fine-Grained to Coarse-Grained Sand

The well-sorted nature of this lithofacies, and alternating magnetite-rich layers with magnetite-poor layers are consistent with a beach foreshore environment, discussed for lithofacies association 2C and the upper portion of 4D (Thompson, 1937; Clifton, 1969). Artifacts recovered from within this lithofacies (Fig. 5.128), indicates occupation contemporaneous with active beach formation.

Unit 512N 529E

This unit revealed lithofacies 11L (Clay-Rich Very Fine-Grained Sand), 12L (Fine-Grained to Medium-Grained sand with few pebbles), and 13L (Silty Fine-Grained Sand with Pebbles). These comprise a poorly-sorted profile with boulders, cobbles and pebbles within a matrix of clay, silt and very fine-grained sand. Also present within lithofacies 11L is charcoal, and roots can be seen throughout the entire profile. Absence of internal structure is consistent with a subaqueous debris flow (Muto & Steel, 1997). However, it is more likely that this profile reveals more recent disturbance also seen adjacent to the road at Woodpecker 2 (Fig. 5.130).

As introduced in the results section, the road has likely been graded and the modern soil was pushed to the west side of the road. This conglomerate of grain-sizes, presence of roots and organic material, and absence of internal structure indicates that a portion of Woodpecker 2 was disturbed and the artifacts within were recovered out of context. However, the area of disturbance appears to be minimal.

6.1.25 Woodpecker 1 and 2 Summary

The Woodpecker ridge is likely the result of erosive wave action, as evidenced by the ridge shape (e.g., Meldahl, 1995; Drake & Bristow, 2006) and the sedimentary sequences. Lithofacies indicate that while Woodpecker 1 represents an erosive coastline, sand was transported alongshore and deposited adjacent to the bedrock/erratic at Woodpecker 2. The elevation is consistent with a shoreline of Lake Minong (Fig. 6.1). Presence of artifacts within the nearshore sequence at Woodpecker 2 indicates occupation contemporaneous with active beach formation. However, the artifacts were dominantly recovered from the upper bioturbated lithofacies at Woodpecker 1 and the majority of Woodpecker 2. Likely, this represents successive occupations on the Woodpecker ridge.

6.1.26 Post-Depositional Processes Affecting the Woodpecker Sites

At Woodpecker 2, there also appears to be modern disturbance that was likely caused by heavy machinery when the road was graded. However, only a few meters on the west side of the road appear to have been impacted. The vast majority of Woodpecker 2 is likely undisturbed, with only minimal reworking by worms (Fig. 5.130).

6.2. Paleogeographic Interpretations

The archaeological sites and exposures discussed in this chapter vary in elevation from about 268m asl (Gravel Pit 3) to 224m asl (Mackenzie South Roadcut). Figure 6.3 shows the elevations of each sequence examined, as well as their horizontal associations, and the depositional environments they represent (the stratigraphic column for the Mackenzie Inn exposure only shows the upper portion of the sediment stratigraphy, although all depositional environments are displayed).

The stratigraphically lowest lithofacies within the study area likely represent a sequence of prodeltas (Fig. 6.4). These must all have been deposited in a subaqueous environment, likely while the majority of the study area was submerged. Southward prograding prodelta sequences were identified at Gravel Pit 1, Mackenzie Trench, Mackenzie Roadcut, and Mackenzie Inn as well as Gravel Pit 3. A northward prograding deltaic sequence was located at Construction Site, and the proximity to a similar grain size below RLF indicates that they may represent the same delta.

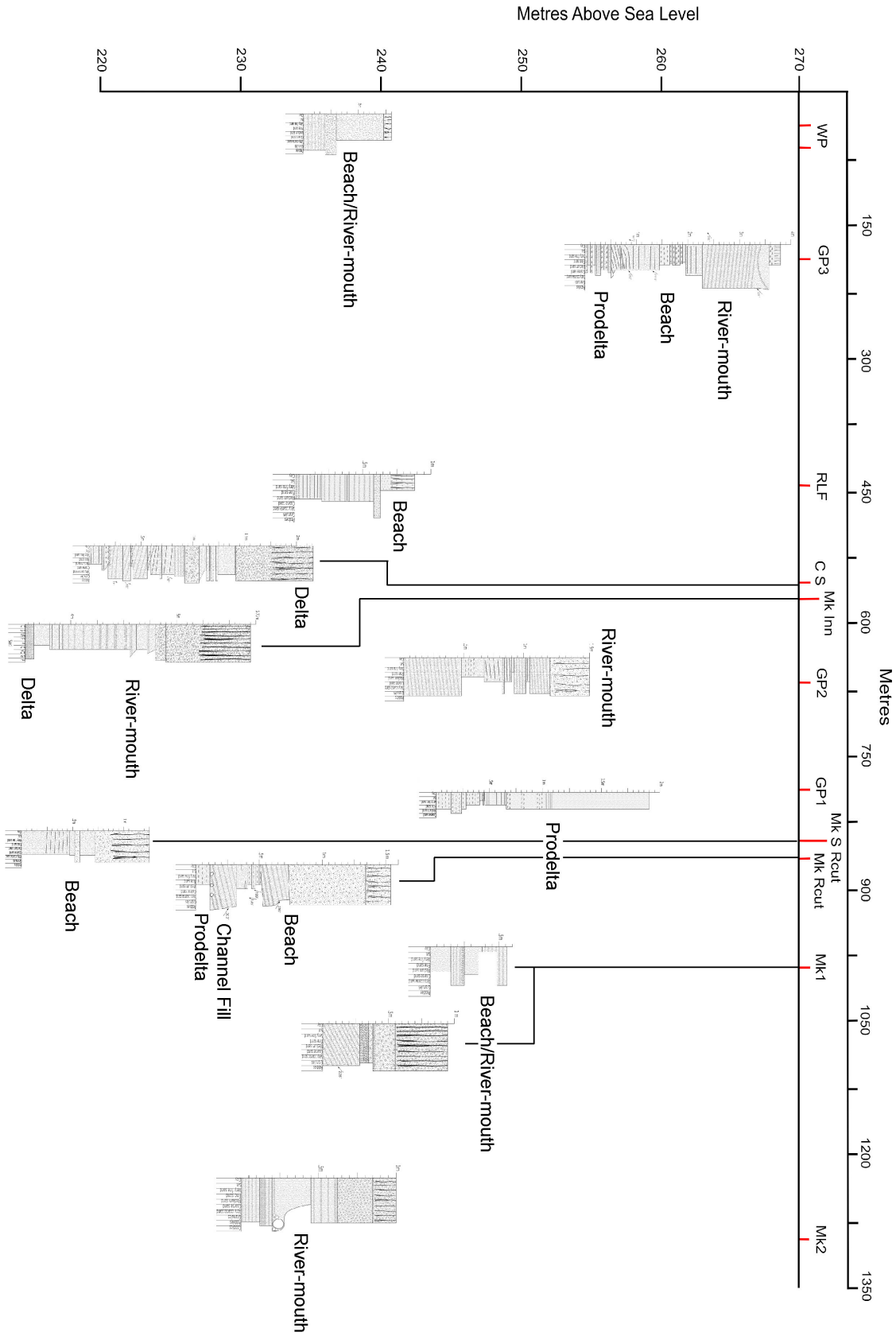

Figure 6.3. The horizontal and vertical association of each sequence examined. The depositional environments they are interpreted to represent are also indicated.

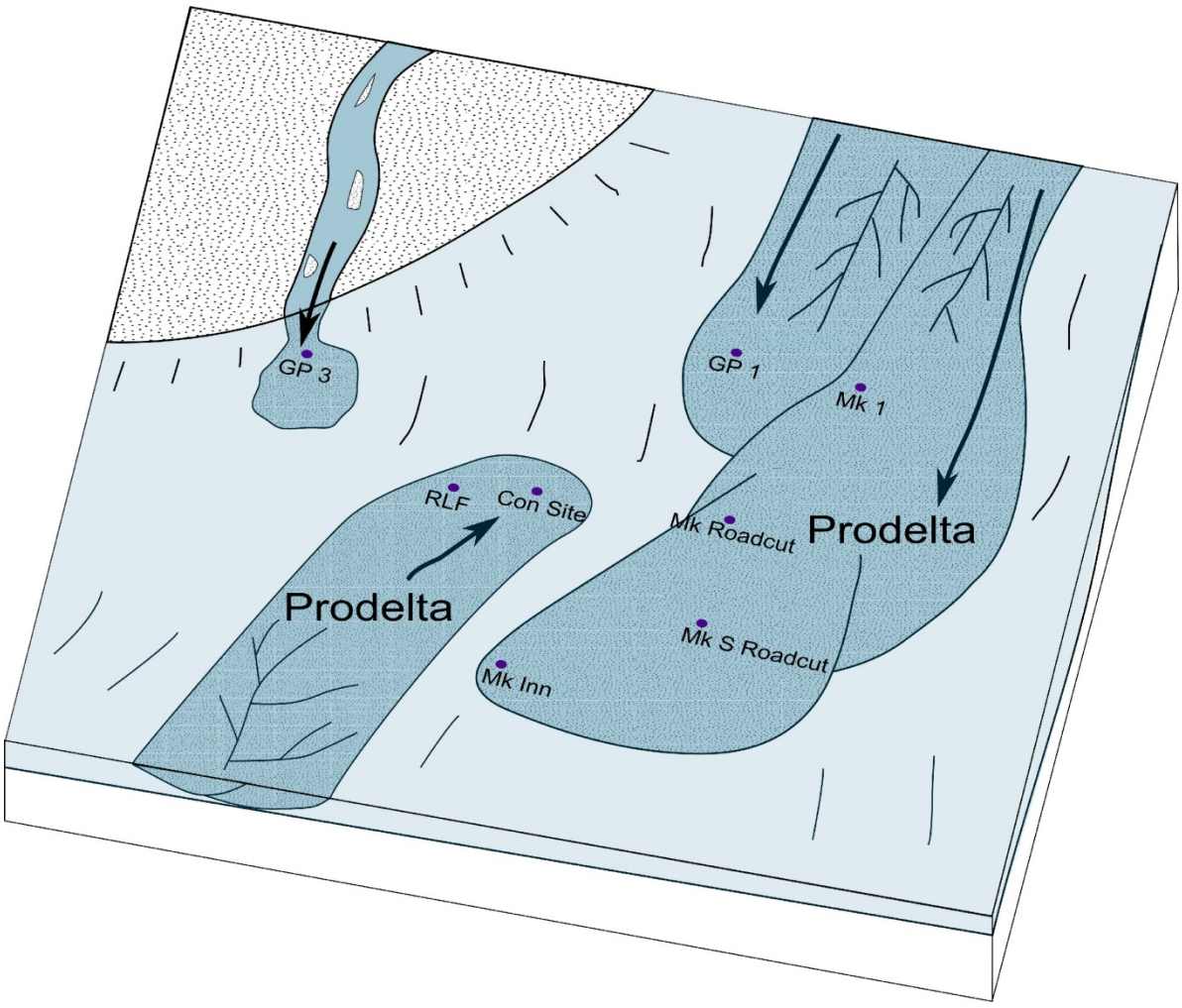

Figure 6.4. Block diagram of prograding deltas within the study area

The sequence at Gravel Pit 3 likely represents a prograding shoreline, indicating that the water level was close to 268m asl for some time. It is possible that the prodelta sequences at Gravel Pit 3, Construction Site, Gravel Pit 1, Mackenzie Trench, and Mackenzie Roadcut were deposited while the lake level was at Gravel Pit 3 (Fig. 6.4). The elevation of the Mackenzie Inn exposure is much lower than the others shown. The prodelta sequence at Mackenzie Inn may have been deposited later than the others, when the water level was lower. Figure 6.4 is dominantly meant to show how the prodelta sequences relate to one another spatially, not temporally.

Overlying the sub-aqueous deltaic sequences are beach and river-mouth deposits that indicate a series of relict shorelines. Since lake level fluctuations

would have caused re-working of sediments, it is likely that these shorelines depict a regressive sequence of lake levels in the Superior basin. Subsequent to the lake level being at 268m asl (at Gravel Pit 3), the water level likely dropped to ~259m asl at Gravel Pit 1 (Fig. 6.5 A). This is evidenced by a prominent ridge extending to north of the Mackenzie 1 site, which likely represents an erosional wave-cut shoreline (e.g. Meldahl, 1995; Drake & Bristow, 2006).

Subsequent shoreline features and sedimentary sequences are located at 249m, 243m, and 240m asl. The Woodpecker ridge is composed of river-mouth sediments along the western portion and beach sediments along the eastern portion (Fig. 6.5 B). It is the only archaeological site with artifacts recovered from within beach sediments, and likely represents one of the earliest occupations in northwestern Ontario. The Mackenzie Roadcut and Mackenzie 2 sequences are at approximately the same elevation, therefore they likely represent the same shoreline inhabited by Paleoindian groups.

The final lake margins within the study area were identified at 233m and 224m asl (Fig. 6.5). As discussed above, it is possible that the prodelta sequence at Mackenzie Inn was deposited later than the other deltaic sediments. A delta could have formed while the lake level was at 259m asl, 249m, 243, or 240m asl.

The sequence at Gravel Pit 2 was likely deposited at a river-mouth. However, the exposure is located in a depression between two ridges seen at Gravel Pit 1 and Gravel Pit 3. Without additional fieldwork, it is difficult to say how this exposure fits into the sequence outlined here.

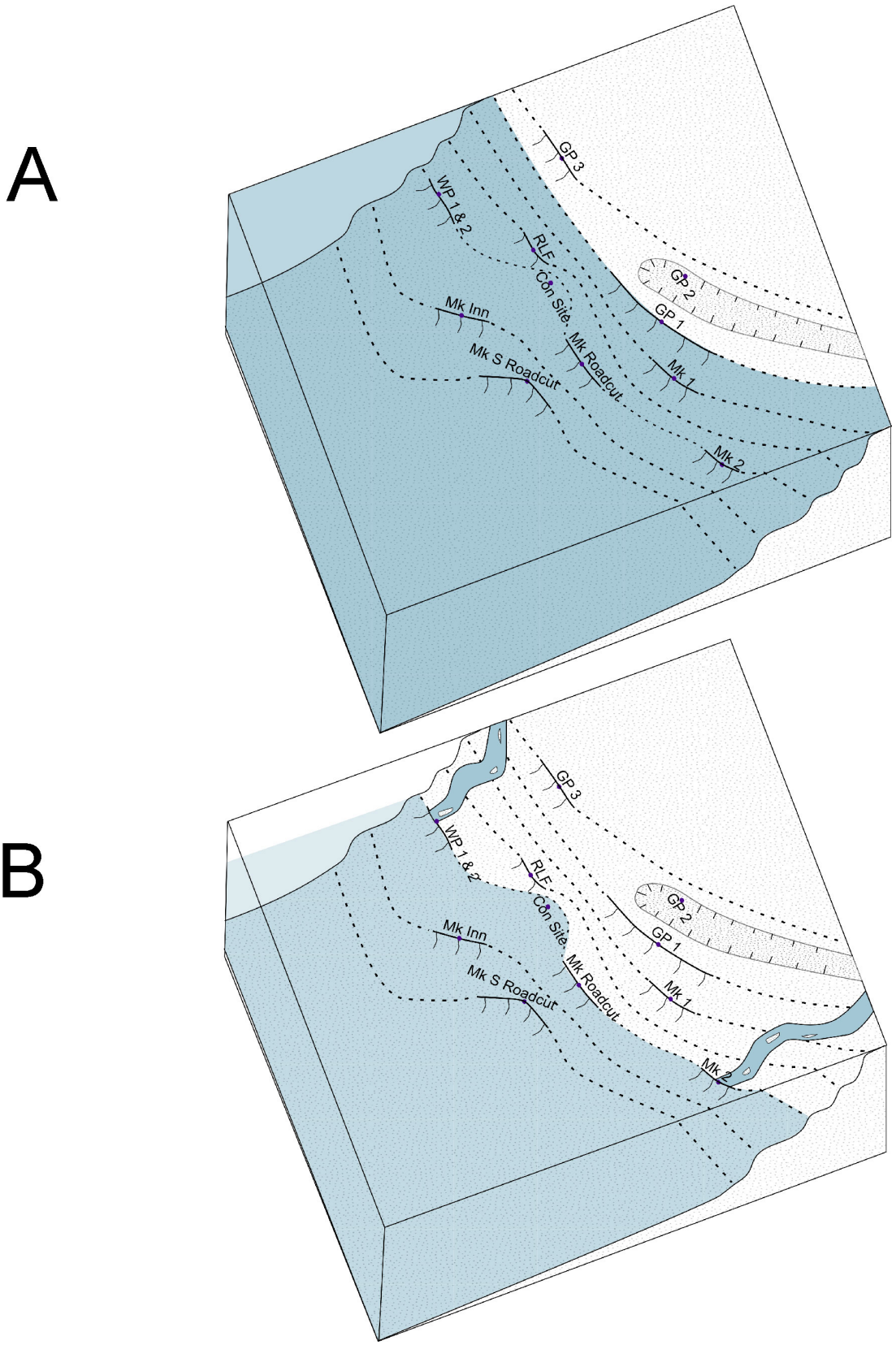

Figure 6.5. Beach and river-mouth sediments representing relict shorelines in the study area

Although the majority of shorelines identified within the study area appear to represent Minong levels, the high elevations of beach/river-mouth sediments at Gravel Pit 3 and lake bottom deposits at Gravel Pit 1 are more consistent with the Lake Beaver Bay stage (Stuart, 1993; Phillips & Fralick, 1994b). After the Marquette readvance, upper Lake Beaver Bay formed as an ice-contact lake along the southwestern margin of the Superior lobe while glacial Lake Baldy formed along its northern margin (Fig. 2.5).

A northward prograding sub-aqueous deltaic sequence at Construction site (236m asl) also likely formed within lower Lake Beaver Bay (Fig. 6.6). Northward flow would have come from the Superior lobe, during its retreat from the northwestern Lake Superior basin (c.f. Phillips & Fralick, 1994b). The low elevation of the topset bed within this sequence indicates that it likely represents the final stage of Lake Beaver Bay as its glacial meltwater flowed into the Superior basin. The elevation of the Construction site, at 236m asl, places it vertically between two Minong shorelines. It is possible that while Lake Minong was at an elevation of ~240m asl (at the Woodpecker ridge, Mackenzie Roadcut and Mackenzie 2 site), the previously deposited deltaic sediments at Construction Site were below wave base and not re-worked. Subsequent relative lake level drop to 233m asl (Mackenzie Inn) may have been rapid enough for preservation of the deltaic sediments.

Strandlines lower than about 268m asl are generally considered to be associated with Lake Minong (Stuart, 1993; Phillips & Fralick, 1994b). At an elevation of 259m asl, Gravel Pit 1 is located on a prominent ridge that likely represents a wave-cut shoreline (e.g., Meldahl, 1995; Drake & Bristow, 2006) consistent with an early elevation of Lake Minong (Burwasser, 1977; Phillips, 1982; Phillips & Fralick, 1994b).

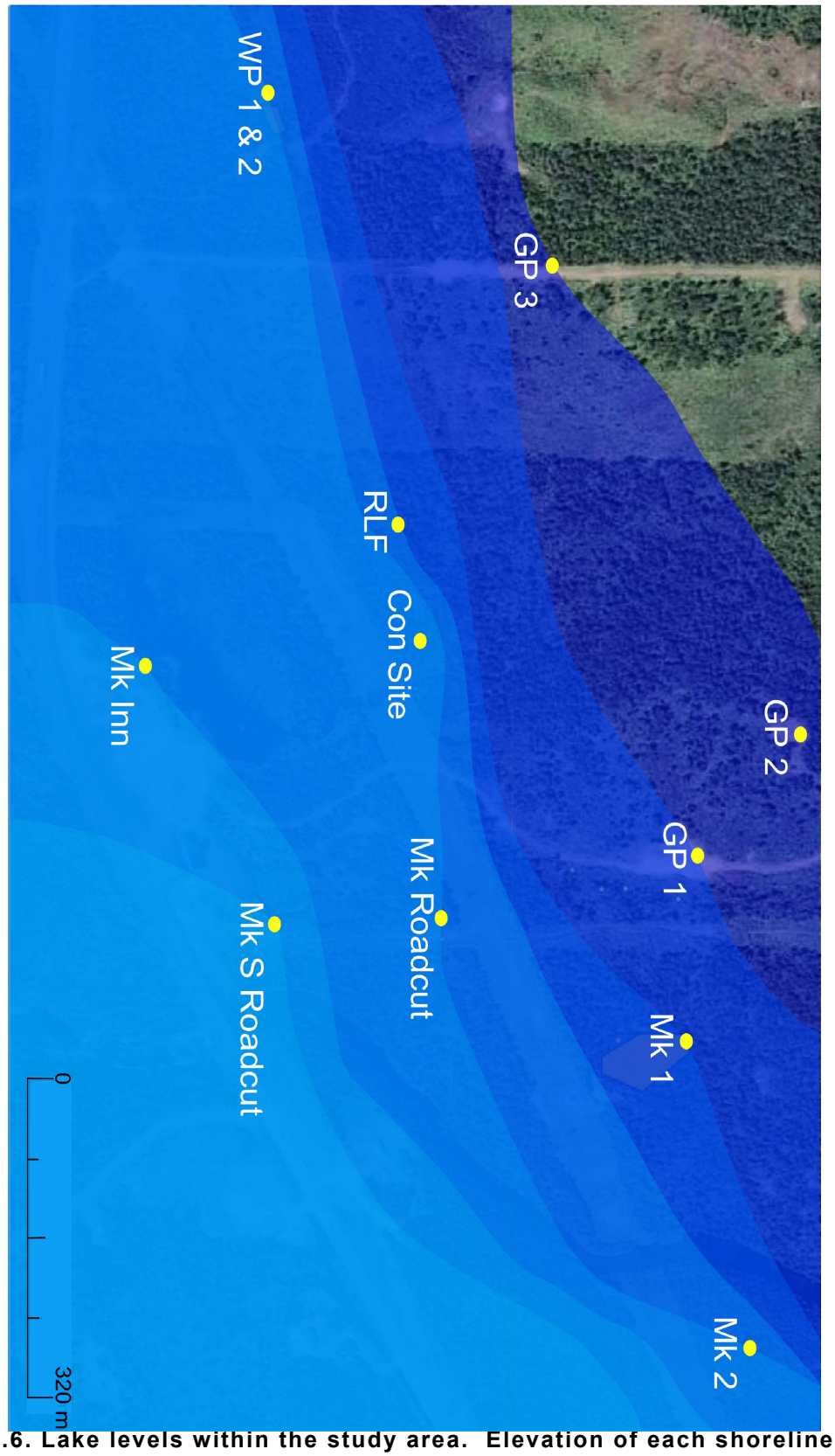

Figure 6.6. Lake levels within the study area. Elevation of each shoreline adjacent to the exposure/archaeological site was estimated utilizing a DEM (LUGDC, 2012a), and GoogleEarth.

6.2.1. Paleogeographic Interpretations of the Archaeological Sites

The Mackenzie 1 site slopes from beach shoreface sediments in the north at ~249m asl (Fig. 6.6), to river-mouth sequences in the south at ~246m asl. A series of lake margin sediments were deposited at lower elevations in the study area (Fig. 6.6) at: RLF (243m asl); the Woodpecker sites, Mackenzie Roadcut, and Mackenzie 2 archaeological site (240m asl); Mackenzie Inn (233m asl); and Mackenzie South Roadcut (224m asl). These elevations are consistent with Minong lake levels (Burwasser, 1977; Phillips, 1982; Julig et al., 1990), and the lowest level of 224m asl at the Mackenzie South Roadcut likely represents a Post-Minong shoreline (Burwasser, 1977). Artifacts recovered from within a nearshore depositional environment indicate that Woodpecker 2 was occupied during active beach formation.

Although contemporaneity between site occupation and active deposition is only demonstrated at Mackenzie 2, it is likely that all five of the Paloindian sites were occupied during the Minong phase (between 9,900 and 9,000 BP). The massive sediment matrix associated with artifacts is consistent with the grain size of adjacent river-mouth and nearshore deposits, making it possible that the artifacts are contemporaneous with active deposition. Subsequent bioturbation would account for the absence of stratigraphy.

6.3. Limitations of Interpretations

This section has outlined a general chronological sequence for the exposures, and a geological context for the archaeological sites. Unfortunately, additional correlations of lithofacies between the exposures and archaeological sites would be too speculative for accurate interpretations and conclusions. For example, river-mouth sequences identified at different locations could represent the same migrating river along a lake margin over time, although additional exposures are required to provide evidence of this.

The Gravel Pit 2 exposure is located in a low-lying area north of the Gravel Pit 1 ridge. It is composed of fluvial and river-mouth sediments that do not correlate with the other exposures and lithofacies associations examined. Additional fieldwork would be required to determine how the sedimentary sequence fits into the deglaciation and lake level chronology.

7. DISCUSSION

7.1 Regional Paleogeographic Reconstruction

The sequence of shorelines identified within the study area is consistent with the known deglaciation sequence and previously identified proglacial lake levels in northwestern Ontario.

Shorelines on the inner flank of the Dog Lake moraine around 442m asl provide evidence of proglacial lakes that formed between the moraine and the wasting margin of the Hudson Bay lobe, while the Superior lobe maintained its position at the Marks moraine (Phillips & Fralick, 1994b). Glacial Lake Baldy began forming on the north side of the Mackenzie interlobate moraine, later extending through the moraine as the Superior ice withdrew southeastward (Phillips & Fralick, 1994b). The Superior lobe likely wasted back from the Marks moraine, gradually retreating eastward along its perimeter and ultimately drawing away from the Mackenzie interlobate portion of the moraine (Phillips & Fralick, 1994b). During this withdrawal, Lake Kaministiquia drained through the Marks moraine along the Kaministiquia River valley, to form the fluvial Kakabeka delta on the edge of Lake Beaver Bay (Burwasser, 1977). The Kakabeka delta bears shorelines from 289m asl, downward to the highest Minong level at 259m asl, indicating a continuous deltaic progradation into a lake of declining level (Phillips & Fralick, 1994b).

Lake Baldy maintained its position between the Mackenzie moraine and the Superior lobe, with fluctuating lake levels as it received water and sediment from the Current River spillway, as well as streams off Lake Baldy, the Mackenzie moraine and the ice sheet (Phillips & Fralick, 1994b). As the Superior lobe retreated from the Intola moraine, the lower level of Lake Beaver Bay inundated Lake Baldy at about 274m asl (Patricia Craig, 1991; Stuart, 1993; Phillips & Fralick, 1994b) (Fig. 7.1). Rapidly dropping water levels are displayed as a series of less distinct shoreline features east of the Intola moraine (Stuart, 1993). The lowest identified strandline of Lake Beaver Bay is at an elevation of 268m asl (Stuart, 1993), and likely corresponds to the beach and river-mouth

sediments located at Gravel Pit 3 (268m asl). The approximate area covered by Lake Beaver Bay at this time is shown in Figure 7.1, although east of the study area additional fieldwork is required to define the lake margin.

Gravel Pit 1 is composed of lake bottom sediments at an elevation of 259m asl. This sequence was likely deposited within a late phase of Lake Beaver Bay. A northward prograding deltaic sequence at Construction site (236m asl) also likely formed within lower Lake Beaver Bay. Northward flow would have come from the Superior lobe, during its retreat from the northwestern Lake Superior basin (c.f. Phillips & Fralick, 1994b). The low elevation of the topset bed within this sequence indicates that it likely represents the final stage of Lake Beaver Bay as its glacial meltwater flowed into the Superior basin. There are two possible scenarios for the dissipation of Lake Beaver Bay.

In the first scenario, as the Superior lobe made its final retreat from northwestern Ontario, it is possible that the water from Lake Beaver Bay drained into the Superior basin until its elevation was about 259m asl, marking the beginning of the Minong phase (c.f. Stuart, 1993; Phillips & Fralick, 1994b). The glacial meltwater from the Superior lobe would have drained to the Superior basin, and it is likely that the Kaministiquia and Current river valleys provided additional outwash from the Hudson Bay lobe (e.g. Phillips & Fralick, 1994b; Boyd et al., 2012). In addition, the Superior basin would have likely been receiving meltwater from glacial Lake Agassiz (Lewis & Anderson, 1989).

Depending on how the Superior lobe retreated from the area, it is also possible that not all of the Lake Beaver Bay water drained into the Superior basin at the same time. In this second scenario, if some water maintained its position north of the glacier margin while the Lobe retreated from the study area, the lake level could have been lower than 259m asl and subsequently risen as the remainder of Lake Beaver Bay water drained into the Superior basin.

The Nadoway sill controlled the lake level in the Superior basin during the Minong phase (Farrand & Drexler, 1985; Yu et al., 2010; Boyd et al., 2012). The elevation of the Nadoway sill was about 271m asl, which has been corrected for differential isostatic rebound to about 230m asl in the Thunder Bay region (Yu et

al., 2010). The lake level in the Superior basin could not have dropped below this elevation, until the Nadoway sill was eroded. It has been demonstrated that the Houghton low phase in the Superior basin was likely caused by a rapid breach at Nadoway Point (Yu et al., 2010). However, it is possible that the Nadoway sill experienced some erosion prior to the rapid lake level drop. Either way, the lake level could not have dropped below an approximate elevation of 230m asl (in the Thunder Bay region) during the Minong phase. This lake level would also have exposed the deltaic sediments at Mackenzie Roadcut, allowing an erosive channel to incise the concave-up base identified.

Gravel Pit 1, at an elevation of 259m asl is located at the top of a slope (Fig. 6.1) that extends eastward north of Mackenzie 1 and southwestward to Gravel Pit 3. It is inconsistent with the size of identified storm beaches that do not indicate a lake level (McMillan & Teller, 2012), and likely represents a wave-cut feature (e.g. Meldahl, 1995; Drake & Bristow, 2006) during the Minong phase.

Subsequent deposition of beach sediments and river-mouth deposits could have occurred as a result of declining lake level, isostatic uplift, or a combination of the two. Possible scenarios are presented below.

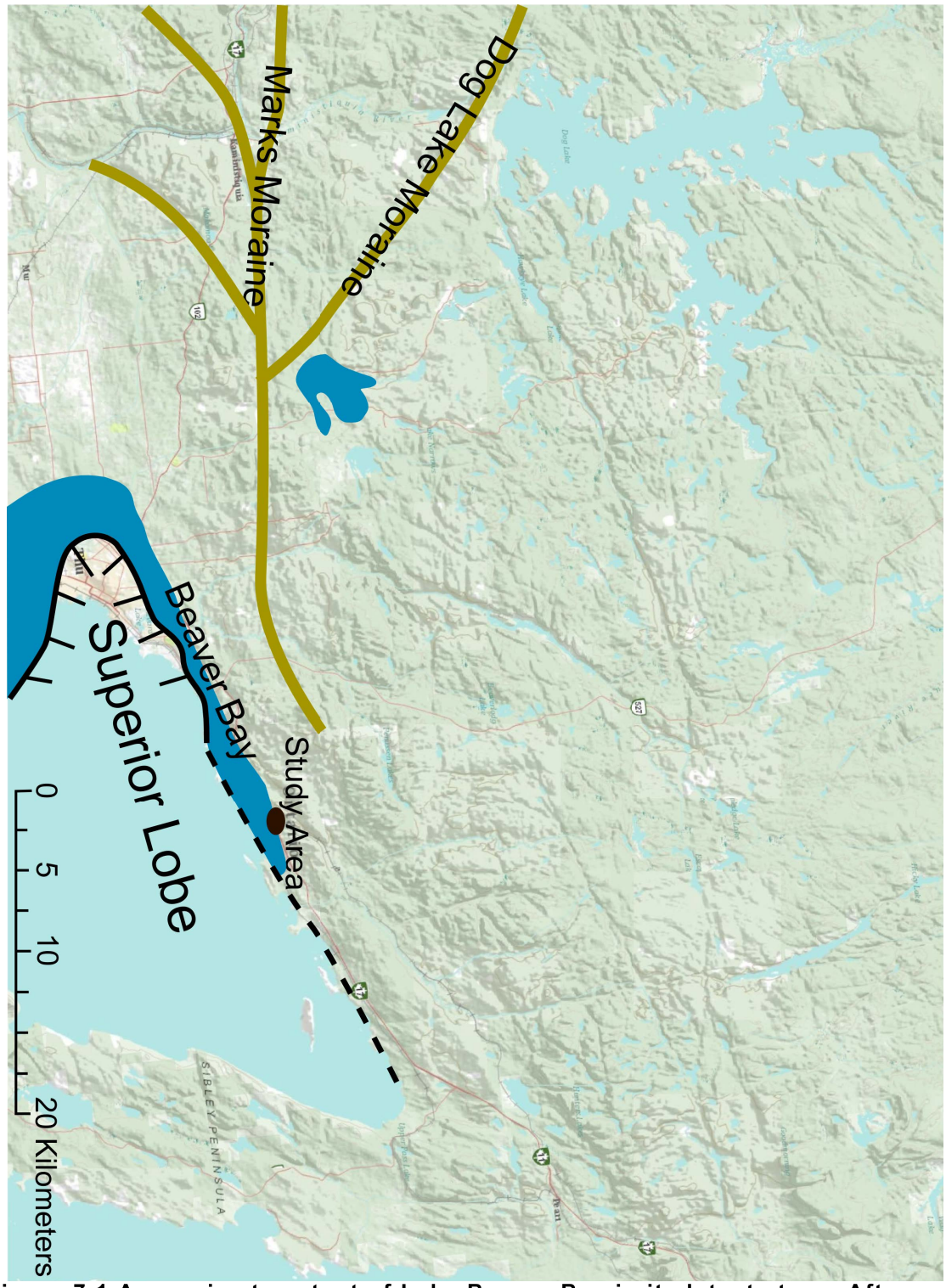

Figure 7.1 Approximate extent of Lake Beaver Bay in its latest stage. After Stuart (1993) and Phillips & Fralick (1994b)

7.1.1 Minong Levels in the Study Area

After creating the wave-cut strandline at 259m asl, Lake Minong likely receded to Mackenzie 1 at 250m asl (Fig. 7.2). Beach sediments in the northern portion of the site become river-mouth sediments in the southern part of Mackenzie 1. This may represent a subsequent regressive sequence. After, the lake level would have dropped to RLF (243m asl). At this elevation, it is possible that the construction site was below wave base and therefore not reworked. In addition, the sediments at Mackenzie Roadcut representing bankfull discharge could have been deposited in a subaqueous environment with lake levels ranging from Mackenzie 1 to RLF (Fig. 6.3).

Further lake level drop to Mackenzie Roadcut and Mackenzie 2 archaeological site (~240m asl) would also have been at the elevation of the Woodpecker ridge. The Woodpecker ridge likely represents a wave-cut feature. Along a coastline with net erosion, sediments are transported along shore to areas of net-deposition. The Woodpecker 2 site has bedrock (or a large erratic), which would have influenced longshore drift currents. It is possible that while Lake Minong was stable at this elevation, the Woodpecker 1 ridge was eroded, and as sediment was transported along shore it was deposited adjacent to the bedrock/erratic.

The sequence identified at Mackenzie Inn (233m asl) is a prograding delta with bottomset and foreset beds that may have been deposited within proglacial Lake Minong. The Cummins site is located on a strandline at 232m asl, and may represent the same lake margin as the topset bed of Mackenzie Inn.

The Mackenzie South Roadcut exposure reveals beach sediments at an elevation of 224m asl. This could represent a low level of Lake Minong. As discussed above, the Nadoway sill controlled lake levels, and it is likely that Minong levels were not lower than about 230m asl (Yu et al., 2010). However, this elevation is an estimate for the morainal sill elevation. It is possible that either the Mackenzie South roadcut represents the lowest possible lake level during the Minong phase, or alternately the Nadoway morainal sill was partially eroded before the rapid breach proposed by Yu et al. (2010).

In the Thunder Bay region, the relative lake level during the Houghton low is approximately the same as the modern Superior lake level or lower (Kingsmill, 2011; Boyd et al., 2012). Another possibility is that the Mackenzie South Roadcut represents a Nipissing level. Rising water levels through the Nipissing phase produced the highest Holocene water levels of the Great Western Lakes by ~4,500 ^{14}C yrs BP (Booth et al., 2002). Due to differential isostatic rebound, this high stand is represented by strandlines lower than Minong and higher than Houghton in some parts of the Superior basin (Farrand & Drexler, 1985; Slattery et al., 2007). However, the Nipissing lake level is likely ~210m asl in the Thunder Bay region (Phillips, 1982; Farrand & Drexler, 1985), and shorelines around 224m asl are generally attributed to a Post-Minong shoreline (Burwasser, 1977).

The proglacial Minong phase in the Superior basin is generally considered to be ~10,500-9,000 cal BP (e.g., Farrand and Drexler, 1985). However, following the Marquette re-advance Lake Beaver Bay was an ice-contact lake along the northern margin of the Superior lobe while the series of deltas identified within the study area were deposited. It was not until after the Superior lobe made its final retreat and Lake Beaver Bay drained into the Superior basin that the Minong phase began, therefore it must have been after 10,000 ^{14}C yrs BP. Although Phillips and Fralick (1994b) speculate that this occurred after ~9,500 ^{14}C yrs BP (the approximate age of Lake Baldy), the radiocarbon date from Woodpecker 2 (~9,700-9,500 cal BP) suggests that it may have been closer to the Marquette re-advance. A tentative date of about 9,900 ^{14}C yrs is here proposed for the beginning of the Minong phase. This likely marks the earliest and highest Minong level identified by wave-cut features west of the study area (Burwasser, 1977; Phillips, 1982; Phillips & Fralick, 1994b), as well as within it (Fig. 7.2).

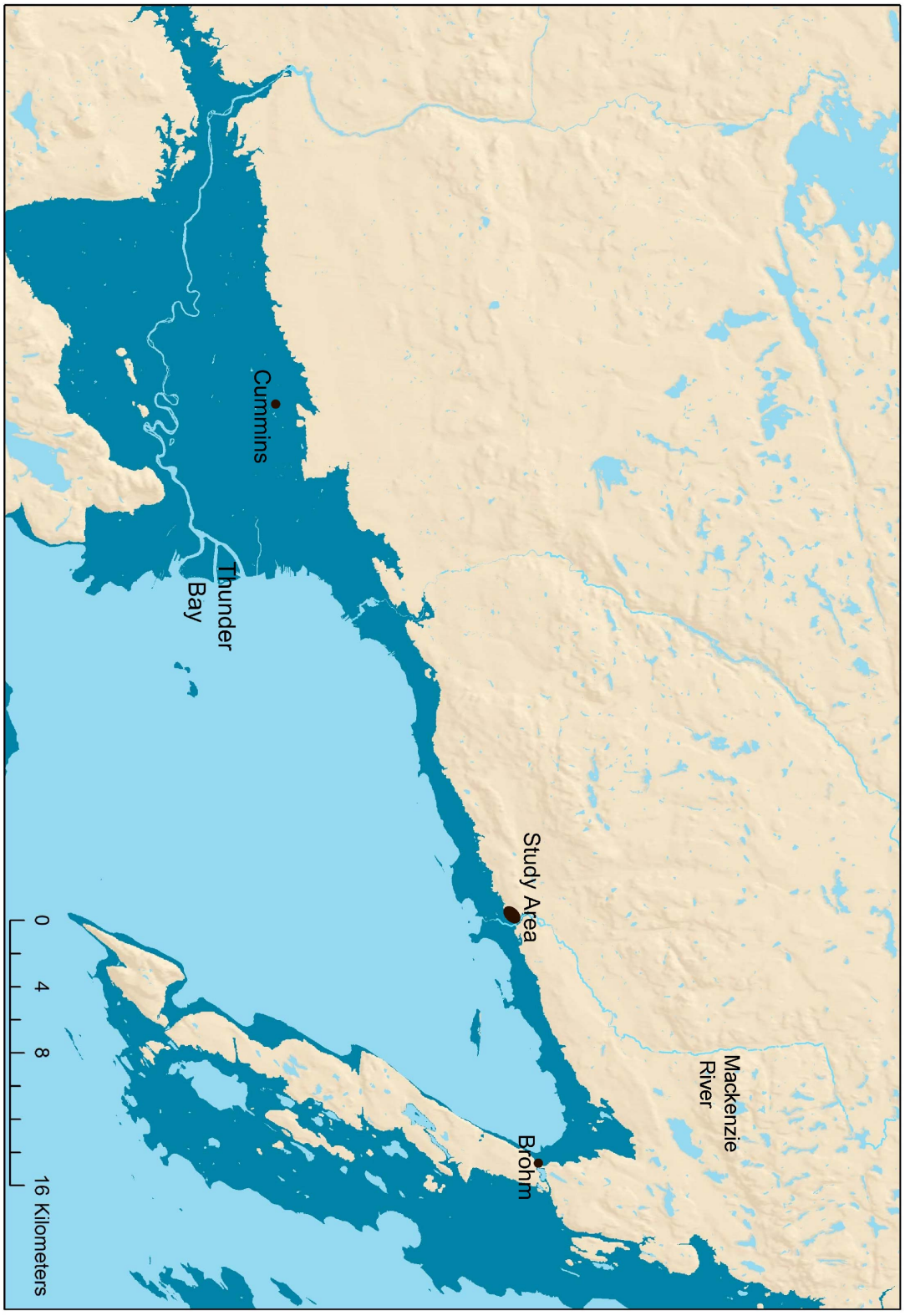

Figure 7.2. Area covered by Lake Minong at an elevation of 259m asl, utilizing a DEM (LUGDC, 2012a)

7.1.2 Isostatic Rebound

The Superior lobe covered the study area, which would have depressed the landscape. Isostatic rebound in this more recently deglaciated region was more rapid than areas located on more southerly isobases, and could also account for the lake margin deposits at different elevations. After the lake margin was at the Mackenzie 1 site, subsequent isostatic rebound can account for the relatively lower beach and river-mouth deposits. As the land was rebounding, it could have been raised to the elevation of RLF, when the channel at Mackenzie Roadcut was infilled.

Subsequent rebound could have raised the landscape relative to Lake Minong, to 240m asl. At this time, the Mackenzie Roadcut and Mackenzie 2 site represent the lake margin where beach and river-mouth sediments were deposited. At approximately the same time, the Woodpecker ridge was formed, and wave reworked sediments were deposited against the outcropping bedrock/erratic at Woodpecker 2.

It is possible that continual isostatic rebound raised the land to 233m asl at the Mackenzie Inn exposure. However, a third possibility for this sequence of events is regression while isostatic rebound influenced the Thunder Bay region. Most likely, both factors influenced relative lake levels in the Thunder Bay region.

7.1.3 Mackenzie River Valley: A Potential Spillway

The Mackenzie River is presently located within a deeply incised valley. There are numerous similar valleys in the Thunder Bay region, which are likely the result of glacial scouring. During the Marquette re-advance, the Mackenzie River valley was likely subglacial (Phillips & Fralick, 1994b) and could have been infilled (at least partly) with subglacial till. Following deglaciation, when the margin of the Hudson Bay lobe was south of Greenwich Lake (B or C in Fig. 2.5), the Mackenzie River valley could have been utilized as a spillway. Since the valley would have been in confluence with the elevation of Lake Minong, it would have been completely filled with sediment either from the glacial meltwater or

from glacial till. Therefore, while the lake was at the elevation of Mackenzie 1 during the Minong phase, the deeply incised valley near the archaeological sites was not present.

The Mackenzie River valley could only have been used as a glacial spillway while the Hudson Bay lobe was south of Greenwich Lake. This is due to high elevations between the Mackenzie River and Lake Nipigon, which currently inhibit direct flow to the Superior basin. Evidence of river-mouth deposits at the Mackenzie 1 and 2 archaeological sites indicates that there was a river transporting fluvial sediments to them. This provides evidence that glacial meltwater from the Hudson Bay lobe flowed through the Mackenzie River Valley.

7.2 Artifact Recoveries within the Study Area

A total of 378 projectile points were recovered from Mackenzie 1 (complete and partial). There is considerable variability in point styles, and no Paleoindian assemblage this big has been found at one archaeological site in northwestern Ontario. This makes it difficult to compare the Mackenzie assemblage to other point styles, although there do appear to be influences from the southwest Plains, Wisconsin, Wyoming, and Florida (Markham, n.d.). No diagnostic artifacts were recovered from the RLF site, and projectile points discovered at Mackenzie 2 and the Woodpecker sites conform to the Mackenzie assemblage (Markham, n.d.). All of these diagnostic artifacts resemble projectile points found at sites around the Great Lakes (Markham, n.d.).

One consistent feature, seen on 99% of the Mackenzie assemblage, is parallel oblique flaking (Markham, n.d.). The majority of points recovered from the Woodpecker sites also have parallel oblique flaking, although it appears to be absent from the point found at Mackenzie 2 (Markham, n.d.).

Five projectile points from Mackenzie 1 appear to have side notches, which typically indicate Archaic occupation. However, they all have a parallel oblique flaking pattern, and it has been argued that the notches are the result of accidental breakage (Markham, n.d.). It is unlikely (albeit possible) that these

projectile points, found throughout the site at various levels, represent an Archaic occupation.

7.3 Optically Stimulated Luminescence (OSL) and Radiocarbon Dates

Sediment samples for OSL dating were taken from Mackenzie 1 as well as Woodpecker 1 (Gilliland, 2012; Kinnaird et al., 2012). At Woodpecker 1, three samples were taken by Dr. Adderley and Dr. Gilliland, and subsequently sent for dating. These were extracted from the west wall of units 500N 468E and 501N 468E. One sample was taken from the middle spillover lobe (lithofacies 3L), one was taken from the bottom of the lithofacies containing artifacts, and the last was from just below surface (also associated with artifact recoveries, both within lithofacies 4L). The spillover lobe was dated to 7,980-7,000 BP, and the bottom and top of the cultural layer(s) yielded a date of 6,840-5,740 BP and 3,100-2,660 BP respectively (Gilliland, 2012; Kinnaird et al., 2012).

Three OSL samples from Mackenzie 1 were sent for dating, all taken from the pit feature in unit 478N 518E (Gilliland, 2012; Kinnaird et al., 2012). One sample was taken from the bottom of the pit feature (within the pit fill), the second was taken from the middle and the third from the top of the pit feature (all samples were within lithofacies 6I). The lower fill yielded and age of 6,500-5,680 BP, the middle of the pit was dated to 6,210-5,330 BP, and the top to 5,820-5,180 BP (Gilliland, 2012; Kinnaird et al., 2012).

During the 2012 field season, charcoal associated with cultural remains was sampled by Western Heritage, from the Woodpecker 2 archaeological site. The charcoal and artifacts were recovered from beach shoreface sediments ~30cm below surface (within lithofacies 13L), and therefore date the Minong lake level as well as occupation at Woodpecker 2. A conventional age of 8,680 ± 50 ^{14}C yrs BP was obtained (Beta 323410), and calibrated to 9,760-9,540 cal BP (Gilliland, 2012).

Western Heritage recovered one charcoal sample from Mackenzie 1, from within the pit fill in unit 497N 506E (lithofacies 7I), about 40cm below surface.

The sample yielded a conventional age of 3,550 ± 30 ^{14}C yrs BP (Beta 301998), and 3,910-3,820 cal BP (Dave Norris 2011, pers. comm).

The spillover lobe at Woodpecker 1 was probably deposited at approximately the same time as the beach deposits at Woodpecker 2 since they are at about the same elevation. However, there is a difference of almost 2,000 to 3,000 years between the OSL and radiocarbon dates. The OSL date of the spillover lobe at Woodpecker 1 is 7,980-7,000 BP (Gilliland et al., 2012; Kinnaird et al., 2012). At this time, all of the Upper Great Lakes except Superior had coalesced with the waters of the Nipissing basin (Lewis & Anderson, 1989). Water in the Superior basin would have been between closer to ~205m asl (Yu et al., 2010). Given this, although there is some debate to the validity of the OSL dates (e.g. Gilliland, 2012), it is unlikely that the OSL date for the spillover lobe is correct. The beach sediments must have been deposited after the Marquette readvance and before the Houghton low, dating between 10,000 ^{14}C yrs BP (Lowell et al., 1999) and 9,300 cal BP (Yu et al., 2010), consistent with the radiocarbon date of 9,760-9,540 cal BP.

OSL profiling results at Woodpecker 1 and Mackenzie 1 indicated a chronology of relative exposure ages (Gilliland, 2012), which conforms to the sequence of OSL dates at each site. This makes it likely that if one date is incorrect, there is a systematic error in the methodology. Another possibility is that the OSL dates on the Mackenzie 1 pit infill sequence is correct, but that it reflects later, post-Paleoindian cultural or natural events. If there is a systematic error in the OSL dates, the ones from sediment associated with artifacts would be too young as well. The OSL dates at both Woodpecker 1 and Mackenzie 1 indicate an Archaic occupation, although the diagnostic artifacts appear to be Paleoindian in age. Archaeological evidence at Mackenzie 1, and stratigraphic evidence at the Woodpecker sites suggest that the OSL dates reported in Gilliland (2012) and Kinnaird et al. (2012) are too recent.

Similarly, the radiocarbon date from Mackenzie 1 is 3,910-3,820 cal BP (Dave Norris 2011, pers. comm.), and cannot reflect the Paleoindian occupation evident by diagnostic artifacts. The pit fill sediment is massive, poorly sorted,

and was likely disturbed during soil sampling prior to archaeological excavations. Absence of Archaic artifacts at Mackenzie 1 makes it highly unlikely that this date represents contemporaneous occupation. More likely, the charcoal could be the result of root burn, which was subsequently mixed in with the older pit fill sediments and artifacts.

7.4 Post-Depositional Processes Affecting Archaeological Sites in the Study Area

At Mackenzie 2, RLF, and Woodpecker 1 the only disturbance appears to be plant bioturbation. All artifacts were recovered from massive and poorly-sorted sediments with common presence of roots. However, at Mackenzie 1 and Woodpecker 2 there appears to be evidence of additional post-depositional disturbance. The disturbance was likely created during construction-related soil sampling at Mackenzie 1, and heavy machinery when the road at Woodpecker 2 was graded.

Wave re-working is apparent at the Cummins site, evidenced by battering and polishing on artifacts in addition to the site stratigraphy (Julig et al., 1990). Preliminary examination of the artifacts from RLF during cataloguing indicates that there may be evidence of rounding caused by wave action. However, no artifacts from the other archaeological sites appear to be water worn. The artifacts recovered from within the beach shoreface sediments at Woodpecker 2 could be reworked, although this is unlikely. There is no evidence of rounding or polishing on the artifacts, and they are associated with charcoal. It is more likely that the artifacts and charcoal were buried by beach shoreface sediments, and preserved. If the layer represented a lag deposit, when wave action transported sand around the artifacts offshore, the charcoal (with its low specific gravity) would have likely been eroded away with the sand.

7.5 Paleoindian Occupation of the Thunder Bay Region

Paleoindian sites are commonly associated with shorelines deposited along former proglacial lake margins (e.g. Deller, 1979; Dawson, 1983a; Buchner

and Pettipas, 1990; Jackson et al, 2000; Boyd et al, 2003; Boyd, 2007b). Beach terraces would have been well-drained, high ridges that could have been utilized as transportation corridors by the mobile hunters and gatherers, and by the prey they hunted (Deller, 1979; Peers, 1985). Similarly, sites in the Thunder Bay region are strategically placed at the mouths of rivers and creeks for procurement of fish, and likely caribou (Fox, 1976).

The nature and timing of initial occupation in northwestern Ontario has remained difficult to discern, due to a lack of geoarchaeological studies at many archaeological sites and general absence of material suitable for dating. One charcoal date at Woodpecker 2 provides evidence that the Thunder Bay region was inhabited 9,760 to 9,540 cal BP, contemporaneous with active beach formation during the Minong phase. However, artifacts recovered from Mackenzie 1 and 2, RLF, and Woodpecker 1 were discovered within bioturbated sediments. Although it is possible that occupation at these sites was also contemporaneous with their associated strandlines, there is no evidence to support this. Active deposition would likely have buried the artifacts and provided recognizable occupation layers, which are only apparent at Woodpecker 2. The other sites may represent occupation along relict strandlines, or alternately bioturbation occurred after deposition ceased.

There is no apparent hiatus between the bioturbated artifact layer(s) and underlying intact stratigraphy. Absence of a soil horizon under the artifact layer(s) indicates that the shorelines at Mackenzie 1 and 2, RLF, and the Woodpecker sites were occupied before soil formation occurred. This provides some evidence that although occupation was not generally contemporaneous with active beach formation, the sites were likely occupied soon after deposition ceased. For example, the northern portion of Mackenzie 1 could have been inhabited while the river-mouth sediments were being deposited in the southern portion of the site. Similarly, the southern portion of Mackenzie 1 may have been utilized by Paleoindian groups while the water level was only a few metres lower at RLF.

In the Thunder Bay region, Paleoindian sites are commonly associated with Minong shorelines, as well as streams and rivers (Dawson, 1983). The Makenzie, RLF, and Woodpecker sites contribute to this strong relationship, providing additional evidence that Paleoindian groups were preferentially occupying beach terraces. In addition, river-mouth deposits underlying occupation layer(s) at Mackenzie 1 and 2, and Woodpecker 1 suggest that locations adjacent to rivers and likely close to river-mouths were also favourable. These may have been ideal locations for fishing, and hunting large game at river crossings.

The large amount of artifacts recovered from the Mackenzie 1 site suggests that the site was utilized over a long period of time, and may represent successive occupations. It was likely an attractive site near a Lake Minong margin as well as a river. However, it is also possible that the site is large because it was used by numerous individuals, or even multiple groups of mobile hunters and gatherers. Additionally, the site was subject to more archaeological excavation than most in northwestern Ontario, and sites of a comparable size may remain unidentified or poorly defined.

The recovered diagnostic tools do appear to resemble early Paleoindian point styles from other areas (Markham, n.d.). As discussed above, the Paleoindian to Archaic transition is not well dated in northwestern Ontario, and Paleoindican occupation could date to any time between ~9,700 ^{14}C yrs BP and ~7,000 ^{14}C yrs BP. However, it is highly likely that the archaeological sites within the study area date to the Minong phase or close to it. Therefore, the Mackenzie, RLF, and Woodpecker sites were likely occupied sometime between about 9,900 and 9,000 ^{14}C yrs BP.

8. CONCLUSIONS

Within the study area, seven exposures were examined for stratigraphic analysis, along with the five archaeological sites identified during stage 2 investigations. Stage four excavations were completed at Mackenzie 1, Mackenzie 2, RLF, and Woodpecker 1, although work is ongoing at Woodpecker 2. The data provides a deglaciation and lake level chronology that fits nicely with previous studies in the Thunder Bay region.

After the Marquette re-advance, the Hudson Bay lobe retreated in a northeastward direction while the Superior lobe wasted southeastward. This created an ice-free area in which Dog Lake and Lake Baldy formed, while Lake Beaver Bay developed southwest of the Superior lobe. Continued glacial retreat caused Lake Beaver Bay to inundate Lake Baldy as well as the study area, at an elevation of about 268m asl. This late stage of lower Lake Beaver Bay ended when the Superior lobe wasted enough for the lake water to drain into the Superior basin, marking the beginning of the Minong phase.

The highest, and likely oldest lake level is at about 259m asl, as evidenced by a wave-cut shoreline to the north of Mackenzie 1 and RLF. Subsequent relative lake level drops occurred as either water level lowered, the land was isostatically rebounding, or a combination of these two factors. This created a series of shorelines in the study area at elevations of 256m, 249m, 243m, 240m, 233m, and 224m asl.

Paleoindian occupation likely took place 9,760-9,540 cal BP at the Woodpecker 2 site, was contemporaneous with a Minong lake level, and may represent the earliest identified inhabitants of northwestern Ontario. The Mackenzie sites, RLF, and the Woodpecker sites were likely occupied around this time and/or more recently. Optically stimulated luminescence dates from Woodpecker 1 and Mackenzie 1 contradict the cultural chronology and lake history in northwestern Ontario, and likely do not reflect the Paleoindian occupation(s) that are indicated by artifact recoveries.

The most destructive post-depositional processes appear to be construction-related at Mackenzie 1 and Woodpecker 2. However, the disturbance is localized in the southern portion of Mackenzie 1 and to the west of the road at Woodpecker 2. The next dominant process is bioturbation; roots have likely caused vertical and horizontal displacement within the occupation layer(s) at all of the archaeological sites. Additional animal burrows and worm trails likely caused minimal movement of artifacts.

Pit features were identified at Woodpecker 1 and Mackenzie 1. Explanations for these include buried ice melt and construction-related disturbance. However, it is possible that a more suitable formation process for these features is yet to be determined.

Occupation at the archaeological sites provides additional evidence that Paleoindian groups preferentially selected habitation areas near lake margins and river-mouths along beach terraces. The artifact matrix was poorly-sorted, contained roots, and was likely bioturbated at all of the archaeological sites. The only exception is Woodpecker 2, where artifacts were recovered from within beach shoreface sediments indicating contemporaneity with a Minong margin. Due to absence of stratigraphy, it cannot be determined whether the other four archaeological sites contain occupation layer(s) contemporaneous with their associated shoreline. However, it is highly likely that the sites represent successive occupations soon after depositition ceased, by mobile Paleoindian groups. The Mackenzie site alone yielded 378 projectile points that suggest one persisting flaking pattern (parallel oblique) on stylistically different diagnostics. The site may have been inhabited by numerous groups over an extended period of time. The Mackenzie, RLF, and Woodpecker sites were likely occupied between about 9,900 ^{14}C yrs BP and 9,000 ^{14}C yrs BP, however additional dates are required to confirm this range.

9. REFERENCES

Aario, R. 1972. Associations of bed forms and palaeocurrent patterns in an esker delta, Haapajarvi, Finland. Annales Academiae Scientiarum Fennicae, Series A, III. 61pp.

Aber, J.S. 1982. Model for glaciotectonism. Bulletin of the Geological Society of Denmark, **30**: 79-90.

Ackerman, R.E. 1996a. Early maritime culture complexes of the Northwestern Northwest Coast. *In* Early Human Occupation in British Columbia. *Edited by* R.L. Carlson, and L. Dallas Bona. University of British Columbia Press, Vancouver, pp. 123-132.

Ackerman, R.E. 1996b. Spein Mountain. *In* Early Human Occupation in British Columbia. *Edited by* R.L. Carlson, and L. Dallas Bona. University of British Columbia Press, Vancouver, pp. 456-460.

Agogino, G.A. 1972. Excavations at a Paleo-Indian Site (Brewster) in Moss Agate arroyo, eastern Wyoming, Research Reports, 1955-1960, Projects 1-6, Washington, DC: National Geographic Society.

Agogino, G.A., and Frankfortner, W.D. 1960. The Brewster Site: An Agate-Basin Folsom multiple component site in eastern Wyoming. The Masterkey, **34**: 102-107.

Aharon, P. 2003. Meltwater flooding events in the Gulf of Mexico revisited: Implications for rapid climate changes during the last detlaciation. Paleoceanography, **18** (4): 1079, doi:10.1029/2002PA000840.

Allen, J.R.L. 1968. Current Ripples: Their Relation to Patterns of Water and Sediment Motion. North-Holland Publishing Company, Amsterdam.

Allen, J.R.L. 1983. Gravel overpassing on humpback bars supplied with mixed sediment: examples from the Lower Old Red Sandstone, southern Britain. Sedimentology, **30**: 285-294.

Allen, J.R.L. 1983b. Studies in fluviatile sedimentation: bars, bar-complexes and sandstone sheets (low-sinuosity braided streams) in the Brownstones (L. Devonian), Welsh borders. Sedimentary Geology, **33**: 237-293.

Amundson, L.J., and Meyer, D. 2003. Late Plano occupation at the St. Louis Site (FfNk-7), central Saskatchewan. Current Research in the Pleistocene, **20**: 1-2.

Anderson, T.W. Pollen stratigraphy and vegetation history, Sheguiandah archaeological site.*In* The Sheguiandah Site: Archaeological, Geological, and Paleobotanical Studies at a Paleoindian site on Manitoulin Island, Ontario. *Edited by* P. Julig, Canadian Museum of Civilization, Archaeological Survey of Canada, Mercury Series Paper 161, pp. 179-194.

Bagnold, R.A. 1954. Experiments on a gravity-free dispersion of large, solid spheres in a Newtonian fluid under shear. London Royal Society Proceedings, **225**: 49-63.

Bajc, A.F., Morgan, A.V., Warner, B.G. 1997. Age and paleoecological significance of an early postglacial fossil assemblage near Marathon, Ontario, Canada. Canadian Journal of Earth Sciences: **34**, 687-698.

Bajc, A.F., Schwert, D.P., Warner, B.G., and Williams, N.E. 2000. A reconstruction of Moorhead and Emerson Phase environments along the eastern margin of glacial Lake Agassiz, Rainy River basin, northwestern Ontario. Canadian Journal of Earth Sciences, **37**: 1335-1353.

Bakken, K. 1988. A middle Woodland beach ridge in Roseau County, Minnesota. Minnesota Archaeologist, **47**: 35-42.

Bamforth, D.B. 2002. The Paleoindian occupation of the Medicine Creek drainage, southwestern Nebraska. *In* Medicine Creek, Seventy Years of Archaeological Investigations. *Edited by* D.C. Roper. University of Alabama Press, Tuscaloosa, AL, pp. 54-83.

Barbour, E.H. and Schulz, C.B. 1932. The Scottsbluff bison quarry and its artifacts. Bulletin of the University of Nebraska State Museum, **34**: 283-286.

Barnett, P.J. 2002. Quaternary geology, stratigraphy, and sedimentology of the Sheguiandah site.*In* The Sheguiandah Site: Archaeological, Geological, and Paleobotanical Studies at a Paleoindian site on Manitoulin Island, Ontario. *Edited by* P. Julig, Canadian Museum of Civilization, Archaeological Survey of Canada, Mercury Series Paper 161, pp. 155-177.

Bennett, G. 2011. Personal Communication.

Bettis, E.A., and Mandel, R.D. 2002. The effects of temporal and spatial patterns of Holocene erosion and alleviation on the archaeological record of the central and eastern Great Plains, USA. Geoarchaeology, **17**: 141-154.

Bigarella, J.J., Becker, R.D., and Duarte, G.M. 1969. Coastal dune structures from Parana (Brazil). Marine Geology, **7**: 5-55.

Bjorck, S., and Keister, C.M. 1983. The Emerson Phase of Lake Agassiz, independently registered in northwestern Minnesota and northwestern Ontario. Canadian Journal of Earth Sciences, **20**: 1536-1542.

Blatt, H., Middleton, G., and Murray, R. 1980. Origin of Sedimentary Rocks, 2nd Edition. Prentice-Hall, Inc.: New Jersey.

Bluck, B.J. 1979. Structure of coarse grained braided stream alluvium. Transactions of the Royal Society of Edinburgh, **70**: 181-221.

Booth, R.K., Jackson, S.T., Thompson, T.A. 2002. Paleoecology of a Northern Michigan Lake and the relationship among climate, vegetation, and Great Lakes water levels. Quaternary Research: **57**: 120-130.

Boyd, M. 2007a. Paleoindiangeoarchaeology of the Assiniboine Delta of glacial Lake Agassiz. Canadian Journal of Archaeology, **31**: 198-221.

Boyd, M. 2007b.Early postglacial history of the southeastern Assiniboine delta, glacial Lake Agassiz basin. Journal of Paleolimnology, **37**: 313-329.

Boyd, M., Running, G.L.,and Havholm, K. 2003. Paleoecology and geochronology of glacial Lake Hind during the Pleistocene-Holocene transition: A context for Folsom surface finds on the Canadian prairies. Geoarchaeology, **18**: 583-607.

Boyd, M., Teller, J.T., Kingsmill, L., and Shultis, C. 2012. An 8900-year-old forest drowned by Lake Superior: Hydrological and paleoecological implications. Journal of Paleolimnology, **47**: 339-355.

Bradley, B., and Stanford, D. 2004. The North Atlantic ice-edge corridor: A possible Palaeolithic route to the New World. World Archaeology, **36**: 459-478.

Brassard, B., Chen, H., and Han, Y.H. 2009. Influence of environmental variability on root dynamics in northern forests. Critical Reviews in Plant Sciences, **28**: 179-197.

Breckenridge, A. 2007. The Lake Superior varve stratigraphy and implications for eastern Lake Agassiz outflow from 10,700 to 8900 cal ybp (9.5-8.0 ^{14}C ka). Palaeogeography, Palaeoclimatology, Palaeoecology: **246**: 45-61.

Breckenridge, A., Lowell, T.V., Fisher, T.G., Yu, S. 2010. A late Lake Minong transgression in the Lake Superior basin as documented by sediments from Fenton Lake, Ontario. Journal of Paleolimnology. DOI 10.1007/s10933-010-9447-z.

Breckenridge, A., Johnson, T.C., Beske-Diehl, S., Mothersill, J.S. 2004. The timing of regional Lateglacial events and post-glacial sedimentation rates from Lake Superior. Quaternary Science Reviews, **23**: 2355-2367.

Broecker, W.S., Kennett, J.P., Flower, B.P., Teller, J.T., Trumbore, S., Bonani, G., and Wolfli, W. 1989. Routing of meltwater from the Laurentide Ice Sheet during the Younger Dryas cold episode. Nature, **341**: 318-321.

Brose, D.S. 1994. Archaeological investigations at the Paleo Crossing site, A Paleoindian occupation in Medina County, Ohio. *In* The First Discovery of America: Archaeological Evidence of the Early Inhabitants of the Ohio Area. *Edited by* W.S. Dancey. The Ohio Archaeological Council, Columbus, OH, pp. 62-71.

Bryan, A.L. 1969. Early man in America and the late Pleistocene chronology of western Canada and Alaska. Current Anthropology, **10**: 339-365.

Buchner, A.P.,and Pettipas, L. 1990. The early occupations of the glacial Lake Agassiz basin in Manitoba, 11,500-7700 BP.*In* Archaeological geology of North America. *Edited by* N.P. Lasca & Donaghue. Boulder: Geological Society of America, pp. 51-59.

Burwasser, G.J. 1977. Quaternary Geology of the City of Thunder Bay and vicinity District of Thunder Bay. Ontario Geological Survey Report GR164, 99 pp.

Byers, D.S. 1954. Bull Brook-A fluted point site in Ipswich, Massachusetts. American Antiquity, **19**: 343-351.

Byers, D.S. 1955. Additional information on the Bull Brook site, Massachusetts. American Antiquity, **20**: 274-276.

Byers, D.S. 1959. Radiocarbon dates for the Bull Brook site, Massachusetts. American Antiquity, **24**: 427-429.

Cannon, M.D., and Meltzer, D.J. 2008. Explaining variability in early Paleoindian foraging. Quaternary International, **191**: 5-17.

Cant, D.J., and Walker, R.G. 1976. Development of a braided-fluvial facies model for the Devonian Battery Point Sandstone, Quebec. Canadian Journal of Earth Sciences, **13**: 102-119.

Church, M. and Gilbert, R. 1975. Proglacial fluvial and lacustrine environments. In Jopling, A.V., and McDonald, B.C. (eds.), Glaciofluvial and Glaciolacustrine Sedimentation. Special Publication Society of Economic Paleontologists and Mineralogists, Tulsa, 23: 22-100.

Clague , J.J., and James, T.S. 2002. History and isostatic effects of the last ice sheet in southern British Columbia. Quaternary Science Reviews, **21**: 71-87.

Clemmensen, L.B. and Houmark-Nielsen, M. 1981. Sedimentary features of a Weichselian glaciolacustrine delta. Boreas, **10**: 229-245.

Clifton, H.E. 1969. Beach lamination: nature and origin. Marine Geology, **7**: 553-559.

Clifton, H.E. 1973. Pebble segregation and bed lenticularity in wave-reworked versus alluvial gravel. Sedimentology, **20**: 173-187.

Collinson, J.D. 1971. Some effects of ice on a river bed. Journal of Sedimentary Petrology, **41**: 557-564.

Cyr, H., MacNamee, C., Amundson, L., Freeman, A. 2011. Reconstructing landscape and vegetation through multiproxy indicators: A geoarchaeological examination of the St. Louis site, Saskatchewan, Canada. Geoarchaeology, **26**: 165-188.

Dabrio, C.J. 1982. Sedimentary structures generated on the foreshore by migrating ridge and runnel systems on microtidal and mesotidal coasts of S. Spain. Sedimentary Geology, **32**: 141-151.

Davidson, D.A., Carter, S.P., Quine, T.A. 1992. An evaluation of micromorphology as an aid to archaeological interpretation. Geoarchaeology, **7**: 55-65.

Davis, L.B., Aaberg, S.A., Eckerle, W.P., Fisher, J.W., and Greisner, S.T. 1989. Montane Paleoindian occupation of the Barton Gulch site, Ruby Valley, southwestern Montana. Current Research in the Pleistocene, **6**: 7-9.

Davis, L.B., Aaberg, S.A., and Greisner, S.T. 1988. Paleoindians in transmontane southwestern Montana: The Barton Gulch Occupations, Ruby River drainage. Current Research in the Pleistocene, **5**: 9-11.

Davis, R.A., Fox, W.T., Hayes, M., and Boothroyd, J.C. 1971. Comparison of ridge and runnel systems in tidal and non-tidal environments. Journal of Sedimentary Petrology, **2**: 413-421.

Davis, L.B., and Greiser, S.T. 1992. Indian Creek Paleoindians: Early occupation of the Elkhorn Mountains' Southeast flank, west-central Montana. *In* Ice Age Hunters of the Rockies. *Edited by* D.J. Stanford, and J.S. Day. University of Colorado Press, Niwot, CO, pp. 285-321.

Dawson, K.C.A. 1983a. Cummins site: A late Paleo-Indian (Plano) site at Thunder Bay, Ontario. Ontario Archaeology, **39**: 3-32.

Dawson, K.C.A. 1983b.Prehistory of the interior forest of Northern Ontario.*In* Boreal Forest Adaptations: The Northern Algonkians. *Edited by* A.T. Steegman Jr. Buffalo, New York.

Deller, D.B. 1976.Paleo-Indian locations on late Pleistocene shorelines, Middlesex County, Ontario. Ontario Archaeology, **26**: 3-20.

Deller, D.B. 1979.Paleo-Indian reconnaissance in the counties of Lambton and Middlesex, Ontario. Ontario Archaeology,**32**: 3-20.

Deller, D.B. 1980. The Parkhill (Brophey) site, AhHk-49: Analyses of Surface Materials. Unpublished MA thesis, Department of Anthropology, Wilfred Laurier University.

Deller, D.B. 1988. The Paleo-Indian Occupation of Southwestern Ontario: Distribution, Technology and Social organization. Unpublished Ph.D. Dissertation, Department of Anthropology, McGill University.

Deller, D.B., and Ellis, C.J. 1984. Crowfield: A preliminary report on a probably Palaeo-Indian cremation in southwestern Ontario. Archaeology of Eastern North America, **12**: 41-71.

Deller, D.B.,and Ellis, C.J. 1988. Early Palaeo-Indian complexes in southwestern Ontario.*In* Late Pleistocene and Early Holocene Paleooecology and Archaeology of the Eastern Great Lakes Region. *Edited by* R.S. Laub, N.G. Miller, D.W. Steadman. Bulletin of the Buffalo Society of Natural Sciences, vol. 33, pp. 251-263.

Deller, D.B.,and Ellis, C.J. 2001. Evidence for late Paleoindian ritual from the Caradoc site (AfHj-104), southwestern Ontario, Canada. American Antiquity, **66**: 267-284.

DeVisscher, J., Wahla, E.J., and Fitting, J.E. 1969. Additional Paleo-Indian campsites adjacent to the Holcome site. American Archaeologist, **16**: 1-23.

Dillehay, T.D.,Pino, M., Davis. E.M.,Valastro Jr., S., Varela A.J., and Casamiquela, R. 1982. Monte Verde: Radiocarbon dates from an early-man site in South-Central Chile. Journal of Field Archaeology, **9**: 547-550.

Dixon, E.J. 2001. Human colonization of the Americas: Timing, technology and process. Quaternary Science Reviews, **20**: 277-299.

Doeglas, D.J. 1962. The structure of sedimentary deposits of braided rivers. Sedimentology **1**:167-192.

Drake, N., and Bristow, C. 2006. Shorelines in the Sahara: geomorphological evidence for an enhanced monsoon from palaeolake Megachad. The Holocene, **16**: 901-911.

Drexler, C.W., Farrand, W.R., and Hughes, J.D. 1983. Correlation of glacial lakes in the Superior basin with eastward discharge events from Lake Agassiz. In: Teller, J.T., Clayton, L. (eds) Glacial Lake Agassiz. Geological Association of Canada Special Paper 26, pp 309-329.

Driver, J.C. 1982. Early Prehistoric killing of bighorn sheep in the southeastern Canadian Rockies. Plains Anthropologist, **27**: 265-271.

Driver, J.C. 1996. The significance of the fauna from the Charlie Lake Cave site. *In* Early Human Occupation in British Columbia. *Edited by* R.L. Carlson, and L. Della Bona. University of British Columbia Press, Vancouver, Canada, pp. 21-28.

Duller, G.A.T. 1991. Equivalent dose determination using single aliquots. Nuclear Tracks and Radiation Measurements, **18**: 371-378.

Dyke, A.S. 2004. An outline of North American deglaciation with emphasis on central and northern Canada.*In*Quaternary glaciations-extent and chronology, part II: North America, vol 2b. *Edited by J.* Ehlers, P.L. Gibbard. Elsevier, Amsterdam, pp 373–424.

Dyke, A.S., Andrews, J.T., Clark, P.U., England, J.H., Miller, G.H., Shaw, J., and Veillette, J.J. 2002. The Laurentide and Innuitian ice sheets during the Last Glacial Maximum. Quaternary Science Reviews, **21**: 9-31.

Ellis. C.J. 1979. Analysis of Lithic Debitage from Fluted Point Sites in Ontario. Unpublished MA thesis, Department of Anthropology, McMaster University.

Ellis, C.J. 1984. Paleo-Indian Lithic Technological Structure and Organization in the Lower Great Lakes Area: A First Approximation. Unpublished Ph.D. Dissertation, Department of Archaeology, Simon Fraser University.

Ellis, C.,Deller, D.B. 1997. Variability in the archaeological record of Northeastern Early Paleoindians: A view from Southern Ontario. Archaeology of Eastern North America, **25**: 1-30.

Ellis, C., Goodyear, A.C., Morse, D.F., and Tankersley, K.B. 1998. Archaeology of the Pleistocene-Holocene transition in eastern North America. Quaternary International, **49/50**: 151-166.

Erlandson, J.M., Rick, T.C., Braje, T.J., Casperson, M., Culleton, B., Fulfrost, B. , Garcia, T., Guthrie, D.A., Jew, N., Kennett, D.J., Moss, M.L., Reeder, L., Skinner, C., Watts, J., and Willis, L. 2011. Paleoindian seafaring, maritime technologies, and coastal foraging on California's Channel Islands. Science, **331**: 1181-1185.

Eynon, G., and Walker, R.G. 1974. Facies relationships in Pleistocene outwash gravels, southern Ontario: a model for bar growth in braided rivers. Sedimentology, **21**: 43-70.

Fagan, B.M. 2000. Ancient North America: The archaeology of a continent. 3rd ed. New York, N.Y.: Thames and Hudson, 1995.

Farrand, W.R., and Drexler, C.W. (1985) Late Wisconsinan and Holocene history of the Lake Superior basin. (Eds) Karrow, P.F. &Calkin, P.E. Quaternary Evolution of the Great Lakes, Geological Association of Canada Special Paper 30.

Fedje, D.W., White, J.M., Nelson, D.E., Vogel, J.S., Southon, J.R. 1995. Vermilion Lakes site: adaptations and environments in the Canadian Rockies during the latest Pleistocene and early Holocene. American Antiquity, **60**: 81-108.

Figueiredo, A.G., Sanders, J.E., and Swift, D.J.P. 1982. Storm-graded layers on inner continental shelves: examples from southern Brazil and the Atlantic coast of the central United States. Sedimentary Geology, **31**: 171-190.

Fisher, T., Lowell, T., Loope, H. 2006. Comment on "Alternative routing of Lake Agassiz overflow during the Younger Dryas: New dates, paleotopography, and a re-evaluation. Quaternary Science Reviews: 25, 1137-1141.

Fisher, T.G., Yansa, C.H., Lowell, T.V., Lepper, K., Hajdas, I., Ashworth, A. 2008. The chronology, climate, and confusion of the Moorhead Phase of glacial Lake Agassiz: New results from the Ojata Beach, North Dakota, USA. Quaternary Science Reviews, **27**: 1124-1135.

Fitting, J.E. 1963. The Hi-Lo site: A Late Paleo-Indian site in western Michigan. The Wisconsin Archaeologist, **44**: 87-96.

Fladmark, K.R. 1979. Alternate migration corridors for early man in North America.American Antiquity, **44**, 55-69.

Forbis, R.G. 1992. The Mesoindian (Archaic) period in the Northern Plains. Revista de Arqueologia Americana, **5**: 27-70.

Fox, W.A. 1975. The Paleo-Indian Lakehead Complex. *In* Canadian Archaeologicial Association, Collected Papers, March 1975, Historical Sites Branch, Division of Parks, Toronto, pp. 29-49.

Fralick, P. and Pufahl, P.K. 2006. Iron formation in Neoarchean deltaic successions and the microbially mediated deposition of transgressive systems tracts. Journal of Sedimentary Research, **76**: 1057-1066.

Frison, G.C. 1975. Mans interaction with Holocene environments on the Plains. Quaternary Research, **5**: 289-300.

Frison, G.C. 1998. Paleoindian large mammal hunters on the plains of North America. Proc. Natl. Acad. Sci. USA, **95**: 14576-14583.

Frison, G.C. and Bradley, B.A. 1980. Folsom tools and technology at the Hanson Site, Wyoming. Albuquerque: University of New Mexico Press.

Frison, G.C., and Stanford, D.J. (Eds.) 1982. The Agate Basin Site, San Diego: Academic Press.

Frison, G.C., and Todd, L.C. (Eds.) 1987. The Horner Site, The type site of the Cody cultural complex, Orlando, Fl: Academic Press.

Fryberger, S.G., Al-Sari, A.M., and Clisham, T.J. 1983. Eolian dune, interdune, sand sheet, and siliciclastic sabkha sediments of an offshore prograding sand sea, Dhahran Area, Saudi Arabia. The American Association of Petroleum Geologists Bulletin, 67: 280-312.

Gilbert, G.K. 1885. The Topographic features of lake shores. Annual Report, U.S. Geological Survey, **5**: 75-123.

Gilbert, G.K. 1890. Lake Bonneville. Monographs, U.S. Geological Survey, **1**: 438 pp.

Gilliland, K. 2012. Lakehead Complex sites, Thunder Bay, Ontario. Geoarchaeological Working Paper 1: Preliminary description and interpretation of chronometric dates in stratigraphic context.

Gilliland, K., Adderley, W.P., Gibson, T., Norris, D. 2012. Context, chronology, and culture: Problem-based geoarchaeology at the Lakehead Complex sites, Thunder Bay. Paper presented May 2012 at the Canadian Archaeological Association annual meeting in Montreal, Quebec.

Goebel, T., Waters, M.R.,and O'Rourke, D.H. 2008. The late Pleistocene dispersal of modern humans in the Americas. Science, **319**: 1497-1502.

Goodyear, A.C. 1995. The Allendale Paleoindian expedition – The search for South Carolina's earliest inhabitants. Pastwatch, **4**: 2-5&9.

Gramly, R.M., and Lathrop, J. 1984. Archaeological investigations of the Potts site, Oswego County, New York, 1982 and 1983. Archaeology of Eastern North America, **12**: 122-147.

Green, F.E. 1962. The Lubbock Lake Reservoir site. The Museum Journal (West Texas Museum Association), **6**: 83-123.

Gryba, E.M. 1983. Sibbald Creek: A Record of 11,000 Years of Human Utilization of the Southern Foothills. Occasional Paper No. 22, Archaeological Survey of Alberta, Edmonton, Canada.

Gustavson, T.C., Ashley, G.M., and Boothroyd, J.C. 1975. Depositional sequences in glaciolacustrine deltas. In Jopling, A.V., and McDonald, B.C. (eds.), Glaciofluvial and Glaciolacustrine Sedimentation. Special Publication Society of Economic Paleontologists and Mineralogists, Tulsa, 23: 264-280.

Hall, D.A. 1995. Ice-Age Wisconsin people left unique cultural record. Mammoth Trumpet, **10**: 5-8.

Halverson, C. 1992. The 1991 excavations of the Simmonds site (DcJh-4): A late Palaeo-Indian site on the Current River. Ontario Ministry of Culture and Communications Conservation Archaeology Report. Northern Region, Report 30, pp. 113.

Hamilton, S. 1996. Pleistocene landscape features and Plano archaeological sites upon the Kaministiquia River Delta, Thunder Bay District. Lakehead University Monographs in Anthropology, 1.

Harris, C., Murton, J., and Davies, M.C.R. 2000. Soft-sediment deformation during thawing of ice-rich frozen soils: results of scaled centrifuge modeling experiments. Sedimentology, **47**: 687-700.

Hart, B.S. and Plint, A.G. 2003. Stratigraphy and sedimentology of shoreface and fluvial conglomerates: insights from the Cardium Formation in NW Alberta and adjacent British Columbia. Bulletin of Canadian Petroleum Geology, **51**: 437-464.

Haynes, C.V. 1975. Pleistocene and recent stratigraphy. *In* Late Pleistocene Environments of the Southern High Plains. *Edited by* F. Wendorf, and J.J. Hester. Publication 9, Taos, NM: Fort Burgwin Research Center, pp. 57-96.

Haynes, C.V. 1995. Geochronology of paleoenvironmental change, Clovis type site, Blackwater Draw, New Mexico. Geoarchaeology, **10**: 317-388.

Haynes, C.V., and Agogino, G.A. 1966. Prehistroci springs and geochronology of the Clovis site, New Mexico. American Antiquity, **31**: 812-821.

Haywood, N.A. 1989. Palaeo-Indians and palaeo-environments of the Rainy River district, northwestern Ontario.Ontario Ministry of Culture and Communications Conservation Archaeology Report. Northwestern Region, Report 11, pp. 91.

Hester, J.J. 1972. Blackwater Locality No. 1: A stratified Early Man site in eastern New Mexico, Publication 8, Taos NM: Fort Burgwin Research Center.

Hill, M.E. 2007. A moveable feast? Variation in faunal resource use among central and western North American Paleoindian sites. American Antiquity, **72**: 417-438.

Hine, A.C. 1979. Mechanisms of berm development and resulting beach growth along a barrier spit complex. Sedimentology, **26**: 333-351.

Hinshelwood, A. 2004. Archaic Reoccupation of Lake Palaeo-Indian Sites in Northwestern Ontario. In Jackson, L.J., and Hinshelwood, A. (Eds), The Late Palaeo-Indian Great Lakes: Geological and Archaeological Investigations of Late Pleistocene and Early Holocene Environments. Mercury Series, Archaeology Paper 165. Canadian Museum of Civilization: Gatineau, Quebec.

Hinshelwood, A., and Webber, E. 1987. Testing and excavation of the Ozbolt property, part of the Biloski site (DcJh-9), a late Palaeo-Indian archaeological site, Thunder Bay, Ontario. Ontario Ministry of Culture and Communications Conservation Archaeology Report. North Central Region Report 25, pp. 101.

Hofman, J.L. 1995. Dating Folsom occupations on the Southern High Plains: The Lipscomb and Waugh sites. Journal of Field Archaeology, **22**: 421-437.

Holliday, V.T. 1989. Middle Holocene drought on the southern High Plains. Quaternary Research**, 31**: 74-82.

Holliday, V.T. 1997. Paleoindian geoarchaeology of the Southern High Plains. University of Texas Press: Austin.

Holliday, V.T. 2000. The evolution of Paleoindian geochronology and typology on the Great Plains.Geoarchaeology,**15**: 227-290.

Holliday, V.t., and Meltzer, D.J. 1996. Geoarchaeology of the Midland (Paleoindian) Site, Texas. American Antiquity, **61**: 755-771.

Hudson, J. 2007. Faunal evidence for subsistence and settlement patterns at the Allen site. *In* The Allen Site: A Paleoindian Camp in Southwestern Nebraska. *Edited by* D.B. Bamforth. University of New Mexico Press, Albuquerque.

Huntley, D.J., Godfrey-Smith, D.I., and Thewalt, M.L.W. 1985. Optical dating of Sediments. Nature, 313: 105-107.

Hurst, S., Johnson, E., Holliday, V.T., Butler, S. 2010. Playa archaeology on the southern High Plains of Texas: a spatial analysis of hunter-gatherer occupations at Tahoka-Walker (41LY53). Plains Anthropologist, **55**: 195-214.

Irwin, H.T.,and Wormington, H.M. 1970. Paleo-Indian tool types in the Great Plains. American Antiquity, **35** (1): 24-34.

Irwin-Williams, C., Irwin, H.T., Agogino, G.A., and Haynes, C.V. 1973. Hell Gap Paleo-Indian occupation on the High Plains. Plains Anthropologist, **18**: 40-53.

Jackson, L.J., Ellis, C., Morgan, A.V., and McAndrews, J.H. 2000. Glacial lake levels and eastern Great Lakes Palaeo-Indians.Geoarchaeology, **15**: 415-440.

Jackson Jr., L.E., Phillips, F.M., Shimamura, K., and Little, E.C. 2002. Cosmogenic^{36}Cl dating of the foothills erratics train, Alberta, Canada. Geology, **25**: 195-198.

Jepson, G.L. 1953. Ancient buffalo hunters of northwestern Wyoming. Southwestern Lore, **19**: 19-25.

Johnson, E. (Ed.) 1987. Lubbock Lake: Late Quaternary studies on the southern High Plains. Texas A&M University Press: College Station.

Jopling, A.V., and Walker, R.G. 1968. Morphology and origin of ripple-drift cross-lamination, with examples from the Pleistocene of Massachusetts. Journal of Sedimentary Petrology, **38**: 971-984.

Josenhans, H., Fedje, D., Pienitz, R., and Southon, J. 1997. Early humans and rapidly changing Holocene sea levels in the Queen Charlotte Islands-Hecate Strait, British Columbia, Canada. Science, **277**: 71-74.

Julig, P.J. 1984. Cummins Paleo-Indian site and paleoenvironment, Thunder Bay, Canada. Archaeology of Eastern North America, **12**: 192-209.

Julig, P.J. 1988. The Cummins site complex and Paleoindian occupations in the northwestern Lake Superior region. PhD Thesis, University of Toronto.

Julig, P.J. 1994. The Cummins site complex and Paleoindian occupations in the northwestern Lake Superior region. Ontario Heritage Foundation, Ontario Archaeological Reports 2.

Julig, P.J. (Ed.) 2002. The Sheguiandah Site: Archaeological, Geological, and Paleobotanical Studies at a Paleoindian site on Manitoulin Island, Ontario. Canadian Museum of Civilization, Archaeological Survey of Canada, Mercury Series Paper 161.

Julig, P.J., and Mahaney, W.C. 2002. Geoarchaeological studies of the Sheguiandah site and analysis of museum collections.*In* The Sheguiandah Site: Archaeological, Geological, and Paleobotanical Studies at a Paleoindian site on Manitoulin Island, Ontario. *Edited by* P. Julig, Canadian Museum of Civilization, Archaeological Survey of Canada, Mercury Series Paper 161, pp. 101-137.

Julig, P.J.,McAndrews, J.H., and Mahaney, W.C. 1990. Geoarchaeology of the Cummins site on the beach of Proglacial Lake Minong, Lake Superior Basin, Canada.*In* Archaeological Geology of North America: Boulder, Colorado, Geological Society of America, Centennial Special Volume 4. *Edited by* N.P. Lasca, and J. Donahue.

Julig, P.J., and Storck, P.L. 2002. Introduction to the Sheguiandah site: Regional context and research questions. *In* The Sheguiandah Site: Archaeological, Geological, and Paleobotanical Studies at a Paleoindian site on Manitoulin Island, Ontario. *Edited by* P. Julig, Canadian Museum of Civilization, Archaeological Survey of Canada, Mercury Series Paper 161, pp. 1-10.

Keith, M.L.,and Anderson, G.M. 1963. Radiocarbon dating: Fictitious results with Mollusk shells. Science, **141** (3581): 643-637.

Kemp, D. 1991. The climate of northern Ontario. Occasional Paper #11, Lakehead University: Centre of Northern Studies.

King, C.A.M. 1972. Beaches and Coasts (2nd Edition). New York: St. Martin's Press.

Kingsmill, L. 2011. Middle Holocene Archaeology and Paleoenvironments of the Thunder Bay region, Lake Superior Basin. Unpublished MES Thesis. Lakehead University, Thunder Bay, Ontario. 224 p.

Kinnaird, T.C., Sanderson, D.C.W., Gilliland, K., and Adderley, P. 2012. Luminescence dating of sediments from the Western Heritage excavation of archaeological sites at Thunder Bay (Ontario, Canada). Scottish Universities Environmental Research Centre: University of Glasgow.

Kocurek, G. 1981. Significance of interdune deposits and bounding surfaces in aeolian dune sands. Sedimentology, **28**: 754-780.

Koldehoff, B., Harrison, W.F.,Markman, C.W., and Karch, C. 1999. The Anderson site: A Paleoindian campsite in Dekalb County, Illinois. The Wisconsin Archaeologist, **80**: 97-109.

Kooyman, B.P., Newman, M.E., Cluney, C., Lobb, M., Tolman, S., McNeil, P., and Hills, V. 2001. Identification of horse exploited by Clovis hunters based on protein analysis. American Antiquity, **66**: 686-691.

Kooyman, B., Hills, L.V., McNeil, P., Tolman, S. 2006. Late Pleistocene horse hunting at the Wally's Beach site (DhPg-8), Canada. American Antiquity, **71**: 101-121.

Kornfeld, M., Frison, G.C., Larson, M.L., Miller, J.C., and Sayette, J. 1999. Paleoindian bison procurement and paleoenvironments in Middle Park of Colorado.Geoarchaeology, **14**: 655-674.

Kunz, M.L., and Reanier, R.E. 1996. Mesa Site, Iteriak Creek. *In* American Beginnings. *Edited by* F.H. West. The University of Chicago Press, Chicago, pp. 505-511.

LaJeunesse, P., St-Onge, G. 2008. The subglacial origin of the Lake Agassiz-Ojibway final outburst flood. Nature Geoscience, **1**: 184-188.

Larson, G., and Schaetzl, R. 2001. Origin and evolution of the Great Lakes. Journal of Great Lakes Research, **27**: 518-546.

Laub, R.S. 1994. The Pleistocene/Holocene transition in western New York state: Fruits of interdisciplinary studies at the Hiscock site. *In* Great Lakes Archaeology and Paleoecology: Exploring Interdisciplinary Initiatives for the Nineties. *Edited by* R.I. MacDonald. Quaternary Sciences Institute, University of Waterloo, Publication, Vol. 10, pp. 155-167.

Laub, R.S., DeRemer, M.F., Dufort, C.A., and parsons, W.R. 1988. The Hiscock site, A rich late Quaternary locality in western New York. *In* Late Pleistocene and Early Holocene Paleoecology and Archaeology of the Eastern Great Lakes Region. *Edited by* R.S. Laub, N.G. Miller, and D.W. Steadman. Bulletin of the Buffalo Society of Natural Sciences, **33**: 67-81.

Lee, T.E. 1957. The antuiquity of the Sheguiandah site. Canadian Field Naturalist, **71**: 117-137.

Leverington, D.W., and Teller, J.T. 2003. Paleotopographic reconstructions of the eastern outlets of Lake Agassiz between 11,000 and 9300 ^{14}C years BP. Canadian Journal of Earth Sciences, **40**: 1259-1278.

Lewis, C.F.M. & Anderson, T.W. (1989) Oscillations of levels and cool phases of the Laurentian Great Lakes caused by inflows from glacial lakes Agassiz and Barlow-Ojibway. Journal of Paleolimnology: 2, 99-146.

Leverington, D.W. & Teller, J.T. 2003. Pelotopographic reconstructions of the eastern outlets of glacial Lake Agassiz. Canadian Journal of Earth Sciences: 40, 1259-1278.

Loope, H.M., Loope, W.L., Goble, R.J., Fisher, T.G., Jol, H.M., Seong, J.C. 2010. Early Holocene dune activity linked with final destruction of Glacial Lake Minong, eastern Upper Michigan, USA. Quaternary Research, **74**: 73-81.

Lowe, D.R. 1982. Sediment gravity flows: II. Depositional models with special reference to the deposits of high-density turbidity currents. Journal of Sedimentary Petrology, **52**: 0279-0297.

Lowe, D.R., and LoPiccolo, R.D. 1974. The characteristics and origins of dish and pillar structures. Journal of Sedimentary Petrology, **44**: 484-501.

Lowell, T.V., Larson, G.J., Hughes, J.D., Denton, G.H. 1999. Age verification of the Lake Gribben forest bed and the Younger dryas advance of the Laurentide Ice Sheet. Canadian Journal of Earth Sciences, **36**: 383-393.

LUGDC. 2012a. National Topographic System Digital Elevation Model. Retrieved from http://www.geobase.ca

LUGDC. 2012b. Great Lakes Aerial Photography. Retrieved from the US National Parks Service.

MacDonald, G.F. 1966. The Debert archaeological project: The position of Debert with respect to the Paleo-Indian tradition. Quaternaria, **8**: 33-47.

MacDonald, G.F. 1968. Debert: A Paleo-Indian site in central Nova Scotia. Anthropology Papers, no. 16, National Museum of Canada.

MacDonald, G.F. 1971. A review of research on Paleo-Indian in eastern North America, 1960-1970. Arctic Anthropology, **8**: 32-41.

Mandryk, C.A.S. 1996. Late-glacial vegetation and environment on the eastern slope foothills of the Rocky Mountains, Alberta, Canada.Journal of Paleolimnology, **16**: 37-57.

Mandryk, C.A.S.,Josenhans, H., Fedje, D.W., and Mathewes, R.W. 2001. Quaternary paleoenvironments of Northwestern North America: Implications for inland versus coastal migration routes. Quaternary Science Reviews, **20**: 301-314.

MacNeish, R.S. 1952. A possible early site in the Thunder Bay district, Ontario. National Museum of Canada Bulletin No.126: 23-47.

Makinen, J., and Rasanen, M. 2003. Early Holocene regressive spit-platform and nearshore sedimentation on a glaciofluvial complex during the Yoldia Sea and the Ancylus Lake phases of the Baltic Basin, SW Finland. Sedimentary Geology, **158**: 25-56.

Makse, H.A., Havlin, S., King, P.R., and Stanley, H.E. Spontaneous stratification in granular mixtures. Nature, **386**: 379-382.

Mallol, C., Marlowe, F.W., Wood, B.M., Porter, C.C. 2007. Earth, wind, and fire: ethnoarchaeological signals of Hadza fires. Journal of Archaeological Science, **34**: 2035-3052.

Marshall, E. (2001) Pre-Clovis sites fight for acceptance. Science, **291**: 1730-1732.

Mason, R.J. 1997. Chapter 5: The Paleo-Indian Tradition. The Wisconsin Archaeologist, **78**: 78-110.

Matthews, W., French, C.A.I., Lawrence, T., Cutler, D.F., and Jones, M.K. 1997. Microstratigraphic traces of site formation processes and human activities. World Archaeology, **29**: 281-308.

McAndrews, J.H. 1982. Holocene environment of a fossil bison from Kenora, Ontario. Ontario Archaeology, **37**: 41-51.

McDonald, B.C. and Shilts, W.W. 1975. Interpretation of faults in glaciofluvial sediments. In Jopling, A.V., and McDonald, B.C. (eds.), Glaciofluvial and Glaciolacustrine Sedimentation. Special Publication Society of Economic Paleontologists and Mineralogists, Tulsa, 23: 123-131.

McLeod, M. 2000. The Palaeo-Indian tradition in the Thunder Bay area, earliest evidence: Periglacial peoples. Abstracts. Canadian Archaeological Association, 33rd Annual Meeting, Ottawa, Ontario.

McMillan, K., Teller, J.T. 2012. Origin of the Herman-Norcross-Tintah sequence of the Lake Agassiz beaches in Manitoba, Canada. Geomorphology, doi:10.1016/j.geomorph.2012.01.015

McNeil, P., Hills, L.V., Kooyman, B., and Tolman, M.S. 2004. Late Pleistocene Geology and Fauna of the Wally's Beach Site (DhPg-8) Alberta, Canada. *In* Archaeology on the Edge: New Perspectives from the Northern Plains. *Edited by* B. Kooyman, and J.H. Kelley. University of Calgary Press, Calgary, pp. 79-94.

Meldahl, K.H. 1995. Pleistocene shoreline ridges from tide-dominated and wave-dominated coasts: northern Gulf of California and western Baja California, Mexico. Marine Geology, **123**: 61-72.

Meltzer, D.J. (1995) Clocking the first Americans.Annual Reviews of Anthropology, **24**: 21-45.

Meltzer, D.J. 1999. Human responses to middle Holocene (Altithermal) climates on the North American Great Plains. Quaternary Research, **52**: 404-416.

Meltzer, D.J., Grayson, D.K., Ardila, G., Barker, A.W., Dincauze, D.F., Vance Haynes, C., Mena, F., Nunez, L., and Stanford, D. 1997. On the Pleistocene antiquity of Monte Verde, southern Chile. American Antiquity, **62:** 659-663.

Miall, A.D. 1977. A review of the braided-river depositional environment. Earth Science Reviews, **13**: 1-62.

Middleton, G.V. 1970. Experimental studies related to problems of flysch sedimentation. *In* Flysch Sedimentology in North America: Geological Association of Canada, Special Paper 7. *Edited by* Lajoie, J., 253-272.

Mills, P.C. 1983. Genesis and diagnostic value of soft-sediment deformation structures – a review. Sedimentary Geology, **35**: 83-104.

Morgan, A.V.,McAndrews, J.H., and Ellis, C. 2000. Geological history and paleoenvironment.*In* An early Paleoindian site near Parkhill, Ontario.*Edited by* C. Ellis, and D.B. Deller. Mercury Series, Archaeological Survey of Canada Paper 159.Canadian Museum of Civilization.Chapter 2, pp 9-30.

Morlan, R.E. 2003. Current perspectives on the Pleistocene archaeology of eastern Beringia. Quaternary Research, **60**: 123-132.

Morris, T.F.,McAndrews, J.H., and Seymour, K.L. 1993. Glacial Lake Arkona-Whittlesey transition near Leamington, Ontario: Geology, plant, and muskox fossils. Canadian Journal of Earth Sciences, **30**: 2436-2447.

Morrow, J.E., and Morrow, T.A. 1999. Geographic variation in fluted projectile points: A hemispheric perspective. American Antiquity, **64**: 215-230.

Mulholland, S.C., Mulholland, S.L., Peters, G.R., Huber, J.K., and Mooers, H.D. 1997. Paleo-Indian occupation in northeastern Minnesota: How early? North American Archaeologist, **18**: 371-400.

Mulligan, C.J., Kitchen, A., and Miyamoto, M.M. 2008. Updated three-stage model for the peopling of the Americas. PLoS ONE, **3**: e3199.

Murton, J.B., Bateman, M.D., Dallimore, S.R., Teller, J.T., Yang, Z. 2010. Identification of Younger Dryas outburst flood path from Lake Agassiz to the Arctic Ocean. Nature, **464**: 740-743.

Muto, T., and Steel, R.J. 1997. The Middle Jurassic Osegerg delta, northern North Sea: a sedimentological and sequence stratigraphic interpretation. American Association of Petroleum Geolgists, **81**: 1070-1086.

Nielsen, L.H., Johannessen, P.N., and Surlyk, F. 1988. A late Pleistocene coarse-grained spit-platform sequence in northern Jylland, Denmark. Sedimentology, **35**: 915-937.

Nishikawa, T., Ito, M. 2000. Late Pleistocene barrier-island development reconstructed from genetic classification and timing of erosional surfaces, paleo-Tokyo Bay, Japan. Sedimentary Geology, **137**: 25-42.

Olley, J.M., Caitcheon, G.G., and Roberts, R.G. 1999. The origin of dose distributions in fluvial sediments, and the prospect of dating single grains from fluvial deposits using optically stimulated luminescence. Radiation Measurements, **30**: 207-217.

Ovenshine, A.T. Observations of iceberg rafting in Glacier Bay, Alaska, and the identification of ancient ice-rafted deposits. Geological Society of America Bulletin, **81**: 891-894.

Overstreet, D.F. 1998. Late Pleistocene geochronology and the Paleoindian penetration of the southwestern Lake Michigan basin. The Wisconsin Archaeologist, **79**: 28-52.

Owens, G. 1996. Experimental soft-sediment deformation: structures formed by the liquefaction of unconsolidated sands and some ancient examples. Sedimentology, **43**: 279-293.

Patricia Craig, S. 1991. Sedimentation Models for Glacial Deltaic Successions in the Thunder Bay Area. Unpublished MSc Thesis, Lakehead University, Thunder Bay, Ontario. 168 p.

Peers, L. 1985.Ontario Paleo-Indians and caribou predation. Ontario Archaeology,**43**: 31-40.

Phillips, B.A.M. 1982. Morphological mapping and paleogeographic reconstruction of former shorelines between Current River and Rosslyn, Thunder Bay, Ontario, including Cummins Site DcJi-1. Report on file with Historical Planning and Research Branch, Ontario Ministry of Citizenship and Culture, Toronto, Ontario.

Phillips, B.A.M. 1993. A time-space model for the distribution of shoreline archaeological sites in the Lake Superior Basin.Geoarchaeology, **8**: 87-107.

Phillips, B.A.M., and Fralick, P. 1994a. A post-lake Minong transgression event on the north shore of Lake Superior, Ontario: possible evidence of Lake Agassiz inflow. Canadian Journal of Earth Sciences, **31**: 1638-1641.

Phillips, B.A.M., and Fralick, P. 1994b. Interpretation of the sedimentology and morphology of perched glaciolacustrine deltas on the flanks of the Lake Superior Basin, Thunder Bay, Ontario. Journal of Great Lakes Research, **20**: 390-406.

Pickering, K.T. 1982. A Precambian upper basin-slope and prodelta in northeast Finnmark, North Norway – a possible ancient upper continental slope. Journal of Sedimentary Petrology, **52**: 0171-0186.

Postma, G., and Nemec, W. 1990. Regressive and transgressive sequences in a raised Holocene gravelly beach, southwest Crete. Sedimentology, **37**: 907-920.

Quimby, G.I. 1959. Lanceolate points and fossil beaches in the upper Great Lakes region. American Antiquity, **24**: 424-426.

Ramos, A., and Sopena, A. 1983. Gravel bars in low-sinuosity streams (Permian and Triassic, central Spain). *In* Modern and Ancient Fluvial Systems. *Edited by* Collinson, J.D., Lewin, J. Special Publication, International Associatiation of Sedimentology, **6**: 301-312.

Ramos, A., Sopena, A., and Perez-Arlucea, M. 1986. Evolution of Buntsandstein fluvial sedimentation in the northwest Iberian Ranges (central Spain). Journal of Sedimentary Petrology, **56**: 862-875.

Rapson, D.J., and Niven, L.B. 2009. The 1960-1966 Locality I faunal assemblage *In* Hell Gap: A Stratified Paleoindian Campsite at the Edge of the Rockies. *Edited by* M.L. Larson, M. Kornfeld, and G.C. Frison. University of Utah Press, pp. 111-134.

Ravensloot, J.C., and Waters, M.R. 2002-2004. Geoarchaeology and archaeological site patterning on the middle Gila River, Arizona. Journal of Field Archaeology, **29**: 203-214.

Reading, H.G., and Collinson, J.D. 1996. Clastic coasts. *In* Sedimentary Environments: Processes, Facies and Stratigraphy, 3rd Edition. *Edited by* H.G. Reading. Elsevier: New York.

Reanier, R.E. 1995. The antiquity of Paleoindian materials in northern Alaska. Arctic Anthropology, **32**: 31-50.

Reeves, B.O.K. 1973. The nature and age of the contact between the Laurentide and Cordilleran ice sheets in the western interior of North America. Arctic and Alpine Research, **5**: 1-16.

Reimer, P.J., Baillie, M.G.L., Bard, E., Bayliss, A., Beck, J.W., Bertrand, C.J.H., Blackwell, P.J., Ramsey, C.B., Buck, C.E., Burr, G.S., Cutler, K.B., Damon, P.E., Edwards, Fairbanks, R.G., R.L., Friedrich, M., Guilderson, T.P., Hogg, A.G., Hughen, K.A., Kromer, B., McCormac, F.G., Manning, S.W., Ramsey, C.B., Reimer, R.W., Remmele, S., Southon, J.R., Stuiver, M., Talamo, S., Taylor, F.W., van der Plicht, J., Weyhenmeyer, C.E. 2004. IntCal04 terrestrial radiocarbon age calibration, 0-26 cal kyr BP. Radiocarbon, **46**: 1029-1058.

Reimer, P.J., Baillie, M.G.L., Bard, E., Bayliss, A., Beck, J.W., Blackwell, P.J., Ramsey, C.B., Buck, C.E., Burr, G.S., Edwards, R.L., Friedrich, M., Grootes, P.M., Guilderson, T.P., Hadjas, I., Heaton, T.J., Hogg, A.G., Hughen, K.A., Kaiser, K.F., Kromer, B., McCormac, F.G., Manning, S.W., Reimer, R.W., Richards, D.A., Southon, J.R., Talamo, S., Turney, C.S.M., van der Plicht, J., Weyhenmeyer, C.E. 2009. Intcal09 and Marine09 radiocarbon age calibration curves, 0-50,000 years cal BP. Radiocarbon, **51**: 1111-1150.

Ritchie, W.A. 1965. The Archaeology of New York State. Natural History Press for American Museum of Natural History, New York.

Roosa, W.B. 1977. Great Lakes Paleoindian: The Parkhill site, Ontario. *In*Amerinds and the Paleoenvironments in Northeastern North America.*Edited by* W.S. Newman, B. Salwen. Annals of the New York Academy of Sciences, **288**: 349-354.

Roosa, W.B.,and Deller, D.B. 1982. The Parkhill complex and eastern Great Lakes Paleo Indian. Ontario Archaeology, **37**: 3-15.

Ross, W. 1997. The interlaces composite:A re-definition of the initial settlement of the Agassiz-Minong peninsula. The Wisconsin Archaeologist, **76**: 244-268.

Rossetti, D.D.F. 1999. Soft-sediment deformation structures in late Albanian to Cenomanian deposits, Sao Luis basin, northern Brazil: evidence for palaeoseismicity. Sedimentology, **46**: 1065-1081.

Rust, B.R. and Romanelli, R. 1975. Late Quaternary subaqueous outwash deposits near Ottawa, Canada. In Jopling, A.V., and McDonald, B.C. (eds.), Glaciofluvial and Glaciolacustrine Sedimentation. Special Publication Society of Economic Paleontologists and Mineralogists, Tulsa, **23**: 177-192.

Saarnisto, M. 1974. The deglaciation history of the Lake Superior region and its climatic implications. Quaternary Research, **4**: 316-339.

Sallenger, A.H. 1979. Inverse grading and hydraulic equivalence in grain flow deposits. Journal of Sedimentary Petrology, **49**: 0553-0562.

Sanderson, D.C.W., and Murphy, S. 2010. Using simple portable OSL measurements and laboratory characterization to help understand complex and heterogeneous sediment sequences for luminescence dating. Quaternary Geochronology, **5**: 299-305.

Schulz, C.B. 1943. Some artifact sites of Early Man in the Great Plains and adjacent areas. American Antiquity, **8**: 242-249.

Schulz, C.B., and Eiseley, L. 1935. Paleontological evidence for the antiquity of the Scottsbluff bison quarry and its associated artifacts. American Anthropologist, **37**: 306-319.

Schweger, C. 1985. Geoarchaeology of northern regions: lessons from cryoturbation at Onion Portage, Alaska. In: Stein, J.K., and Farrand, W.R. (eds.) Archaeological Sediments in Context. Center for the Study of Early Man, Institute for Quaternary Studies, University of Maine: Orono, pp. 127-141.

Sellards, E.H. 1952. Early Man in America. University of Texas Press, Austin.

Sharpe, D.R., Pullan, S.E., Warman, T.A. 1992. A basin analysis of the Wabigoon area of Lake Agassiz, a Quarternary clay basin in Northwestern Ontario. Geographie Physique et Quaternaire, **46**: 295-309.

Slattery, S.R., Barnett, P.J., Long, D.G.F. (2007) Constraints on paleolake levels, spillways and glacial lake history, north-central Ontario, Canada. Journal of Paleolimnology: **37**, 331-348.

Smith, I.R. 2000. Diamictic sediments within high Arctic lake sediment cores: evidence for lake ice rafting along the lateral glacial margin. Sedimentology, **47**: 1157-1179.

Smith, G.L.B., and Eriksson, K.A. 1979. A fluvioglacial and glaciolacustrine deltaic depositional model for Permo-Carboniferous coals of the northeastern Karoo basin, South Africa. Palaeogeography, Palaeoclimatology, Palaeoecology, **27**: 67-84.

Steel, R.J. and Thompson, D.B. 1983. Structures and textures in Triassic braided stream conglomerates ('Bunter' Pebble Beds) in the Sherwood Sandstone Group, North Staffordshire, England. Sedimentology, **30**: 341-367.

Steinbring, J. 1967. A short note on materials from the Cummins quarry site (DcJi-1) near Thunder Bay, Ontario. Ontario Archaeology, **26**: 21-30.

Stevenson, M.G. 1985. The formation of artifact assemblages at workshop/habitation sites: models from Peace Point in Northern Alberta. American Antiquity, **50**: 63-81.

Stevenson, M.G. 1986. Window on the past: archaeological assessment of the Peace Point site, Wood Buffalo National Park, Alberta. National Historic Parks and Sites Branch, Parks Canada, Environment Canada: Quebec.

Stewart, A. 1984. The Zander site: Paleo-Indian occupation of the southern Holland Marsh region of Ontario. Ontario Archaeology, **41**: 45-79.

Stoltman, J.B. 1998. Paleoindian adaptive strategies in Wisconsin during Late Pleistocene times. The Wisconsin Archaeologist, **79**: 53-67.

Storck, P.L. 1972. An unusual late Paleo-Indian projectile point from Grey County, southern Ontario.Ontario Archaeology, **18**: 25-36.

Storck, P.L. 1983. The Fisher site, fluting techniques, and early Palaeo-Indian cultural relationships. Archaeology of Eastern North America, **11**: 80-92.

Storck, P.L. 1984. Research into the Paleo-Indian occupations of Ontario: A review. Ontario Archaeology, **41**: 3-28.

Stow, D.A.V., Reading, H.G., and Collinson, J.D. 1993. Deep Seas. *In* Sedimentary Environments: Processes, Facies and Stratigraphy, 3rd Edition. *Edited by* H.G. Reading. Elsevier: New York.

Strong, W.L., and Hills, L.V. 2003. Post-Hypsithermal plant disjunctions in western Alberta, Canada. Journal of Biogeography, **30**: 419-430.

Stuart, A.J. 1993. Palaeogeographical Reconstructio of Lake Beaver Bay Raised Shorelines, with Correlation to possible Palaeoindian Settlement, Thunder Bay Region, Ontario. Unpublished HBA Thesis. Lakehead University, Thunder Bay, Ontario. 83 p.

Sturm, M., and Matter, A. 1978. Turbidites and varves in Lake Brienz (Switzerland): deposition of clastic detritus by density currents. Spec. Publs int. Ass. Sediment., **2**: 147-168.

Sun, C., and Teller, J.T. 1997. Reconstruction of glacial Lake Hind in southwestern Manitoba, Canada. Journal of Paleolimnology, **17**: 9-21.

Syms, E.L. 1977.Cultural ecology and ecological dynamics of the ceramic period in southwestern Manitoba.Plains Anthroplogist, mem. 12, part 2.

Tamm, E., Kivisild, T., Reidla, M., Metspalu, M., Smith, D.G., Mulligan, C.J., Bravi, C.M., Rickards, O., Martinez-Labarga, C., Khusnutdinova, E.K., Fedorova, S.A., Golubenko, M.V., Stepanov, V.A., Gubina, M.A., Zhadanov, S.I., Ossipova, L.P., Damba, L., Voevoda, M.I., Dipierri, J.E., Villems, R., and Malhi, R.S. 2007. Beringian standstill and spread of Native American founders.PLoS ONE, **2** (9): e829.

Taylor, R.B. and McCann, S.B. 1983. Coastal depositional landforms in northern Canada. In: Smith, D.E., and Dawson, A.G. (eds.), Shorelines and Isostasy. Academic Press: New York, NY, p. 53-75.

Teller, J.T. & Boyd, M. 2006. Two possible routings for overflow from Lake Agassiz during the Younger Dryas: Reply to comment by Fisher et al. Quaternary Science Reviews: **25**, 1142-1145.

Teller, J.T., Boyd, M., Yang, J., Kor, P.S.G., Fard, A. 2005. The alternative routing of Lake Agassiz overflow during the Younger Dryas: new dates and a re-evaluation. Quaternary Science Reviews, **24**: 1890-1905.

Teller, J.T., Leverington, D.W., Mann, J.D. 2002. Freshwater outbursts to the oceans from glacial Lake Agassiz and their role in climate change during the last deglaciation. Quaternary Science Reviews: **231**, 879-887.

Teller, J.T. and Mahnic, P. (1988) History of sedimentation in the northwestern Lake Superior basin and its relation to Lake Agassiz overflow. Canadian Journal of Earth Sciences: **25**, 1660-1673.

Teller, J.T., Risberg, J., Matile, G., and Zoltai, S. 2000. Postglacial history and paleoecology of Wampum, Manitoba, a former lagoon in the Lake Agassiz basin. Geological Society of America Bulletin, **112**: 943-958.

Teller, J.T., Thorleifson, L.H. 1983. The Lake Agassiz-Lake Superior Connection. In: Teller, J.T., Clayton, L. (eds) Glacial Lake Agassiz. Geological Association of Canada Special Paper 26, pp 261-290.

Teller, J.T., Thorleifson, L.H., Matile, G., Brisbin, W.C. 1996. Sedimentology, geomorphology and history of the central Lake Agassiz basin. Field Trip Guidebook, B2, Geology Association of Canada/Minerology Association of Canada, p. 84.

Thompson, W.O. 1937. Original structures of beaches, bars, and dunes. Bulletin of the Geological Society of America, **48**: 723-752.

Van Den Berg, J.H., and Van Gelder, A. 1993. A new bedform stability diagram, with emphasis on the transition of ripples to plane bed in flows over fine sand and silt. Spec. Publs Int. Ass. Sediment, **17**: 11-21.

Vaneste, K., Meghraoui, M., Camelbeeck, T. 1999. Late Quaternary earthquake-related soft-sediment deformation along the Belgian portion of the Feldbiss Fault, Lower Rhine Graben system. Tectonophysics, **309**: 57-79

Visser, J.N.J., Colliston, W.P., and Terblanche, J.C. 1984. The origin of soft-sediment deformation structures in Permo-Carboniferous glacial and proglacial beds, South Africa. Journal of Sedimentary Petrology, **54**: 1183-1196.

Waguespack, N.M. 2007. Why we're still arguing about the Pleistocene occupation of the Americas. Evolutionary Anthropology, **16**: 63-74.

Wallinga, J. 2002. Optically stimulated luminescence dating of fluvial deposits: a review. Boreas, **31**: 303-322.

Wang, S., Lewis, C.M., Jakobsson, M., Ramachandran, S., Ray, N., Bedoya, G., Rojas, W., Parra, M.V., Molina, J.A., Gallo, C., Mazzotti, G., Poletti, G., Hill, K., Hurtado, A.M., Labuda, D., Klitz, W., Barrantes, R., Bortolini, M.C., Salzano, F.M., Petzl-Erler, M.L., Tsuneto, L.T., Llop, E., Rothhammer, F., Excoffier, L., Feldman, M.W., Rosenberg, N.A., and Ruiz-Linares, A. 2007. Genetic variation and population structure in Native Americans. PLOS Genetics, **3**: 2049-2067.

Ward, B.C., Wilson, M.C., Nagorsen, D.W., Nelson, D.E., Driver, J.C., andWigen, R.J. 2003. Port Eliza cave: North American West Coast interstadial environment and implications for human migrations. Quaternary Science Reviews, **22**: 1383-1388.

Washburn, A.L. 1973. Periglacial processes and environments. St. Martin's Press: New York.

Waters, M.R. 1986. The Sulphur Spring stage and its place in New World Prehistory. Quaternary Research, **25**: 251-256.

Waters, M.R., Forman, S.L., Jennings, T.A., Nordt, L.C., Driese, S.G., Feinberg, J.M., Keene, J.L., Halligan, J., Lindquist, A., Pierson, J., Hallmark, C.T., Collins, M.B., and Wiederhold, J.E. 2011. The Buttermilk Creek Complex and the origins of Clovis at the Debra L. Friedkin site, Texas. Science, **331**, 1599: DOI: 10.1126/science.1201855.

Waters, M.R., and Stafford Jr., T.W. 2007. Redefining the age of Clovis: Implications for the peopling of the Americas. Science, **315**: 1122-1126.

Wedel, W.R. 1986. Central plains prehistory. Lincoln: University of Nebraska Press.

Wendorf, F., and Krieger, A.D. 1959. New light on the Midland discovery. American Antiquity, **25**: 66-78.

Wendorf, F., Krieger, A.D., Albritton, C.C., and Stewart, T.D. 1955. The Midland discovery. University of Texas Press: Austin.

Williams, G.E. 1970. Flood deposits of the sand-bed ephemeral streams of central Australia. Sedimentology, **17**: 1-40.

Williams, J.W., Shuman, B.N., and Webb, T. 2001. Dissimilarity analyses of Late-Quaternary vegetation and climate in eastern North America. Ecology, **82**: 3346-3362.

Wood, W.R., and Johnson, D.L. 1978. A survey of disturbance processes in archaeological site formation. Advances in Archaeological Method and Theory, **1**: 315-381.

Wright, J.V. 1963. Field Notes in 1963 Cummins Site Excavations. On file at Archaeological Survey of Canada, Ottawa.

Wright, L.D. 1977. Sediment transport and deposition at river mouths: a synthesis. Geological Society of America Bulletin, **88**: 857-868.

Zoltai, S.C. 1965. Glacial Features of the Quetico-Nipigon area, Ontario. Canadian Journal of Earth Sciences. **2**: 247-269.

Zonnefeld, J-P., and Moslow, T.F. 2004. Exploration potential of the Falher G shoreface conglomerate trend: evidence from outcrop. Bulletin of Canadian Petroleum Geology, **52**: 23-38.

Zumberge, J.H., and Wilson, J.T. 1953. Effect of ice on shore development. In: Johnson, J.W. (ed) Fourth Conf. Coastal Eng. Chicago Proc.: Berkeley, University of California, pp 201-205.